THE UNIVERSITY *of* EDINBURGH

THE UNIVERSITY *of* EDINBURGH

MITF in Melanoma Progression, Pathology and Survival *in vivo*

Amy Capper

Presented for the Degree of

Doctor of Philosophy

The University of Edinburgh

2014

I hereby declare that this thesis has been composed by me, this work has not been submitted for any other degree or professional qualification, the work is my own and contribution from others has been clearly indicated.

Amy Capper

May 2014

Acknowledgements

I am forever grateful to all those who have helped me throughout my PhD.

I would firstly like to acknowledge my supervisor Liz Patton for all her support over the last four years. From our first collaboration during my Masters rotation to giving me such a great project and a lab environment to develop as a scientist, all of which could never be done without a good cup of earl grey! I would also like to thank my second supervisor Ian Jackson who has given me endless support from the start, from advice about RNA-seq to running tips (!) and Nick Hastie for his continued belief and inspiration.

I am very grateful for our strong collaborations with Jim Lister from Virginia Commonwealth University School of Medicine and Jennifer Yen, Derek Stemple and Andy Futreal at the Sanger Institute, Hinxton. I would also like to thank collaborators in Edinburgh, in particular Marie Mathers for her time in helping with pathology, Ian Overton for his help with network analysis and James Prendergast and Graeme Grimes for their IT and genomic analysis expertise.

It has been a pleasure to work in a lab within the IGMM, Edinburgh with all the support from technical, imaging and admin teams. Huge thanks must go to Paul Perry, Matt Pearson, Allyson Ross and Craig Nicol. I must also thank everyone in my lab and the fish room both past and present for all their support...Corina, Jenny, Kerrie, Zhiqiang, Nick, Emma, Amy, Nicola, Juan, Judith, Witek, Wei and Karthika.

Lastly, I would like to thank friends and family. Although most are blissfully unaware of everything that goes on in the lab they know how much I appreciate their continual support and love. Both near and far, I would like to thank Kiran, Kathrz, Lucy and Colleen, Gill, Aly, Corina, Kerrie and Sehrish. Mum, Dad, Tess and of course Nige. Thank you all for everything.

Abstract to Thesis

MITF is the master melanocyte transcription factor and has a complex role in melanoma. Both gain- and loss-of function mutations in MITF have been identified in melanoma, although its' role in melanoma development and the effects of targeting MITF are unknown. Using a temperature-sensitive *mitf* zebrafish mutant I show that low levels of MITF are oncogenic with $BRAF^{V600E}$ in melanoma progression. By pathology and MITF target gene expression, $BRAF^{V600E}mitfa^{vc7}$ tumours are distinct from $BRAF^{V600E}p53^{M214K}$ tumours, and represent two melanoma subtypes. Melanomagenesis can also be driven independently of $BRAF^{V600E}$, in a transgenic zebrafish with mutations in *mitf* and *p53*, representing a new melanoma model.

Abrogating MITF activity in $BRAF^{V600E}mitfa^{vc7}$ melanoma leads to regression of the tumour, characterised by macrophage infiltration and increased apoptosis. This result confirms the dependence on MITF activity in $BRAF^{V600E}mitfa^{vc7}$ melanomas and highlights the role of MITF as a therapeutic target for melanoma. Exome and transcriptome sequencing has been carried out to gain insight into the expression and genomic mutational landscape that is driven by these melanoma transgenic models and results in these genotype-phenotype specific subtypes observed.

Table of Contents

Chapter 5 Exploring the melanoma genomic mutation and expression landscape

Chapter 6 Concluding Remarks and Future Directions

Chapter 7 Materials and Methods

List of Figures

Chapter 1 Introduction

Chapter 2 MITF is a cancer gene

Chapter 3 MITF mutations direct pathological and molecular features of melanoma

Chapter 4 MITF is essential for melanoma survival

Chapter 5 Exploring the melanoma genomic mutation and expression landscape

List of Abbreviations

ALM	Acral lentiginous melanoma
C>T	Cytosine to thymine transition
cAMP	Cyclic adenosine monophosphate
CD68	Cluster of Differentiation 68
cDNA	Complementary DNA
cGMP	Cyclic guanosine monophosphate
cSCC	Cutaneous squamous cell carcinoma
Ct	Threshold cycle
DAVID	Database for Annotation, Visualisation and Integrated Discovery
DMBA	7,12-Dimethylbenz(a)anthracene
DMSO	Dimethylsulfoxide
DNA	Deoxyribonucleic acid
EHNA	erythro-9-(2-hydroxy-3-nonyl)adenine
ENU	N-ethyl-N-nitrosourea
FDA	Food and Drug Administration
GO-term	Gene Ontology – (term)
H&E	Haematoxylin and eosin
H2AX	H2A histone family, member X
HCC	Hepatocellular carcinoma
HDAC	Histone deacetylase
HGFR	Hepatocyte growth factor receptor
IHC	Immunohistochemistry
IMP	Integrative Multi-species Prediction
KEGG	Kyoto Encyclopaedia of Genes and Genomes
LMM	Lentigo maligna melanoma
MAPK	Mitogen-activated protein kinase
MPNST	Malignant peripheral nerve sheath tumour
mRNA	Messenger RNA

MSC	Melanocyte Stem Cell
N:S	Non-synonymous/synonymous mutation ratio
NCI-60	National Cancer Institute-60 cell line
NCPC	Neural Crest Progenitor Cell
NGS	Next generation sequencing
NHS	National Health Service
NMDA	N-methyl-D-aspartate receptor
OS	Overall survival
PCR	Polymerase Chain Reaction
PTK	Protein tyrosine kinase
RCC	Renal cell carcinoma
RFS	Relapse-free survival
RGP	Radial growth phase
RNA	Ribonucleic acid
RPE	Retinal pigment epithelium
RT-PCR	Reverse Transcription PCR
siRNA	Small interfering RNA
SNP	Single Nucleotide Polymorphism
SSM	Superficial spreading melanoma
STRING	Search Tool for the Retrieval of Interacting Genes/Proteins
SUMO	Small ubiquitin-like modifier
TGF-β	Transforming growth factor beta
TILLING	Targeted Induced Local Lesions in Genomes
TMR	Tumour mitotic rate
TNM	Tumour-node-metastasis
TS	Tietz syndrome
TSS	Transcription start site
UV	Ultraviolet (light)
VEGF	Vascular endothelial growth factor
VGP	Vertical growth phase
WS2	Waardenburg syndrome type 2
WTSS	Whole transcriptome shotgun sequencing

Gene names

BRAF	v-raf murine sarcoma viral oncogene homolog B
CDKNA2	cyclin-dependent kinase inhibitor 2A
CRAF	v-raf-1 murine leukemia viral oncogene homolog 1
ERK/MAPK	extracellular signal-regulated kinase/mitogen-activated protein kinase
KIT	v-kit Hardy-Zuckerman 4 feline sarcoma viral oncogene homolog
MEK/MAP2K	Mitogen-activated protein kinase-kinase
MITF	microphthalmia-associated transcription factor
NF2	neurofibromin 2
NRAS	neuroblastoma RAS viral (v-ras) oncogene homolog
p53	Tumour protein 53
PAX3	paired box 3
PDGFR	platelet-derived growth factor receptor
PREX2	phosphatidylinositol-3,4,5-trisphosphate-dependent Rac exchange factor 2
SMURF2	SMAD specific E3 ubiquitin protein ligase 2
TGF-β	transforming growth factor, beta
VEGFR2	vascular endothelial growth factor receptor 2

N.B Gene/protein nomenclature

- **Human** gene symbols are italicised and all letters are in upper case (e.g. *MITF*); protein designations are same as gene symbol but not italicised (e.g. MITF)
- **Mouse/Rat/Chicken** gene symbols are italicised with first letter in upper case and rest in lower case (e.g. *Mitf*); protein designations are same as gene symbol but not italicised and all in upper case (e.g. MITF)
- **Fish** gene symbols are italicised and all in lower case (e.g. *mitf*); protein designations are same as gene symbol but not italicised and first letter only in upper case (e.g. *Mitf*)

Chapter 1 – Introduction

1.1 Melanoma as a clinical disease

Malignant melanoma is the most deadly form of skin cancer (The Skin Cancer Foundation, 2014) and the 5th most common cancer in the UK (Cancer Research UK, 2011). The word 'melanoma' comes from the Greek word '*melas*,' meaning black and '*-oma*,' meaning tumour and was first coined in the 1830s to describe a pigmented growth (Oxford English Dictionary, 2014). It is cancer of the melanocytes, the pigment-producing cells found in our skin, hair and eyes. It develops most commonly in the skin, but also less frequently in the eye, on palms of the hands and in the nails, as well as in the linings of the nose and mouth.

Skin cancer statistics from Cancer Research UK show the impact of malignant melanoma on patients in the UK in 2011. In this year, 13,348 people in the UK were diagnosed with malignant melanoma and there were 2,209 deaths from the disease (Cancer Research UK, 2011). In contrast, in the same year, around 100,000 people in the UK were diagnosed with non-melanoma skin cancer, with only 585 deaths from this disease (Cancer Research UK, 2011). This statistic highlights the severity of malignant melanoma in particular and its aggressive nature compared to other forms of skin cancer. The incidence of malignant melanoma in the UK has increased significantly over the last 30 years and interestingly, cases in melanoma have increased more rapidly than any of the current ten most common cancers in both males and females (Figure 1.1). This increase is thought to be mostly due to changes in sun-related behaviour, including an increase in frequency of holidays abroad and the use of sunbeds. The impact of these factors is supported by a study published in 2011, which estimated that 86% of malignant melanomas in the UK in 2010 were linked to UV radiation exposure from the sun and sunbeds (Parkin *et al*., 2011). The authors of this study assume that the high percentage of melanomas linked to UV radiation is due to altered patterns in human behaviour, through our choice of

clothing and recreational sunshine, which causes an increase in incidence that is population-specific (Parkin *et al*., 2011).

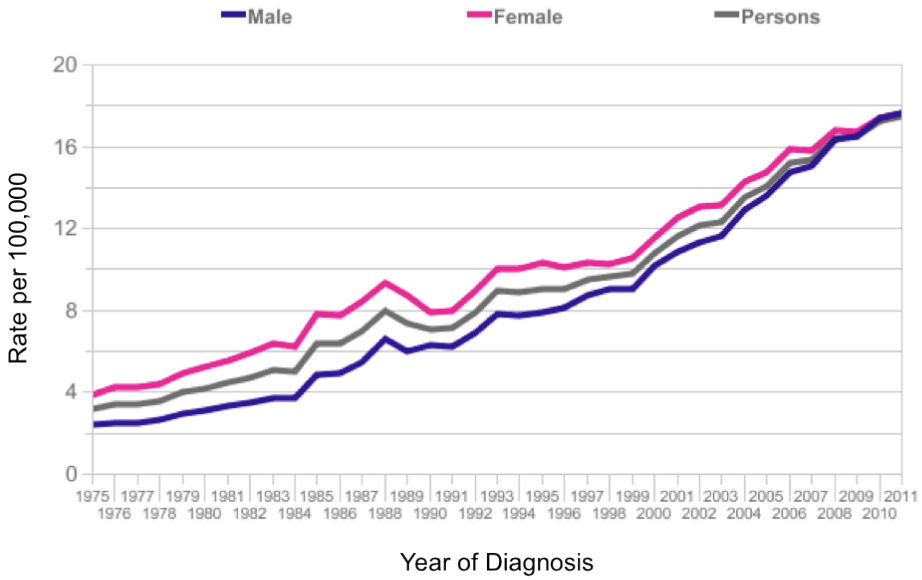

Figure 1.1 Malignant melanoma incidence trend in the UK (Adapted from Cancer Research UK, 2011)
Malignant melanoma, European age-standardised incidence rates per 100,000 population, by sex, in the UK between 1975 and 2011.

The critical moment in melanoma development takes place when the clonal evolution generates a cell that has the potential to enter the vertical growth phase (VGP) (Clark, 1989; Crotty, 2004). There are several key steps, from structurally normal melanocytes to metastatic melanoma, which underline the stages of melanoma progression. It begins simply with normal melanocytes, the cell type that is essential for pigmentation and from which melanomas are derived. Normal melanocytes together can form commonly acquired or congenital nevi. The melanocyte structure has the capacity to change and form dysplastic nevi. These are atypical or unusual, benign moles which could resemble early melanomas. It is at this point at which some patients may present to their general practitioners or dermatologists for an accurate, early diagnosis. The first growth phase from a dysplastic nevus is called the radial growth phase (RGP), in which the nevus transforms but is still non-tumorigenic without the ability to metastasise. After this stage, vertical growth allows the nevus to become tumorigenic with the potential to metastasise. The final stage of melanoma progression describes the ability of a melanoma to metastasise and invade other tissues. As the stages progress, the patients' prognosis worsens. Models from both Clark (1989), who describes a method to classify the layers of skin to which the melanoma has penetrated and Breslow (1970), who stages melanoma by thickness are referred to when making decisions on melanoma stage for diagnosis. The extent to which the melanoma has progressed through these stages will enable choices to be made on treatment, the risk of re-development of the tumour after treatment and whether a test is required to check for spreading of the tumour to the lymph nodes (Cancer Research UK, 2013). As well as the Clark and Breslow methods, the TNM method, which stands for tumour (T), nodes (N) and metastases (M), is a staging system that describes melanoma progression (Cancer Research UK, 2013). In more detail, it can explain the size of a primary tumour (T), whether the tumour cells have invaded the lymph nodes (N) and whether the melanoma has spread to other areas, known as metastasis (M).

According to Cancer Research UK (2013), most patients diagnosed with melanoma in the UK will have only have a 'T' value. In other words, in the majority of

melanoma patients the tumour will not have begun to spread to either lymph nodes or any other area in the body. Treatment by surgery is the most common in the UK, by which tumours are simply removed without the need for drug intervention. Surgery is usually possible for melanomas that have progressed up to 4mm in thickness, but with no sign of lymph node infiltration or metastasis. In the case of lymph node spread or metastasis, further treatments are required. Currently, these treatments include further surgery to lower the risk of melanoma recurrence, removal of lymph nodes by surgery, chemotherapy, radiotherapy or another biological therapies.

The genetic make-up of a melanoma patient can determine the type of biological therapies available to them. The discovery of *BRAF* mutations in melanoma by Davies and colleagues in 2002 was a standout example of the potential of cancer genome characterisations. Mutations in *BRAF* are found in approximately 50% of melanoma patients, the most common form being V600E, in which valine (V) is substituted for a glutamic acid (E) at position 600 (Davies *et al*., 2002). *BRAF* mutations are also found in melanocytic nevi suggesting that these alterations occur early in the cancer's progression (Pollock *et al*., 2003; Kumar *et al*., 2004). Vemurafenib, a BRAF inhibitor for example, has been shown to shrink tumours in patients with a $BRAF^{V600E}$ mutation and may be a treatment option for those with this particular *BRAF* mutation (Chapman *et al*., 2011). Combined genetics and environmental factors play a role in determining melanoma susceptibility. The heritability of melanoma, i.e. the contribution that genetics plays in melanoma development is estimated to be between 18-55% (Hemminki *et al*., 2001; Shekar *et al*., 2009). The advance in genomic technologies has allowed for a better understanding of the genetic pathways contributing to the disease and hence a shift in the therapeutic options available to patients. Multiple oncogenic pathways that lead to melanomagenesis have been identified (Figure 1.2) and this has opened doors for the development of new therapeutics to treat this disease.

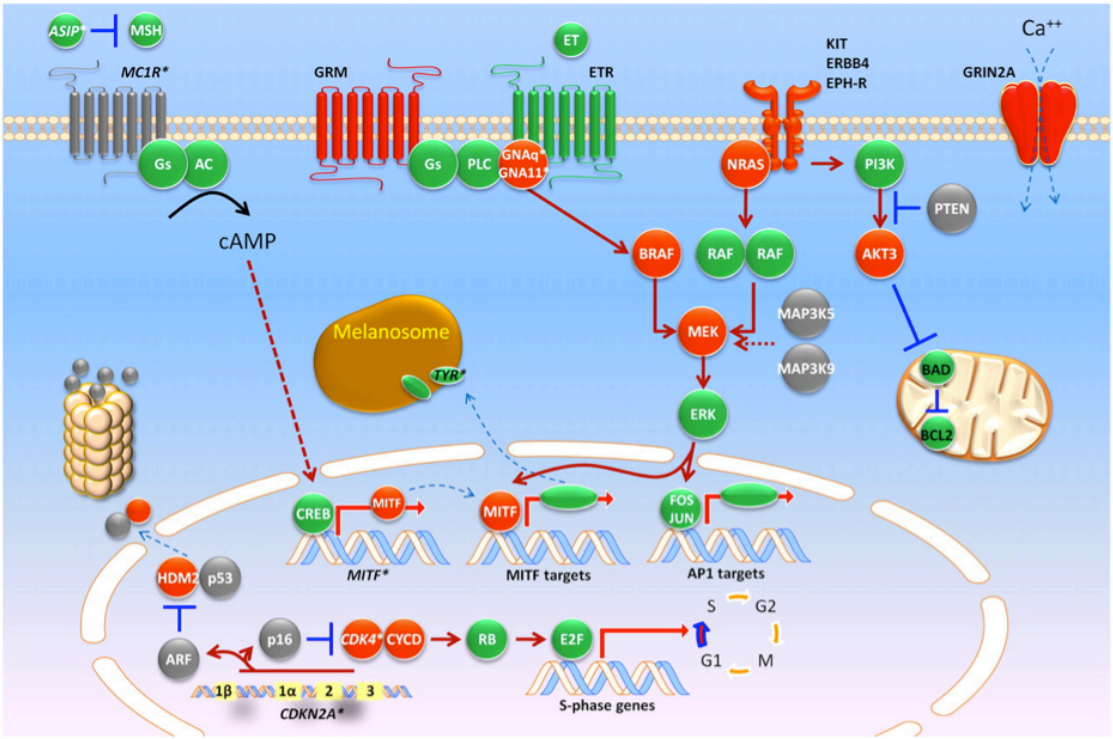

Figure 1.2 Molecular pathways and genes involved in melanoma (Tsao *et al.*, 2012)
Somatic alterations that result in either gain of function (red; e.g. BRAF) or loss of function (grey; e.g. PTEN) and heritable loci with risk alleles or SNPs (italic and with asterisks; e.g. *MC1R**) are shown.

Many of the genetic factors that have been identified through genomic technologies and shown to contribute to melanoma have been shown to act in parallel, although some are mutually exclusive. *NRAS* mutations are found in 15-20% of melanomas and activate RAF kinases in response to growth factor receptor activation (van 't Veer *et al*., 1989). *BRAF* mutations confer RAS-independent activation of the MAPK pathway and therefore it is not surprising that $BRAF^{V600E}$ and *NRAS* mutations are rarely found together. Mutation, deletion or transcriptional silencing of the *CDKN2A* locus causing loss of *p16* expression is also frequent in melanomas and is found to overlap with mutations in $BRAF^{V600E}$ (Daniotti *et al*., 2004). Less common mutations in *CCND1* and *CDK4* are also associated with mutations in $BRAF^{V600E}$ and are mutually exclusive with loss of *p16* (Curtin *et al*., 2005). The most common, recurrent mutations in melanoma have been found to reside within important signaling or developmental pathways that are essential for the survival and proliferation of the melanocyte lineage, for example the MAPK pathway (Flaherty *et al*., 2012). As well as these, there are also examples of lineage-restricted oncogenes, such as *MITF* and *KIT* that are part of pathways that lineage-specific and contribute to the metastatic potential of melanoma. Although metastatic melanoma remains a destructive disease, the identification of the described oncogenes and others and the development of small-molecule inhibitors to target these have provided significant therapeutic benefit to patients.

1.2 Therapeutic strategies for melanoma

'If melanoma is diagnosed early, the survival statistics are very good.'

(Cancer Research UK, 2013).

The current therapeutic strategies available to melanoma patients are dependent on the stage of the disease at the time of presentation. The overall outlook for melanoma patients without spread to either lymph nodes or other parts of the body is positive. In most of these cases, surgery to remove the melanoma is a cure. As the tumour thickness increases and the cancer stages progress over time however, the treatment becomes more difficult and the patient prognosis worsens. Metastatic melanoma is the leading cause of death from skin disease due to its propensity to metastasise from the skin to other areas of the body including the lymph nodes. Most patients diagnosed with melanoma that has acquired the ability to metastasise die within two years. The following facts summarise the current therapeutic strategies undertaken in the UK to treat melanoma patients, as outlined by Cancer Research UK (2013).

Patients with early stage melanoma have tumours less than 2mm thick with no sign of metastasis. The usual procedure in these cases is for doctors to remove the unusual, suspected mole as well as a small area of surrounding tissue by surgery. This is then sent for laboratory analysis for diagnosis. If melanoma is confirmed, the patient will undergo a second surgery to remove further tissue from around the cancerous site. A lymph gland/node check may also be carried out to check for spread of the tumour to these sites, which if positive is a sign that the melanoma has metastasised. Lymph gland metastasis can be carried out by ultrasound, fine needle aspiration or biopsy. If the lymph gland/node test returns negative and the second surgery is successful, the cancer has been cured at the early stage and prognosis is good. Follow up appointments with a doctor will usually take place and any other

changes in moles or tissue around the primary melanoma will be continually monitored. No further treatment is required unless further melanomas develop.

With medium stage melanomas, those which are >2mm thick or >1mm with ulcerations, a similar surgical approach to patients with early stage melanomas is taken. As well as the primary surgery for disease diagnosis, a second surgery will also take place to remove further tissue around the cancer. This is known as wide local excision and is carried out to lower the risk of melanoma developing in the future. A sentinel lymph node biopsy will usually also be carried out to assess the state, if any, of metastasis. This is more likely with tumours that are thicker and have therefore penetrated deeper through layers of the skin. If the nodes are tumour-negative then no cancer cells have reached this area and no further treatment is required. If however, the nodes do contain tumour cells then lymph node dissection, surgical removal of the nodes is required. Adjuvant therapy, the treatment after surgery to prevent recurrence, may also be required and could include chemotherapy, radiotherapy, and/or biological therapy such as interferon therapy. If the melanoma recurs, this can be either at a location nearby the primary melanoma that was removed (locoregional melanoma) or another site. The prognosis is better for locoregional melanoma, but again surgery and further treatment is required to remove the melanoma and reduce the risk of recurrence. If the tumour arises at a location in an area away from the initial site of trauma this is categorised as stage four melanoma. This is the final, most dangerous stage at which a patient can be diagnosed.

Advanced melanoma occurs when a tumour recurs at a different area of the body after initial surgery and treatment of an initial melanoma. The most common areas that melanomas spread to are the lungs, liver, bone, brain, abdomen and lymph nodes. The treatment options for this late stage cancer are dependent on the location of the melanoma, a patient's symptoms and the previous treatment that was used to treat the primary melanoma. Any treatment choice, from further surgery to intensive chemo- or radio- therapy, will not cure the disease but hopes to prolong the patient's

lifetime by causing tumour shrinkage or halting its proliferation. The side effects that the therapies cause must be taken into account and be balanced with their ability to control the melanoma growth and increase patient survival time. Clinical trials are also available as an option for advanced stage melanoma patients. These may combine chemotherapy with new biological therapeutics with the aim of identifying the best treatments for advanced stage melanomas.

The biological therapies available to medium and advanced stage melanoma patients vary greatly. Until recently, interferon therapy was the only therapeutic that showed positive results in both relapse-free survival (RFS) and overall survival (OS) of melanoma patients (Mitchell *et al*., 2007). The benefits of interferon treatment, although positive, were minor – a 5-10% increase in RFS and 2-5% increase in OS (Hauschild, 2009). A breakthrough in therapy for more advanced stage melanoma patients came in 2011 with the approval of ipilimumab and vemurafenib. Ipilimumab targets immune checkpoints, while vemurafenib inhibits mutated oncoproteins and both are proving promising clinical approaches to treatment for advanced stages of this disease.

Ipilimumab is a monoclonal antibody that blocks the cytotoxic T-lymphocyte antigen-4 (CTLA-4) pathway from inhibiting T cell activation. The US Food and Drug Administration (FDA) approved it for the treatment of metastatic melanoma in 2011 and clinical trials have shown overall survival benefit for patients compared to other treatment options (Acharya and Jeter, 2013). Use of ipilimumab simply stimulates a patient's own immune response, which is important to destroy cancerous cells. Clinical trial results have shown that around 30% of patients who are administered ipilimumab will have a beneficial long-term outcome (Hodi *et al*., 2010). Positive results when taking the drug include shrinkage of melanocytic lesions and a reduction in the total number of tumours. Side effects when using ipilimumab are also observed however, including immune-mediated adverse reactions (Weber, 2007) and therefore further trials and possible combined therapeutic studies are

required for the maintenance of the benefits of this drug for metastatic melanoma patients.

Also in 2011, there was further hope for metastatic melanoma patients when Plexxikon and Genentech developed the BRAF inhibitor vemurafenib. For patients harbouring the V600E activating mutation in *BRAF*, known to be found in ~60%, vemurafenib was shown to yield a positive response in more than 50% of patients (Chapman *et al*., 2011). Vemurafenib is a selective inhibitor of BRAF and its development follows the failure of another drug, sorafenib, which was developed as a broad-spectrum tyrosine and serine-threonine kinase inhibitor. The inhibitory action of sorafenib targeted BRAF, CRAF, PDGFR, VEGFR2, p38 and CKIT and was the first RAF-inhibitor to be trialled in melanoma patients (Wilhelm *et al*., 2006). It failed to elicit a response in the clinical trials however, as either a single agent or combination therapy, due to its inability to adequately inhibit the MAPK pathway. Due to the failure of sorafenib, more potent and selective inhibitors of BRAF were developed, including the successful vemurafenib. Treatment with vemurafenib reduces the levels of pERK by >80% in $BRAF^{V600E}$ mutant tumours and correlates with a clinical response (Bollag *et al*., 2010). Importantly, inhibition of the MAPK pathway by vemurafenib is specific only to tumour cells harbouring the *BRAF* mutation, as other cells maintain this signalling pathway through CRAF.

Despite the impressive clinical activity of vemurafenib in $BRAF^{V600E}$ mutant melanomas, the drug elicited many common side effects including fatigue and nausea. As well as these side effects, more than a quarter of patients treated with vemurafenib developed cutaneous squamous cell carcinomas (cSCC) and 60% of these tumours harboured *HRAS* mutations (Su *et al*., 2012). One mechanism for the promotion of tumourigenesis in a different cell type through targeted therapy is thought to be that while MAPK signaling is blocked in $BRAF^{V600E}$-mutant cells, the RAF inhibitors increase MAPK signaling in either mutated or activated RAS cells (Oberholzer *et al*., 2012). RAS activation in cutaneous cell populations interacts with RAF inhibition therapy to promote cell proliferation and can therefore result in the

development of cSCCs, suggesting that formation of these tumours is caused by a 'pro-proliferative interaction between RAF inhibitors and latent RAS mutant keratinocytes' (Oberholzer *et al*., 2012). This finding highlights the need to identify strategies to prevent secondary tumour development that occurs as a result of inhibitor treatments for melanoma. As well as this, strategies to overcome resistance to these inhibitors must also be addressed. Although BRAF inhibitor therapy has been shown to produce tumour response in most patients, these are largely partial and evidence of clinical tumour resistance usually occurs between 5-7 months.

The clinical benefits of BRAF inhibitors have been limited by both de novo (pre-existing) and acquired resistance mechanisms. The presence of de novo resistance mechanisms has been revealed by the 10% of melanoma patients who do not observe a response after drug treatment and in which tumour progression continues (Chapman *et al*., 2011; Hauschild *et al*., 2012). As well as this 10%, another 30% of melanoma patients given BRAF inhibitor treatment will achieve only a minor response, characterized by less than 25% reduction in tumour size, and only 5% will achieve complete response (Chapman *et al*., 2011; Hauschild *et al*., 2012). This heterogeneity towards BRAF inhibitors supports the presence of pre-existing molecular characteristics that determine patient response. Of the remainder of patients that achieve a positive response to BRAF inhibitors, the majority (80-90%) will develop acquired resistance within 12 months of treatment, leading to progression of melanoma. Many mechanisms of the resistance to BRAF inhibitors have been identified and broadly either reactivate the MAPK pathway or activate other proliferative or pro-survival pathways (Bucheit and Davies, 2014). To reactivate the MAPK pathway, alterations in both BRAF itself and other components not involving BRAF have been identified. Both aberrant splicing of *BRAF* (Poulikakos *et al*., 2011) and a gain in copy number of *BRAF* (Shi *et al*., 2012) have been observed in melanomas that progressed after an initial response to BRAF inhibitors. An increased BRAF inhibitor dosage was able to overcome resistance acquired due to the gain in copy number of *BRAF* but not when due to aberrant splicing (Poulikakos *et al*., 2011; Shi *et al*., 2012). Alterations of other components

of the RAS/RAF/MEK/ERK signaling pathway have also been observed during resistance and act to reactivate the MAPK pathway. Activating *NRAS* mutations are found in 20% of tumours after BRAF inhibitor resistance (Nazarian *et al*., 2010) an unexpected result as *BRAF* and *NRAS* mutations are usually mutually exclusive in untreated melanomas. Secondary mutations in *MEK1* have also been shown to emerge as a result of BRAF inhibition and result in resistance (Emery *et al*., 2009; Wagle *et al*., 2011). Overexpression of COT kinase, which directly phosphorylates MEK and/or ERK, has also been shown to assist reactivation of the MAPK pathway through its regulation of MEK and ERK downstream of BRAF (Johannessen *et al*., 2010). Lastly, resistance mechanisms have been shown to utilize BRAF heterodimers that use RAF isoforms, ARAF and CRAF, instead of BRAF, hence supporting reactivation of the pathway (Villanueva *et al*., 2010).

In addition to reactivation of the MAPK pathway, other mechanisms of BRAF inhibitor resistance have included activation of the PI3K-AKT pathway. This signaling pathway, which is activated genetically by many of the common somatic alterations observed in cancer including activating point mutations of *PIK3CA*, gene amplification of *HER2* and loss of function mutations of negative regulators of the pathway including *Pten,* plays key roles in proliferation, growth and survival and is commonly activated in tumours. Loss of PTEN function has been observed in tumours resistant to BRAF inhibitors, suggesting that this mechanism is associated with resistance. PTEN negatively regulates the PI3K-AKT pathway and in multiple tumour types loss of PTEN correlates with activation of AKT, a critical effector of the pathway. Loss of PTEN is found in 10-30% of human melanomas (Wu *et al*., 2003) and frequently associated with BRAF activating mutations. BRAF inhibitors cause apoptosis in BRAF mutant tumours with normal PTEN function, whereas BRAF mutant tumours with PTEN loss are resistant to apoptosis (Paraiso *et al*., 2011). As well as PTEN loss, receptor tyrosine kinases (RTKs) that activate the PI3K-AKT pathway have also been shown to be involved in BRAF inhibitor resistance. The increased expression of two RTKs, PDGFβR and IGF1R, blocked apoptosis through increased PI3K-AKT activation (Nazarian *et al*., 2010; Villanueva *et al*., 2010) and hence acted as a resistance mechanism. Activation of the PI3K-AKT pathway is also regulated by the tumour microenvironment, specifically by

non-malignant cells within the stroma that produce hepatocyte growth factor (HGF). Production of HGF induces resistance through activation of the PI3K-AKT pathway (Straussman *et al*., 2012).

The majority of resistance mechanisms stem from reactivation of downstream factors of BRAF within the MAPK pathway and therefore to overcome this resistance, a combinational treatment targeting BRAF and its targets is required. Combination treatments with inhibitors of MEK and ERK have been useful in an attempt to overcome most of the acquired resistance mechanisms. Dual BRAF and MEK inhibition using dabrafenib and trametinib for example, significantly improved progression-free survival in $BRAF^{V600E}$ melanomas compared to monotherapy (76% compared to 54%) (Flaherty *et al*., 2012). As well as improved survival, addition of the MEK inhibitor also reduced the development of cSCCs compared to monotherapy (7% compared to 19%) (Flaherty *et al*., 2012) suggesting that the paradoxical activation of the MAPK pathway described was blocked.

1.3 Zebrafish as a model of melanoma

One of the earliest animal models of melanoma was developed in the freshwater fish, *Xiphophorus* (Anders *et al*., 1984; Schartl *et al*., 1985). First recognised in the 1920s, the *Xiphophorus* hybrid melanoma model was utilised by Schartl and colleagues to discover that overexpression of the *xmrk* oncogene in pigment cells is the primary change that results in the formation of malignant melanoma (Schartl *et al*., 1999). *Xmrk* is a duplicate of an orthologue of the mammalian epidermal growth factor receptor gene *EGFR* (Meierjohann *et al*., 2004). This discovery established the use of this model system to identify novel genetic modifiers of nevi and melanoma phenotypes.

Despite the opportunities to study melanoma provided by the *Xiphophorus* model, 'for genome-wide genetic screens and dissecting the mechanisms of melanocyte development and melanoma progression, the zebrafish and medaka model fish systems offer distinct advantages' (Patton and Nairn, 2010). One main advantage that these species offer over the *Xiphophorus* is their ability to fertilise embryos externally. This feature allows visualisation and analysis of embryo development, as well as the ability to carry out chemical and genetic screens *in vivo*. Additionally, pairs can be bred and provide hundreds of embryos every week, offering a more high throughput approach to experiments.

The zebrafish in particular has become a good disease model for melanoma. In addition to the advantages of external embryo fertilisation and high offspring numbers, the genomic resources available and the shared tissue, organ and molecular pathways with humans allow scientific studies to be carried out in relation to human disease. As well as melanoma, other human cancers can be modelled in zebrafish and one well established example is liver cancer. The Gong laboratory has been central in developing zebrafish liver cancer models and recently showed that these share

molecular signatures with human hepatocellular carcinoma (HCC) (Zheng *et al*., 2014). Three oncogene transgenic zebrafish lines with inducible expression of *xmrk*, *kras* or *Myc* in the liver were generated and each tumour signature showed significant correlation with human HCC (Zheng *et al*., 2014). Together, the three models represented almost half (47.2%) of human HCCs, which makes them valuable tools for molecular classification of human HCCs and understanding molecular drivers of hepatocarcinogenesis of different subtypes (Zheng *et al*., 2014).

Our understanding of zebrafish genetics has progressed rapidly in the last 10-15 years. The first vertebrate genome to be sequenced, after the human was a large marine fish known as *fugu*. This was carried out using the whole-genome shotgun method and completed in 2002 (Aparicio *et al*., 2002). In 2001, the Sanger Institute began to sequence the zebrafish genome. They initiated the sequencing of the Tübingen strain as the reference genome, as this was previously used to identify mutations that affected embryogenesis. To carry out the sequencing they used a clone-by-clone approach, a similar technique to that used to sequence both the mouse and human genomes. The most recent version of the sequenced genome, Zv9, is available online. It shows that zebrafish have more than 26,000 protein-coding genes, and that interestingly, they have more species-specific genes than any other previously sequenced vertebrate (Howe *et al*., 2013). By comparing zebrafish and human protein-coding genes, Howe and colleagues find that more than 70% of human genes have at least one zebrafish orthologue and equally, 69% of zebrafish genes also have at least one human orthologue (Howe *et al*., 2013). Access to an annotated, fully sequenced zebrafish genome has enabled scientists to make valuable discoveries. These include the ‘positional cloning of hundreds of genes from mutations affecting embryogenesis, behaviour, physiology, and health and disease’ and the ‘generation of accurate whole-exome enrichment reagents, which are accelerating both positional cloning projects and new genome-wide mutation discovery efforts’ (Howe *et al*., 2013).

The zebrafish genome is now well understood, owing to the high-throughput sequencing projects and widely available. Within the zebrafish field there are a range of techniques that have been developed to manipulate the genome in an attempt to model human disease. Importantly for this project, many techniques have been developed to generate zebrafish cancer models, including melanoma. These include forward and reverse genetic screens, chemical treatments and transplantation of mammalian cells.

Traditionally, forward genetic approaches such as chemical and insertional mutagenesis screens have been used to generate zebrafish disease models. This has allowed for the identification of a large range of mutants with disruption of conserved genes that correlate with human disease loci. Almost two decades ago, the Nusslein-Volhard laboratory carried out the first mutagenesis screens in zebrafish (Mullins *et al*., 1994). Since then, screens for almost all phenotypes, including cancer, have been carried out. In 2004, Amsterdam and colleagues published a screen carried out for embryonic lethality, which by chance identified cancer-related genes. They used retroviral insertions to carry out the screen for embryonic lethality but noticed that heterozygous founders showed an increased tumour incidence. Eleven of the twelve lines with increased tumour incidence carried insertions in ribosomal genes, while the other was mutated in one of the two zebrafish homologues of neurofibromatosis 2 (*nf2*), a human tumour suppressor gene (Amsterdam *et al*., 2004). This example shows that forward genetic screens are suitable for use in the zebrafish and can provide important information that can directly relate to human disease and importantly human cancer. Another example is provided by research from the Zon laboratory. Here, another zebrafish forward genetic screen was used to identify a number of cell proliferation mutants including *crb*, which represents a loss-of-function mutation in *bmyb*, a transcriptional regulator and part of a putative proto-oncogene family (Shepard *et al*., 2005). The *crb* heterozygous mutants have increased cancer susceptibility, demonstrating that loss of function of *bmyb* can be associated with cancer and that similar zebrafish screens are useful in uncovering cancer pathways (Shepard *et al*., 2005).

Reverse genetic approaches, including morpholino and mRNA injection have also resulted in the development of zebrafish disease models. These are both techniques used to either transiently knock down or overexpress a disease gene. In order to create a stable zebrafish mutant, a technique called target-selected mutagenesis or TILLING can be used. This technique, first described in 2000 for mutation detection in *Arabidopsis* (McCallum *et al*., 2000) combines standard ENU mutagenesis with gene targeting. The TILLING method involves the formation of DNA heteroduplexes during PCR amplification and the subsequent separation of these DNA strands by size using techniques such as high-performance liquid chromatography (HPLC). Targeted-selected mutagenesis was first used in the zebrafish system in 2004 (Wienholds and Plasterk, 2004) and since then several zebrafish mutants, including those for known human tumour suppressors have been generated. An example of the use of reverse genetics in the zebrafish to create a tumour model is that of *tp53*, one of the most frequently mutated genes in human cancer. The $tp53^{M214K}$ zebrafish mutant contains a missense mutation in the DNA-binding domain of the gene and 28% of mutants develop tumours by 14 months of age (Berghmans *et al*., 2005). All but one of these tumours were shown to be malignant peripheral nerve sheath tumours (MPNSTs), the other was found to be a melanoma. The $tp53^{M214K}$ zebrafish mutant is a good example of how reverse genetic techniques can be used to study human disease in this model organism.

The forward and reverse genetic techniques described showcase the ability to manipulate the zebrafish genome and model human disease. As well as this, the now fully sequenced zebrafish genome also allows high-throughput sequencing projects of zebrafish tissues, including cancers and those from phenotypic mutants to be carried out (Howe *et al*., 2013). The mapping of sequencing reads, from transcriptome, exome or whole genome to an annotated reference genome allows the detection of mutations and other variants. As the human and zebrafish genomes show a high degree of conservation, relationships between genes and pathways identified in the zebrafish can be translated to a human context. During this project, the latest version of the zebrafish genome, Zv9 (Howe *et al*., 2013) has enabled high

confidence mapping of RNA-seq reads and the sequential analysis of the transcriptome data by bioinformatics. For this reason, the comprehensive genetics that are known today and our ability to utilise these makes the zebrafish an ideal animal model to work with as an aid to understand human disease.

Similar to the high conservation between the human and zebrafish genomes identified through sequencing projects, the tissues, organs and molecular pathways of these two organisms are found to share many characteristics (Zon, 1999). This, in addition to the genetics is another advantage of the zebrafish as a model organism for which to study human disease.

Importantly for this project, melanocytes are found in both humans and zebrafish and perform similar functions. In humans, melanocytes are the pigment-producing cells that colour the hair, skin and eyes and play an important role in protecting the skin from the harmful effects of UV radiation. When they are stimulated by UV radiation, human melanocytes produce melanin that is then distributed to surrounding epidermal cells as a form of protection. In zebrafish, melanocytes are one of three pigment cell types that pigment the body and make up their characteristic stripe pattern. Zebrafish melanocyte development is highly conserved with other vertebrates, including humans and therefore our understanding of human melanocytes can be improved by studying this cell type in the zebrafish. The main difference between human and zebrafish melanocytes is that unlike humans, zebrafish do not distribute melanin from their cells, but rather move it around within melanocytes during background adaptation. Distinguishing melanocytes that cluster to form nevi and those that have progressed to melanoma can be carried out by observation (Figure 1.3). Nevi are simple clusters of melanocytes that lie within the epidermal layer but do not have the capacity to protrude either through this or the underlying dermal layer and tissues (Figure 1.3A,B). Tumours are made up of densely packed melanoma cells (black) that can be seen forming nodules and invading underlying tissues (Figure 1.3C).

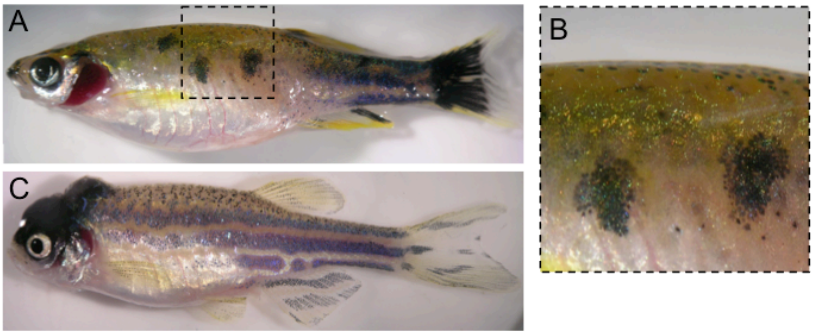

Figure 1.3 Observing zebrafish nevi and tumours.
A. Distinct clusters of melanocytes on body of zebrafish represent nevi. B. Close up of nevi (A), which remain flat and do not invade underlying dermal layers. C. Tumour shown on head region protrudes through epidermis to become nodular and disrupts underlying dermal layer and tissues.

1.4 Melanoma cancer gene discovery

Our understanding of zebrafish genetics has improved greatly due to high-throughput sequencing projects such as those carried out at the Sanger Institute, Hinxton by Howe and colleagues (2013). These and other projects have been key to further identification of important genes and biological pathways involved in melanoma and this in turn has led to the development of better therapeutic strategies for melanoma patients.

Melanoma is a complex disease influenced by many genetic and environmental factors and it has therefore been a challenge to understand its development and improve therapeutics. The classical melanoma genes known are *BRAF*, *NRAS* and those coded by the *CDKNA2* locus, *p14* and *p16*. The mutational burden of commonly altered genes *BRAF* and *RAS* is responsible for approximately 70% of melanoma progression. Over the last 10 years, our understanding of the roles of these classical genes, as well as the discovery of novel genes that contribute to melanoma development has been greatly improved using new techniques in DNA sequencing.

In 2007, Greenman and colleagues described one of the first projects using deep-sequencing methods on a large scale covering the whole genome. In this study 210 human cancers, including melanomas were sequenced and the results found over 1000 somatic mutations in 274Mb of DNA corresponding to the coding exons of over 500 protein kinase genes (Greenman *et al*., 2007). An average of 18.54 mutations/Mb were found in melanoma cell lines and of these more than 90% (of a total of 144) were shown to be C to T transitions, which is a typical UV signature (Greenman *et al*., 2007).

In parallel to the Greenman study, Pleasance and colleagues (2010) provided the first comprehensive catalogue of somatic mutations from an individual cancer, using the whole genome of a melanoma cell line and lymphoblastoid cell line from the same patient. They identified over 33,000 somatic mutations including 292 somatic base substitutions in protein-coding sequences, of which 187 were non-synonymous mutations leading to amino acid changes (Pleasance *et al*., 2010). Similar to the Greenman study (2007), about 75% of the total number of mutations were found to be C to T mutations, again indicating their association with UV exposure. The group also noticed that there was an 'uneven distribution of mutations across the genome, with a lower prevalence in gene footprints' (Pleasance *et al*., 2010), suggesting that the DNA repair mechanisms were used preferentially in transcribed regions. In conjunction with the results from Greenman and colleagues (2007), this study highlights the power of the cancer genome sequence in our understanding of the processes of cancer development.

More recently, Berger and colleagues (2012) advanced the use of sequencing technologies to understand cancer genome signatures by using metastatic melanoma samples and tumours from different areas of body mass. In agreement with both Greenman (2007) and Pleasance (2010), this study found an elevated mutational rate and a UV-associated signature in melanomas. Analysis of melanomas from different areas of the body, including acral and trunk, also provided information on differences in mutational rate and C to T substitution number between melanoma subtypes. One of the most interesting findings from the whole-genome sequence data was the identification of *PREX2* as a new, recurrently mutated gene in melanoma (Berger *et al*., 2012). *PREX2* mutations were found at a frequency of 14% (15/107) in non-synonymous mutations and functional analysis of these mutations showed that overexpression of *PREX2* accelerates tumourigenicity (Berger *et al*., 2012). This suggests that some melanoma cells could gain oncogenic activity through *PREX2* mutations and that it could be a novel therapeutic target.

As well as whole genome sequencing described by the Greenman, Pleasance and Berger studies, exome sequencing has also been beneficial in identifying novel genes involved in melanoma development. One study by Nikolauv and colleagues in 2011 carried out exome sequencing of seven melanoma cell lines with donor-matched germline cells and, like the whole genome sequencing studies described previously, showed that all samples had a high number of somatic mutations and showed a hallmark of UV-induced DNA repair (Nikolauv *et al*., 2011). The study also identified recurrent somatic *MAP2K1* and *MAP2K2* (*MEK1* and *MEK2* respectively) mutations in the melanoma samples and new potentially candidate genes *FAT1*, *LRP1B* and *DSC1* (Nikolauv *et al*., 2011). A separate exome-sequencing project in 2011 by Stark and colleagues used eight metastatic melanoma samples and found new somatic mutations in *MAP3K5* and *MAP3K9*, both members of the MAPK pathway. Both mutations resulted in a decrease in the kinase activity of the proteins as well as a reduction in the level of phosphorylated MEK-ERK and JNK, which are both pathways involved in apoptosis, differentiation, survival and senescence (Stark *et al*., 2011). A third exome-sequencing project carried out by Krauthammer and colleagues (2012) used a much higher sample size, a total of 147 melanomas, and were able to identify new cancer genes including *PPP6C* and a recurrent UV-signature in the *RAC1* gene. An activating mutation in *RAC1* was identified in 9.2% of sun-exposed melanomas and through functional studies they were able to show that this alteration promoted melanocyte proliferation and migration (Krauthammer *et al*., 2012). RAC1 had previously been shown to play an important role in melanoblast migration, cytokinesis and cell cycle progression during normal development (Li *et al*., 2011), which are suggestive of its role within melanoma.

Although both whole genome and exome sequencing efforts have identified many mutations in melanoma, most of these can be categorised as ‘passenger’ mutations, those that do not contribute to cancer development but have occurred during its growth phase. The challenge proposed therefore was to be able to distinguish this type of mutations from ‘driver’ mutations, those that push cells towards cancer and are critical for its development. In 2012, Hodis and colleagues presented data that

could overcome this problem by sequencing both the exons and introns of melanoma samples and comparing their frequency to identify positively selected genes. They were able to identify six novel melanoma genes, *PPP6C, RAC1, SNX31, TACC1, STK19 and ARID2,* as well as provide an insight into *BRAF* and *NRAS*-driven melanomas and those that are independent of *BRAF/NRAS* mutations (Hodis *et al*., 2012).

1.5 Motivation

The motivation for this body of work lies in the statistics of increasing melanoma incidence, particularly in young females in the UK, and the deficit of successful drug treatments currently available for these patients. With most of the basic scientific research and therapeutic developments presently focused on *BRAF* and other MAPK pathway inhibition strategies, I felt it was essential to broaden our understanding of other important genes and pathways that play key roles in melanomagenesis. Through research and improved understanding of genes such as *MITF*, it is hoped that novel or combination therapeutics will be developed and lead to more successful outcomes for melanoma patients.

Chapter 2 – *MITF* is a cancer gene

Chapter 2: *MITF* is a cancer gene

In this first results chapter, I describe the genetics that I have used to identify *MITF* as a cooperating mutation with $BRAF^{V600E}$ in zebrafish to drive melanomagenesis. I will introduce the role of *MITF* in development, human disease and cancer and then outline the importance of the $BRAF^{V600E}$ $mitfa^{vc7}$ zebrafish as an *in vivo* cancer model.

With the $BRAF^{V600E}p53^{M214K}$ mutant already established as a melanoma model (Patton *et al*., 2005), I (in collaboration with J.A. Lister) describe how $BRAF^{V600E}$ cooperates with a mutation in *mitf* (Johnson *et al*., 2011) to promote melanoma. I also describe a new model of melanoma that is independent of a *BRAF* mutation, in $mitfa^{vc7}p53^{M214K}$ zebrafish.

2.1 Introduction

2.1.1 The role of MITF in development

Named the 'master' melanocyte regulator, MITF is one of the key transcription factors in regulating melanocyte development and is essential for melanocyte cell survival (McGill *et al*., 2002; Levy *et al*., 2006; Arnheiter, H., 2010). The gene is encoded by the microphthalmia locus and expressed in developing neural crest-derived melanocyte precursors and the neuroepithelium-derived retinal pigmented epithelium (RPE). With multiple target genes and an essential role in melanocyte development and cell survival, MITF is also important in cellular processes including proliferation, differentiation and cell cycle progression.

In a comprehensive review by Steingrímsson and colleagues (2004), the authors describe four key experiments that highlight the importance of *MITF* as a determinant of melanocyte development. In the first experiment, Tachibana and colleagues showed that by ectopically expressing *MITF* they were able to transform fibroblasts into cells with characteristics of melanocytes (Tachibana *et al*., 1996). The transformed cells were dendritic and expressed melanocyte-specific marker genes including tyrosinase and tyrosinase-related protein 1, which indicated that *MITF* is involved in melanocyte differentiation (Tachibana *et al*., 1996). In the second experiment, Planque and colleagues investigated the role of *Mitf* in cell proliferation and pigmentation by transfecting mouse *Mitf* cDNA into chicken neuroretinal cells (Planque *et al*., 1999). They showed that the transfected cells quickly became pigmented and expressed QNR-71 mRNA, which encodes a melanosomal protein, both of which indicated that *Mitf* could transdifferentiate neural cells into pigment cells (Planque *et al*., 1999). In the third experiment, Lister and colleagues identified a new mutation in the zebrafish neural crest that affected pigment cell fate (Lister *et al*., 1999). *Nacre* zebrafish mutants carry a mutation in

the zebrafish *mitf* gene and are unable to develop melanophores, however this pigmentation phenotype can be rescued by injecting wild-type *mitf* into early-stage embryos (Lister *et al*., 1999). In the last set of experiments, Béjar and colleagues showed that *mitf* expression is sufficient for the 'differentiation of medaka pluripotent stem cells into melanocytes' (Béjar *et al*., 2003). By expressing *mitf* in medaka ES-like cells, they induced fully differentiated pigment cells (Béjar *et al*., 2003). Together, these four experiments using four different species – human, chicken, zebrafish and medaka – suggest that *Mitf* functions as the master regulator of melanocyte development in vertebrates and is a determinant of melanocyte differentiation (Steingrímsson *et al*., 2004).

In addition to these four species, the mouse model has also played an important part in understanding the role of *Mitf* in melanocyte development. Melanocyte precursors arise from neural crest progenitor cells (NCPCs) and are dependent on *Mitf* for their survival and migration from the neural tube (Hornyak *et al*., 2001). The maintenance of melanocyte stem cells (MSC), a self-renewing population of melanocytes found in the bulge region of hair follicles in the mouse (Nishimura *et al*., 2002), is also dependent on MITF activity. In an *Mitf* mouse mutant, loss of MITF causes a premature loss of MSCs and results in premature hair greying (Nishimura *et al*., 2005). The maintenance of these MSCs by MITF prevents physiological hair greying, which is part of the aging process developed through loss of the differentiated progeny (Nishimura *et al*., 2005).

During development and throughout adulthood, the expression of *Mitf* is highly regulated. Its expression is first observed in 22-somite-stage embryos within the optic vesicle of the developing eye (Nguyen and Arnheiter, 2000). Later, its expression is limited to the RPE, before being expressed in cells with neural crest characteristics, firstly in the head and later towards the tail region (Nakayama *et al*., 1998). These mitf-positive cells were presumed to be neural crest-derived melanoblasts as their location, expression markers and number all fit with this description (Steingrímsson *et al*., 2004). As well as embryos, *Mitf* expression has been explored in adult tissues from both mouse and human. In adults, as well as in

melanocytes and melanoma cells, MITF protein is expressed in osteoclasts (Weilbaecher *et al*., 1998) and mast cells (King *et al*., 2002). Although mutations in *Mitf* have been identified in all four of these mitf-positive cell types, none have been found in mouse heart or skeletal muscle, although *Mitf* expression has also been shown to be present in these tissues (Hodgkinson *et al*., 1993).

Mitf mouse mutants display a range of distinctive defects including loss of pigmentation leading to a white phenotype, reduced eye size compared to wild-type, early onset deafness, failure of secondary bone resorption and a reduced number of mast cells (Hodgkinson *et al*., 1993). MITF (and its human counterpart) is a structure containing a basic helix-loop-helix-leucine zipper (bHLH-LZ) that is essential for DNA binding and dimerization. It consists of 419 amino acids and shares more than 90% identity with human MITF (Tachibana *et al*., 1994). MITF consists of at least nine isoforms that differ in their amino termini including MITF-A, MITF-B, MITF-C, MITF-H and MITF-M (Amae *et al*., 1998). The *Mitf* gene itself consists of at least four promoters, their consecutive first exons (1A, 1H, 1B and 1M) and eight downstream exons that are common to all isoforms (Udono *et al*., 2000). The different promoters generate transcriptional diversity while the different isoforms themselves provide functional diversity (Shibahara *et al*., 2001).

The zebrafish has two mitf genes, namely *mitfa* and *mitfb*, which occur as a result of a gene duplication event. *mitfa* is essential for the development and specification of all neural-crest derived melanocytes, while *mitfb* is responsible for development of melanocytes in the retinal pigment epithelium (RPE) (Lister *et al*., 2001). *mitfa* was the first *mitf* gene to be identified in zebrafish and shares the most similarity with the mouse neural crest-specific *Mitf-M* isoform. *mitfb* shares greater similarity to Mitf isoforms present in the mouse RPE, especially in the amino terminal region (Lister *et al*., 2001). Conservation between both *Mitf* gene structure and function in humans, mice and zebrafish has been shown ((Steingrímsson *et al*., 2004) with mutations affecting the development of neural crest-derived pigment cells and those in the RPE of the eye.

2.1.2 MITF mutations in human disease

In humans, there is a single *MITF* gene located at chromosome 3p14.1, encompassing 229kb and 9 exons. There are 9 isoforms (A, B, C, D, E, H, J, M and MC) each of which has its' own 5' specificity and have exons 2-9 in common. Exon 1, in which the transactivation domain (TAD) and basic helix-loop-helix-leucine zipper (bHLH-LZ) are found, varies between isoforms. Some isoforms are cell type-specific, such as MITF-M and –MC, which are only found in melanocytes and mast cells respectively (Steingrímsson *et al*., 2004).

In 1994, Tassabeliji and colleagues identified mutations in *MITF* that caused Waardenburg Syndrome type 2 (WS2), an autosomal dominant inherited condition that causes hearing loss and abnormal pigmentation of the eyes, hair and skin. Prior to this identification, the mouse microphthalmia mutant was suggested as a possible candidate homologue of some forms of WS, as all *mi* mutant mice have no or reduced pigmentation in their eyes and coat, as well as a no or small eye phenotype (Asher and Friedman, 1990). By screening WS2 patients for mutations in *MITF*, Tassabeliji and colleagues identified mutations in two WS2 families that affected the splice sites of *MITF* (Tassabeliji *et al*., 1994).

Tietz syndrome patients, similar to those with WS2, suffer from profound deafness and generalised hypopigmentation (Tietz, 1963). In 2000, Smith and colleagues re-ascertained the original family reported with these features described by Tietz (1963). From these family members with Tietz syndrome, Smith identified a missense mutation in the basic region of the *MITF* gene (Smith *et al*., 2000). Amiel and colleagues also found this mutation in another family of Tietz syndrome (Amiel *et al*., 1998).

Interestingly, *in vitro* studies show that the mutant mitf protein predicted by the Tietz syndrome mutation has a dominant-negative effect, whereas the proteins predicted for the mutations in WS2 do not (Nobukuni *et al*., 1996; Tachibana, 1997) As both conditions are autosomal dominant, the symptoms of each occur in patients that are heterozygous, with one copy of the wild-type gene and one copy carrying the mutation. In Tietz syndrome, the mutant mitf protein is thought to interfere with the normal mitf protein causing a depletion of mitf function and a failure in the development of melanocytes (Tachibana, 2000). In contrast, the mutant mitf protein in WS2 patients does not have a dominant-negative effect and so although the mitf protein is present, its level is not sufficient to allow the full development of melanocytes (Nobukuni *et al*., 1996; Tachibana, 1997). The variation in levels of functioning mitf protein in WS2 patients explains the variation in the severity of symptoms observed in the patients (Tachibana, 2000).

As MITF has been shown to play a multifaceted role in supporting differentiation, proliferation and cell death of normal melanocytes (White and Zon, 2008) this suggests that changes in MITF signalling could support melanoma formation. In addition to the amplification of *MITF* in 10-20% of melanoma cases (Garraway *et al*., 2005) in 2009, Cronin and colleagues identified somatic *MITF* mutations in metastatic melanoma cell lines. By sequencing 13 *MITF* exons that encompass the full coding sequences of all *MITF* isoforms and comparing tumour to patient-matched normal DNA, they found six changes including four non-synonymous point mutations and one splice-site alteration (Cronin *et al*., 2009). These mutations, shown in Figure 2.1, were located in the regions encoding the transactivation, DNA binding or basic-helix-loop helix domains, and interestingly, were found to occur in a mutually exclusive pattern to *MITF* amplifications. More recently, a SUMOylation *MITF* mutation ($MITF^{E318K}$) that associated with melanomagenesis was identified by two separate studies (Yokoyama *et al*., 2011; Bertolotto *et al*., 2011) and shown to affect the activation domain of *MITF* (Figure 2.1). In total, seven *MITF* mutations have been identified in melanoma cell lines or patient samples and it is estimated that

20% of metastatic melanoma cases have alterations in the MITF pathway, through MITF itself or its downstream targets (Cronin *et al*., 2009).

Recently, a study of 24 human MITF mutations in WS2, TS and melanoma patients has revealed how mutations in a single gene, MITF, can lead to such great variation in disease phenotype (Grill *et al*., 2013). In a graphical representation of the human MITF protein, Figure 2.1 shows the locations of these mutations causing both melanoma (red) and WS2 or TS (blue) in patients. The research in this paper characterised the DNA-binding and transcription activation properties of different MITF mutations found in these two pigment deficiency syndromes and melanoma. Eleven of 18 WS2 and TS mutations were found within the bHLH-LZ domains of MITF where they fail to bind DNA and are unable to activate melanocyte-specific promoters (Grill *et al*., 2013). The remaining seven mutations had normal or reduced DNA-binding and transcription activity. In contrast, MITF mutations in melanoma were found in the amino- and carboxyl domains of MITF where they were able to bind DNA at a level similar to wild-type MITF. These mutations affect the transactivation potential of MITF however and hence it was concluded that the structural location of these MITF mutations identified in melanoma plays an important role in both transactivation and oncogenic potentials of MITF (Grill *et al*., 2013).

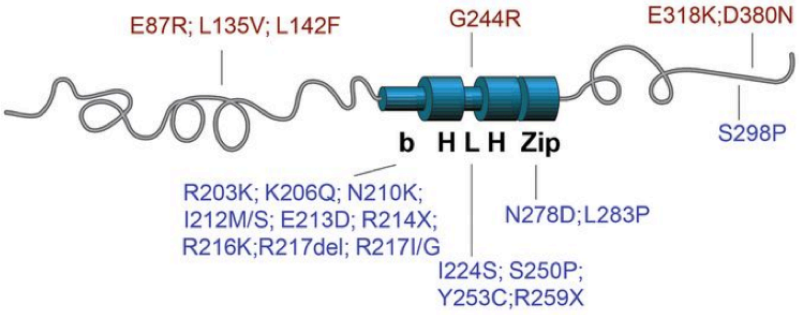

Figure 2.1 Structure of the human MITF protein and the locations of identified mutations (Grill *et al*., 2013)
The protein has a basic helix-loop-helix leucine zipper (bHLHZip) structure. Mutations found in melanoma patients are shown in red, with all apart from one (G244R) at the amino- and carboxyl- ends. Mutations found in Waardenburg syndrome type 2 (WS2) and Tietz syndrome (TS) patients are shown in blue, with most in the basic (b), helix-loop-helix (HLH) and leucine zipper (Zip) regions of the protein.

2.1.3 The role of MITF in cancer

Since 1999, anti-MITF antibodies have been used as sensitive and specific markers for malignant melanoma histologic specimens (King *et al*., 1999) suggesting that MITF could play an oncogenic role in melanoma. In the first study by King and colleagues, 100% (76/76) of human melanomas stained positively for MITF in the nucleus, in some cases where the most commonly used markers of melanoma, HMB-45 and S-100, had failed (King *et al*., 1999). Human melanoma black (HMB)-45 is a monoclonal antibody that recognises melanosomal glycoprotein gp100 (Pmel17) (Gown *et al*., 1986), whereas S-100 is an acidic protein. Although both have previously been shown to be markers of melanoma, other more specific markers have been superior in diagnosis of melanoma micrometastases (Shidham *et al*., 2001). In the study by King and colleagues using non-melanoma samples, no nuclear staining of MITF was observed (0/60) although 2 (2/60) samples showed cytoplasmic staining (King *et al*., 1999). The two samples with positive MITF cytoplasmic staining were derived from breast cancer specimens. As MITF is normally expressed in both osteoclasts and mast cells and many breast cancers are known to express genes involved in bone resorption, it was suggested that the expression of MITF may play a role in bone metastasis of breast cancer and be a predictor of osteotrophic tumours (King *et al*., 1999). In a second study by Dorvault and colleagues (2001), 81 cell blocks from patients with both melanoma and non-melanoma tumours were immunostained with a monoclonal antibody against mitf (D5). They found that 100% of melanomas (44/44) stained positively for MITF and only one (1/37) non-melanoma malignancy showed mitf staining, which was rare (<10%) and weak (Dorvault *et al*., 2001). In contrast to the 100% sensitivity staining of malignant melanomas with MITF, staining with two current standard melanoma markers, HMB-45 antigen and S-100 protein was not as specific (Dorvault *et al*., 2001). In a third study, Sheffield and colleagues used the same anti-MITF antibody to stain 72 melanoma and non-melanoma malignant neoplasms, alongside antibodies S-100, HMB-45, Melan-A and tyrosinase (Sheffield *et al*., 2002). Similar to Dorvault and

colleagues (2001), they found that MITF stained 100% (40/40) of melanomas and only one non-melanocytic tumour. In addition, they used a combination of anti-MITF and anti-Melan-A staining to show that this was the most sensitive and specific tool, with 100% of melanomas and no non-melanocytic tumours stained using this method (Sheffield *et al*., 2002). Taken together, the results from King, Dorvault and Sheffield confirm that MITF is a sensitive and specific marker for malignant melanoma in histologic sections and superior to the current markers used for diagnosis (King *et al*., 1999; Dorvault *et al*., 2001; Sheffield *et al*., 2002).

In 2005, Garraway and colleagues used high-density SNP arrays to investigate chromosomal alterations in human cancer cell lines and their results reinforced an oncogenic role for *MITF* in human melanoma. They combined SNP array-based genetic maps and gene expression signatures to identify *MITF* as the target of a novel melanoma amplification. They identified six out of eight melanoma cell lines from the NCI60 tumour cell lines containing a region of amplification on chromosome 3p and *MITF* was the only highly expressed gene to be found within this amplified region (Garraway *et al*., 2005). They also examined human tumours and found that while no benign moles harboured this amplification, 10% of primary melanomas and 21% of metastatic melanomas did, indicating an association between *MITF* amplification and the ability to metastasise. In metastatic melanomas, the amplification was associated with a decreased 5-year survival, implicating an association between the amplification and lethality. The identification of the genomic amplification of *MITF* also suggested that the melanocyte lineage dependency on *MITF* might be maintained in melanoma cells. Garraway and colleagues tested this theory by introducing an adenovirus that expressed a dominant-negative *MITF* mutant (*Ad-dnMITF*) into NCI60 melanoma cell lines with varying levels of *MITF* amplification. They found that the *Ad-dnMITF*, as well as a knockdown of *MITF* using short hairpin (sh) RNAs resulted in growth inhibition of the melanoma cells. This suggests that deregulation of *MITF* through amplification or other mechanisms may preserve a critical lineage survival function in melanoma (Garraway *et al*., 2005).

As Garraway and colleagues discovered the *MITF* oncogenic amplification in human melanomas, also in 2005 Wellbrock and Marais confirmed interplay between MITF and BRAF (Wellbrock and Marais, 2005). They showed that in melanocytes, MITF expression is suppressed by oncogenic BRAF and if re-expressed in BRAF-transformed melanocytes, proliferation is inhibited. In melanoma cells, they showed that low levels of MITF were present with oncogenic BRAF, but that if MITF expression is increased by differentiation-inducing factors, proliferation is inhibited. Together, the data suggested that the down-regulation of MITF by BRAF signalling is crucial for progression of oncogenic BRAF melanomas and that MITF may play an anti-proliferative role in melanoma (Wellbrock and Marais, 2005).

The study by Garraway and colleagues that identified a novel amplification of *MITF* in between 10-20% of human melanomas, suggesting that *MITF* could act as a dominant oncogene, is in contrast to data from both Carreira (2005) and Loercher (2005). Their data shows that MITF regulation of *p21*, a cell cycle gene, and mutations of melanoma-associated genes that would lower the transcriptional activity of *MITF* could remove its control of the cell cycle (Carreira *et al*., 2005; Loercher *et al*., 2005). An explanation for these contrasting results came from Hoek and colleagues (2006), whose data provided a model for the metastatic potential of melanomas that is defined by a specific gene expression profile (Hoek *et al*., 2006). This study carried out three separate microarray analyses on 86 cultures of melanoma. In contrast to previous studies, which identified correlations between gene expression and activating mutations in *BRAF* or *NRAS*, Hoek and colleagues showed through multiple testing correction that there was no relationship between gene expression pattern and a mutation in these two MAPK pathway genes. Instead, they were able to identify three distinct sample groups that represented differing degrees of melanoma metastatic potential and were regulated by changes in Wnt and TGF-β signalling (Hoek *et al*., 2006). Their gene regulation model for melanoma metastatic potential describes two different phenotypes driven by different signalling pathways and defined by individual patterns of gene regulation. The first are highly proliferative cells with weak metastatic potential, which maintain a neural crest-like

signature through Wnt signalling. The second are weakly proliferative cells with high metastatic potential that are driven by TGF-β signalling, which activates a positive feedback loop, changes the extracellular environment and inhibits Wnt signalling. With respect to MITF, this model describes how low levels of MITF drive an invasive and more metastatic phenotype, while high levels of MITF drive a more proliferative but less metastatic phenotype (Hoek *et al*., 2006). As melanoma cells are known to be a heterogeneous population (Fidler, 1978) driven by environmental factors (Postovit *et al*., 2006), the rheostat model also predicts that levels of MITF could drive phenotypic switching between the different states, as described by Hoek and Goding (2010).

As the evidence presented so far implicated a central role for *MITF* in melanoma progression and somatic mutations are relevant to the progression of cancer, in 2009 Cronin and colleagues sequenced melanoma tumour DNA to assess whether *MITF* was somatically mutated in melanoma (Cronin *et al*., 2009). They compared sequences of *MITF* from primary and metastatic melanomas to patient-matched normal DNA. Out of 50 metastatic melanoma tumour lines, they identified 4 with genomic amplifications of *MITF* and 4 with *MITF* mutations in regions encoding transactivation, DNA binding and basic, helix-loop-helix domains (8/50, 16%) (Cronin *et al*., 2009). As they had found *MITF* mutations in the 50 samples analysed, they hypothesised that other *MITF* pathway genes may also be altered in the melanoma samples. One of these genes, *SOX10*, is a transcription factor found upstream of *MITF* and is known to synergise with *MITF* in transactivation of *DCT* and *TYR*. Cronin and colleagues found three mutations in *SOX10* in the same 50 metastatic samples, but showed that *MITF* and *SOX10* were mutated in a mutually exclusive fashion, confirming disruption of a common genetic pathway (Cronin *et al*., 2009). As well as metastatic tumours, they also evaluated whether somatic mutations in *MITF* and *SOX10* were present in primary melanoma samples. They identified 2 *MITF* mutations in 26 primary samples (7.7%) and 6 *SOX10* mutations in 5 of 55 primary samples (9%), none of which were observed in a control panel of lymphocyte DNA, suggesting that these mutations arose somatically. None of the

primary lesions contained amplifications, hinting that *MITF* amplification may only occur in the later stages of melanoma development. Overall, the study successfully identified both non-synonymous mutations and amplifications with frequencies of 13.2% in *MITF* and 8.6% in *SOX10* in primary and metastatic melanomas, emphasising the involvement of the *MITF* signalling pathway in melanomagenesis (Cronin *et al*., 2009).

As described, *MITF* is amplified in some melanomas and its ectopic expression has been shown to cooperate with $BRAF^{V600E}$ to transform both human melanocytes and neural crest cells (Garraway *et al*., 2005, Kumar *et al*., 2013). Recently, Kumar and colleagues showed that *MITF* cooperates with $BRAF^{V600E}$ to increase the proliferative capacity of human neural crest progenitor cells (hNCPCs) and that overexpression of *MITF* in these cells increases tumorigenicity, resulting in fully transformed tumour cells (Kumar *et al*., 2013).

Although the identification of amplifications and somatic mutations of *MITF* in human melanoma samples provided good evidence that the *MITF* signalling pathway played an important role in melanomagenesis, as yet very few mutations have been linked to familial melanoma. The two most established, but rare, high-penetrance genes for melanoma are *CDKN2A* and *CDK4* (Hussussian *et al*., 1994; Liu *et al*., 1995; Zuo *et al*., 1996). Since the discovery of these two high-risk alleles, only other more common, moderate- or low-penetrant genes have been associated with melanoma. At the end of 2011 however, two papers were published simultaneously that showed the discovery of an *MITF* mutation in melanoma patients (Bertolotto *et al*., 2011, Yokoyama *et al*., 2011). The identified germline SUMOylation E318K mutation is a melanoma risk factor and confers differential gene expression of *MITF* target genes. Patients carrying the mutation have a five-fold increased risk of developing melanoma, as well as an increased risk of developing renal cell carcinoma (RCC) (Bertolotto *et al*., 2011). The mutation identified occurs in a small-ubiquitin-like modifier (SUMO) consensus site and impairs the ability of MITF to be SUMOylated (Bertolotto *et al*., 2011). SUMOylation is a post-translational

modification that determines transcriptional activity and stability. The E318K mutation of *MITF* enhances its protein binding ability to the *HIF1A* promoter and in turn increases its transcriptional activity compared to wild type controls. The mutant MITF protein enhances melanocyte and renal cell clonagenicity, migration and invasion, which is consistent with a gain-of-function role for MITF in both melanoma and RCC. Two studies using different populations, from Italy and Queensland, Australia, also identified carriers of the E318K mutation of *MITF* (Ghiorzo *et al*., 2013; Sturm *et al*., 2014) and support the finding that *MITF* is a medium-penetrance melanoma gene.

Despite our improved understanding of melanoma genetics in recent years, one outstanding problem in the field is the identification of novel driver mutations, owing to the high number of passenger mutations, which are caused by UV exposure. To address this problem, Hodis and colleagues analysed whole exome sequencing data from over 120 melanoma tumour and normal pairs and used an approach that 'infers positive selection at each gene locus based on exon/intron mutational distributions, as well as the predicted functional impact of each mutation' (Hodis *et al*., 2012). This allowed them to 'control for passenger mutational load on a per gene basis' and in doing so they were able to identify six new melanoma genes, three of which harboured functional, potentially targetable mutations, as well as driver mutations that were directly attributable to UV exposure (Hodis *et al*., 2012). The study also included an analysis of somatic copy number aberration profiles, allowing them to confirm expected melanoma alteration including gains of *MITF*.

The importance of MITF and its role in the melanocyte lineage during melanoma MAPK pathway inhibitor resistance was recently highlighted. Although RAF and MEK inhibitors have shown clinical efficacy in $BRAF^{V600E}$ mutant melanomas (Flaherty *et al*., 2012), resistance to these agents still poses a challenge. Johannessen and colleagues discovered that a cyclic-AMP-dependent melanocytic signalling network was associated with this drug resistance and was also conferred through expression of downstream transcription factors of both the MAPK and cAMP

pathways, including *MITF* (Johannessen *et al*., 2013). Using a combination of MAPK and histone-deacetylase (HDAC) inhibitors (the latter of which impairs *MITF* expression) they could suppress both *MITF* expression and cAMP-mediated resistance. Their results 'support a model in which aberrant signalling from melanocyte lineage pathways may converge on *MITF* or other transcription factors to drive resistance to MAPK pathway inhibitors' (Johannessen *et al*., 2013). This suggests that the addition of HDAC inhibitors in combination with RAF-MEK inhibition may be a novel therapeutic strategy to successfully control the growth of some $BRAF^{V600E}$ melanomas and overcome resistance.

In relation to my research, an important study was carried out in 2011 showing that *MITF* is required to coordinate differentiation with cell cycle arrest (Taylor *et al*., 2011). Using a transgenic zebrafish *mitf* model, they identified a subpopulation of differentiated melanocytes that arose through cell division. These were separate from those that are derived from undifferentiated precursor cells, the primary mechanism that results in the adult melanocyte population of developing adults (Parichy, 2003; Yang and Johnson, 2006). Although *MITF* is known to control both differentiation and cell cycle progression in melanocytes (Levy and Fisher, 2011), the effect of MITF levels in differentiated cells had not been studied in an animal model as MITF first affects specification and survival. Taylor and colleagues found, using the temperature-sensitive $mitfa^{vc7}$ model, that *mitfa* hypomorphic melanocytes underwent serial differentiated cell divisions (Taylor *et al*., 2011). In other experiments using the $mitfa^{vc7}$ model, they were able to show that the human melanoma $MITF^{4T\Delta 2B}$ mutation (Cronin *et al*., 2009) could stimulate cell division and differentiation in melanocytes. This result 'underscores the importance of MITF anti-proliferative activity *in vivo*' (Taylor *et al*., 2011).

The temperature-sensitive $mitfa^{vc7}$ zebrafish model utilised by Taylor and colleagues (2011) and described above was successfully used throughout my research as a tool to manipulate mitf activity and further our understanding of the role of mitf in melanomagenesis. The $mitfa^{vc7}$ allele is a 'mutation in a splice donor site that reduces

the level of correctly-spliced transcripts' and was first identified through an ENU-mutagenesis screen (Johnson *et al*., 2011). The *vc7* mutation is found in the intron 6 splice donor site and results in various alternative transcripts, all with a preserved reading frame (Figure 2.2). The predominant transcript is a product that extends through intron 6 to exon 7, introducing 39 amino acids within the basic region (Figure 2.2B). Two minor transcripts are also produced as a result of the *vc7* mutation – one correctly spliced and of the correct size, suggesting that the mutation does not completely abrogate splicing, and one that skips exon 6 and leaves a truncated basic region (Figure 2.2B) (Johnson *et al*., 2011). These alternative spliced transcripts are not functionally active and therefore allow regulation of MITF activity to study its role *in vivo*.

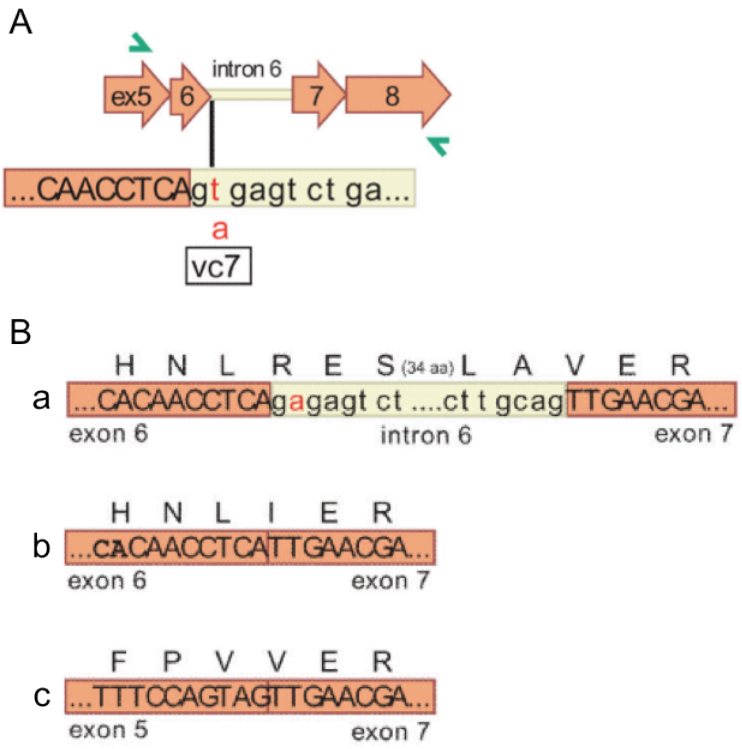

Figure 2.2 The mitfa^{vc7} allele affects splicing of mitfa (adapted from Johnson *et al.*, 2011)
A. The *vc7* mutation, a t>a substitution (red), is located at the intron 6 splice donor site.
B. The reading frames of 3 alternative transcripts as a result of the *vc7* mutation: predominant translation product extends through intron 6 and continues into exon 7, preserving the correct reading frame and introducing 39 amino acids in the middle of the basic region (a); minor product of the correct size with proper splicing (b); minor product with skipping of exon 6, which preserves reading frame but truncates basic protein (c).

2.2 Results

2.2.1 BRAF^{V600E} cooperating mutations drive melanomagenesis

BRAF^{V600E} cooperates with p53 to induce melanoma in zebrafish

In 2005, Patton and colleagues described the role of *BRAF* in nevi and melanoma in the zebrafish. They generated a transgenic zebrafish that expressed the most common *BRAF* mutation, V600E, under the control of the melanocyte *mitfa* promoter (Patton *et al*., 2005). Expression of this mutant, in contrast to wild-type (Figure 2.3A), led to a cloak-like clustering of melanocytes on the surface of the skin, which obscures the stripe patterning (Figure 2.3B). When *mitfa-BRAF^{V600E}* was injected into zebrafish embryos harbouring a homozygous missense mutation in exon 7 of the *zp53* gene (*zp53^{M214K}*) the activated *BRAF* induced melanocytic lesions that progressed to invasive tumours and closely resembled human melanomas (Patton *et al*., 2005). The key result from this significant paper was that *BRAF* activation is sufficient for nevi formation, but that a cooperating mutation, for example in *p53*, is required to induce melanoma (Patton *et al*., 2005). I replicated this experiment by crossing *BRAF^{V600E}* homozygote mutants to *p53^{M214K}* homozygote mutants to give *BRAF$^{V600E/+}$p53$^{M214K/+}$* transgenic zebrafish. This generation of heterozygous zebrafish mutants were then incrossed to create double homozygote *BRAF$^{V600E/V600E}$ p53$^{M214K/M214K}$* transgenic zebrafish (Figure 2.3C). These fish are grown at a stable temperature of 28°C in the aquatic system and develop nevi and melanoma.

Although mutations and deletions of *TP53* are found in approximately 50% of human cancers, they are less common in melanomas (0-10%) (Box and Terzian, 2008). Mouse models expressing a melanocyte-specific activated HRAS allele on a p53-null background provided initial evidence for p53 inactivation during

melanomagenesis (Bardeesy *et al*., 2001) and more recently, an epithelial-like subtype of melanoma was identified in which p53 inactivation was significantly more frequent than first described (Shields *et al*., 2007). In 2009, Yu and colleagues identified a subpopulation of *BRAF*^{V600E} mutant melanocytes in which oncogene-induced senescence had been bypassed. The additional disruption of p53 immortalizes these cells and leads to a transformed cell phenotype both *in vitro* and *in vivo* (Yu *et al*., 2009). This data supports a tumour suppressor role for p53 in melanoma and, similar to the *BRAF*$^{V600E/V600E}$ *p53*$^{M214K/M214K}$ transgenic zebrafish, identifies the cooperation of alterations in these genes to promote melanoma.

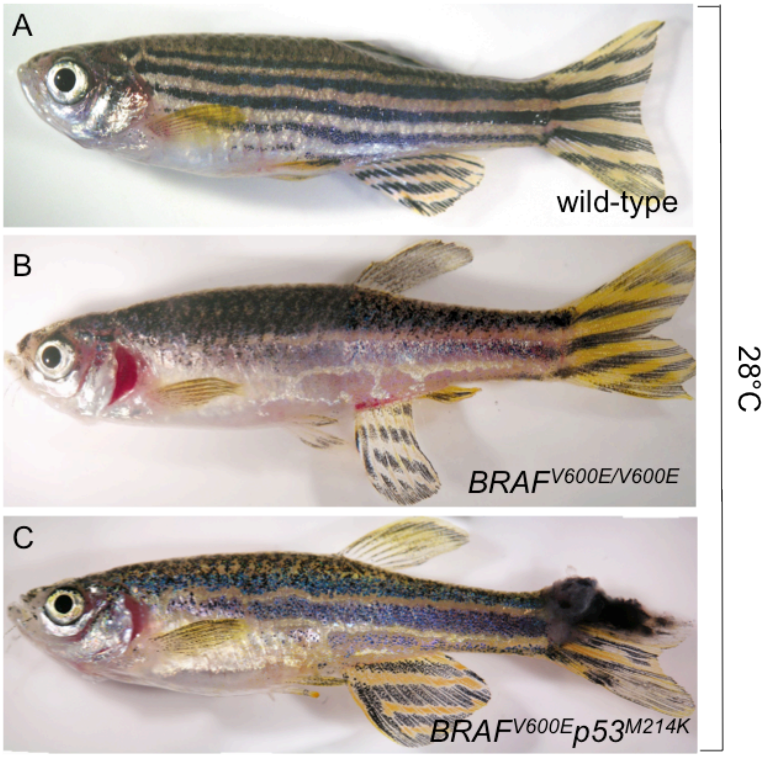

Figure 2.3 Adult wild-type (A), mutant *BRAF*$^{V600E/V600E}$ (B) and *BRAF*$^{V600E/V600E}$*p53*$^{M214K/M214K}$ zebrafish (C) raised at 28°C. *BRAF*$^{V600E/V600E}$ mutants display a cloak-like clustering of melanocytes disturbing normal stripe patterning. *BRAF*^{V600E}*p53*^{M214K} zebrafish develop melanoma, here show at the tail fin region.

BRAF^{V600E} cooperates with mitfa to induce melanoma in zebrafish

I used the hypomorphic temperature-sensitive *mitfa* mutant, *mitfa^{vc7}*, to study the role of *mitf* in melanoma and test its function as a cancer gene in the zebrafish. The main advantage of the temperature-sensitive *mitfa^{vc7}* mutant is that we can alter the *mitf* activity by simply changing the temperature of the water. At high, restrictive temperatures of 32°C *mitf* activity is too low to allow normal development of melanocytes and both the embryos and adult appear non-pigmented or white in colour. At lower temperatures of 28°C, levels of *mitf* activity is still insufficient to promote the development of melanocytes and both embryos and adults appear white. At even lower temperatures <26°C, *mitf* activity is sufficient for some body melanocytes to develop, which are observable in embryos and adults grown at this temperature. To illustrate the temperature-sensitive activity of the *mitfa^{vc7}* allele, wild- type and mutant *mitfa^{vc7}* embryos were grown at different temperatures to 48hpf (or until stage-matched) and the melanocyte development was observed (Figure 2.4). The number of melanocytes able to develop at each temperature varied as the *mitf* activity was altered by temperature. At 24°C, *mitfa^{vc7}* mutant embryos develop similar numbers of melanocytes to wild-type embryos. Increasing temperature to 26°C reduces *mitf* activity and the number of melanocytes able to develop in embryos is reduced. At both 28°C and 32°C, *mitf* levels are insufficient to allow development of any melanocytes and so the embryo appears white.

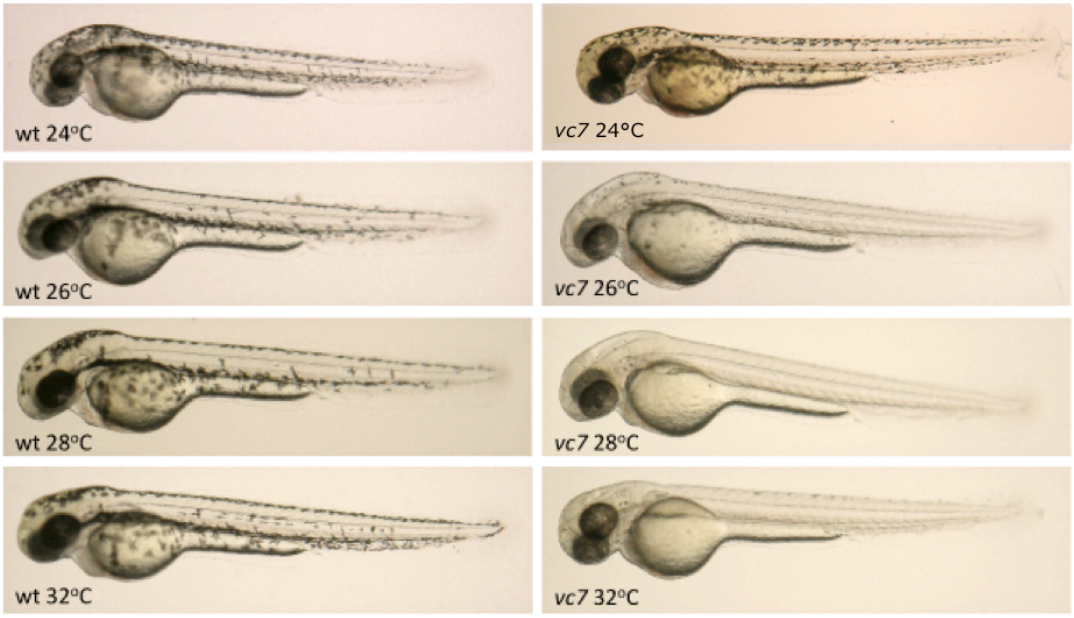

Figure 2.4
Melanocyte development in wild-type (left) and *mitfa*^{vc7} (right) in 48hpf stage-matched embryos grown at temperatures between 24-32°C.

In collaboration with J.A. Lister, I crossed the *mitfa*^{vc7} mutants with the *BRAF*^{V600E} mutants. I hypothesised that at temperatures at which *mitf* was sufficient to allow melanocyte development, but not cell cycle arrest (Taylor *et al*., 2011) it would cooperate with *BRAF*^{V600E} to promote melanomagenesis. I found that *BRAF*$^{V600E/V600E}$ *mitfa*$^{vc7/vc7}$ zebrafish grown at the permissive temperatures below 26°C, at which melanocytes are able to develop normally, developed melanocytic tumours (Figure 2.5).

Figure 2.5 Adult *BRAF*^{V600E}*p53*^{M214K} (A) zebrafish raised at 28°C and *BRAF*^{V600E}*mitfa*^{vc7} zebrafish (B) raised at <26°C develop melanocytic tumours.

2.2.2 The mitfa allele in tumour samples

To confirm that the *mitfa*^{vc7} allele was present in the *BRAF*^{V600E} *mitfa*^{vc7} melanomas, I carried out an RT-PCR using RNA prepared from four *BRAF*^{V600E} *mitfa*^{vc7} tumour samples. To act as controls, I repeated the RT-PCR experiment using RNA prepared from a wild-type adult, an *mitfa*^{vc7} mutant embryo grown at 28°C and four *BRAF*$^{V600E/V600E}$ *p53*$^{M214K/M214K}$ tumour samples. From this experiment I could confirm that the *mitfa*^{vc7} mutant allele was present in all four of the *BRAF*^{V600E} *mitfa*^{vc7} melanomas tested as it produced the same molecular weight band on an agarose gel as the RT-PCR product from the *mitfa*^{vc7} mutant embryo grown at 28°C (Figure 2.6). In contrast, a wild-type *mitf* band was found in the four *BRAF*$^{V600E/V600E}$ *p53*$^{M214K/M214K}$ tumour samples and corresponded to the same molecular weight band as the wild-type sample. These results confirm that the *mitfa*^{vc7} allele is present in the *BRAF*^{V600E} *mitfa*^{vc7} melanomas as expected.

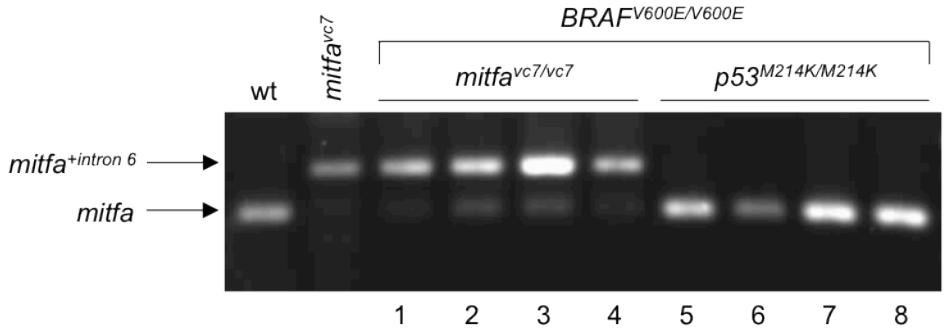

Figure 2.6 RT-PCR analysis of the *mitfa* transcript in *BRAF*^{V600E}*mitfa*^{vc7} and *BRAF*^{V600E}*p53*^{M214K} melanomas.

2.2.3 Incidence of zebrafish melanoma

By counting the number of fish that developed tumours from a single genetic background, I could quantitate the incidence of melanoma. Collecting tumour numbers from other genotypes, as well as recording the age of tumour occurrence allows for a comparison of tumour incidence between different genetic backgrounds.

After collating tumour incidence data for both *BRAF*^{V600E}*mitfa*^{vc7} and *BRAF*^{V600E}*p53*^{M214K} zebrafish, I compared both the age of onset and frequency of tumours in these genetic backgrounds. Eighteen tumours were observed and collected from a total of 67 *BRAF*^{V600E} *mitfa*^{vc7} zebrafish (18/67), while 48 tumours were observed from a total of 177 *BRAF*^{V600E}*p53*^{M214K} zebrafish (48/177). Converting these numbers into percentage gives an overall tumour incidence of 26.9% for *BRAF*^{V600E}*mitfa*^{vc7} zebrafish and 27.1% for *BRAF*^{V600E}*p53*^{M214K} zebrafish (Table 1). The similar percentages calculated indicate that the tumour incidence in *BRAF*^{V600E}*mitf* and *BRAF*^{V600E}*p53*^{M214K} zebrafish is similar. Both genetic backgrounds were also similar in the age of tumour onset. In both *BRAF*^{V600E}*mitfa*^{vc7} and *BRAF*^{V600E}*p53*^{M214K} zebrafish, tumours first occurred between 4-5 months of age and continued to present up to one year old. Median tumour onset was calculated for each melanoma subtype, with *BRAF*^{V600E}*p53*^{M214K} zebrafish showing an earlier median age of onset at 10 months than *BRAF*^{V600E}*mitfa*^{vc7} zebrafish, which showed a median tumour onset of 12 months (Table 1). To compare the tumour incidence between *BRAF*^{V600E} *mitfa*^{vc7} and *BRAF*^{V600E}*p53*^{M214K} zebrafish a log-rank test was used. This analysis tests the null hypothesis that there is no difference between these two genotypes in the probability of developing a tumour at any age and is based on the age in months at which the tumour develops. For each month, I calculated the observed number of tumours in each genotype and the number expected if there were no difference between genotypes. For example, the first melanomas to develop were observed at 5 months of age, at which point one tumour was observed in the

BRAF^{V600E}*p53*^{M214K} population and four tumours were observed in the *BRAF*^{V600E}*mitfa*^{vc7} population. In total, there were 66 tumours that developed between the two populations, so the risk of developing a tumour at 5 months was 5/66 (0.0758). There were a total of 18 tumours that developed in the *BRAF*^{V600E}*mitfa*^{vc7} background so if the null hypothesis were true the expected number of tumours developing at this stage is 1.364 (18*0.0758). Similarly, there were a total of 48 tumours that developed in the *BRAF*^{V600E}*p53*^{M214K} background, so if the null hypothesis were true, the expected number of tumours developing at this stage is 3.636 (48*0.0758). The same calculations were carried out for 5-18 months until the experiment was ended. From these, the total numbers of expected melanomas were 22.16 in the *BRAF*^{V600E}*mitfa*^{vc7} background and 44.84 in the *BRAF*^{V600E}*p53*^{M214K} background. To then test the null hypothesis, $X^2 = \Sigma\ (O\text{-}E)^2/E$, where O and E are the total numbers of observed and expected tumours respectively, is calculated. In this case, $((18\text{-}22.16)^2/22.16 + (48\text{-}44.84)^2/44.84) = 1.167$. The degrees of freedom (*DF*) are the number of groups (genetic backgrounds) compared minus one, i.e. 2-1=1 (*DF*=1). The p-value is found by referring the outcome of the log rank test (1.167) to a X^2 distribution with 1 degree of freedom. By calculating this, the p-value given is 0.280019 (>0.05) and therefore the difference in tumour incidence between *BRAF*^{V600E} *mitfa*^{vc7} and *BRAF*^{V600E}*p53*^{M214K} genetic backgrounds is not statistically significant.

Tumour incidence and age of onset for both *BRAF*^{V600E}*mitfa*^{vc7} and *BRAF*^{V600E}*p53*^{M214K} zebrafish are displayed graphically in Figure 2.7. As opposed to the incidence of tumours within a population, the percentage of tumour-free individuals is presented as a variable on the y-axis. This allows the data to be clearly interpreted as tumour incidence can be correlated with age and the percentage of tumour incidence from both genetic backgrounds shown.

Table 1 Tumour incidence and median onset of distinct zebrafish melanoma subtypes

Genotype	Median tumour onset (months)	Observed tumour incidence	Expected tumour incidence	Overall tumour incidence (%)
$BRAF^{V600E/V600E}mitfa^{vc7/vc7}$	12	18	22.16	26.87
$BRAF^{V600E/V600E}p53^{M214K/M214K}$	10	48	44.84	27.12
$BRAF^{V600E/V600E}mitfa^{vc7/vc7}p53^{M214K/M214K}$	7	31	23.96	100
$BRAF^{V600E/V600E}mitfa^{vc7/vc7}p53^{M214K/wt}$	6	49	49.04	100
$mitfa^{vc7/vc7}p53^{M214K/M214K}$	10	94	28.25	72.9

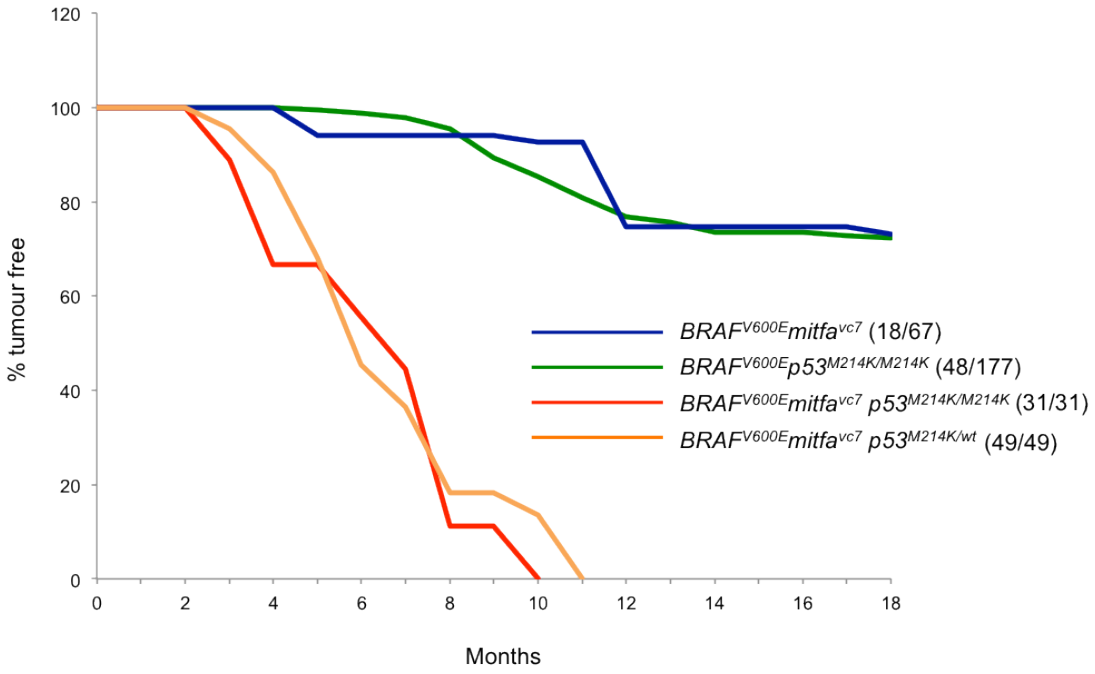

Figure 2.7 Melanoma incidence curves of $BRAF^{V600E}mitfa^{vc7}$, $BRAF^{V600E}p53^{M214K}$ and $BRAF^{V600E}$ $mitfa^{vc7}$ $p53^{M214K}$ genetic crosses at <26°C.

2.2.4 Zebrafish mutants of BRAF, mitfa and p53

One question I asked after we confirmed that both *mitfa*^{vc7} and *p53* could cooperate with *BRAF*^{V600E} to promote melanoma was if a triple zebrafish mutant, with mutations in *BRAF*, *MITF* and *p53*, would cooperate to induce melanoma with increased incidence. To create a zebrafish transgenic containing mutations in all three genes I crossed *BRAF*^{V600E} *mitfa*^{vc7} mutants with the *p53*^{M214K} mutant fish. This genetic cross resulted in mutant fish with heterozygous mutations in *BRAF*, *MITF* and *p53*, so these were then incrossed to achieve homozygous mutants.

A *BRAF*^{V600E}*mitfa*^{vc7}*p53*^{M214K} zebrafish mutant (Figure 2.8) developed both nevi and melanoma when grown at temperatures between 24-28°C, which are hypomorphic for levels of *mitf* activity. Melanomas from this transgenic line could be observed from 3 months and occurred more frequently than both *BRAF*^{V600E}*mitfa*^{vc7} and *BRAF*^{V600E}*p53*^{M214K} double mutants (Figure 2.7). I observed tumour incidence in both *BRAF*^{V600E}*mitfa*^{vc7}*p53*$^{M214K/M214K}$ and *BRAF*^{V600E}*mitfa*^{vc7}*p53*$^{M214K/wt}$ mutants, in which the only difference is the homozygous vs. heterozygous *p53* mutation. To assess whether the difference in *p53* mutation affected tumour incidence I carried out the log-rank test, with the null hypothesis that there is no difference in incidences between these two genetic backgrounds. I found no significant difference between tumour incidence in zebrafish with *p53* homozygous and heterozygous mutations ($p=0.150$).

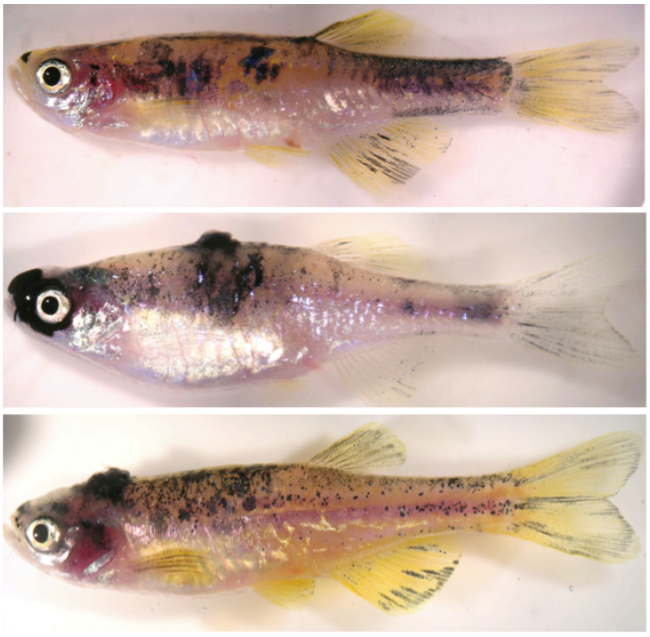

Figure 2.8 Triple mutant zebrafish with mutations in *BRAF*^{V600E}, *mitfa*^{vc7} and *p53*^{M214K} develop melanoma.

2.2.5 A BRAF – independent melanoma model

mitfa^{vc7} cooperates with p53^{M214K} to induce melanoma in zebrafish

One experiment that evolved from a genetic cross in the fish facility has proved to be fruitful in our understanding of the importance of MITF in BRAF-independent melanoma progression. Zebrafish with homozygous mutations in both *mitfa^{vc7}* and *p53^{M214K}*, but lacking a *BRAF^{V600E}* mutation, develop melanomas at 28°C (Figure 2.9). As controls, neither *mitfa^{vc7}* or *p53^{M214K}* mutants develop melanomas, although two *mitfa$^{vc7/vc7}$* mutants develop nevi and seven *p53$^{M214K/M214K}$* mutants develop malignant peripheral nerve sheath tumours (MPNSTs) (not shown).

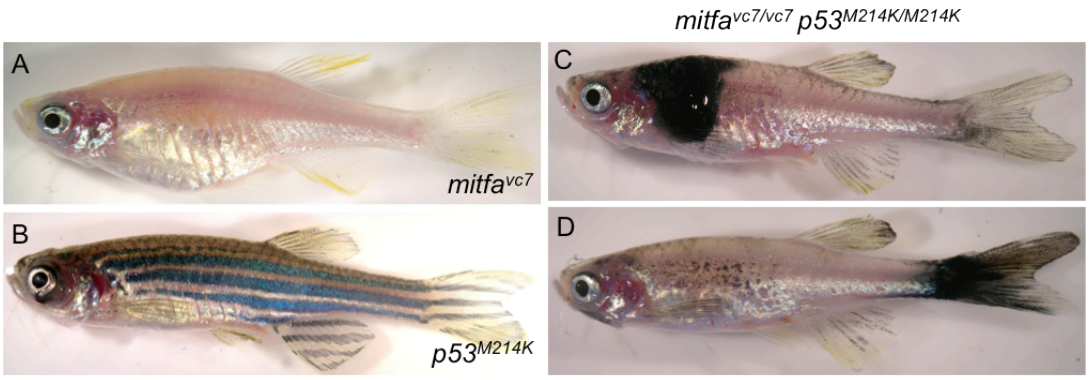

Figure 2.9 A novel melanoma model independent of a *BRAF^{V600E}* mutation. *mitfa$^{vc7/vc7}$* (A) and *p53$^{M214K/M214K}$* (B) zebrafish mutants raised at 28°C do not develop nevi or melanoma. *mitfa$^{vc7/vc7}$p53$^{M214K/M214K}$* zebrafish mutants (C,D) develop both nevi and melanoma when raised at temperatures of 28°C.

mitfa^{vc7} p53^{M214K} melanomas occur with higher frequency but at later age than BRAF^{V600E} p53 ^{M214K} and BRAF^{V600E} mitfa^{vc7} melanoma models

In a similar manner to the *BRAF^{V600E} p53^{M214K}* and *BRAF^{V600E} mitfa^{vc7}* melanoma models, I collected tumour incidence data for the *mitfa^{vc7} p53* zebrafish to compare both the age of onset and frequency of tumours. As well as this, I counted both *mitfa$^{vc7/vc7}$* and *p53$^{M214K/M214K}$* mutant zebrafish populations, none of which developed melanomas. All *mitfa$^{vc7/vc7}$*, *p53$^{M214K/M214K}$* and *mitfa^{vc7} p53* zebrafish included in the population counts were raised at 28°C.

Of 142 *mitfa$^{vc7/vc7}$* zebrafish, 2 developed nevi (2/142, 1.4%), and of 22 *p53$^{M214K/M214K}$* zebrafish, 7 developed malignant peripheral nerve sheath tumours (MPNSTs) (7/22, 31.8%). Zebrafish MPNSTs are identifiable upon external visualisation because of ocular or abdominal cavity localisation and by histopathological staining in which the tumours are composed of mainly spindle-shaped cells (Berghmans *et al*., 2005). In comparison, 94/129 *mitfa^{vc7}p53 ^{M214K}* zebrafish developed melanomas (72.9%). This tumour incidence is extremely high compared to both *BRAF^{V600E}p53^{M214K}* (27.1%) and *BRAF^{V600E}mitfa^{vc7}* (26.9%) zebrafish melanoma models. It is comparable to the incidence of *BRAF^{V600E}mitfa^{vc7}p53^{M214K}* zebrafish mutants, in which 51/60 (85%) develop tumours.

The age of tumour onset also differed between *mitfa^{vc7}p53^{M214K}* zebrafish and the previously described models. In *BRAF^{V600E}mitfa^{vc7}* and *BRAF^{V600E}p53^{M214K}* zebrafish, tumours were observed between 4-5 months of age and continued to present up to one year old. In *mitfa^{vc7} p53 ^{M214K}* zebrafish, tumours were first observed after 8 months and by 10 months of age, 46.5% (60/129) had developed tumours. From observation, tumours from *mitfa^{vc7}p53^{M214K}* zebrafish, once initiated, were quick to progress. Although the age of tumour onset is greater than both *BRAF^{V600E}mitfa^{vc7}*

and *BRAF*^{V600E}*p53*^{M214K} mutants, the impact of tumour initiation in *mitfa*^{vc7}*p53*^{M214K} zebrafish is more severe. Once melanomas develop in *mitfa*^{vc7}*p53*^{M214K} zebrafish, their health deteriorates rapidly and this requires them to be sacrificed. Similar to the median tumour onset calculated for *BRAF*^{V600E}*p53*^{M214K} mutants (Table 1), *mitfa*^{vc7}*p53*^{M214K} zebrafish showed a median tumour onset of 10 months.

To compare tumour incidence between these three genetic backgrounds, *mitfa*$^{vc7/vc7}$, *p53*$^{M214K/M214K}$ and *mitfa*$^{vc7/vc7}$*p53*$^{M214K/M214K}$ and the effect of combining the *mitfa*^{vc7} and *p53*^{M214K} mutations, I carried out a three-way log-rank test. The null hypothesis for this statistical analysis is that there is no difference between these three genotypes in the probability of developing a tumour at any age. The p-value, found by referring the outcome of the log rank test (215.19) to a X^2 distribution with 2 degrees of freedom, is <0.00001. The difference in tumour incidence between *mitfa*$^{vc7/vc7}$, *p53*$^{M214K/M214K}$ and *mitfa*$^{vc7/vc7}$*p53*$^{M214K/M214K}$ zebrafish is therefore statistically significant.

Both tumour incidence and age of onset for *mitfa*$^{vc7/vc7}$, *p53*$^{M214K/M214K}$ and *mitfa*^{vc7}*p53*^{M214K} zebrafish are displayed graphically in Figure 2.10. As Figure 2.7, the percentage of tumour-free individuals is presented as a variable on the y-axis.

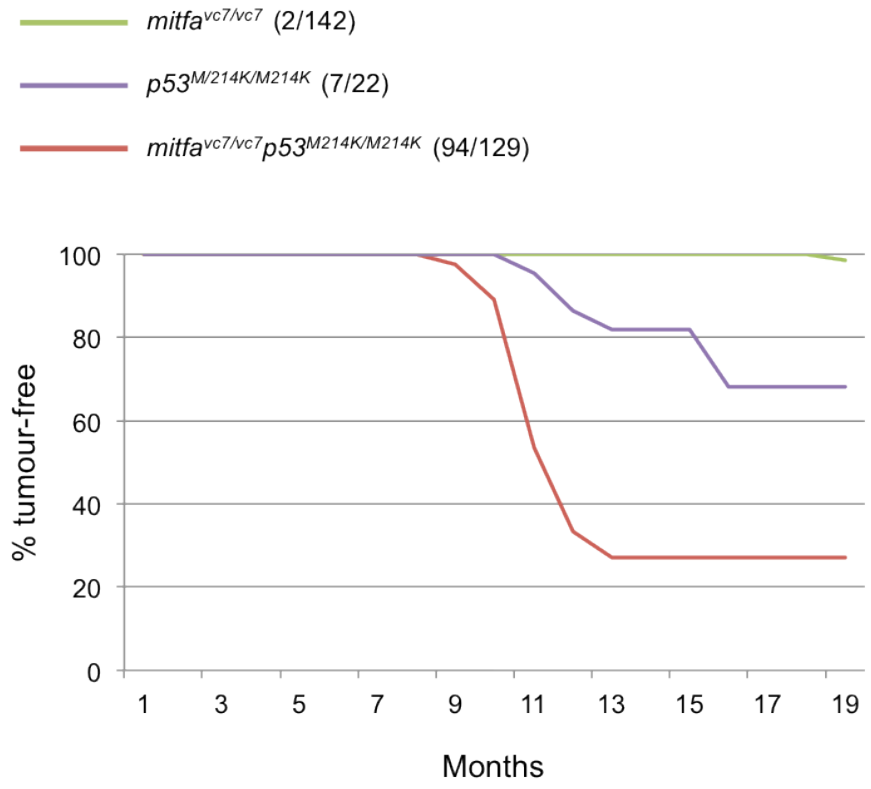

Figure 2.10 Melanoma incidence curves of *mitfa*$^{vc7/vc7}$, *p53*$^{M214K/M214K}$ and *mitfa*$^{vc7/vc7}$*p53*$^{M214K/M214K}$ zebrafish mutants at 28°C.

2.3 Discussion

In this first results chapter I focused on the role of MITF in melanoma and asked if, like a mutation in *p53*, the temperature-sensitive *mitfa*^{vc7} allele could cooperate with *BRAF*^{V600E} to drive melanoma progression. Identifying new mutations that cooperate with *BRAF*^{V600E} to induce melanoma in this model is an essential step in the development of new therapeutics and understanding the resistance that occurs with current drugs. As reviewed by Tsao and colleagues (2012), the activity of MITF is an important contributing factor in melanoma. Here, I show for the first time in an animal model that a low level of wild-type *mitf* activity is oncogenic with *BRAF*^{V600E}.

Initially, I aimed to replicate the work of Patton and colleagues (2005) to create *BRAF*^{V600E}*p53*^{M214K} transgenic zebrafish and confirm that these animals develop melanoma (Patton *et al*., 2005). I then took advantage of the temperature-sensitive nature of the *mitfa*^{vc7} allele (Johnson *et al*., 2011) to create a *BRAF*^{V600E}*mitfa*^{vc7} model. Over 26% of *BRAF*^{V600E}*mitfa*^{vc7} zebrafish developed melanomas from 3-4 months of age when grown at temperatures <26°C, a similar incidence rate to *BRAF*^{V600E}*p53*^{M214K} zebrafish.

Our model of melanoma in the *BRAF*^{V600E}*mitfa*^{vc7} zebrafish is relevant to human melanoma as it was found that a low level of MITF is oncogenic with BRAF^{V600E}, a trend that is also observed in human melanoma patients in which low MITF expression levels are associated with disease progression and poor prognosis (Levy *et al*., 2006). As described by Salti and colleagues, patients with < 50% MITF expression have significantly more nodal metastases after nodal dissection than those with > 50% MITF expression (Salti *et al*., 2000) suggesting that *MITF* or its target genes are commonly downregulated in cases of advanced melanoma, with the exception of those with *MITF* amplifications. In these cases with low MITF

expression, exogenous expression of MITF leads to inhibition of proliferation (Selzer *et al*., 2002; Wellbrock and Marais, 2005).

In contrast to low levels of MITF in association with melanoma progression, MITF amplification has also been shown to be an indicator of poor prognosis of the disease, as it cooperates with $BRAF^{V600E}$ to transform melanocytes (Garraway *et al*., 2005). One argument for the differences in the relationship between MITF activity and disease prognosis is that they may reflect different melanoma subtypes. A second possibility is that in the context of high $BRAF^{V600E}$ signalling, MITF activity must be maintained at a sufficient level to guarantee melanoma cell survival, and MITF amplification reflects this requirement (Garraway *et al*., 2005; Wellbrock *et al*., 2008). One of the essential features of melanoma therefore would be 'fine-tuning' MITF activity. There must be a sufficient level of MITF activity for survival and proliferation, but higher levels of activity that would promote cell cycle arrest and differentiation, or lower levels that would lead to cell cycle arrest and apoptosis must be limited (Gray-Schopfer *et al.*, 2007; Hoek and Goding, 2010).

In this project, the temperature-sensitive nature of the zebrafish $mitfa^{vc7}$ mutant allele has enabled MITF activity to be varied within an individual animal by altering the water temperature. Taking advantage of this allele has revealed the role of MITF activity levels in melanomagenesis and survival *in vivo*, although it is possible that it also has additional functions that contribute to melanoma.

The potential of MITF as a drug target for melanoma is highlighted by the novel finding that the $mitfa^{vc7}$ mutation cooperates with a mutation in *p53* to drive melanoma in zebrafish. It is important to note that this new melanoma model presented is independent of a $BRAF^{V600E}$ mutation. Much of the recent therapeutic developments have focused on the use of inhibitors that target BRAF, as this is found mutated in about 40% of melanomas (Bamford *et al*., 2004). The degree of this focus seems unjustified however, owing to the development of resistance mechanisms and

side effects that arise as a consequence of BRAF inhibitor treatments such as vemurafenib. It is necessary to broaden the therapeutic development scope to include BRAF-independent melanomas as these represent more than half of melanoma cases and would therefore greatly benefit from novel therapeutics. As the research and literature is dominated by BRAF mutant melanomas and lacks that of BRAF-independent melanomas, our finding of a BRAF-independent zebrafish model is important.

In the context of MITF and the identification of the first animal model presented here in which low levels of wild-type MITF activity is oncogenic with $BRAF^{V600E}$, it is important to relate this to the recent development of MITF as a resistance mechanism for current BRAF inhibitors or BRAF/MEK combination therapies. MITF was recently found to be a novel regulator of ERK-independent de novo and acquired resistance to BRAF and MEK inhibitors (Smith *et al*., 2013). In this study, an increase in MITF levels was observed in patients treated with BRAF inhibitors, which then decreased at time of progression. In resistance to either MEK inhibition or a combination of BRAF/MEK inhibition however, these high levels of MITF continued to be elevated. The authors found that SMAD-specific E3 ubiquitin protein ligase 2 (SMURF2) depletion reduced MITF levels as well as lowering the threshold of MEK inhibitor-induced apoptosis (Smith *et al*., 2013). This suggested that targeting SMURF2 could be a novel therapeutic strategy to increase the efficacy of MEK inhibitors that are currently used in combination with BRAF inhibitors. The study both highlights the discovery of MITF as a resistance mechanism and addresses this by way of a new inhibitor that could contest this resistance.

Chapter 3 – *MITF* mutations direct pathological and molecular features of melanoma

Chapter 3: MITF mutations direct pathological and molecular features of melanoma

In the first results chapter, I described the genetics of the *BRAF*^{V600E}*mitfa*^{vc7} melanoma model. I showed that, like *p53*, a mutation in *mitf* could cooperate with *BRAF*^{V600E} to drive melanomagenesis in the zebrafish.

The aim of this second data chapter was to use pathology to determine whether melanomas driven by *BRAF*^{V600E} and a cooperating mutation in either *p53* or *mitfa* could be characterised as distinct subtypes. I will first introduce features of human melanoma pathology and describe how these can relate to characteristics of melanomas induced in zebrafish. I will then outline the target genes of MITF that have been discovered and are detailed in the literature.

I will show how I have used the *BRAF*^{V600E} mutant line to identify two melanoma subtypes that can be distinguished by their pathology. I will also describe how these subtypes differ in the expression of MITF target genes.

3.1 Introduction

3.1.1 Human melanoma pathology

In humans, there are four types of cutaneous melanoma – superficial spreading, nodular, lentigo maligna and acrallentigineous (McGovern *et al*., 1973). These subtypes can be histopathologically distinguished by examining serial sections cut through the tumour mass, using haematoxylin and eosin (H&E) stain and identifying characteristic cellular features. As well as histologic subtype, other prognostic factors in melanoma include time of diagnosis, tumour thickness, Clark level of invasion, anatomic site, mitotic rate and growth phase. A combination of these prognostic factors and a histological analysis is useful in providing answers relating to patient prognosis and the most suitable therapeutic regimens for successful treatment to achieve the best overall outcome.

An accurate diagnosis of a human melanoma relies on the ability to determine what stage of tumour progression the melanoma has reached upon presentation (reviewed by Balch *et al*., 2001). The progression of melanoma from small patches of pigmented skin through radial and vertical growth phases to allow tumour cells to enter and spread within the lymphatic and vascular networks was described in Chapter 1. With each growth stage progression comes increased survival risk. Important factors when deciding stage progression are the 'Clark level' (Clark *et al*., 1969) and 'Breslow's depth' (Breslow, 1970), which both refer to the degree of tumour invasion at a microscopic level.

As well as tumour thickness and invasion, the cellular proliferation within a primary tumour, reflected by the mitotic rate, is now used to stage melanoma patients and predict survival. In 2003, Azzola and colleagues showed that tumour mitotic rate

(TMR) was 'an important, independent predictor of survival for melanoma patients.' They showed that patients with 0 mitoses/mm^2 had a significantly better survival rate than those with 1 mitoses/mm^2 (Azzola *et al.*, 2003). More recently, Thompson and colleagues (2011) concluded from a study that, of the independent predictors of melanoma-specific survival, mitotic rate is the strongest predictor after tumour thickness.

Like a pathologist's investigation into a human melanoma, zebrafish melanomas can be dissected and studied using similar methods. Zebrafish and other teleost cancers share many histopathological features with human cancers (Amatruda *et al*., 2002; Stern and Zon, 2003). In 1985, Hawkins and colleagues induced tumours using carcinogens in seven small fish species, including medaka and guppies (Hawkins *et al*., 1985). This work highlighted the importance of these fish and others as models of cancer from which to study the human disease. In 2000, Spitsbergen and colleagues emphasised that zebrafish were an invaluable tool 'in which to study the mechanistic aspects of the carcinogenesis process,' using the carcinogen DMBA to induce a range of tumours in different tissues characterising individual histologic types (Spitsbergen *et al*., 2000). Likewise, in 2000, Beckwith and colleagues used ethylnitrosourea (ENU) to induce epidermal lesions or papillomas, which established the feasibility of the zebrafish as an experimental model for the study of skin tumours (Beckwith *et al*., 2000).

Drawing parallels between features of melanoma in the zebrafish and that of the human patient demonstrates that the zebrafish is a good model to study this disease. In this chapter, I will examine the histological sections of melanoma and stain with antibodies to identify specific parts of tumour tissue architecture and molecular characteristics. We can then compare features observed in the zebrafish melanoma with tumour characteristics already known to be present in the human melanoma and use this to establish how MITF for example contributes to melanoma pathology.

3.1.2 MITF target genes

The so-called 'master melanocyte regulator' MITF is essential for melanocyte development (Steingrímsson *et al*., 2004). As well as its role in melanocytes, it plays an important function in the development and homeostasis of other cell types including the retinal pigment epithelia (RPE) (Planque *et al*., 2004). It has also been shown to be a critical factor in regulating proliferation in melanoma (Carreira *et al*., 2006; Hoek *et al*., 2008).

Due to its complex and important role in both development and melanoma, this transcription factor is thought to function in multiple pathways and affect many other target genes. It was initially shown to control the transcription of just three genes involved in pigmentation – tyrosinase (*TYR*) (Hou *et al*., 2000), tyrosinase-related protein 1 (*TYRP1*) (Fang *et al*., 2002) and dopachrome tautomerase (*DCT*) (Yasumoto *et al*., 2002). MITF is now known to regulate the transcription of a wide range of genes. The transcription of other genes involved in growth and/or survival were shown to be under the control of MITF, as suggested by the lack of melanocytes in *Mitf*-deficient mice (reviewed by Cheli *et al*., 2010). Now, many target genes of MITF have been confirmed, including those involved in growth and survival – *BCL2* and *CDK2*.

In a study by Hoek and colleagues in 2008, a list of around 40 genes were given as already confirmed MITF target genes. Their research aimed to continue the search for novel genes whose expression was regulated by MITF, in order to 'further characterise the role of MITF in melanocyte and melanoma development' (Hoek *et al*., 2008). Using an approach combining two DNA microarray studies and a cross-validation protocol to help eliminate false-positives in the data, they confirmed 13 previously identified targets and discovered 71 novel targets of MITF (Hoek *et al*., 2008).

One observed relationship between MITF and melanoma development is its role as a transcriptional activator of senescence- and proliferation-associated genes. By driving changes to overcome cellular senescence and promote proliferation, MITF can initiate events leading to tumorigenesis. Senescence mediator proteins p14, p16 and p21, encoded by MITF target gene *CDKN2A*, may be transcribed to assist a transformation between a melanocyte and a melanoma cell for example. Similarly, MITF target gene *TBX2* (Carreira *et al*., 2000) is highly expressed in melanomas and has been shown to repress *p19* and *p21*, which are effectors of senescence, promote proliferation and suppress senescence in melanoma (Vance *et al*., 2005). Both of these examples demonstrate the ability of MITF to transcriptionally activate genes involved in senescence and proliferation, which are properties essential in melanomagenesis and therefore provide an additional link between MITF and melanoma.

As well as anti-senescence and proliferation, anti-apoptosis is another key process in melanoma development. One known anti-apoptotic gene, *BCL-2* is widely expressed in melanomas (Cerroni *et al*., 1995; Ramsay *et al*., 1995) and has been confirmed as an MITF target gene (McGill *et al*., 2002). Similarly, hypoxia-inducible factor 1 α (*HIF-1α*) has been shown to be an anti-apoptotic factor in melanoma cells (Buscà *et al*., 2005) and MITF has been shown to bind directly to the HIF-1α promoter site to activate its transcription. The $MITF^{E318K}$ mutation identified in melanoma and renal cell carcinoma (Bertolotto *et al*., 2011) was shown to enhance MITF protein binding to the HIF-1α promoter and increase its transcriptional activity compared to wild-type MITF.

The MITF target gene *HIF-1α* targets vascular endothelial growth factor (*VEGF*), a gene that contributes largely to angiogenesis (Buscà *et al*., 2005), another critical step in the process of tumorigenesis. As well as angiogenesis, the ability of cells to invade structures is also important for tumour development. Another MITF target, the *C-MET* proto-oncogene, which encodes hepatocyte growth factor receptor (HGFR), is highly expressed in melanomas and has been linked with its ability to

metastasize (Halaban *et al*., 1992; Natali *et al*., 1993; Hendrix *et al*., 1998; McGill *et al*., 2006). In 2006, McGill and colleagues investigated whether the HGF/c-Met signaling pathway elicited some of its downstream signaling through Mitf. They found that stimulating both melanocytes and melanoma cells with HGF leads to phosphorylation of Mitf via the MAPK pathway (McGill *et al*., 2006). In addition, they identified 'conserved Mitf binding sequences in the human and mouse c-Met promoters that are bound by Mitf' and regulate the expression of c-Met in melanocytes (McGill *et al*., 2006). Importantly, they also found that while HGF could stimulate invasive growth in melanocytes and melanoma cells, suppressing endogenous Mitf could abrogate this invasiveness. This suggests that there is potential to inhibit the invasive capacity of melanomas by targeting Mitf.

In summary, MITF has many known target genes and with this the ability to upregulate both melanoma-inducing (*BLC-2, C-MET*) and -repressing genes (*p16, p21*). It is likely that the level or activity of MITF changes to drive either a melanoma-promoting or -inhibiting role and so this must be carefully regulated to transform melanocytes to melanoma cells. Low levels of MITF expression promote proliferation in melanoma, whereas high levels promote differentiation driven by senescence and melanin production (Goding and Meyskens, 2006; Hoek and Goding, 2010). Due to these opposing roles that are dependent on MITF expression, it seems that it is a balancing act to regulate MITF and in doing so either promote or inhibit the change from melanocyte to melanoma cell.

In this chapter, I will examine the expression of these known, described MITF target genes in $BRAF^{V600E}mitfa^{vc7}$ and $BRAF^{V600E}p53^{M214K}$ melanomas using qRT-PCR.

3.2 Results

3.2.1 Pathology of BRAF^{V600E} melanomas

After fixation and embedding, transverse sections were cut through the body of the tumours and stained with H&E (Figures 3.1 and 3.2). From the *BRAF^{V600E} mitfa^{vc7}* genetic cross, 26 tumour sections were examined and in the same process, 21 *BRAF^{V600E} p53^{M214K}* tumours were also examined by pathology. This body of work was carried out under the supervision of NHS pathologist Marie Mathers, a clinical pathologist specializing in skin cancer. For each tumour from either genetic background, several characteristics were examined including tumour growth pattern, degree of pigmentation, cell type within the tumour mass and the presence or absence of mitoses. The similarities and differences between subtypes of each of these parameters are subsequently described.

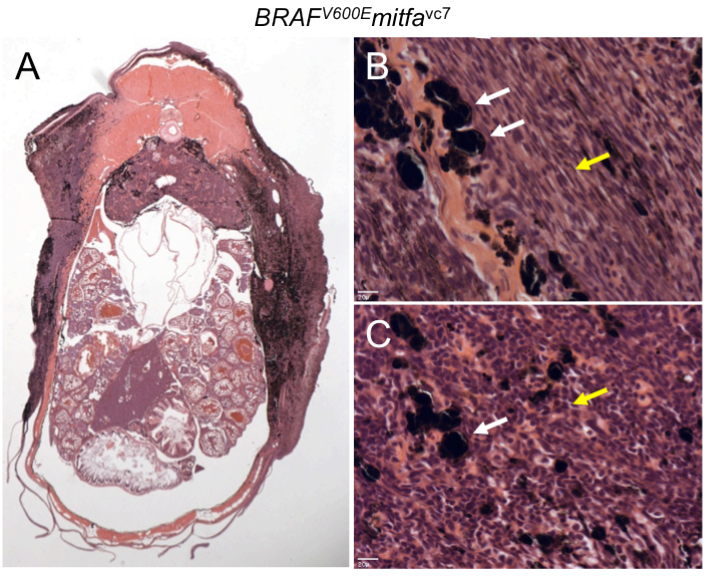

Figure 3.1 H&E staining of a *BRAF^{V6000E}mitfa^{vc7}* melanoma.
A. Transverse section through body of zebrafish, showing superficial spreading tumour on right side.
B,C. Close up of tumour tissue A, containing macromelanophages (white arrows) and both epithelioid and spindle-like cells (yellow arrows). Scale bar=20μm.

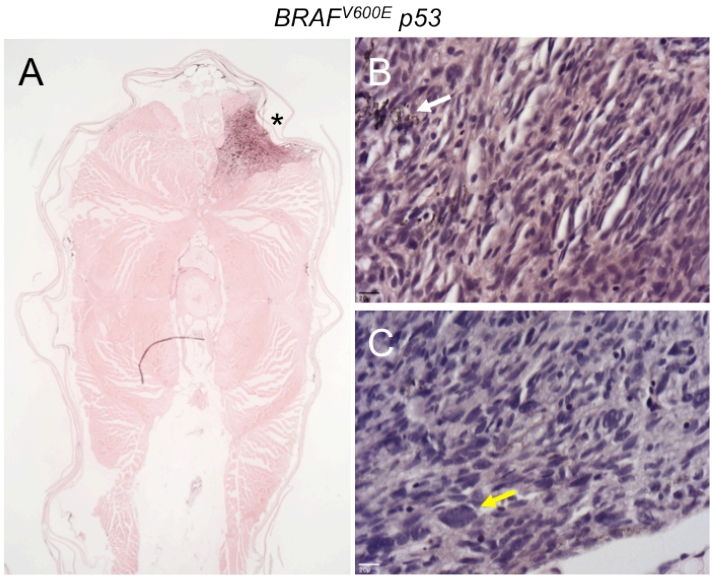

Figure 3.2 H&E staining of a *BRAF*^{V6000E} *p53* melanoma. A. Transverse section through body of zebrafish, showing nodular-like tumour (*) B,C. Close up of tumour tissue A, containing scattered pigment (white arrow) and a nuclear pleomorphism (yellow arrow). Scale bar=20μm.

Tumour growth

The first trait observed was the growth pattern of the melanoma. Although the tumour initiation site is difficult to distinguish, by looking at the area and location of tumour progression and its invasive potential, I can describe an individual tumour's growth pattern in detail. A clear difference in the pattern of tumour growth was visible between the genetic backgrounds from which the tumour had arisen.

In the *BRAF*^{V600E} *mitfa*^{vc7} tumours (Figure 3.1), 22/26 showed a superficial spreading pattern of growth, with some invasion into the underlying muscle. Exclusive to this type of growth, the tumour cells spread along the surface dermal layer of the skin with minimal, if any, invasion into other muscle or organs. In contrast, 19/21 *BRAF*^{V600E} *p53*^{M214K} tumours (Figure 3.2) displayed a growth pattern described as nodular and highly invasive, with tumour cells found in multiple organs. In this subtype of melanoma, the tumour growth was more aggressive than that seen in

BRAF^{V600E}*mitfa*^{vc7} tumours. In most of these tumours, although the melanoma seems to have initialised within the skin, tumour cells have been able to penetrate through dense muscular regions and organs such as the kidney. In Table 2, levels of invasion are determined by observation of H&E stained tumour sections (Figure 3.1; Figure 3.2). Low levels of invasion were observed in tumours in which a superficial spreading growth pattern was dominant and there was minimal invasion into underlying musculature. Tumours with high levels of invasion, as shown in Figure 3.2, showed highly aggressive invasive behaviour in which melanoma cells progressed through musculature and to nearby organs including the kidney.

The distinction between a superficial spreading type of tumour growth and one that is highly invasive is a simple way to distinguish between melanomas from these two genetic backgrounds. With each melanoma harbouring a homozygous *BRAF*^{V600E} transgene and a different cooperating mutation, it is clear that mutations in *mitfa* and *p53* drive unique patterns of melanoma growth that are individual to that genotype.

Pigmentation

As well as distinct growth patterns, the two melanoma subtypes also displayed a different degree of pigmentation. In the *BRAF*^{V600E}*mitfa*^{vc7} mutant melanomas, macro-melanophages are recognisable as dark brown stained cells, the colour coming from the melanin contained within the cell. These cells also appear larger than other surrounding cells in the tumour tissue and have poorly defined cytoplasmic borders, characteristics typical of melanophages (Busam *et al*., 2001).

In *BRAF*^{V600E}*mitfa*^{vc7} stained melanoma sections, a high degree of pigmentation was observed in the tumour cell population, with many macro-melanophages present (white arrows, Figure 3.1B, C). In contrast, although pigmented cells were also present in the tumour tissue of *BRAF*^{V600E}*p53*^{M214K} melanomas (white arrow, Figure 3.2B), no macro-melanophages were present. This difference allows classification of

melanoma subtype by the presence or absence of macro-melanophages within the tumour tissue.

Cell type

Tumour tissue can be composed of different cell shapes, namely spindle-like (long, narrow, stretched-like cells) and epithelioid (rounded, condensed, sphere-like cells). Differences in cell shape can be observed in different tumours or in areas of the same tumour that may have developed at different time points. In $BRAF^{V600E}mitfa^{vc7}$ tumours, both spindle and epithelioid shaped cells were present (yellow arrows, Figure 3.1B, C). In contrast, only epithelioid shaped cells were present in the tumour tissue of $BRAF^{V600E}p53^{M214K}$ melanomas, allowing these melanoma subtypes to be distinguished by the dominant cell shape within the tumour cell population. Whether the dominant cell type is spindle or epithelioid shaped may affect prognosis. Spatz and colleagues for example, found that tumours with mostly spindle cell populations were more frequently observed in long-term survivors of the disease (Spatz *et al*., 1998), suggesting that dominance of this cell type is correlated with improved prognosis.

Mitoses

The last distinguishable feature between $BRAF^{V600E}mitfa^{vc7}$ and $BRAF^{V600E}p53^{M214K}$ tumours was identified by looking for the presence of mitoses in each tumour cell population. Mitotic events were observable by identifying single cells in the tumour population that were undergoing mitosis. Very few mitotic events were observed in the $BRAF^{V600E}mitfa^{vc7}$ tumour sections we looked at, compared to a high number in the tumour sections from $BRAF^{V600E}p53^{M214K}$ melanomas. The comparison of mitotic events here are descriptive observations only and need to be followed up by quantification to ascertain true differences between melanoma subtypes. Notably, a high degree of nuclear pleomorphism was observed in $BRAF^{V600E}p53^{M214K}$ tumour tissue, recognisable by either an increase or variability in the size or number of nuclei present within some cells (yellow arrow, Figure 3.2C). In human melanoma, marked

nuclear pleomorphism is typical of aggressive tumour behaviour (Broekart *et al*., 2010; Patton *et al*., 2011). Similar to the observation of mitotic events, presence of nuclear pleomorphism identified here is descriptive and should be quantified to strengthen this difference between melanoma subtypes.

In summary, I saw clear differences in tumour growth pattern, pigmentation, cell shape and mitoses between tumours from *BRAF*^{V600E}*mitfa*^{vc7} and *BRAF*^{V600E}*p53*^{M214K} genetic backgrounds (summarised in Table 2). From these observations, I can conclude that *BRAF*^{V600E} - cooperating mutations, *mitfa* and *p53*, direct specific characteristic features of melanoma pathology.

Table 2. Characteristic features of the *BRAF*^{V600E}*mitfa*^{vc7} and *BRAF*^{V600E}*p53*^{M214K} melanoma subtypes defined by pathology.

Pathology feature	***BRAF*^{V600E}*mitfa*^{vc7}**	***BRAF*^{V600E}*p53*^{M214K}**
Growth pattern	Superficial spreading	Nodular
Invasion	Low	High
Pigmentation	Heavy in macro-melanophages	No macro-melanophages Pigmentation in melanoma cells
Tumour cell shape	Spindle and epithelioid	Primarily epithelioid
Presence of mitoses	Few	Many

3.2.2 Macrophages in BRAF^{V600E}mitfa^{vc7} tumours

One of the characteristics that distinguished *BRAF^{V600E}mitfa^{vc7}* tumours from *BRAF^{V600E}p53^{M214K}* tumours was the degree of pigmentation. Although there were pigmented tumour cells present in the *BRAF^{V600E}p53^{M214K}* melanomas, there were higher numbers of pigmented cells observed in the tumour tissues of *BRAF^{V600E}mitfa^{vc7}* melanomas. Also noticeable was the presence of 'macro-melanophages' in the *BRAF^{V600E}mitfa^{vc7}* tumours – large, heavily pigmented cells that were densely packed with melanin so they appeared solid and almost black in colour (white arrows, Figure 3.1B, C). These cells were absent in the *BRAF^{V600E}p53^{M214K}* melanomas.

To confirm the presence of macrophages in the *BRAF^{V600E}mitfa^{vc7}* tumour tissue population, a macrophage-specific antibody marker (anti-CD68) was used to stain the tissue of six fixed tumours from this genotype. Positively stained cells, depicting macrophages, were observed in all *BRAF^{V600E}mitfa^{vc7}* tumours and were distributed randomly (Figure 3.3). This staining confirmed our observation of macrophages present in the *BRAF^{V600E}mitfa^{vc7}* tumours and these became another distinguishing feature when describing the two melanoma subtypes from *BRAF^{V600E}mitfa^{vc7}* and *BRAF^{V600E}mitfa^{vc7}* genetic backgrounds.

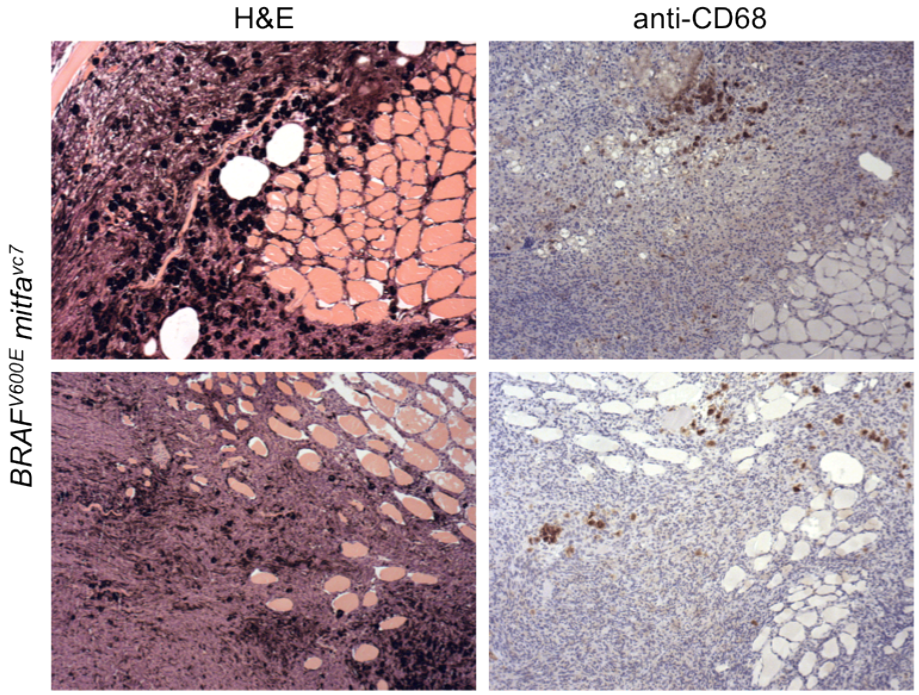

Figure 3.3 Immunohistological staining showing macrophages. H&E staining (left) and antibody staining using anti-CD68 (right) of two *BRAF*^{V600E} *mitfa*^{vc7} melanoma sections.

3.2.3 Pathology of $BRAF^{V600E}$-independent $mitfa^{vc7}p53^{M214K}$ melanomas

In collaboration with NHS pathologist Marie Mathers, the histopathology of melanomas from the $mitfa^{vc7}p53^{M214K}$ genetic background was also examined (Figure 3.4). In 7/8 melanomas, the tumour growth pattern was similar to that of the $BRAF^{V600E}p53^{M214K}$ melanomas, with a highly aggressive behaviour and invasion into musculature and internal organs. In 3/8 $mitfa^{vc7}p53^{M214K}$ melanomas examined, the tumour growth was also reminiscent of the $BRAF^{V600E}mitfa^{vc7}$ subtype, with superficial spreading along the dermis in addition to invasion. All $mitfa^{vc7}p53^{M214K}$ melanoma tissues (8/8) were highly pigmented, with melanin observable in most tumour cells, but no macro-melanophages were present. A mixture of both spindle and epitheliod cell types were present within the tumour cell populations and all $mitfa^{vc7}p53^{M214K}$ melanomas displayed a high degree of nucleur pleomorphism (8/8).

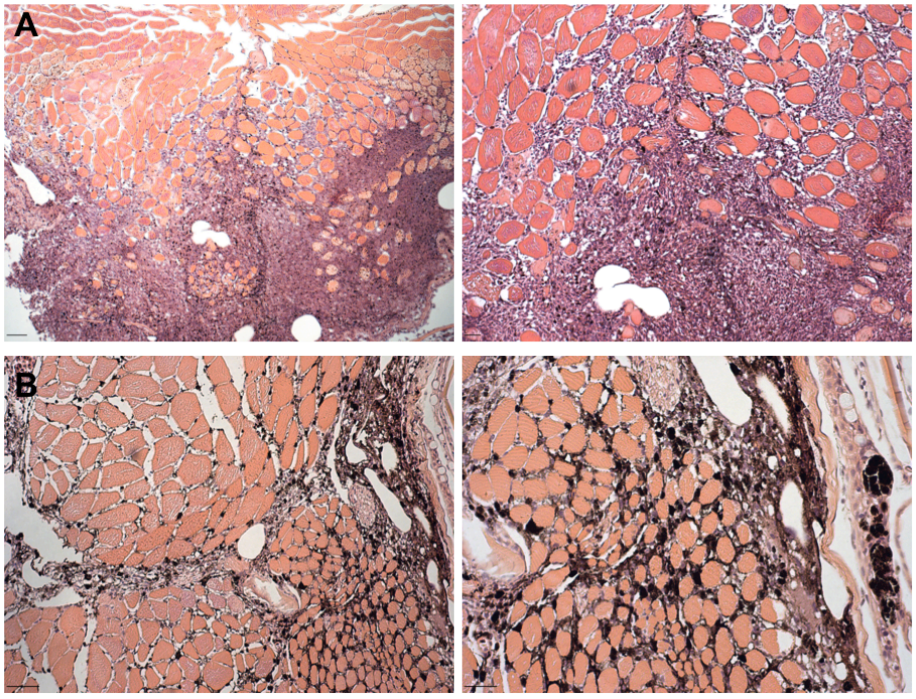

Figure 3.4 Histopathology of $mitfa^{vc7/vc7}p53^{M214K/M214K}$ zebrafish melanomas. Cross-sections of two $mitfa^{vc7/vc7}p53^{M214K/M214K}$ melanomas (A, B) stained with hematoxylin and eosin (H&E) to identify characteristic histological features. Scale bars = 20μm.

3.2.4 Immunohistochemistry of $BRAF^{V600E}$ and $BRAF^{V600E}$-independent melanomas

Immunohistochemical staining, using a variety of antibodies was carried out to determine further differences between melanoma subtypes identified by pathology.

Positive melan-A staining in both tumour subtypes confirms melanoma status

Melan-A, isolated as a melanoma-specific antigen, is expressed in the skin, retina, melanocytes and melanomas (Busam and Jungbluth, 1999; Shidham *et al*., 2001). The melan-A stain used in IHC is useful to confirm that our zebrafish tumours are melanoma. All *$BRAF^{V600E}$mitfa^{vc7}* and *$BRAF^{V600E}$p53^{M214K}* stained positively with this stain (Figure 3.5), confirming the tumour type as melanoma.

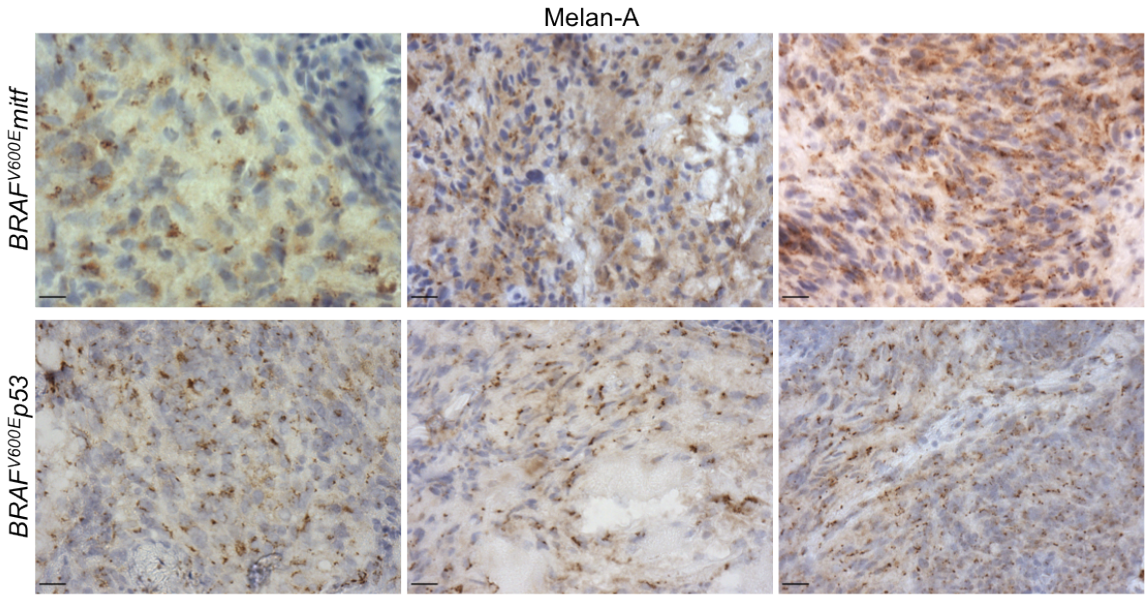

Figure 3.5 Positive melan-A staining in both tumour subtypes confirms melanoma status. Anti-melan-A positive staining (stained brown cells) in *$BRAF^{V600E}$mitf* (top panel) and *$BRAF^{V600E}$p53* (lower panel) melanomas. Scale bars=50μm.

Activation of the MAPK cascade in both melanoma subtypes

Members of the MAPK/ERK pathway (mitogen-activated protein kinases, once called extracellular signal-regulated kinases) include ERK and MEK. Antibody staining using anti phospho-ERK and anti phospho-MEK was carried out on *BRAF*^{V600E}*mitfa*^{vc7} and *BRAF*^{V600E}*p53*^{M214K} tumour sections to look at the activity of these signalling molecules in these important pathways.

Positively stained cells were observed in the tumour populations of both melanoma subtypes using these two antibodies (Figure 3.6). This result confirmed that the MAPK pathway was highly active both *BRAF*^{V600E}*mitfa*^{vc7} and *BRAF*^{V600E}*p53*^{M214K} tumours.

Activation of the MAPK cascade in mitfa^{vc7}*p53*^{M214K} *melanomas*

The same antibody staining using anti phospho-ERK and anti phospho-MEK was carried out on *mitfa*^{vc7}*p53*^{M214K} tumour sections. This assessed whether, like BRAF^{V600E} melanomas, this BRAF^{V600E}-independent melanoma subtype had MAPK cascade activity. Few positively stained cells were observed in *mitfa*^{vc7}*p53*^{M214K} tumour tissue these antibodies (Figure 3.7), however sections focused on musculature to which these tumours had invaded. To ascertain whether either ERK or MEK are active in these melanomas it would be useful to repeat this antibody staining on sections containing the tumour mass.

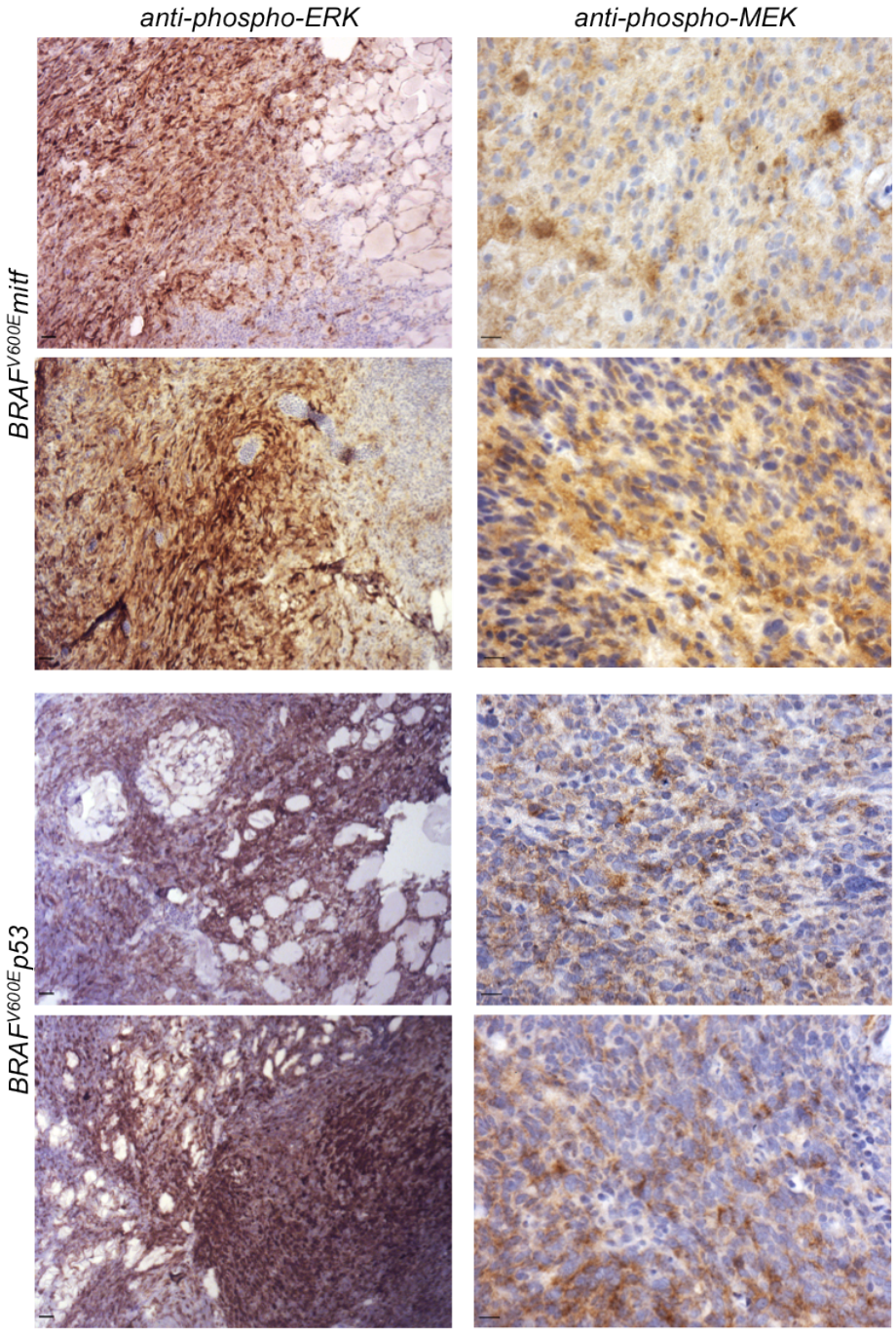

Figure 3.6 Activation of MAPK cascade in both melanoma subtypes. *BRAF*^{V600E}*mitf* (top panel) and *BRAF*^{V600E}*p53* (bottom panel) melanoma samples show activation of the MAPK pathway through positive staining with antibodies against phospho-ERK (left) and phospho-MEK (right) in fixed tumour sections. Scale bar=50μm.

Increased levels of p53 mutant protein in BRAF^{V600E}p53^{M214K} tumours

Using an antibody to detect mutant p53 protein allowed the comparison of levels of mutant p53 between *BRAF^{V600E}mitfa^{vc7}* and *BRAF^{V600E}p53^{M214K}* tumours (Figure 3.7). The anti-p53 monoclonal antibody (gifted by David Lane) was validated using IHC to show that exposure of zebrafish embryos to p53-activating agents resulted in p53 protein accumulation in the gut, liver and pancreas (Lee *et al*., 2008).

By IHC it was clear that no staining was present in tumour sections from the *BRAF^{V600E}mitfa^{vc7}* genotype, indicating that this melanoma subtype did not have mutant p53 (Figure 3.7). In contrast, all *BRAF^{V600E}p53^{M214K}* tumours stained positively for mutant p53 (Figure 3.7).

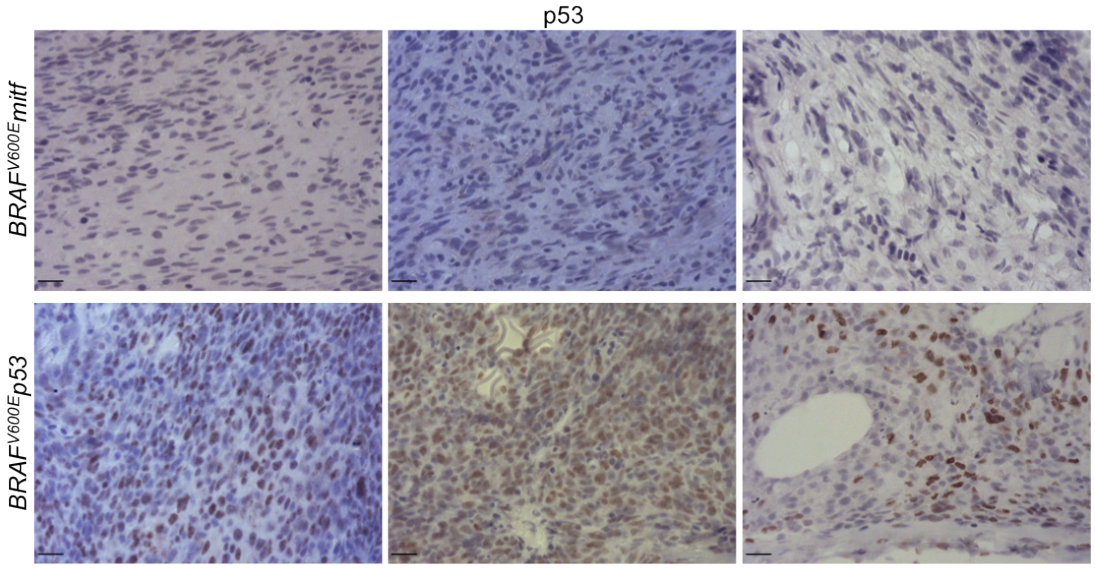

Figure 3.7 Increased levels of p53 mutant protein in *BRAF^{V600E}p53* tumours *BRAF^{V600E}mitf* (top panel) and *BRAF^{V600E}p53* (bottom panel) melanoma samples stained with an antibody raised against p53. *BRAF^{V600E}p53* melanomas show increased staining (stained brown cells) with anti-p53 compared to *BRAF^{V600E}mitf* melanomas, indicating increased levels of p53 in this melanoma subtype. Scale bar=50μm.

Similar levels of phospho-H2AX activity in both melanoma subtypes

To assess levels of DNA damage in tumour populations, an antibody against p-H2AX was used in IHC. The polyclonal anti-p-H2AX antibody (gifted by James Amatruda) recognises the zebrafish p-H2AX histone variant. Phosphorylation of the H2AX histone variant occurs along tracks of chromatin at double strand breaks, which enables detection of DNA damage sites using the antibody (Sharma *et al*., 2012).

Phospho-H2AX-positively stained cells were found in both *BRAF*^{V600E}*mitfa*^{vc7} and *BRAF*^{V600E}*p53*^{M214K} tumours (Figure 3.8). This result indicates that both melanoma subtypes show a similar degree of DNA damage, of which H2AX is marker.

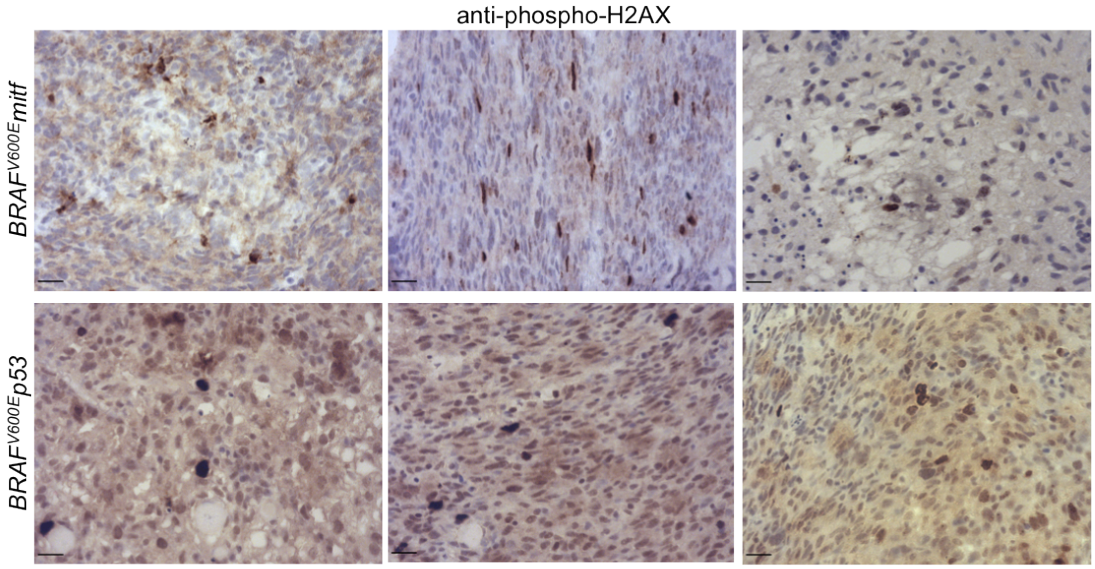

Figure 3.8 Similar levels of phospho-H2AX activity in both melanoma subtypes. *BRAF*^{V600E}*mitf* (top panel) and *BRAF*^{V600E}*p53* (bottom panel) melanoma samples stained with anti-phospho-H2AX. Both *BRAF*^{V600E}*mitf* and *BRAF*^{V600E}*p53* melanomas show positive staining (dark brown cells) with anti-phospho-H2AX, indicating similar levels of phospho-H2AX in each melanoma subtype. Scale bar=50μm.

Increased mitotic activity in $BRAF^{V600E}p53^{M214K}$ tumours

Levels of mitotic activity were assessed using an anti-phospho-Histone H3 antibody. Tumours were stained with the antibody and in both subtypes positively stained cells were observed (Figure 3.9A).

By simple visualisation of the staining, I hypothesised that there was a difference in the degree of positively stained cells between tumour tissues from each melanoma subtype. To test this hypothesis, I quantified the number of positively stained cells in a population from each tumour. Dark brown (positive) cells were counted within a cell population for each tumour and each subtype to quantify the degree of anti-phospho-Histone H3 staining. The results were represented as a boxplot (Figure 3.9B).

Higher numbers of phospho-Histone H3 stained cells were found in $BRAF^{V600E}p53^{M214K}$ tumours compared to $BRAF^{V600E}mitfa^{vc7}$ tumours. Using a T-test, I could show that the difference in phospho-Histone H3 staining was significant between melanoma subtypes ($p=0.0078$). This result confirms that there is a statistically significant difference in mitotic activity levels between melanoma subtypes $BRAF^{V600E}mitfa^{vc7}$ and $BRAF^{V600E}p53^{M214K}$. In humans a high mitotic rate, measured by number of mitoses/mm^2, is associated with a lower survival probability (Thompson *et al.*, 2011) suggesting that $BRAF^{V600E}p53^{M214K}$ melanomas, with a higher mitotic activity, are representative of a more aggressive and dangerous subtype.

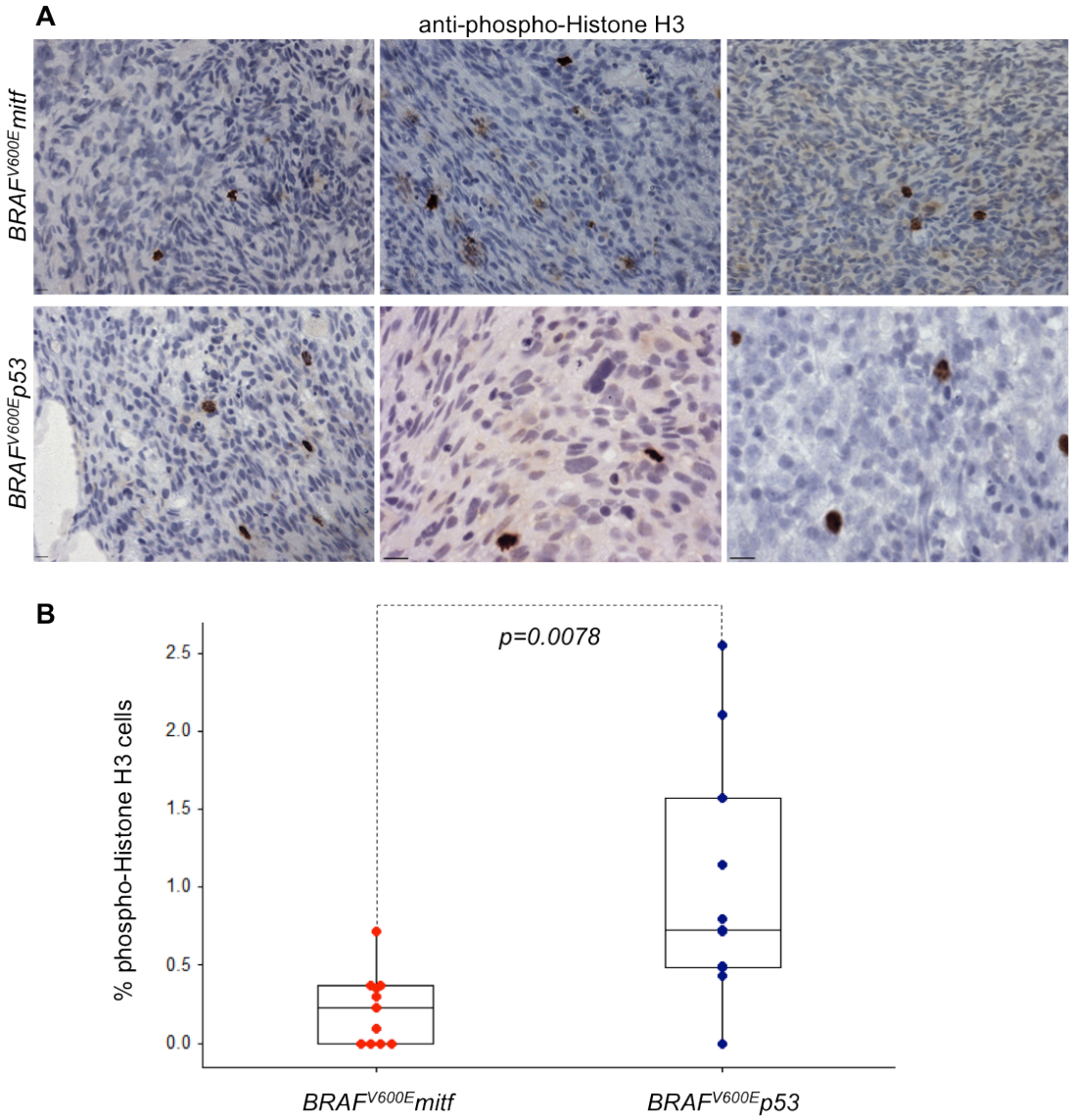

Figure 3.9 Increased mitotic activity in *BRAF*^{V600E}*p53*$^{-/-}$ tumours as shown by levels of phospho-Histone H3 antibody staining.
A. *BRAF*^{V600E}*mitf* (top panel) and *BRAF*^{V600E}*p53* (bottom panel) melanoma samples stained with anti-phospho-Histone H3. Both *BRAF*^{V600E}*mitf* and *BRAF*^{V600E}*p53* melanomas show positive staining (dark brown cells) with anti-phospho-Histone H3. Scale bar=50μm. B. Quantification of positive anti-phospho-Histone H3 staining in *BRAF*^{V600E}*mitf* and *BRAF*^{V600E}*p53* melanomas. Box plot represents mean percentage of phospho-Histone H3 positive cells in *BRAF*^{V600E}*mitf* and *BRAF*^{V600E}*p53* melanomas (n=11). Bars represent interquartile range. Student's T-test, p=0.0078 (significant).

3.2.5 Using quantitative real-time PCR to quantify the expression levels of MITF target genes in melanoma subtypes

As an important transcription factor involved in processes including differentiation and the cell cycle, many target genes of MITF have been identified (Figure 3.10). Genes involved in proliferation, cell survival and oxygen stress including *CDK2*, *TBX2, BCL-2, MET, HIF-1α* and *APE-1* are all MITF target genes. MITF also controls transcription of genes involved in cell cycle arrest including *p16* and *p21*. Genes involved in pigmentation, including *DCT* and *TYR* are also under the transcriptional control of MITF. Important for their role in melanoma, genes involved in metastasis and invasiveness such as *SLUG, MET* and *DIA* have also been shown to be target genes of MITF.

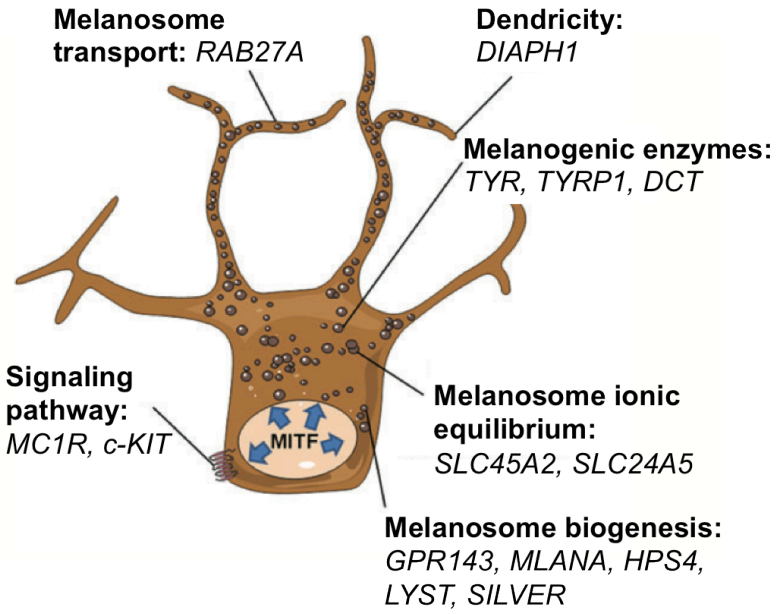

Figure 3.10 (adapted from Cheli *et al*., 2010) Graphic showing the numerous functional pathways and genes targeted by MITF

The aim of the following experiments was to ascertain the expression levels of some of these known MITF target genes in our melanoma subtypes. I hypothesised that these target genes may be differentially expressed between the melanoma subtypes *BRAF*^{V600E}*mitfa*^{vc7} and *BRAF*^{V600E}*p53*^{M214K}. To address the aim, I carried out quantitative real-time PCR using cDNA prepared from *BRAF*^{V600E}*mitfa*^{vc7} and *BRAF*^{V600E}*p53*^{M214K} tumours and a range of primer sequences specific to the MITF target gene in question. The results of this set of experiments are described in the following sections and as boxplots.

Target genes expressed at similar levels of melanoma subtypes

I found that certain MITF target genes were expressed at a similar level in both melanoma subtypes. These included genes *CDK2, p16* and *p21* (Figure 3.11A-C respectively), which are involved in proliferation and cell cycle arrest. Using an anti-phospho-Histone H3 antibody in IHC, *BRAF*^{V600E}*p53*^{M214K} tumours showed a higher level of staining, indicating a higher degree of proliferation in this melanoma subtype compared to *BRAF*^{V600E}*mitfa*^{vc7} tumours.

As well as MITF target genes involved in proliferation showing no change in expression, genes *BCL-2, HIF-1α* or *p53* were also expressed at similar levels between melanoma subtypes (Figure 3.12A-C).

These results show that the tumour genotype and the *BRAF*^{V600E} – cooperating mutation have no affect on the levels of expression of MITF target genes *CDK2, p16, p21, BCL-2, HIF-1α* and *p53*. Together they indicate that despite the reduced levels of MITF in *BRAF*^{V600E}*mitfa*^{vc7} melanomas, there is sufficient MITF activity to control MITF target genes involved in cell proliferation and survival.

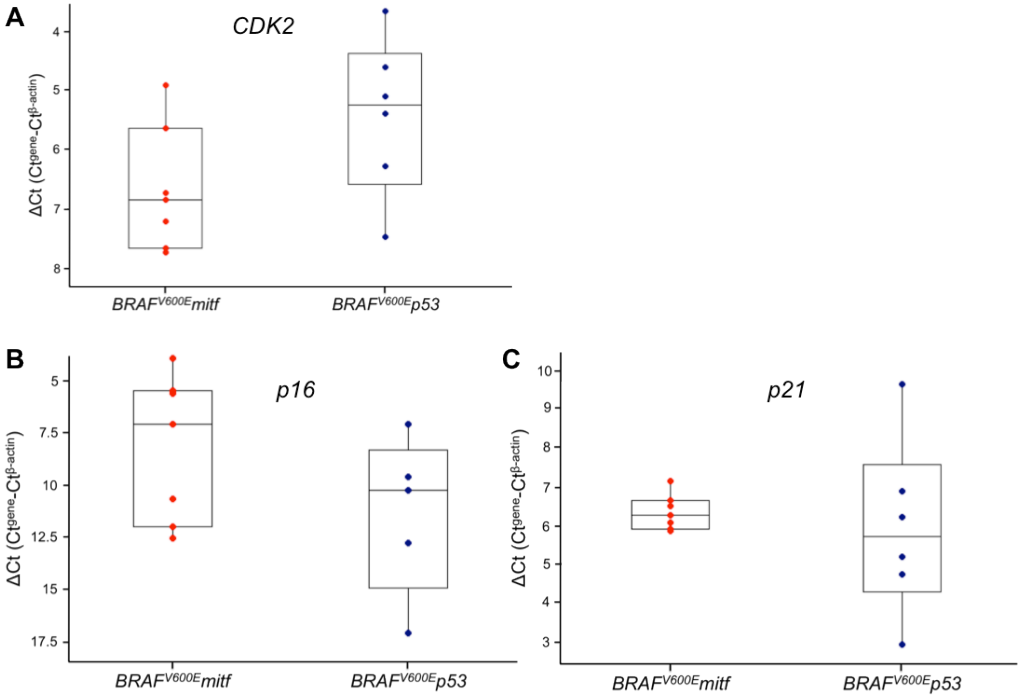

Figure 3.11 Box plots of quantitative real-time PCR of MITF target genes *CDK2* (A), *p16* (B) and *p21* (C). The y-axis shows the difference between the Ct value of the gene of interest and the Ct value of β-actin for each sample.

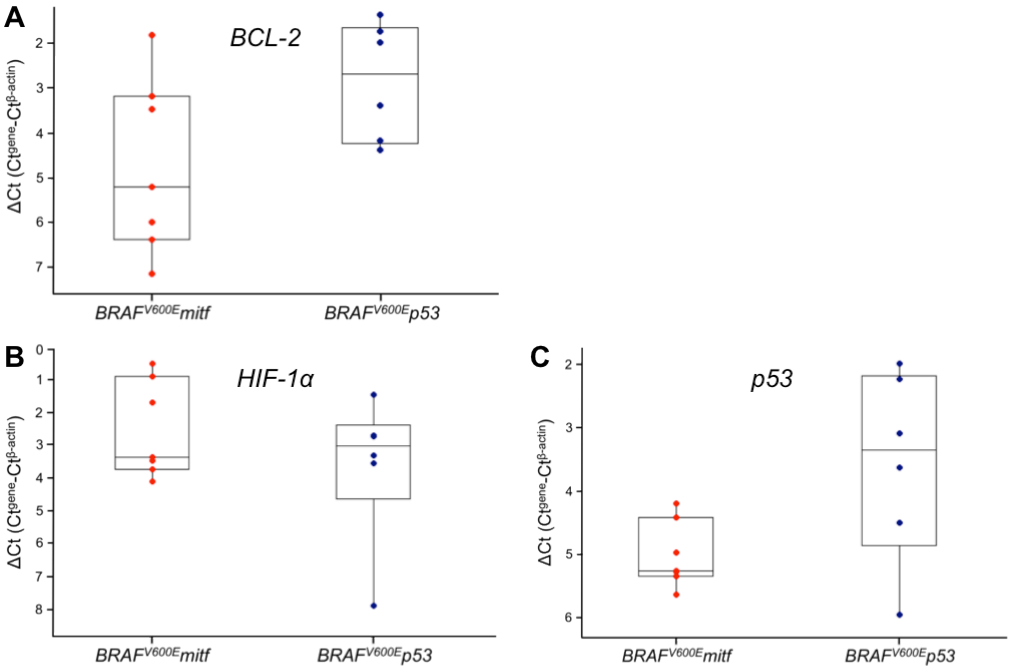

Figure 3.12 Box plots of quantitative real-time PCR of MITF target genes *BCL-2* (A), *HIF-1α* (B) and *p53* (C). The y-axis shows the difference between the Ct value of the gene of interest and the Ct value of β-actin for each sample.

Differentiation genes TYR and DCT are expressed at lower levels in BRAF^{V600E}mitfa^{vc7} tumours

Differences in cycle threshold (Ct) values, which indicate levels of expressed RNA, were observed in other MITF target genes when comparing melanoma subtypes *BRAF^{V600E}mitfa^{vc7}* and *BRAF^{V600E}p53^{M214K}* by qRT-PCR. Pigmentation genes *DCT* and *TYR* were expressed at lower levels in *BRAF^{V600E}mitfa^{vc7}* tumours, indicated by higher Ct values. These values were statistically significant (p=0.00025) (Figure 3.13).

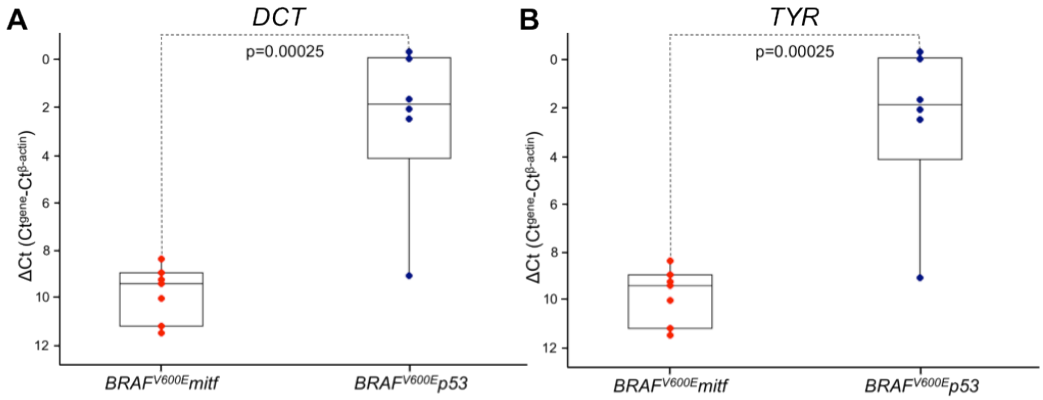

Figure 3.13 Box plots of quantitative real-time PCR of MITF target genes *DCT* (A) and *TYR* (B). The y-axis shows the difference between the Ct value of the gene of interest and the Ct value of β-actin for each sample. Bars represent interquartile range. P-values were calculated using the Student's T-test.

Differential expression of C-MET between melanoma subtypes

Another difference observed between melanoma subtypes was in the MITF target gene, *C-MET* (Figure 3.14). A statistically significant difference in RNA expression was observed between $BRAF^{V600E}mitfa^{vc7}$ and $BRAF^{V600E}p53^{M214K}$ tumours (p=0.00024). $BRAF^{V600E}mitfa^{vc7}$ tumours expressed significantly higher levels of c-met compared to $BRAF^{V600E}p53^{M214K}$ melanoma.

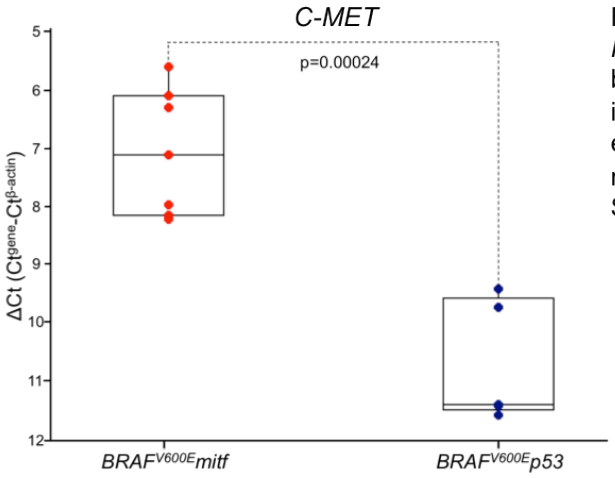

Figure 3.14 Box plot of qRT-PCR of *C-MET*. The y-axis shows the difference between the Ct value of the gene of interest and the Ct value of β-actin for each sample. Bars represent interquartile range. P-values were calculated using the Student's T-test.

3.3 Discussion

'Zebrafish cancer models for a variety of human cancers demonstrate similar features both histopathologically and genetically, underscoring the tight conservation of cancer-related pathways between fish and human' (Liu and Leach, 2011).

In this chapter, I investigated whether previously identified *BRAF*^{V600E}-cooperating mutations *p53* and *mitf* contributed to melanoma pathology. The histopathological characteristics of human melanoma are determined by many factors including genetic background (Whiteman *et al.,* 2011). As an example of this, BRAF^{V600E} melanomas are clinically classified as a subtype of melanoma owing to their histomorpological features (Viros *et al*., 2008). Melanomas with *BRAF* mutations have distinct morphological features including upward migration of intraepidermal melanocytes, thickening of the epidermis and heavy pigmentation (Viros *et al*., 2008). As a consequence, melanoma *BRAF* mutational status can be predicted with ~90% accuracy by simply observing histological features. Using histologically stained sections of zebrafish melanomas, I show for the first time that BRAF^{V600E}-cooperating mutations play an important role in determining pathological features of melanoma.

The growth pattern of melanomas can be a distinguishing subtype-distinct feature. In humans, three different subtypes of melanoma can be differentiated, based on their intraepidermal growth pattern or radial growth phase (Whiteman *et al.,* 2011). Superficial spreading melanoma (SSM), lentigo maligna melanoma (LMM) and acral lentiginous melanoma (ALM) all differ within their early growth phase in which the tumour spreads on the surface of the skin. With SSM in particular, as opposed to LMM and ALM, the growth pattern is described as 'pagetoid,' referring to the resemblance to the intraepidermal spread of breast cancer in the nipple epidermis

(Paget's disease) (Whiteman *et al.,* 2011). SSM also presents with enlarged melanocytes that often aggregate into clusters.

Similar to human melanoma, the *BRAF*^{V600E}*mitfa*^{vc7} zebrafish melanomas contain large, heavily pigmented cells that are not present in the *BRAF*^{V600E}*p53*^{M214K} subtype. They also display a superficial spreading growth pattern with evidence of invasion into the underlying muscle. Characteristic *BRAF*^{V600E}*mitfa*^{vc7} melanoma histological features include the presence of large, heavily pigmented cells throughout the tumour mass, few mitoses and a low degree of nuclear pleomorphism. With these features, an NHS skin pathologist could reliably identify tumours from *BRAF*^{V600E}*mitfa*^{vc7} zebrafish on blind assessment.

As well as their differences in pathology, BRAF^{V600E} melanomas with cooperating mutations in either *p53* or *mitf* also differ in their mitotic activity. *BRAF*^{V600E}*p53*^{M214K} melanomas have increased mitotic activity compared to *BRAF*^{V600E}*mitfa*^{vc7} tumours, a result confirmed by immunostaining for phospho-Histone H3, a marker of late G2/M phase. As expected, *BRAF*^{V600E}*p53*^{M214K} melanomas also have increased levels of p53 mutant protein, providing another method of distinction between these two melanoma subtypes. These results, taken together with those from histopathology, show that there is a strong genotype-phenotype correlation for cooperating mutations that can directly affect growth features and cellular histology.

Although they share some similar features, the histopathology of the *mitfa*^{vc7}*p53*^{M214K} melanomas, which are BRAF^{V600E} – independent, represents a novel phenotype compared to the BRAF^{V600E} melanomas described. The most distinguishing feature of these tumours is their invasiveness nature. Although invasion was observed in the *BRAF*^{V600E}*p53*^{M214K} subtype, it is much more pronounced in this genetic background with tumour masses forcing themselves into areas of musculature and organs. Due to the observation of this aggressive and invasive behaviour it would be useful to determine the mitotic activity within these tumours using immunohistochemical

staining such as phospho-Histone H3. Comparing the number of positively stained cells using the phospho-Histone H3 antibody between *mitfa*^{vc7}*p53*^{M214K} and the other melanoma subtypes, particularly *BRAF*^{V600E}*p53*^{M214K}, would give further insight into the relative degree of aggressiveness of the tumours and how it could relate to a human melanoma subtype.

To further understand how hypomorphic MITF activity contributed to melanoma I assessed the levels of MITF target gene expression in the melanoma subtypes. I used real-time PCR to calculate expression levels of known MITF target genes involved in important cellular processes including proliferation (*CDK2*), differentiation (*TYR, DCT*), cell cycle arrest (*p16, p21*) and survival (*BCL-2, HIF-1α* and *C-MET*). Despite the observed difference in phospho-Histone H3 staining between *BRAF*^{V600E}*mitfa*^{vc7} and *BRAF*^{V600E}*p53*^{M214K} melanomas, expression of *CDK2, p16 and p21* were not significantly different between the melanoma genotypes. There was also no difference between melanoma subtypes in expression, as indicated by cycle threshold values of *p53*, *BCL-2* or *HIF-1α*. Together, these results indicate that despite the lower levels of MITF in *BRAF*^{V600E}*mitfa*^{vc7} melanomas, there is a sufficient level of MITF activity to control those target genes involved in proliferation and cell survival. One striking difference observed from the real-time PCR was the expression of differentiation genes, *DCT* and *TYR*. *BRAF*^{V600E}*mitfa*^{vc7} melanomas expressed both of these genes at a much lower level than *BRAF*^{V600E}*p53*^{M214K} melanomas. In contrast, and unexpectedly, *BRAF*^{V600E}*mitfa*^{vc7} melanomas expressed significantly higher levels of *C-MET* than *BRAF*^{V600E}*p53*^{M214K} melanomas. Although the tumours are known to be heterogeneous, both the low expression of differentiation genes, *DCT* and *TYR*, and the high expression of *C-MET* suggest that hypomorphic MITF activity may maintain melanocytes in a less differentiated state that is more susceptible to BRAF^{V600E} transformation.

It is important to note that the low levels of oncogenic MITF shown here to cooperate with *BRAF*^{V600E} to promote melanoma are distinct from data from both

mouse models and human. As described by Nobukuni and colleagues in 1996, loss-of-function mutations of the MITF gene results in haploinsufficiency of the MITF protein, which is necessary for normal melanocyte development. These mutations are found in individuals with Waardenburg syndrome type 2 (WS2) causing defects in pigmentation and hearing due to the lack of normal melanocytes (Nobukuni *et al*., 1996). To date however, no patient with either WS2 or Tietz syndrome, a similar disease also characterised by pigmentation and hearing defects caused by alterations in MITF, has developed melanoma. This distinction between the low levels of MITF promoting melanoma in the zebrafish and loss-of-function/hypomorph mitf mutants modelled in mice and observed in patients, in which there is no increased incidence in melanoma compared to wild-type, must be recognised. Our temperature-sensitive *BRAF*^{V600E}*mitfa*^{vc7} zebrafish, which has shown that low levels of MITF are oncogenic, has provided the scientific field with a model to assess varying MITF conditions and how these are linked to melanomagenesis.

The differential expression of *C-MET* between BRAF^{V600E} melanoma subtypes was an interesting finding as there is an abundance of genetic and biochemical research demonstrating that the growth and motility hepatocyte factor/scatter factor (HGF/SF) and its receptor MET have a causal role in uncontrolled cell survival, growth, angiogenesis and metastasis, many of the essential hallmarks of cancer (To and Tsao, 1998). In many human cancers overexpression of *MET* contributes to invasive growth and MET activation confers selective advantage to cancer cells in tumour progression and during drug resistance (Stella *et al*., 2010). The overexpression of *MET* accompanies *ras*-mediated cellular transformation (Webb *et al*., 1998) and directly contributes to this *ras*-mediated tumorigenesis and metastasis (Furge *et al*., 2001). As some of the research leading to these findings used melanoma cell lines and *MET* overexpression is found consistently in melanoma it is justified that inhibitors of c-MET are currently in preclinical development (Flaherty, 2006). Inhibitors of MET are also being thought of as part of combination treatment with BRAF inhibition, after it was shown that the tumour microenvironment confers innate resistance to therapy via MET activation (Straussman *et al*., 2012). After RAF

inhibitor treatment of BRAF mutant melanomas, Straussman and colleagues found that stromal cell secretion of HGF resulted in activation of MET, reactivation of MAPK and PI(3)K-AKT pathways and immediate resistance to RAF inhibition. They identified a similar resistance mechanism in both BRAF mutant colorectal and glioblastoma cells lines, suggesting that RAF inhibition in combination with either HGF or MEK inhibition could act as a potential therapy for BRAF mutant cancers (Straussman *et al*., 2012). As I found *C-MET* to be expressed at a higher level in $BRAF^{V600E}mitfa^{vc7}$ melanomas compared to $BRAF^{V600E}p53^{M214K}$, it may be interesting to compare these levels with that found in human melanoma both before and after BRAF inhibitor treatment. High *C-MET* levels identified in this tumour subtype also provide an animal model in which to test novel MET inhibitors and combination therapies with BRAF inhibitors.

Chapter 4 – MITF is essential for melanoma survival

Chapter 4: MITF is essential for melanoma survival

In the first two results chapters I showed how *BRAF*^{V600E} could cooperate with a mutation in *MITF* to drive an individual melanoma subtype. I also showed that *BRAF*^{V600E}*mitfa*^{vc7} melanomas were distinct from those of *BRAF*^{V600E}*p53*^{M214K} background by histopathology and MITF target gene expression.

The aims of this third data chapter are to test if MITF activity is required for melanoma survival in our *BRAF*^{V600E}*mitfa*^{vc7} model and identify the cellular process by which MITF-dependent melanomas regress.

I will first describe how animal models, including zebrafish, have been vital in identifying and confirming the status of *MITF* and other cancer genes. I will then outline examples of tumour regression in relation to melanoma and explain the evidence that MITF could act as a future therapeutic target for melanoma.

In the results section of this chapter, I will demonstrate how the temperature-sensitive nature of the *mitfa*^{vc7} allele in cooperation with the *BRAF*^{V600E} mutation has allowed me to show that loss of MITF causes melanoma regression in zebrafish. With this result I conclude that *MITF* is a critical gene for melanoma survival *in vivo*.

4.1 Introduction

4.1.1 Importance of animal models in establishing a role for cancer genes in vivo

The emergence of animal models has been vital in the establishment of the roles for cancer genes such as *BRAF* and *MITF*. Using *BRAF* as an example, its identification and mechanistic action as an oncogene was established through studies using human tumour samples and cell lines. In the past, one of the limitations of this method was the accessibility of human cancer material, in particular from early stage tumours that could potentially be used to identify genes and pathways involved in tumour progression. To overcome this restriction and aid further understanding of cancer genes, genetically engineered animal models, such as mice and zebrafish, have now been generated. More recently, the availability of primary human melanoma samples for research has greatly improved, although again, samples from early stage tumours are rare. The generation of disease models is therefore vital to improve understanding of disease progression and to test new therapeutics.

As the most commonly found mutation in human melanoma, $BRAF^{V600E}$ has been shown to stimulate constitutive cell signalling and growth factor independent proliferation (Davies *et al*., 2002; Goodall *et al*., 2004; Wellbrock *et al*., 2004; Hoeflich *et al*., 2006; Wellbrock *et al*., 2008). *In vitro* studies have shown that $BRAF^{V600E}$ inhibitors block proliferation and induce apoptosis in melanoma, while *in vivo* studies have shown that they slow the growth of melanoma xenografts. Despite this data confirming that $BRAF^{V600E}$ is necessary for human melanoma survival and progression, an animal model of $BRAF^{V600E}$ in the zebrafish showed that overexpression of $BRAF^{V600E}$ only induces nevi, which do not progress to melanoma unless *p53* is also deleted (Patton *et al*., 2005). In addition to this finding, $BRAF^{V600E}$

was shown to induce classical oncogene-induced senescence (Michaloglou *et al*., 2005). Together, this data implied that in addition to *BRAF*^{V600E}, other genetic or epigenetic alterations are required to drive melanomagenesis. To determine these additional changes, Dhomen and colleagues engineered a *Braf*^{V600E} mouse model of melanoma that emulated the human disease (Dhomen *et al*., 2009). This was an important model as the close similarities between tumours that developed in the mouse model and those observed in human advanced the ability to study melanoma genetics and pathology.

As previously described, despite the success of BRAF inhibitors, many BRAF^{V600E}-treated melanomas develop resistance. This highlights the requirement for additional melanoma pathways to be targeted, and as suggested by Johannessen and colleagues, one of these may involve MITF (2013). Prior to the development of novel therapeutics against targetable pathways however, our understanding of these must be improved through study, for example, of animal models. Das Thakur and colleagues provide one standout example of the use of an animal model in melanomagenesis (2013). They developed two primary human melanoma xenograft mice models to study the cause and consequences of vemurafenib resistance in BRAF^{V600E} mutant melanomas. Drug resistance was selected for by continuous vemurafenib administration and it was found that resistant tumours showed 'continued dependency on BRAF^{V600E} → MEK → ERK signaling owing to elevated BRAF^{V600E} expression' (Das Thakur *et al*., 2013). They also found that vemurafenib resistant tumours became drug dependent for their continued proliferation, as when drug treatment was stopped the established drug-resistant tumours regressed. Das Thakur and colleagues went on to show that a discontinuous dosing strategy using vemurafenib would delay the onset of lethal drug-resistant disease and suggest that this alternative therapeutic approach may improve the durability of the vemurafenib response. The xenograft mice used in this study demonstrate the importance of using animal models to study human disease.

In the subsequent results section of this chapter, I will present evidence that MITF may be a potential target for melanomagenesis. Zebrafish models of melanoma have been engineered and, for the first time, provide *in vivo* data to show that MITF is essential for $BRAF^{V600E}$ – driven melanoma survival.

4.1.2 Melanoma regression and MITF as a potential therapeutic target

In 2010, the first trial of PLX4032 (Plexxikon and Roche), an orally available inhibitor of mutated BRAF, was conducted in humans (Flaherty *et al*., 2010). Using a dose-escalation method of administration, treatment of the drug in 16 patients with $BRAF^{V600E}$ mutant melanoma resulted in 10/16 having a partial response and one having a complete response, while in patients with metastatic disease, 24/32 showed a partial response while two had a complete response (Flaherty *et al*., 2010). For all patients receiving BRAF inhibitor treatment, PLX4032 induced either partial or complete regression in 81% of patients and produced a median progression-free survival estimate of more than 7 months (Flaherty *et al*., 2010). The 'response' referred to here indicates regression, both partial and complete as stated. In pre-clinical trials using human melanoma tumours transplanted onto immune-compromised mice, the drug first simply inhibited the growth and then at higher concentrations induced regression (Tsai *et al*., 2008). The promising results from both the mouse and human trials with PLX4032 meant that the drug was accelerated through clinical trial phases quickly, a trend that has been observed for other target cancer drugs such as crizotinib, an ALK inhibitor used to treat non-small cell lung carcinoma (Chabner, 2011). Targeting *c-KIT* mutant melanomas using tyrosine kinase inhibitors such as imatinib have also been shown to lead to tumour regression. Imatinib mesylate is the most well established tyrosine kinase inhibitor for melanomas harboring *c-KIT* mutations with response rates of more than 20% in two separate clinical human trials (Guo *et al*., 2011; Carvajal *et al*., 2011). As well as molecular targeted therapy, targeted immunotherapy has also proved to be an important direction for research and therapeutic development in the treatment of

melanoma. This concept relies on the idea that tumours are immunogenic and can independently stimulate an immune-mediated anti-tumour response (Liu and Colegio, 2013). In early studies, melanoma patients were treated with a human antibody to cytotoxic T-lymphocyte antigen-4 (anti-CTLA-4) and results showed both complete (2/56) and partial (5/56) tumour regression (Attia *et al*., 2005). More recently, a monoclonal antibody known as ipilimumab, which acts by promoting T-cell activation, has been shown to elicit anti-tumour effects on melanoma (Hodi *et al*., 2010). Results of initial trials using this treatment regime were promising but improved significantly in combination with dacarbazine, a common chemotherapeutic agent (Robert *et al*., 2011). Future treatment regimes for melanoma patients are leading in the direction of combination therapies including BRAF inhibitors with MEK inhibitors (discussed in Chapter 2) and immunotherapy. An interesting finding that connects these two methods of treatment is that BRAF inhibitors increase the expression of melanocyte differentiation antigens, which is associated with improved recognition by antigen-specific T lymphocytes (Boni *et al*., 2010). This result suggests that combining BRAF inhibition with an immunotherapy such as ipilimumab could improve tumour response rates compared to individual treatment regimes.

As described in Chapter 2, MITF is a potential therapeutic target in melanomas treated with BRAF inhibitors that have developed resistance. BRAF inhibition with vemurafenib has been shown to cause an increase in MITF levels (Smith *et al*., 2013), a result that suggests a potential to include MITF inhibitors in combination therapy to overcome resistance mechanisms. As a transcription factor without a ligand dependency, aiming to target MITF incurs difficulties, however HDAC inhibitors have been shown to repress MITF expression in both clear cell carcinoma and melanoma cells (Yokoyama *et al*., 2008). It is well established that inhibiting oncokinases, such as BRAF in melanoma, is the foundation of current, successful cancer treatments but also that this therapeutic strategy is hindered by innate drug resistance mediated by upregulation of the HGF receptor, MET (Webster *et al*., 2014). In a recent study, lineage-specific MET enhancers were identified, including a

melanoma-specific enhancer downstream of the MET TSS that displayed inducible chromatin looping with the MET promoter to upregulate MET upon BRAF inhibition (Webster *et al*., 2014). Interestingly, the study also found that MITF mediates this enhancer function and that deleting the MITF motif in the MET enhancer suppresses inducible chromatin looping and drug resistance, while maintaining MITF-dependent, inhibitor-induced melanoma cell differentiation (Webster *et al*., 2014). This result demonstrates how MITF can be targeted in a novel way to block resistance to BRAF inhibition.

4.2 Results

4.2.1 Regression of tumour growth in BRAF^{V600E}mitfa^{vc7} mutants at 32°C

Melanoma developed in *BRAF^{V600E}mitfa^{vc7}* fish after 3 months at <26°C (Figure 2.3). To test the role of MITF in these tumours, I utilised the temperature-sensitive nature of this genetic cross to control the levels of MITF. By upshifting the fish to static tanks at 32°C after the tumours have developed at <26°C, I could observe changes that occurred when the level of MITF activity is insufficient to promote melanocyte development. Photographs were taken before and after the upshift to track any changes in tumour growth.

It is noteworthy that at the restrictive temperature of 32°C, Johnson and colleagues (2011) confirmed that none of the aberrant *mitfa^{vc7}* splice products are sufficient for melanocyte development and MITF activity is not required to maintain the activity of the *mitfa* promoter fragment driving the *BRAF^{V600E}* transgene (Dooley *et al*., 2013).

Twelve *BRAF^{V600E}mitfa^{vc7}* fish with tumours grown at <26°C were upshifted to 32°C for 2 weeks. Before and after photographs were taken of each fish to identify changes that had taken place during the upshift period at 32°C. After 2 weeks, 8/12 melanomas had dramatically regressed (Figure 4.1). This was clear simply by observation, as the tumour pigmentation and size had significantly reduced.

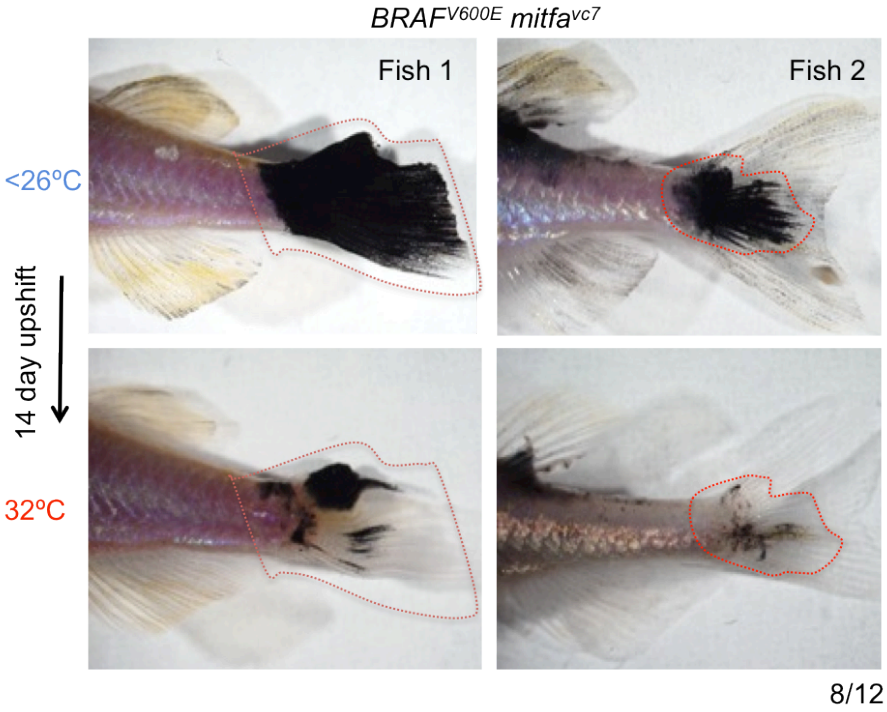

Figure 4.1 Two adult *BRAF*^{V600E} *mitfa*^{vc7} zebrafish grown at a semi-permissive temperature, <26°C, develop melanoma in tail region (top panel). Fish are then transferred to water at 32°C for 14 days. Red dotted lines outline the tumours before and after the temperature shift. Image is representative of 8/12 fish upshifted that showed tumour regression.

The upshift experiment was also continued for a total of 2 months with 15 *BRAF*^{V600E}*mitfa*^{vc7} fish. After 2 months at the upshift temperature of 32°C, 12/15 very large tumours had regressed and 6/15 showed complete regression, as well as healing at the tumour site (Figure 4.2).

In an additional experiment, *BRAF*^{V600E}*mitfa*^{vc7} zebrafish that showed melanoma regression at the restrictive temperature (32°C) were transferred back to the semi-permissive temperature (<26°C). Despite the striking loss of tumour mass that occurred after 2 weeks at 32°C, after one month at <26°C melanomas recurred (6/6). I hypothesise that there is a small subpopulation of melanoma cells with very low or no MITF levels that are able to survive. It is also possible that during upshift at 32°C, the tumour microenvironment is maintained and acts as a niche for the recurring tumours. After the tumour regression and subsequent temperature downshift to <26°C for one month, this population of melanoma cells is able to repopulate the original tumour site. This is shown by the observation that tumours recur in the same original location of the zebrafish.

Figure 4.2 Adult *BRAF*^{V600E} *mitfa*^{vc7} zebrafish grown at <26°C, then transferred to water at 32°C for 2 months. Red dotted lines outline the tumours before and after the temperature shift.

4.2.2 BRAF^{V600E}p53$^{M214K/M214K}$ mutants at the restrictive temperature do not regress

To confirm that the melanoma regression was due to the change in levels of MITF and not the temperature of the water, the upshift experiment was carried out with *BRAF^{V600E}p53^{M214K}* fish, which do not have a mutation in *mitf*. Six *BRAF^{V600E}p53^{M214K}* zebrafish with melanomas were upshifted to 32°C for 2 weeks as a control. In 6/6 fish, no melanoma regression was observed and the tumours continued growing (Figure 4.3). Additional nodules also formed within the tumours of the controls during the temperature upshift period. This result confirms that tumour regression is not induced by changes in water temperature.

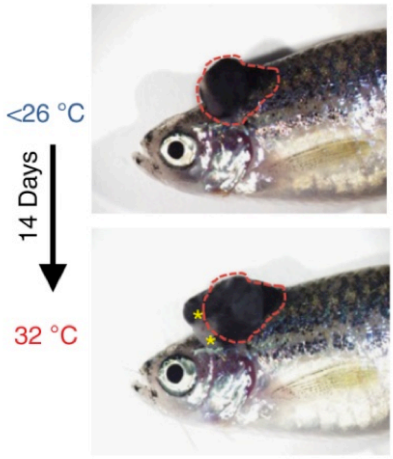

Figure 4.3 Control *BRAF^{V600E} p53* zebrafish grown at <26°C, then transferred to water at 32°C for 14 days. Red dotted lines outline the tumours before and after the temperature shift. Yellow asterisks show areas of increased tumour growth.

4.2.3 Mechanism of regression in BRAF^{V600E} melanomas involves macrophage infiltration and apoptosis

To understand the mechanism of *BRAF^{V600E}mitfa^{vc7}* tumour regression, I aimed to capture a time point at which the tumour had began to regress but some tumour tissue still remained. To do this, I upshifted 7 *BRAF^{V600E}mitfa^{vc7}* fish with tumours to the restrictive temperature (32°C) for 7 days. After this time, melanoma regression was obvious by eye, however tumour tissue was still present indicating only partial regression. I analysed the melanoma regression in progress by sacrificing the fish at this stage.

Histological analysis of these partially regressing tumours allowed us to understand the mechanism of regression. By haematoxylin and eosin (H&E) staining, I could observe the extent to which the tumour had regressed and showed that the regression was characterised by marked loss of tumour density and an accumulation of heavily pigmented macrophages (Figure 4.4A). In 7/7 of partially regressing *BRAF^{V600E}mitfa^{vc7}* melanomas, these characteristics were present.

Our initial hypothesis as to the mechanism of regression, after observation of the characteristics shown by H&E staining, was apoptosis. This was largely due to the presence of large melanophages within the regressing melanoma, which may have played a role in clearance of the dying or dead tumour cells, brought about by apoptosis. To address whether apoptosis contributed to the regression mechanism I stained sections of the partially regressing *BRAF^{V600E}mitfa^{vc7}* melanomas with an antibody to detect active (cleaved) caspase-3 (Adams *et al*., 2007) (Figure 4.4B). I found that high levels of active (cleaved) caspase-3 were present in these regressing tumours (5/5). In contrast, as a control, I also stained non-regressing *BRAF^{V600E}mitfa^{vc7}* melanomas with the same antibody and no activity was observed (5/5).

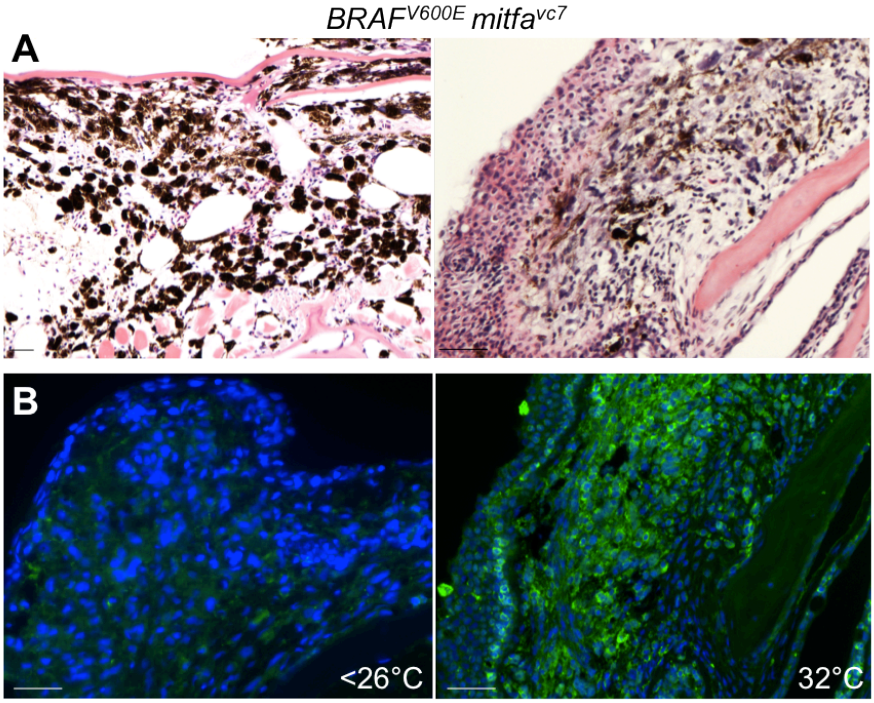

Figure 4.4 Melanoma regression in *BRAF*^{V600E}*mitfa* melanomas is associated with melanophage infiltration and apoptosis.
A. H&E staining of regressing *BRAF*^{V600E}*mitfa* melanomas with melanophage infiltration (Scale bars=200μm(left); 100μm(right)).
B. Cleaved caspase-3 antibody (green) and DAPI (blue) staining of non-regressing (<26°C) and regressing (32°C) *BRAF*^{V600E}*mitfa* melanomas. Scale bars=50μm.

4.2.4 Regression of tumour growth in mitfa^{vc7} p53^{M214K} (BRAF^{V600E}-independent) mutants at 32°C

To take further advantage of the temperature-sensitive nature of the mitfa^{vc7} allele and test the dependence of *mitfa^{vc7}p53^{M214K}* melanomas on MITF, I upshifted *mitfa^{vc7}p53^{M214K}* zebrafish with pre-established tumours grown at 28°C, to 32°C for 14 days. Before, during and after the upshift period, I took photographs of the zebrafish to record external, visible changes in the tumours. I observed melanoma regression in 11/11 *mitfa^{vc7}p53^{M214K}* zebrafish upshifted to 32°C for 14 days, visible by reduced tumour size and pigmentation (Figure 4.5). The experiment was continued for a subsequent 14 days and continued regression was observed 28 days post-upshift.

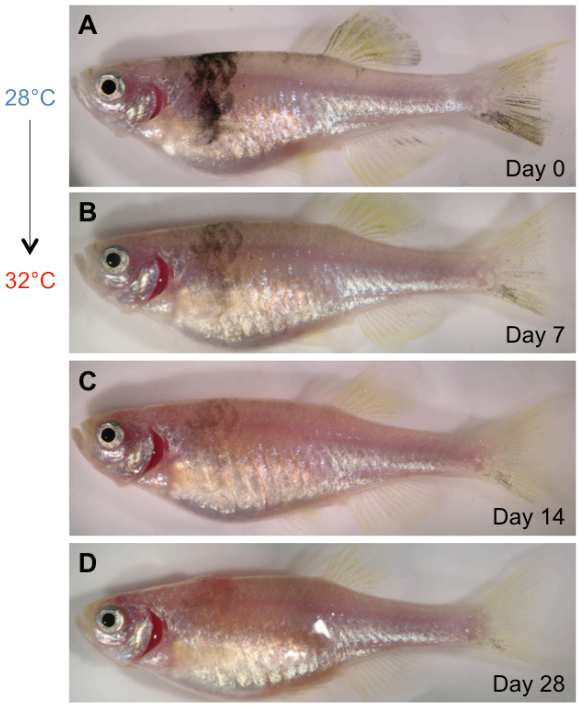

Figure 4.5 *mitfa^{vc7}p53^{M214K}* melanoma is dependent on MITF for survival. Adult *mitfa^{vc7}p53^{M214K}* zebrafish develops nevus/melanoma at 28°C (A). *mitfa^{vc7}p53^{M214K}* zebrafish with established nevus/melanoma is upshifted to 32°C for 7 days, after which regression is visible (B). Continued temperature upshift at 32°C for 14 days (C) shows progressive regression, until almost no pigmentation is visible after 28 days (D) .

4.3 Discussion

Aside from the identification of the somatic mutation, $MITF^{E318K}$ (Bertolotto *et al*., 2011, Yokoyama *et al*., 2011), *MITF* mutations in human melanoma are rare compared to *MITF* amplifications, which are found in 10-20% of melanomas. Garraway and colleagues first identified *MITF* as an amplified oncogene in melanoma using integrated SNP array and expression profile analyses. They also found that these amplifications were more prevalent in metastatic disease and correlated with a reduced patient survival rate and that MITF cooperates with oncogenic BRAF to transform melanocytes (Garraway *et al*., 2005). MITF is expressed in most human melanomas and its continued expression is essential for the survival of melanoma cells as well as for their proliferation (Levy *et al*., 2006). Its expression however, is much lower in melanoma cells than normal melanocytes and if increased, melanoma cell proliferation is reduced, even in the presence of oncogenic BRAF (Wellbrock and Marais, 2005). High expression of MITF has also been shown to reduce melanoma cell tumorigenicity (Levy *et al*., 2006). In 2007, Gray-Schopfer and colleagues proposed that 'MITF regulates distinct functions in melanocytic cells at different levels of expression,' suggesting that levels of MITF protein must be carefully controlled in a melanoma environment to maintain tumorigenicity (Gray-Schopfer *et al*., 2007). MITF expression levels vary considerably between melanoma specimens; in some they are high (in cases of amplifications) and in others expression is low or decreased (Steingrímsson *et al*., 2004).

How can MITF be simultaneously lost and amplified during melanoma progression?

The discovery of *MITF* amplifications highlights the need for melanoma cells to be able to maintain a sufficient level of MITF activity for survival, in the presence of oncogenic BRAF. A common feature of melanomas therefore, may involve the

maintenance of sufficient levels of MITF activity for survival and proliferation, or in other words, carefully regulating the MITF rheostat described by Carreira and colleagues (2006). The rheostat model provides a framework to further our understanding of the role of MITF in both melanocyte development and its opposing pro- and anti-proliferative roles in melanoma progression (Carreira *et al*., 2006). In melanoma, the balance of MITF activity must be finely regulated. Both high levels of MITF that promote cell cycle arrest and differentiation, as well as lower levels, which lead to cell cycle arrest and apoptosis must be restricted (Carreira *et al*., 2006). The rheostat accounts for MITF function in melanoma and provides a model in which low MITF is a hallmark of stem cell-like cells and higher MITF levels promote proliferation or differentiation (Carreira *et al*., 2006). Although we now understand that different levels of MITF promote different cellular phenotypes, what controls this MITF rheostat is still unclear. One possibility is simply that MITF levels control it, but other factors including post-transcriptional modifications and the transcriptional regulation of downstream target genes may also be important.

Our *BRAF*^{V600E}*mitfa*^{vc7} melanoma model shows that low levels of MITF are oncogenic with BRAF^{V600E} and, for the first time, MITF is required for the survival of melanoma *in vivo*. By taking advantage of the temperature-sensitive nature of the *mitfa*^{vc7} allele, I have shown that upshifting established *BRAF*^{V600E}*mitfa*^{vc7} tumours grown at <26°C to 32°C causes regression due to insufficient MITF levels. From this result, we can confirm that *BRAF*^{V600E}*mitfa*^{vc7} melanomas are dependent on MITF for their maintenance.

As I have shown that depleting endogenous MITF activity *in vivo* causes dramatic tumour regression, we can speculate that MITF may be a good therapeutic target. The current status of melanoma treatment remains challenging due to the recurrence of tumours after BRAF^{V600E} inhibition (Das Thakur *et al*., 2013). The ability to use combination therapies that target alternative melanoma pathways is therefore essential to improve patient survival. Our work suggests that MITF may be a potential target and an effective approach to melanoma therapy, which correlates

with research from the literature attempting to target MITF using different approaches.

CDK2 has been shown to be a target gene of MITF (Du *et al*., 2004) and therefore one approach to target melanomas with amplification of *MITF*, as well as a *BRAF* mutation was to use a combination of CDK2 and BRAF inhibitors. Du and colleagues found that depletion of CDK2 suppressed growth and cell cycle progression in melanoma and, as CDK2 activity is tightly regulated at the transcriptional level by MITF, it also represents an additional drug target in melanoma.

A second pharmacological approach by Yokoyama and colleagues (2008) utilised histone deacetlyase (HDAC) inhibitors to suppress MITF and promote anti-melanoma efficacy *in vitro* and in mouse xenografts. One of the problems of targeting MITF is that it is a transcription factor that is not dependent on ligand binding. This means that drugs cannot simply be designed that will block its transcriptional activation. Despite this disadvantage, Yokoyama and colleagues showed that HDAC inhibitors could antagonize MITF specifically in melanocytes through transcriptional downregulation of the MITF promoter. This suggests that HDAC inhibitor drugs are potential candidates as therapeutics to target conditions affecting the melanocyte lineage, including melanoma (Yokoyama *et al*., 2008).

There is potential for MITF inhibitors to be part of future melanoma therapeutics as MITF is a lineage survival factor in melanocytes and many melanomas retain and depend on MITF as a survival factor. It is possible therefore to suspect that even for melanomas without an MITF amplification, targeting against MITF may be therapeutically beneficial. McGill and colleagues for example showed that suppression of MITF expression was lethal to most melanoma cell lines, causing apoptosis that could be rescued by overexpression of BCL2, an MITF target gene (McGill *et al*., 2002).

In contrast to the potential use of MITF inhibitors described, it is expected that a subset of melanomas with downregulated or loss of MITF will not respond to MITF-targeted therapeutics. From our data, it is also important to note that while targeting MITF may be effective in a melanoma therapeutic setting, we must address this strategy with careful attention as we have also shown that low levels of MITF are oncogenic.

Our results also highlight the variation of MITF expression observed in human melanoma samples and this would have a direct effect on the therapeutic range for which MITF inhibitors may be beneficial. I found that 4/12 $BRAF^{V600E}$ $mitfa^{vc7}$ tumours did not regress when temperature was increased to 32°C, at which levels of MITF were reduced. Explanations for this could include differences in initial levels of MITF expression or the degree of melanoma progression prior to the temperature upshift. These tumours may also possess additional mechanisms to overcome MITF shutdown, similar to those identified for BRAF inhibition resistance. Whatever the reason for this divergence, it is important for the way in which MITF inhibitor treatment is managed. MITF inhibitors may prove beneficial to some patients not others and, like trials with the BRAF inhibitor vemurafenib, prolonged use of the drug may lead to tumours developing resistance. As suggested by Das Thakur and colleagues (2013), it may be important to take drug 'holidays' during treatment regimes to prolong their use and prevent resistance developing.

Chapter 5 – Melanoma genomic mutation and expression landscape

Chapter 5: Exploring the melanoma genomic mutation and expression landscape

In Chapter 4, I showed how *BRAF*^{V600E}-cooperating mutations *mitf* and *p53* play an important role in determining pathological features of melanoma and are responsible for drive two distinct melanoma subtypes.

In this final data chapter, my aims are to explore the gene expression landscape of *BRAF*^{V600E}*mitfa*^{vc7}, *BRAF*^{V600E}*p53*^{M214K}, and *BRAF*^{V600E}*mitfa*^{vc7}*p53*^{M214K} melanomas using RNA-seq and identify novel mutations in these tumour samples through exome sequencing. This was an important part of my research, as it would not only identify differences in gene expression that characterise the individual melanoma subtypes, but also has the potential to discover new genes and pathways involved in melanomagenesis.

I will first introduce the current melanoma target genes that have been identified through multiple sequencing projects and briefly describe the protocol taken to acquire data from RNA-seq (in collaboration with Genepool, Dr James Prendergast, Graeme Grimes and Dr Ian Overton) of my zebrafish melanomas. I will then describe the results from the exome sequencing (in collaboration with Jennifer Yen, Sanger Institute, Hinxton) and RNA-seq of the zebrafish melanomas collected from different genetic backgrounds.

5.1 Introduction

5.1.1 Current melanoma target genes identified by sequencing methods

The advances in genomic technologies have allowed us to gain better understanding of melanoma genetics. Techniques have progressed from single candidate gene- and family- sequencing to whole exome- and genome-sequencing. This has greatly improved our ability to identify new drug targets and develop personalised therapeutics for melanoma patients.

The mutational burden of melanoma is greater than that of other cancer types, as it harbours a larger number of genomic changes. The reason for this is the major environmental factor that influences melanoma development, UV light, which induces point mutations that cause cytosine to thymidine (C>T) nucleotide substitutions (Pleasance *et al*., 2010). Mutated genes are classified as either oncogenes or tumour suppressors and the mutations themselves are either drivers or passengers. To distinguish between driver and passenger mutations, four characteristics are taken into account: recurrence; non-synonymous to synonymous (N:S) ratio; bioinformatic analysis; and biochemical or biological analysis (Walia *et al*., 2012).

Primary studies using candidate gene sequencing, a technique that focused on genes that had a previous association with cancer, identified mutations in genes including *p14* and *p16* in melanomagenesis. These mutations were accountable for only a small proportion of sporadic and familial melanomas (Chin, 2003). Additional genes with identified mutations using this early, basic type of sequencing include *BRAF*, *NRAS*, *CKIT*, *MITF, GNAQ* and others.

After completion of the human genome project, single candidate gene identification progressed to candidate gene family sequencing. Using this technique, hundreds of genes could be studied at once instead of singly, allowing a faster and more high-throughput approach. The protein tyrosine kinase (PTK) family of genes was the first family to be fully sequenced using this method. It was chosen because many members of this family had already been associated with tumorigenesis and, as part of the kinase superfamily they were known to be susceptible to pharmalogical inhibition and so were potential new drug targets. Prickett and colleagues (2009) carried out the mutational analysis of this gene family in cutaneous metastatic melanoma and identified 30 somatic mutations affecting the kinase domains of 19 PTKs in 79 melanoma samples. The study found *ERBB4* to be the most commonly mutated PLK gene, with mutations resulting in increased kinase activity and transformation ability (Prickett *et al.* 2009). This result showed that candidate gene family sequencing could identify mutations in genes within families and these could be used as potential new therapeutic targets.

Although sequencing gene families proved to be a powerful tool to identify melanoma candidate genes, new high-throughput technologies became available that allowed whole exomes and genomes to be sequenced. Wei and colleagues carried out the first exome-wide study of melanoma in 2011. They performed exome-sequencing of 14 matched normal and metastatic tumour samples from untreated melanoma patients (Wei *et al*., 2011). The study identified 68 genes that were 'somatically mutated at an elevated frequency' and most importantly found a previously unidentified gene, *GRIN2A*, mutated in 33% of the melanoma samples (Wei *et al*., 2011). *GRIN2A* is part of a family of genes that encode glutamate receptors that bind NMDA. Together the data from Prickett and colleagues (2011) showing that 16% of melanomas have mutations in *GRM3*, and Shin and colleagues (2008) showing that the expression of *GRM1* results in melanocyte transformation, implicates the importance of glutamate receptor signalling in melanoma.

In contrast to whole-exome sequencing, which was fruitful in its ability to identify new cancer genes as described above, whole-genome sequencing provided a more in-depth investigation into mutational changes, including those within regulatory gene regions. In 2010, Pleasance and colleagues described the first whole-genome study of melanoma, comparing somatic mutations found in malignant melanoma and lymphoblastoid cell lines derived from the same patient. Missense mutations were identified in two novel cancer genes, *SPDEF* and *UVRAG* and overall the study showed that DNA repair mechanisms were initiated preferentially at transcribed DNA regions rather than those untranscribed (Pleasance *et al*., 2010).

As sequencing technologies have progressed from single-gene to whole-genome so has our ability to learn more about the human genome and the way it is altered in, for example, cancer. Our approach to carry out RNA-seq/whole transcriptome shotgun sequencing (WTSS) of zebrafish melanomas from different genetic backgrounds was chosen with the aim to explore their expression landscape and identify to changes in gene expression between melanoma subtypes.

5.1.2 Whole transcriptome shotgun sequencing (WTSS) (RNA-seq) of tumour tissue from zebrafish melanomas

The approach I took to explore the expression landscape of melanoma involved the preparation of RNA from zebrafish melanomas, paired-end transcriptome sequencing (carried out by an University of Edinburgh-based company, Genepool) and bioinformatical analysis of the output reads. Details of RNA preparation and quality control testing are detailed in Chapter 7: Material and Methods.

Prepared RNA from 34 zebrafish melanomas was sent to Genepool, a next-generation genomics and bioinformatics facility based within the School of Biological Sciences at The University of Edinburgh (http://genepool.bio.ed.ac.uk). Here, an Illumina platform was used to carry out paired-end sequencing of the tumour samples from different genetic backgrounds.

The more recent development of next generation sequencing (NGS) has allowed for the sequencing of RNA transcripts and, as a consequence, the ability to investigate alternative splicing, gene fusion, post-translational modification and changes in gene expression. Prior to NGS, these types of transcriptome and gene expression level change studies were carried out using expression microarrays. An expression (or DNA) microarray is a collection of DNA sequences that are spotted onto a solid surface, which is then used to measure expression levels of many genes at the same time. One advantage that RNA-seq has over expression microarrays is the depth of coverage obtained. The arrays used were only ever as good as the database they were designed from, so for this reason they had a limited application. Importantly for my project, many types of cancer are caused by very rare mutations and would be undetectable using microarrays. NGS technologies such as RNA-seq are therefore essential tools to identify small, but important, changes in gene expression, which

could lead identification of novel therapeutic targets. For this reason, RNA-seq technology was chosen as the technique to use for this project with an aim to understand the genetic expression landscape of zebrafish melanomas. Combining RNA-seq and exome sequencing in this project is also advantageous as it allows detection of both gene mutation and expression.

To summarise the RNA-seq workflow in brief, the RNA prepared from the sample tissue is converted to cDNA through a process of fragmentation. From the cDNA, short reads are obtained and then aligned to the reference genome, which can then be classified as exonic, junction or poly (A) reads to form a comprehensive, base-resolution expression profile (Wang *et al*., 2009). An Illumina platform is then used to carry out paired-end transcriptome sequencing and produces millions of reads, which can then be aligned to a reference genome and analysed further by bioinformatics.

5.2 Results of exome sequencing

In collaboration with Dr Jennifer Yen, Dr Derek Stemple and Professor Andy Futreal (Wellcome Trust Sanger Institute, Hinxton, UK), we carried out exome sequencing of zebrafish melanomas to explore their genetic heterogeneity and mutational burden (Yen *et al*., 2013).

My role in this study was to provide melanoma and non-tumour samples from $BRAF^{V600E}$ – driven transgenic zebrafish. The protein coding exons of these samples, in combination with melanomas from $NRAS^{Q61K}$ mutant zebrafish, were sequenced. The main finding from the exome sequencing was that, surprisingly, the engineered zebrafish melanomas harboured a low mutational burden with a strong, inverse association with the number of initiating germline driver mutations (Figure 5.1; Yen *et al*., 2013). The number of coding mutations identified in the zebrafish samples was significantly lower that that previously reported in human melanoma (4 as opposed to 171, Krauthammer *et al*., 2012). As well as a low number of substitutions, the study identified very few recurrent mutations, providing evidence that very few additional mutations are required to drive melanomagenesis in $BRAF^{V600E}$ and $NRAS^{Q61K}$ – driven transgenic zebrafish. This result also suggests that these models could be used to estimate the number of events in human cancer. A reassuring finding was that 60% of the genes mutated in the zebrafish melanomas were also found with at least one mutation in human melanoma.

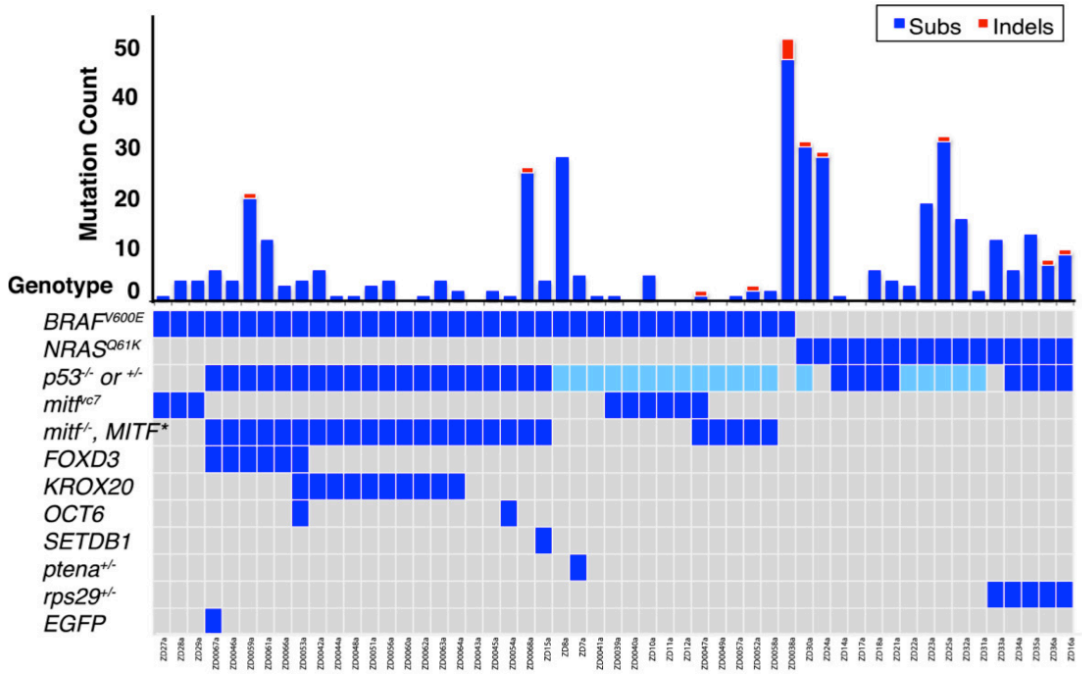

Figure 5.1 An overview of the substitutions and indels identified in engineered zebrafish melanomas. (adapted from Yen *et al*. (2013))
Graph shows the total number of substitutions (blue) and indels (red) identified per sample. The lower shaded area shows the initiating germline mutation of each sample. For p53 mutations, light blue indicates *p53*$^{+/-}$ and dark blue corresponds to *p53*$^{-/-}$ mutations. The asterisk marks *mitf:MITF* expression in an *mitf*$^{-/-}$ background.

One aspect of the study involved the comparison of UV- and non-UV- mutational spectra. Recent studies have shown that more than half of the driver mutations identified in human melanoma are not associated with the UV radiation signature. As the zebrafish melanoma samples were collected from an environment without UV light exposure, they could be used as an example of a UV-independent dataset. Consistent with other human cancers, including melanoma, the most common mutational change identified in the zebrafish melanomas was the C > T substitution. This type of change accounted for 24.4% of the total number of mutations identified across all samples in the experiment. As reported by Krauthammer and colleagues (2012), like melanomas from non sun-exposed areas, zebrafish melanomas showed no significant bias in mutations from any class on any strand. This is in contrast to human melanoma from sun-exposed areas, which have a characteristic UV mutation signature and a mutation strand-bias due to transcription-coupled repair. The loss of

this signature in the zebrafish melanomas suggests that these repair pathways are not activated unless they are triggered by a stress or DNA damage factor such as UV.

The presence of indels in the melanoma samples from zebrafish was much lower than the average identified in human melanoma (Figure 5.1; Krauthammer *et al*., 2012). One interesting result however, was the identification of a single nucleotide deletion that resulted in a frameshift mutation in *pik3ip1*. This gene is a negative regulator of PI3K and has a known role in cancer as a suppressor of hepatocellular carcinoma development (He *et al*., 2008). The mutation was identified in one of the $BRAF^{V600E}$ melanoma samples that I provided for the study. The identification of this mutation in this particular sample is consistent with a role for PI3K cooperation with MAPK deregulation in human melanoma, as first described by Davies in 2012.

One of the key findings of this sequencing project was the identification of a recurrently amplified region in a subset of melanoma samples. The most frequently amplified genes in this region were *prkacaa*, *samd1*, *as1ba*, *wu:fj41e11* and *tecra*. No evidence of amplification of these genes has been found in human cancer datasets or other melanoma studies. In addition to these genes, another gene called *tert* was found to amplified in fewer zebrafish melanoma samples but with statistical significance. The *tert* gene is of interest in particular as it is the only known cancer gene that is recurrently mutated in this dataset. *TERT* is amplified in human melanoma (Garraway *et al*., 2005 and Hodis *et al*., 2012) and has promoter mutations in 90% of melanoma patients (Huang *et al*., 2013 and Horn *et al*., 2013).

Among the homozygous deletions identified in this zebrafish melanoma sample set were four *nitr* genes from the novel immune type receptor family found in teleosts. Unlike immune receptors, these genes do not rearrange, but show structural similarities to the T-cell and Ig-like receptors found in mammals. The loss of these genes could be relevant in cancer progression in terms of their ability to avoid

immune surveillance, consistent with a critical role for immune regulation in human melanoma (Miller and Mihm, 2006).

The final analysis of the exome sequencing looked at the functional characterization of the most frequently mutated genes in the zebrafish melanomas. Like human cancers, the zebrafish melanomas were highly heterogeneous and the majority (68%) of genes were mutated in only one tumour sample. Using KEGG pathway analysis, it was shown that although most genes are not frequently mutated and significant alone, the biological pathways to which they belong are significantly mutated. Importantly, the most enriched pathways identified in this study are directly linked to the hallmarks of cancer – apoptosis and VEGF signalling. The MAPK signalling and cell cycle pathways were also found to have significant enrichment in this study, supporting functions important in human melanoma development.

In summary, this study was the first to describe the spectrum of sporadic coding mutations in an engineered model of melanoma. The analysis of the exome sequencing described provides an understanding of the genetic paths that lead to melanomagenesis in *BRAF*- and *NRAS*- driven melanoma models. It also provides the field with a standard for further studies using engineered animal models of cancer, including melanoma.

5.3 Results of transcriptome sequencing

5.3.1 Alignment of raw reads to the zebrafish transcriptome

The raw reads produced from the RNA-seq were first aligned to the reference genome, in this case the latest assembly of the zebrafish genome, Zv9 (Howe *et al*., 2013) using TopHat (Trapnell *et al*., 2009). The reads were mapped using a tool called Bowtie (Langmead *et al*., 2009), one of the applications available on an in-house Galaxy server – a general-purpose platform for computational biology that supports RNA-seq analysis. Read counts were then estimated using Cufflinks (Trapnell *et al*., 2010), another application available on the Galaxy server.

5.3.2 Differential gene expression between melanoma subtypes

The approach I took to explore the differences in gene expression between our melanoma subtypes was using a method called DESeq. This is based on the 'negative binomial distribution, with variance and mean linked by local regression' (Anders and Huber, 2010). It is often used to analyse data produced from high-throughput sequencing assays, including RNA-seq and test for differential expression (Anders and Huber, 2010).

With help from Dr James Prendergast, a heatmap to visualise the differential gene expression patterns between melanoma subtypes was developed (Figure 5.2). This shows variation in expression of over 50 genes between three melanoma subtypes. The zebrafish genotypes from which the melanomas were collected are shown on the x-axis: six $BRAF^{V600E}mitfa^{vc7}$, thirteen $BRAF^{V600E}p53^{M214K}$ and thirteen $BRAF^{V600E}mitfa^{vc7}p53^{M214K}$ melanomas. On the right are Ensembl gene identities of

the genes differentially expressed. The colours represent variation in gene expression: down-regulated genes compared to other subtypes are blue, up-regulated genes compared to other subtypes are yellow. Black dotted lines surround clusters of up- or down-regulated genes that group within genetic subtypes. The dendrograms (or tree diagrams) show how closely related both the melanoma subtypes and genes are.

A total of 53 genes were differentially expressed between melanoma subtypes and are represented in the heatmap (Figure 5.2). Of particular interest were the genes that clustered as up- or down-regulated in only one subtype, for example those shown in yellow in the lower right corner of the heatmap (Figure 5.2). In this cluster, 28 genes are up-regulated in the majority of *BRAF*^{V600E}*p53*^{M214K} melanomas (yellow/green) compared to *BRAF*^{V600E}*mitfa*^{vc7} and *BRAF*^{V600E}*mitfa*^{vc7}*p53*^{M214K} melanomas in which they are down-regulated (blue/green). Of these 28 genes, many were unique to zebrafish while others included *URAH, PGBD4, NTRK3A, HOXD9A* and *HOXD10A*. Using DAVID, no functional association between the set of 28 genes was found, which could be true or as a result of the high number of un-annotated zebrafish genes for which function is unknown. Another interesting cluster included those genes found to be mostly up-regulated in both *BRAF*^{V600E}*mitfa*^{vc7} and *BRAF*^{V600E}*mitfa*^{vc7}*p53*^{M214K} melanoma subtypes (yellow/green) compared to *BRAF*^{V600E}*p53*^{M214K} melanomas (blue) shown in the top half of the heatmap (Figure 5.2). Included within this set of 25 genes were *NPH2, ENTPD3, HOMER1B, CPA2, CPA4, CALCR, FGFR1B* and *HYAL2*. Similar to the first cluster, no functional association between these genes was identified.

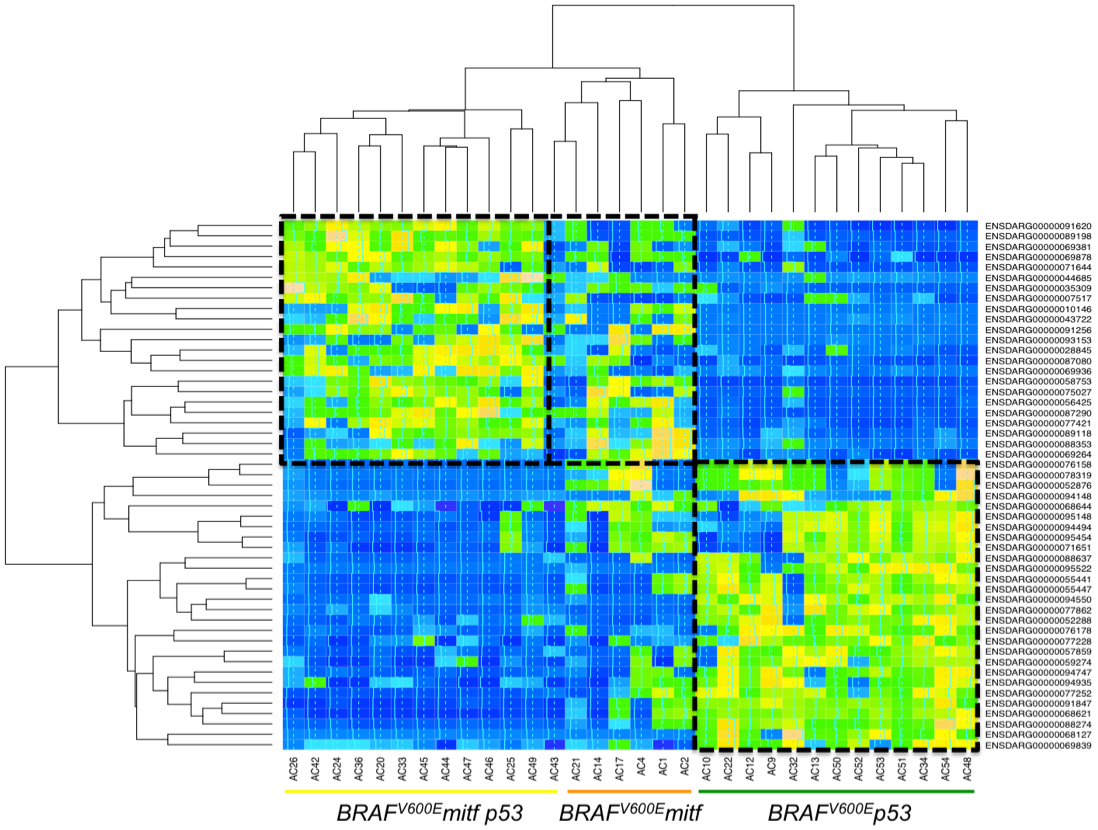

Figure 5.2 A heatmap showing the result of clustering the melanoma samples using the expression levels of genes found to be differentially expressed between the tumour subtypes. Melanoma genotypes on x-axis: *BRAF*^{V600E} *mitfa*^{vc7} *p53*^{M214K}; *BRAF*^{V600E} *mitfa*^{vc7} and *BRAF*^{V600E} *p53*^{M214K} (left to right). Rows correspond to genes labeled with Ensembl gene identifiers. Colours depict level of expression compared to other subtypes: down-regulated (blue); up-regulated (yellow). Dendrograms (shown as trees, to left and above map) indicate how closely related both the genes and melanoma subtypes are. Black dotted-lines surround distinct areas of the map in which genes are expressed at a similar level in an individual melanoma subtype.

5.3.3 Validation of differential gene expression

I attempted to validate the differential gene expression shown to cluster by melanoma subtype in the heatmap (Figure 5.2). In an approach similar to that described in section 3.2.5 to identify differentially expressed MITF target genes, I carried out qRT-PCR to quantify the expression level of two genes that were differentially expressed by RNA-seq. The genes were homeo box D9a (ENSDARG00000059274) and homeo box D10a (ENSDARG00000057859). Both of these genes were shown to be up-regulated in all $BRAF^{V600E}p53^{M214K}$ melanomas (Figure 5.2, yellow) and down-regulated in most tumours from both $BRAF^{V600E}mitfa^{vc7}$ and $BRAF^{V600E}mitfa^{vc7}p53^{M214K}$ genetic backgrounds. I hypothesised that this same trend would be observed using qRT-PCR, and expression of both *hoxd* genes would be greater in $BRAF^{V600E}p53^{M214K}$ tumours than the two other melanoma genotypes. Using six tumour samples from each genotype, I carried out qRT-PCR for both *hoxd* genes and found that neither matched the expression patterns shown by the RNA-seq data (not shown). As well as being unable to observe the same trend in gene expression by qRT-PCR, the number of differentially expressed genes that clustered in the heatmap was low (51), causing a bottleneck in further analysis. To overcome this, the next step utilised network analysis to identify greater numbers of differentially expressed genes that were biologically significant.

5.4 Network analysis of RNA-seq data

For this analysis, I focused on the comparison of *BRAF*^{V600E}*mitfa*^{vc7} versus *BRAF*^{V600E}*p53*^{M214K} melanomas. This simplified the data analysis so I could concentrate on the cleanest genetic subtypes, as all tumours in this comparison were from double homozygote backgrounds.

5.4.1 STRING network

Two types of network were used to carry out analysis of differentially expressed genes identified by RNA-seq. The first was a STRING network, which represents pathway co-membership based on KEGG. STRING is a database of known and predicted protein interactions constructed for the analysis of associations between proteins and the genes that encode them (von Mering *et al*., 2003). These interactions can be either direct (physical) or indirect (functional) and are derived from sources including genomic context, high-throughput experiments, co-expression and previous knowledge (Franceschini *et al*., 2013). The database currently describes over 5.2 million proteins from over 1100 different species. The Kyto Encyclopedia of Genes and Genomes (KEGG) is a collection of databases, including the KEGG Pathway database, which collects and stores information on networks of molecular interactions in cells and their variants. Using the STRING network, which integrates data from the KEGG Pathway, I inputted the DESeq data from RNA-seq using an R package. Of the differentially expressed genes identified by DESeq, I took the top and bottom 1500 genes to take forward for the network. I then visualized the STRING network results using Cytoscape, a software platform that allows visualization of molecular interaction networks and biological pathways (Figure 5.3). The groups of genes (listed in Appendix I, Table A-1) shown by Cytoscape represent clustered genes, as defined by the network. Each node (circle within a cluster) represents an individual gene and the different coloured nodes represent different

tumour genotype comparisons (Yellow: *BRAF*^{V600E}*mitfa*^{vc7} vs. *BRAF*^{V600E}*p53*^{M214K}; blue: *BRAF*^{V600E}*mitfa*^{vc7} vs. *BRAF*^{V600E}*mitfa*^{vc7}*p53*^{M214K}; orange: *BRAF*^{V600E}*mitfa*^{vc7} vs. *BRAF*^{V600E}*p53*^{M214K} and *BRAF*^{V600E}*p53*^{M214K} vs. *BRAF*^{V600E}*mitfa*^{vc7}*p53*^{M214K}; purple: *BRAF*^{V600E}*p53*^{M214K} vs. *BRAF*^{V600E}*mitfa*^{vc7}*p53*^{M214K} and *BRAF*^{V600E}*mitfa*^{vc7} vs. *BRAF*^{V600E}*mitfa*^{vc7}*p53*^{M214K}*).* The node edges differentiate between up-regulated (red) and down-regulated (green) gene expression, when comparing *BRAF*^{V600E}*mitfa*^{vc7} and *BRAF*^{V600E}*p53*^{M214K} melanomas. Cytoscape allows simple modification of colour, shape and background and images can be exported as picture files for presentation.

As a result of the STRING network analysis, twenty clusters of differentially expressed genes that shared pathway membership were identified (annotated in Figure 5.3). A few of these pathways overlapped, including those involved in ion binding, membrane-association and proteolysis. One of the clusters identified, which through DAVID annotation was associated with voltage-gated potassium channels, contained thirteen genes, seven of which were members of the voltage-gated potassium channel family – *KCNC1A*, *KCNC4, KCNH5B*, *KCNF1B, KCNAB1, KCNH3* and *CKMB*. These genes were all up-regulated in *BRAF*^{V600E}*mitfa*^{vc7} tumours compared to *BRAF*^{V600E}*p53*^{M214K} tumours (shown as red-edged nodes, Figure 5.3). In contrast, another cluster identified a group of genes mostly down-regulated in *BRAF*^{V600E}*mitfa*^{vc7} tumours compared to *BRAF*^{V600E}*p53*^{M214K} tumours that were associated with the cytochrome p450 (CYP) superfamily of hemoproteins (Figure 5.3). The cluster also contained thirteen genes, eight of which were members of the CYP superfamily – *CYP17A2, CYP2AA3, CYP2AA9, CYP2K16, CYP2K17, CYP2P7, CYP2X9* and *CT737*. All eight of these genes were down-regulated in *BRAF*^{V600E}*mitfa*^{vc7} melanomas (shown as green-edged nodes, Figure 5.3).

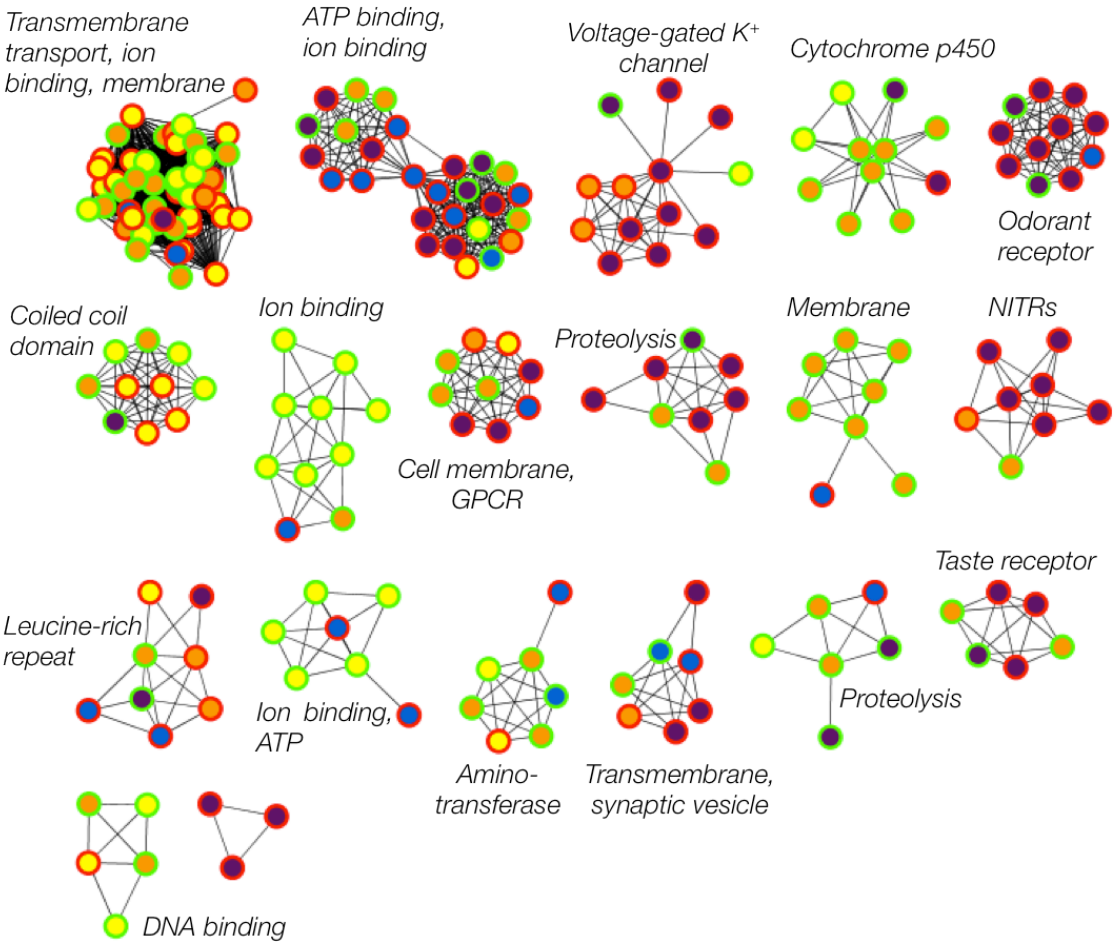

Figure 5.3 STRING network analysis of differentially expressed genes between *BRAF*^{V600E}*mitf* and *BRAF*^{V600E}*p53* genotypes shown using the Cytoscape platform. Clusters represent genes with pathway co-membership, based on KEGG. Node colours of individual genes represents different genotype comparison (Yellow: *BRAF*^{V600E}*mitf* vs. *BRAF*^{V600E}*p53*; blue: *BRAF*^{V600E}*mitf* vs. *BRAF*^{V600E}*mitf p53*; orange: *BRAF*^{V600E}*mitf* vs. *BRAF*^{V600E}*p53* and *BRAF*^{V600E}*p53* vs. *BRAF*^{V600E}*mitf p53*; purple: *BRAF*^{V600E}*p53* vs. *BRAF*^{V600E}*mitf p53* and *BRAF*^{V600E}*mitf* vs. *BRAF*^{V600E}*mitf p53).* Edge colour shows either genes up-regulated in *BRAF*^{V600E}*mitf* tumours compared to *BRAF*^{V600E}*p53* tumours (red), or down-regulated in *BRAF*^{V600E}*mitf* tumours compared to *BRAF*^{V600E}*p53* tumours (green). Functionally-related clusters of genes annotated using DAVID.

5.4.2 IMP network

The second network used in the analysis was the IMP network, which represents functional similarity defined by GO-term co-annotation. Integrative multi-species prediction (IMP) is an interactive web server that provides access to a large, cross-organism collection of functional predictions and networks (Wong *et al*., 2012). This network was used subsequent to the STRING network in order to provide a direct comparison of the clusters of genes differentially expressed between *BRAF*^{V600E}*mitfa*^{vc7} and *BRAF*^{V600E}*p53*^{M214K} melanomas. Similar to the first analysis, I took the top and bottom 1500 genes from the DESeq results and inputted them into IMP network using an R package. I then visualized the IMP network results using Cytoscape (Figure 5.4). The groups of genes (listed in Appendix I, Table A-2) shown by Cytoscape represent clustered genes, as defined by the network. Each node (circle within a cluster) represents an individual gene and are coloured either green or red to represent whether they are up- or down-regulated in *BRAF*^{V600E}*mitfa*^{vc7} melanomas compared to *BRAF*^{V600E}*p53*^{M214K} melanomas, respectively.

As a result of the IMP network analysis, another twenty clusters of differentially expressed genes that shared functional properties were identified (annotated in Figure 5.4). Similar to the STRING network analysis, a few of these pathways overlapped, including those involved in ion binding, transmembrane transport and fibroblast growth factors (FGFs). Interestingly, two of the clusters identified and classified as associated with transmembrane transport were found to contain genes both up- and down-regulated in *BRAF*^{V600E}*mitfa*^{vc7} melanomas compared to *BRAF*^{V600E}*p53*^{M214K} melanomas. In one cluster of four genes, *SLC22A7A*, *SLC22A7B, SLC22A11* and *SLC22A16* were found to be up-regulated in *BRAF*^{V600E}*mitfa*^{vc7} tumours (shown as green nodes, Figure 5.4). In another cluster of five genes, *CKMB, SLC1A3*, *SLC5A1, SLC5A5* and *SLC7A1* were found to be down-regulated in *BRAF*^{V600E}*mitfa*^{vc7} tumours (shown as red nodes, Figure 5.4). This result demonstrates how genes from the same family can be differentially regulated within

a single tumour subtype. Another interesting and positive result was the presence of genes within clusters from the IMP network analysis that were also identified within clusters using the STRING network. These genes were found in clusters that were functionally related by their association with G protein-coupled receptors and included *GRIN2AA*, *GRIN2AB* and *GRIN2BB*. Similar to the gene clusters associated with transmembrane transport, the *GRIN* genes and others associated with G protein-coupled receptors were found to be both up- and down-regulated in $BRAF^{V600E}mitfa^{vc7}$ tumours compared to $BRAF^{V600E}p53^{M214K}$ tumours.

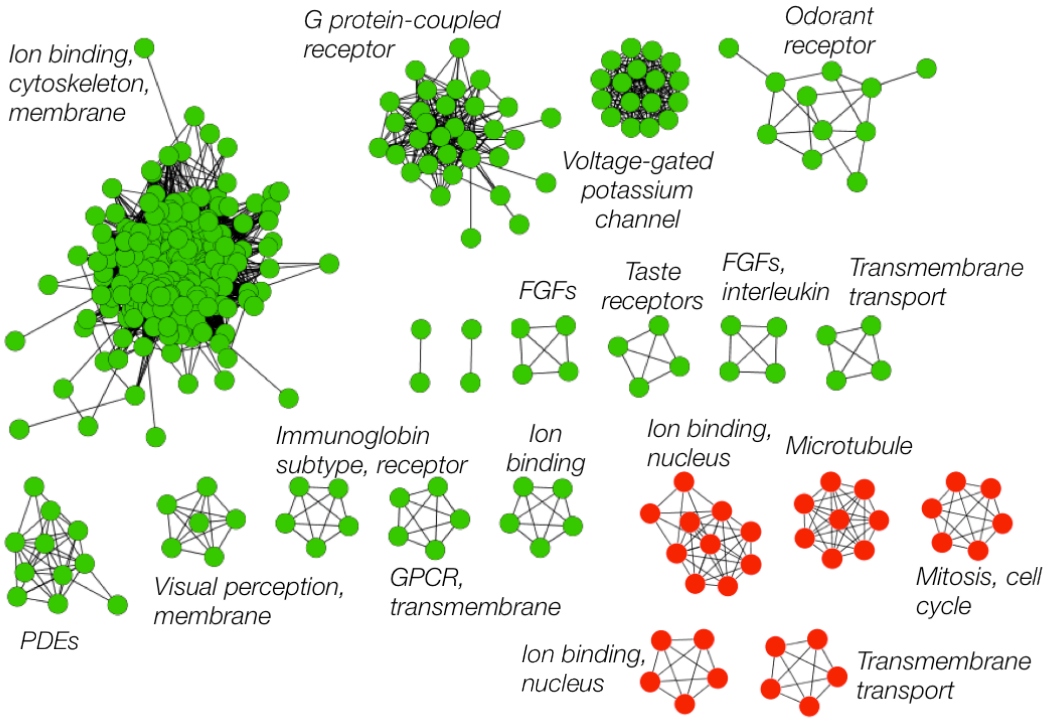

Figure 5.4 IMP network analysis of differentially expressed genes between *BRAF*^{V600E}*mitf* and *BRAF*^{V600E}*p53* genotypes shown using the Cytoscape platform. Clusters represent genes with functional similarity, defined by GO term co-annotation. Node colour shows either genes up-regulated in *BRAF*^{V600E}*mitf* tumours compared to *BRAF*^{V600E}*p53* tumours (green), or down-regulated in *BRAF*^{V600E}*mitf* tumours compared to *BRAF*^{V600E}*p53* tumours (red). Functionally-related clusters of genes annotated using DAVID.

Using both STRING and IMP networks during the analysis allowed for a more comprehensive exploration of the differentially expressed genes between *BRAF*^{V600E}*mitfa*^{vc7} and *BRAF*^{V600E}*p53*^{M214K} melanoma subtypes. Whereas the STRING network reflects biological pathway co-membership based on KEGG, the IMP network reflects functional similarity and is based on GO-term annotation. Initial analysis using the STRING network alone provided a good set of clustered, differentially expressed genes with overlapping functions including ion binding, cell membrane-associated and proteolysis. A second, subsequent analysis using the IMP network allowed for a comparison of the functional annotation of the clusters, with similar groups including ion binding, transmembrane transport and G protein-coupled receptors. By combining the analyses using STRING and IMP networks, I was able to recognise genes identified using both networks providing confidence in those selected for further validation.

5.4.3 qRT-PCR validation of differentially expressed genes identified by network analysis

Clusters of differentially expressed genes identified by network analysis, with functional relevance through annotation by DAVID, were selected for further study. Two groups of genes were of particular interest, the phosphodiesterases (*PDEs*) and glutamate receptors (*GRINs*). Of the phosphodiesterases, *PDE1a*, *PDE4a* and *PDE11a* were chosen for validation. *GRIN2aa*, *GRIN2ab* and *GRIN2bb* from the glutamate receptor family were validated.

DESeq determines the log fold change values for the difference in expression of these genes between $BRAF^{V600E}mitfa^{vc7}$ and $BRAF^{V600E}p53^{M214K}$ melanomas (Table 3). A positive log fold change value shows expression is higher in $BRAF^{V600E}mitfa^{vc7}$ compared to $BRAF^{V600E}p53^{M214K}$ melanomas. A negative log fold change value shows expression is higher in $BRAF^{V600E}p53^{M214K}$ compared to $BRAF^{V600E}mitfa^{vc7}$ melanomas.

Table 3. Log fold change values for the expression of genes in $BRAF^{V600E}mitfa^{vc7}$ and $BRAF^{V600E}p53^{M214K}$ melanomas.

Gene	$BRAF^{V600E}mitfa^{vc7}$ vs. $BRAF^{V600E}p53^{M214K}$
PDE1a	0.528
PDE4a	2.798
PDE11a	-3.058
GRIN2aa	3.542
GRIN2ab	-1.602
GRIN2bb	1.588

To validate these values, I carried out qRT-PCR using five tumours from each tumour genetic background. I hypothesised that I would observe the same trends of gene expression from both DESeq (RNA-seq) and qRT-PCR.

I found that 2/3 of the expression trends for both the *PDE* and *GRIN* genes matched between the DEseq and qRT-PCR methods (Figure 5.5; 5.6). For the phosphodiesterases, the expression of *PDE4a* was significantly higher in *BRAF*^{V600E}*mitfa*^{vc7} melanomas than in *BRAF*^{V600E}*p53*^{M214K} (p=0.0217) (Figure 5.5). The expression of both *PDE1a* and *PDE11a* was also greater in *BRAF*^{V600E}*mitf* melanomas compared to *BRAF*^{V600E}*p53*^{M214K} tumours, although neither of these expression trends was found to be statistically significant (Figure 5.5). Using both DESeq data and qRT-PCR validation, the expression of both *PDE1a* and *PDE4a* were higher in *BRAF*^{V600E}*mitfa*^{vc7} melanomas compared to *BRAF*^{V600E}*p53*^{M214K} tumours (Table 3; Figure 5.5). In contrast, the DESeq data showed that expression of *PDE11a* was greater in *BRAF*^{V600E}*p53*^{M214K} tumours (Table 3, log fold change = -3.058), while qRT-PCR showed that it was greater in *BRAF*^{V600E}*mitfa*^{vc7} tumours (Figure 5.5), although this was not statistically significant.

In a similar fashion to the *PDEs*, 2/3 of the expression trends for *GRIN* genes matched between the DEseq and qRT-PCR methods (Table 3; Figure 5.6). By qRT-PCR, the expression of *GRIN2aa* was significantly greater in *BRAF*^{V600E}*mitfa*^{vc7} melanomas compared to *BRAF*^{V600E}*p53*^{M214K} melanomas (Figure 5.6). This qRT-PCR data validated the expression difference calculated by DESeq, in which the expression of *GRIN2aa* was also shown to be greater in *BRAF*^{V600E}*mitfa*^{vc7} tumours compared to *BRAF*^{V600E}*p53*^{M214K} tumours (Table 3, log fold change = 3.542). Using both DESeq data and qRT-PCR validation, the expression of *GRIN2bb* was also found to be greater in *BRAF*^{V600E}*mitfa*^{vc7} melanomas compared to *BRAF*^{V600E}*p53*^{M214K} tumours (Table 3; Figure 5.6). In contrast, while the DESeq data showed that the expression of *GRIN2ab* was greater in *BRAF*^{V600E}*p53*^{M214K} tumours (Table 3, log fold change = -1.602), qRT-PCR data showed that it was greater in *BRAF*^{V600E}*mitfa*^{vc7} tumours (Figure 5.6), although this was not statistically significant.

To summarise the validation approach, network analysis identified functionally-related groups of genes that were differentially expressed between two melanoma subtypes. The phosphodiesterases and glutamate receptors were selected from these groups as biologically interesting and chosen for further study. I was able to validate the significant changes in gene expression identified by network analysis by qRT-PCR in 4/6 genes (*PDE1a*, *PDE4a*, *GRIN2aa* and *GRIN2bb*). This broadly validates the network finding that these groups of genes are of interest.

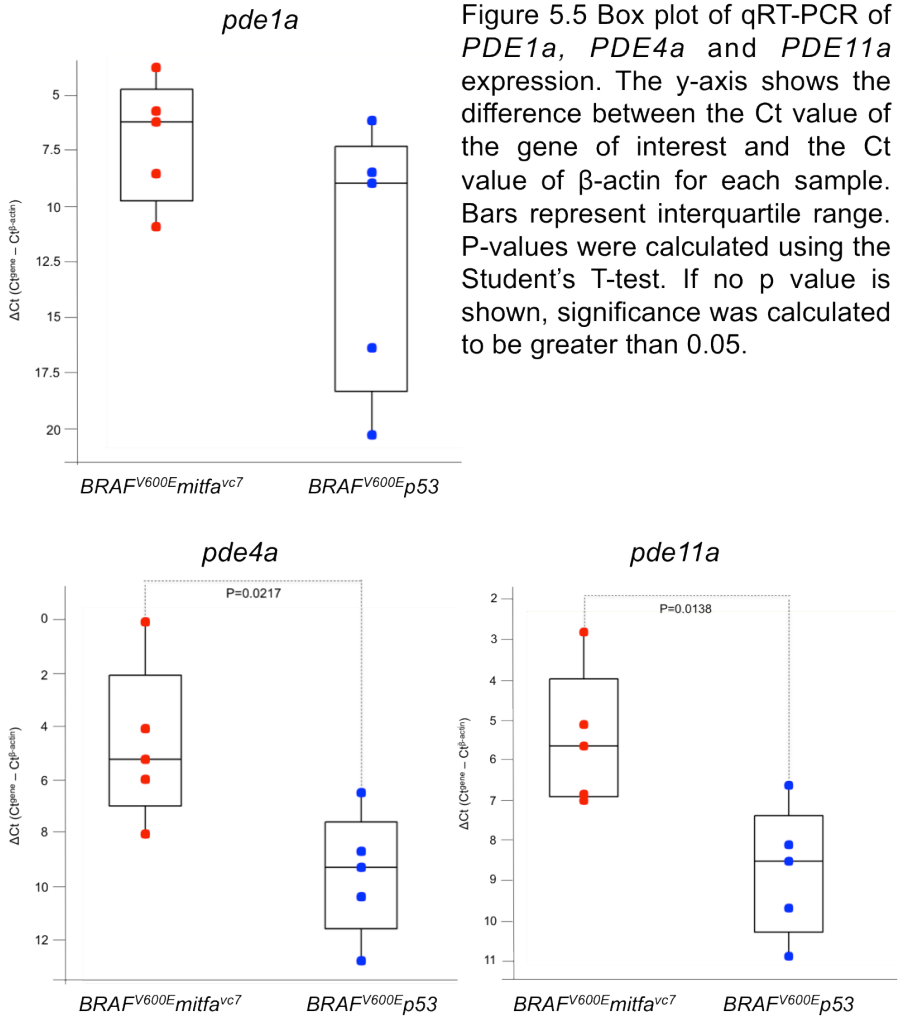

Figure 5.5 Box plot of qRT-PCR of *PDE1a*, *PDE4a* and *PDE11a* expression. The y-axis shows the difference between the Ct value of the gene of interest and the Ct value of β-actin for each sample. Bars represent interquartile range. P-values were calculated using the Student's T-test. If no p value is shown, significance was calculated to be greater than 0.05.

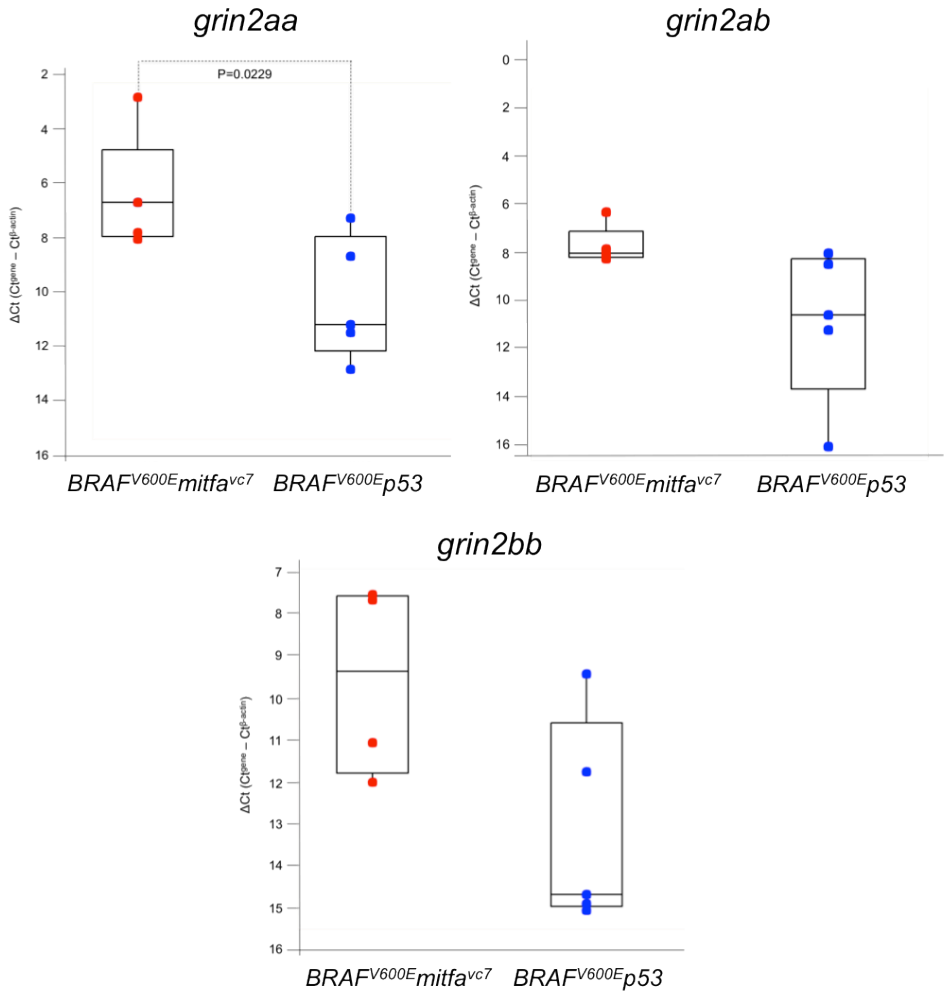

Figure 5.6 Box plot of qRT-PCR of *grin2aa*, *grin2ab* and *grin2bb* expression. The y-axis shows the difference between the Ct value of the gene of interest and the Ct value of β-actin for each sample. Bars represent interquartile range. P-values were calculated using the Student's T-test. If no p value is shown, significance was calculated to be greater than 0.05.

5.4.4 Validation of differentially expressed phosphodiesterase genes identified by network analysis using a cAMP assay

The differential gene expression of the phosphodiesterases and particularly the high *PDE4a* expression in the *BRAF*^{V600E}*mitfa*^{vc7} melanomas shown by both RNA-seq and qRT-PCR (Figure 5.5; Table 3) lead to a hypothesis that cAMP levels may be lower in this tumour subtype. The role of phosphodiesterases is to degrade the phosphodiester bond in second messenger molecules cAMP and cGMP; hence if levels of these enzymes were higher in a tumour, I predicted that levels of cAMP and/or cGMP would be lower.

To test this hypothesis, I carried out a cAMP ELISA assay using tumour tissue from *BRAF*^{V600E}*mitfa*^{vc7} and *BRAF*^{V600E}*p53*^{M214K} melanomas. I calculated the cAMP concentration of six tumour samples from each melanoma subtype (Figure 5.7) and found that there was no significant difference between *BRAF*^{V600E}*mitfa*^{vc7} and *BRAF*^{V600E}*p53*^{M214K} melanoma cAMP concentration (p=0.395). To confirm this result it would be useful to include more tumours in the experiment to overcome variation and eradicate outliers, as well include wild-type adult tissue samples to compare cAMP concentrations in tumour to normal tissue.

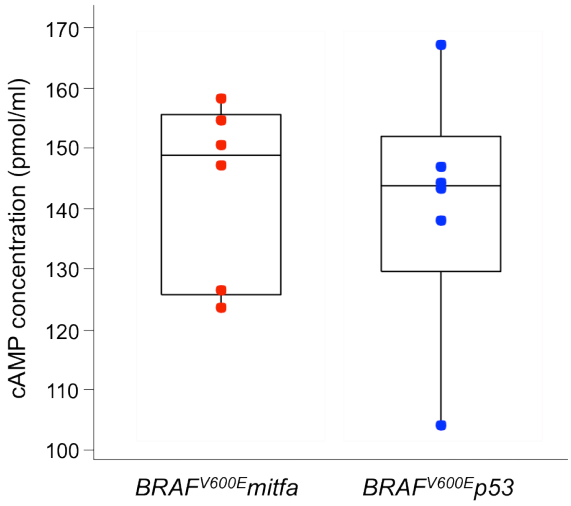

Figure 5.7 Box plot of cAMP concentrations (pmol/ml) in six tumours from *BRAF*^{V600E}*mitfa* and *BRAF*^{V600E}*p53* melanoma subtypes. cAMP concentrations are calculated from a standard curve regression equation before being plotted. Bars represent interquartile range. The Student's T-test was used to calculate a p-value of 0.395.

5.5 Discussion

Sequencing technologies have rapidly advanced to allow greater understanding of the human genome and the way in which it is altered in cancer. To explore both the gene mutation and expression landscape of *BRAF*^{V600E} melanomas, I took an approach utilising both exome and transcriptome sequencing. By employing RNA-seq (transcriptome sequencing) methodology, I was able to investigate gene expression levels and the presence of splice variants, which exome and whole-genome sequencing do not provide. I hypothesised that differential gene expression identified between the two melanoma subtypes, driven by *BRAF*^{V600E}-cooperating mutations *mitf* and *p53,* would provide greater understanding of the different histological characteristics of these melanomas.

In 2010, Berger and colleagues carried out RNA-seq using eight patient-derived melanoma cultures and two melanoma cell lines. RNA-seq data in combination with chromosomal copy number data identified 11 novel melanoma gene fusions and 12 novel readthrough transcripts (Berger *et al*., 2010). The tumour suppressor *RB1* was part of one of the gene fusions identified and found in a region commonly deleted in melanoma, suggesting that inactivation of *RB1* may contribute to melanoma pathology (Berger *et al*., 2010). This research provided a platform for future transcriptome studies and demonstrated 'the capability of RNA-seq to interrogate the full spectrum of RNA-based alterations relevant to cancer through integrative analysis' (Berger *et al*., 2010).

With the premise initiated by previous successful RNA-seq studies, including that of Berger and colleagues (2010), I collected 34 melanoma samples from *BRAF*^{V600E}*mitfa*^{vc7}, *BRAF*^{V600E}*p53*^{M214K}, and *BRAF*^{V600E}*mitfa*^{vc7}*p53*^{M214K} genetic backgrounds to take forward for transcriptome sequencing. The initial analysis of the data using DESeq was inadequately fruitful, returning only 51 differentially

expressed genes in biologically unconnected pathways (Figure 5.2). It did, however, demonstrate similar expression levels of clusters of genes unique to one melanoma subtype.

It was interesting that no fusion transcripts were identified by RNA-seq in any of the melanoma subtypes. Gene fusions that arise from translocations and other chromosomal abnormalities are a common and important feature of cancer, and until recently very few were known in melanoma. The study by Berger and colleagues (2010) identified eleven novel gene fusions involving four genes on separate chromosomes, but also suggested that unlike other tumour types with common gene fusions, these are low frequency events in melanoma (Berger *et al*., 2010). The absence of gene fusions from our RNA-seq data may therefore reflect this low frequency or the fact that these are very rapid onset tumours and hence provide much less time to rearrange and accumulate mutations compared to humans.

To further explore the differential gene expression, I carried out network analysis, which returned functionally relevant clusters of genes in interesting molecular pathways. Due to time restraints, I selected two of these clusters to validate using qRT-PCR. This selection was based on established links between the associations of these genes with melanoma.

The differential expression of genes from the glutamate receptor family, *GRIN2aa*, *GRIN2ab* and *GRIN2bb*, were of particular interest due to the recent association of several glutamate receptor signalling members and a pathogenic pathway in melanoma. The *GRIN* family members encode for glutamate (N-methyl-(D)-aspartic acid (NMDA)) receptor subunits of an ionotropic glutamate receptor. As previously described, *GRIN2A* was found to be the highest mutated gene in a screen of 14 metastatic melanoma samples by Wei and colleagues (2011). Gene amplifications of *GRIN2B* and *GRIN2C* in melanoma cell lines have also been identified using combinations of RNA-seq, SNP-analysis and comparative genome hybridization

(CGH) (Valsesia *et al*., 2011). *GRM3*, a group 2 glutamate receptor, was also found frequently mutated in a targeted exome sequencing study of 11 metastatic melanomas (Prickett *et al*., 2011). Together, these three studies highlight the significance of glutamate receptor signalling in melanoma and indicate a potential novel therapeutic strategy. From RNA-seq and qRT-PCR data, I found the expression of both *GRIN2aa* and *GRIN2bb* to be greater in $BRAF^{V600E}mitfa^{vc7}$ melanomas than $BRAF^{V600E}p53^{M214K}$ melanomas (Figure 5.6; Table 3). The differential expression of these genes identified by RNA-seq and validated by qRT-PCR, suggests these, and potentially other glutamate receptor family members may in part be responsible for the distinction between $BRAF^{V600E}mitfa^{vc7}$ and $BRAF^{V600E}p53^{M214K}$ melanoma subtypes.

The differential gene expression of the phosphodiesterases and particularly the high *PDE4a* expression in the $BRAF^{V600E}mitfa^{vc7}$ melanomas shown by both RNA-seq and qRT-PCR (Figure 5.5; Table 3) led to a hypothesis that cAMP levels may be lower in this tumour subtype. As the role of phosphodiesterases is to degrade the phosphodiester bond in second messenger molecules cAMP and cGMP, I predicted that levels of cAMP and/or cGMP would be lower. Using three tumour samples from each melanoma subtype, I found no significant difference in cAMP levels between $BRAF^{V600E}mitfa^{vc7}$ and $BRAF^{V600E}p53^{M214K}$ melanomas (Figure 5.7). Despite this result, it would be interesting to confirm this finding using greater numbers of tumour samples and include a wild-type control tissue sample, which would support more extensive follow-up experiments with phosphodiesterases.

One of these follow-up experiments in relation to phosphodiesterases could involve the use of PDE inhibitors, which block the enzymatic activity of PDEs and prevent the inactivation of cAMP and cGMP. PDE inhibitors are currently used in a clinical setting: PDE4 inhibitors have shown promise for treatment of patients with autoimmune diseases (Kumar *et al*., 2013), while PDE5 specific inhibitors are used as a first-line treatment for patients with erectile dysfunction (Corona *et al*., 2011). In addition to the specificity of these PDE inhibitors currently used in a clinical setting,

of importance to this research are the relationships that have been identified between phosphodiesterases and melanoma.

In 2011, Arozarena and colleagues found that downregulation of *PDE5A* elicits melanoma cell invasion. They showed that oncogenic, activated BRAF acts through *MEK* and *BRN-2* to down-regulate *PDE5A*. This then leads to an increase in cGMP, which causes a rise of intracellular Ca^{2+} levels and a dramatic, consequential increase in melanoma cell invasion (Arozarena *et al*., 2011). They also showed that ectopic expression of any PDE5 isoform suppresses the invasive capacity of $BRAF^{V600E}$ mutant melanoma cells, and that PDE5A is downregulated in a number of melanoma lines that harbour oncogenic BRAF (Arozarena *et al*., 2011). This indicates that PDE5A downregulation may be a novel biomarker for increased invasiveness and consequent poor prognosis in melanoma. It also implies a novel therapeutic potential of up-regulating PDE5A in oncogenic BRAF melanomas, which in theory may reduce invasiveness and metastatic potential.

More recently, Hiramoto and colleagues identified a role for PDE2 in melanoma growth and invasion. They showed that a specific PDE2 inhibitor, erythro-9-(2-Hydroxy-3-nonyl) adenine (EHNA) inhibited the growth and invasion of a human malignant melanoma PMP cell line (Hiramoto *et al*., 2014). The effect of EHNA was mimicked by transfecting PDE2A-specific siRNA into melanoma cells. The authors conclude from these results that PDE2 could 'play an important role in growth and invasion of the human malignant melanoma PMP cell line' and that 'selectively suppressing PDE2 might possibly inhibit growth and invasion of other malignant tumour cell lines' (Hiramoto *et al*., 2014).

Both of these studies provide evidence that members of the phosphodiesterase enzyme family could play an important role in melanoma invasion and lead to a hypothesis that specific phosphodiesterase inhibitors could be used as therapeutics to reduce invasive potential. In the Patton laboratory, a specific inhibitor of PDE4,

rolipram, has been used in the past as a chemical modifier of the cAMP pathway and shown to affect melanosome dispersal (Richardson *et al*., 2008). As the use of this drug is already established within the laboratory, it can be used to treat adult fish and directly test the effect of altering PDE activity and cAMP/cGMP levels. As well as testing PDE4 using rolipram, it would also be useful to test inhibitors of both PDE2 and PDE5, as these have both been shown to affect levels of invasion in melanoma (Arozarena *et al*., 2011; Hiramoto *et al*., 2014). As the melanomas developed in the $BRAF^{V600E}p53^{M214K}$ background are characteristically invasive compared to $BRAF^{V600E}mitfa^{vc7}$ melanomas, it would be interesting to test the effect of these PDE inhibitors on the invasive nature of these tumours. I could hypothesise that treatment of $BRAF^{V600E}p53^{M214K}$ melanomas with a PDE inhibitor would lead to a less invasive phenotype and losing this histopathological feature they would become more similar to $BRAF^{V600E}mitfa^{vc7}$ melanomas. Ultimately, if use of any PDE inhibitor in this type of experiment affects the characteristic histopathlogical features of the $BRAF^{V600E}mitfa^{vc7}$ or $BRAF^{V600E}p53^{M214K}$ zebrafish melanomas, it may help to uncover the role of phosphodiesterases and their inhibitors and show whether it would beneficial to explore their therapeutic use in melanoma.

Chapter 6 – Concluding Remarks and Future Directions

6.1 Concluding Remarks

To refer back to the motivation of this thesis, in recent years the incidence of melanoma has increased more than any other cancer type (Seigel *et al*., 2012) and although there have been exceptional advances in therapeutics, the survival rate of patients diagnosed with metastatic melanoma is poor. Despite the improvement in our understanding of the genes and pathways that contribute to melanomagenesis, the driving force behind much of both academic and pharmaceutical research has been focused on BRAF and other MAPK pathway inhibitor strategies. In combination with BRAF inhibitors, MEK inhibitors such as trametanib (GlaxoSmithKline) have shown to improve rates of progression-free survival of patients with metastatic melanoma that harbour the $BRAF^{V600E}$ mutation, compared to chemotherapy (Flaherty *et al*., 2012). Combination therapies to address other mechanisms of BRAF inhibitor resistance including activation of the PI3K/Akt pathway are also being developed. AKT inhibition has been shown to reverse acquired drug resistance to BRAF inhibitors in melanoma cell lines and therefore provides evidence of the antitumour effect of this combination in patients currently receiving BRAF inhibitor therapy (Lassen *et al*., 2014). KIT inhibitors such as imatinib mesylate have also been developed and shown to result in significant clinical responses in patients with advanced melanoma harbouring KIT alterations (Carvajal *et al*., 2011).

Although these therapeutic approaches have shown significant benefit to patients, particularly the use of vemurafenib in $BRAF^{V600E}$ mutant melanomas, the innate drug resistance and development of side effects associated with these strongly suggests the need for novel targets towards this disease. One such target could be MITF, as research including that shown here has highlighted the importance of this gene in melanoma progression, pathology and survival.

MITF has a complex role in melanoma and since 2005, when Garraway and colleagues identified a genomic amplification of *MITF* in melanoma (Garraway *et al*., 2005) and Wellbrock and Marais (2005) determined a relationship between MITF and BRAF, recent research has shown that $BRAF^{V600E}$ plays an important role in ensuring an "intermediate level" of MITF is sustained to allow tumour growth (Hoek and Goding, 2010). Until now, the effects of targeting MITF *in vivo* have not been understood as modulating MITF levels within an animal model had not been tested. Here, I present conclusive data showing that low levels of MITF are oncogenic with $BRAF^{V600E}$ to promote melanoma (Lister *et al*., 2014). Key to this research is that the melanomas developed in the $BRAF^{V600E}mitfa^{vc7}$ zebrafish share similar features to human melanoma pathology, with a superficial spreading growth pattern and the presence of heavily pigmented macro-melanophages. In addition to these findings, the most remarkable discovery from this research was that abrogating MITF activity in $BRAF^{V600E}mitfa^{vc7}$ causes tumour regression, which is characterised by melanophage infiltration and an increase in apoptosis. The observed melanoma regression caused by a reduction in MITF is a significant discovery and a major contribution to understanding the impact of MITF on melanoma development. It demonstrates that targeting MITF activity is an effective mechanism to prevent and/or inhibit tumour growth. Together, the results confirm a direct interaction between MITF and the survival of $BRAF^{V600E}$ melanoma and show that MITF plays a key role in the survival of $BRAF^{V600E}$ melanomas.

As well as in melanoma, *MITF* mutations have been identified in pigment deficiency syndromes and renal cell carcinoma (RCC). A link between MITF and RCC lies in hypoxia inducible factor (*HIF1A*), which is a shared target of both *MITF* and kidney cancer susceptibility genes. In 2011, a germline variant in MITF (E318K) was identified in an individual with melanoma that affected SUMOylation and was significantly over-represented in cases with a family history of melanoma (Yokoyama *et al*., 2011). Also in 2011, Bertolotto and colleagues identified the same MITF variant that co-occurred in both melanoma and RCC patients. The $MITF^{E318K}$ mutation increased global MITF binding and its transcriptional activity and carriers

of the mutation have a 5-fold increased risk of developing melanoma, RCC or both cancers (Bertolotto *et al*., 2011). In addition to melanoma and RCC, mutations in MITF are found in patients with Waardenburg syndrome type 2A (WS2A) and Tietz syndrome (TS), both characterised by hypopigmentation and deafness. Recently Grill and colleagues described how mutations in this single gene, *MITF*, could cause both of the pigment deficiency syndromes and melanoma. The study showed that different DNA-binding and transcription activation abilities of the MITF mutations were responsible for the different phenotypes they caused (Grill *et al*., 2013). These studies highlight the range of diseases in which MITF plays an important role and describe the way in which MITF mutations can lead to distinct disease phenotypes.

As *MITF* amplifications as well as both somatic and germline mutations of *MITF* have been identified and I have shown that abrogating MITF in $BRAF^{V600E}$ melanomas causes regression, it seems valuable to consider MITF as a therapeutic target. In previous studies, HDAC inhibitors have been shown to target MITF and suppress its expression in melanocytes, melanoma and clear sarcoma cells (Yokoyama *et al*., 2008). *In vitro* studies have also shown that HDAC inhibitors suppress tumour growth in a human melanoma xenograft model (Yokoyama *et al*., 2008). Although the mechanism by which HDAC inhibition suppresses MITF is unclear, it is thought to involve the suppression of one of its upstream transcriptional regulators. A better understanding of this mechanism and experiments testing the use of these drugs in a $BRAF^{V600E}$ mutant melanoma for example, may lead to identification of the true target of these drugs and the development of MITF inhibitors with increased specificity.

As well as the genetic and *in vivo* evidence supporting *MITF* as a target gene for melanoma, it has also been supported by the discovery that MITF could act as a resistance mechanism for melanomas treated with the currently available therapeutics (Smith *et al*., 2013; Johannessen *et al*., 2013; Van Allen *et al*., 2014). In 2013, Smith and colleagues used human melanoma cells with both induced and de novo resistance to MEK inhibitors to show that the resistance correlated with an

overexpression of MITF. They found that the expression of MITF in these cells was regulated epigenetically by signalling related to TGF-β (Smith *et al*., 2013). The resistance also correlated with an increase in SMURF2 expression, a ubiquitin ligase that down-regulates the expression of inhibitory SMADS, including those that regulate *PAX3* (Smith *et al*., 2013, Davies and Kopetz, 2013). Inhibiting MITF expression by treatment with TGF-β or knockdown of SMURF2, PAX3 or MITF itself using siRNAs sensitised the melanoma cells to apoptosis induction by MEK inhibition (Smith *et al*., 2013). The results of this recent study are extremely promising and if further research employed clinical specimens and achieved the same result, the case for MITF to be presented as a druggable target, in combination therapy with MEK inhibitors for example, would be very strong.

In addition to the results from Smith and colleagues (2013), whole-exome sequencing identified an amplification of *MITF* in a melanoma patient with MAPK resistance (Van Allen *et al*., 2014). To test whether the amplification of *MITF* contributed directly to the resistance phenotype, Van Allen and colleagues overexpressed mutated *MITF* in $BRAF^{V600E}$ melanoma cells and cultured them in the presence of RAF, MEK and ERK inhibitors. They found that the forced overexpression of *MITF* rendered these $BRAF^{V600E}$ melanoma cells resistant to MAPK pathway inhibition (Van Allen *et al*., 2014). *MITF* was also overexpressed in two different $BRAF^{V600E}$ melanoma cell lines and the cells were treated with the $BRAF^{V600E}$ inhibitor PLX4720 (Plexxikon/Roche) before a cell growth inhibition assay was performed (Van Allen *et al*., 2014). In both cell lines, *MITF* overexpression increased the PLX4720 -driven growth inhibition by between 30- and 80-fold (Van Allen *et al*., 2014). Both of these experiments confirm that alterations in MITF contribute to a clinical resistance mechanism in $BRAF^{V600E}$ melanoma and, together with results from Smith and colleagues, highlight the need to target MITF in $BRAF^{V600E}$ melanoma.

6.2 Future Directions

6.2.1 Exploring MITF as a drug target

The *BRAF*^{V600E}*mitfa*^{vc7} zebrafish melanoma model is temperature-sensitive and this has proven to be valuable in our ability to modulate MITF activity by temperature change. By taking advantage of this feature I have shown that low levels of MITF activity in BRAF^{V600E} mutant zebrafish promote melanoma and that completely shutting off its activity causes melanoma regression. The regression observed in this model highlights the possibility that MITF could be a good drug target for human melanoma and also that successful therapeutics must be able to turn off MITF activity fully to elicit positive effects.

As a transcription factor lacking ligand dependency, MITF is considered to be a difficult drug target using current therapeutics (Yokoyama *et al*., 2008). Yeh and colleagues (2013) now show that recent advances in drug delivery strategies that specifically target tumour cells as well as pharmacologic agents will allow transcription factors to be directly targeted in cancer (Yeh *et al*., 2013). Using these new technologies would allow specific inhibition of MITF to be tested. The crystal structure of MITF has recently been determined and identified both the DNA-binding and dimerization domains of MITF (Pogenberg *et al*., 2012). Together with advanced targeting technologies, identifying ligands that specifically bind to pockets within the MITF structure could elude to drugs that successfully inhibit its activity.

To identify compounds that have potential to target MITF, a high-throughput drug screen could be initially used as an *in vitro* approach. If successful, such a screen could identify compounds that affect the expression of MITF and its downstream targets, which could be subsequently used to test the effect of targeting MITF in

BRAF mutant cells. It would also be very important to model the effects of targeting MITF *in vivo* and the *BRAF*^{V600E}*mitfa*^{vc7} melanoma model presented here would be a good animal model in which to do this. Newly identified compounds and inhibitors designed that target MITF could be used in future experiments to test if similar regression patterns are observed to those shown by shutting off MITF by temperature shift.

BRAF^{V600E}*mitfa*^{vc7} melanomas that regressed after MITF activity was switched off were shown to recur when MITF activity was restored. One possible theory for this recurrence is that melanoma-initiating cells, which lie dormant when MITF is shut off, are stimulated upon MITF activity and repopulate the tumour. Using previously established fluorescent reporter lines such as *mitfa-GFP* (Dooley *et al*., 2013) and making genetic crosses with *BRAF*^{V600E}*mitfa*^{vc7} mutants we could visualise the mechanisms of tumour regression and recurrence using live imaging. This would provide an understanding of how melanoma-initiating cells repopulate the tumour site as well as how these cells respond to drug treatment.

As MITF has been shown to act as a resistance mechanism to BRAF and MEK inhibition (Smith *et al*., 2013; Johannessen *et al*., 2013; Van Allen *et al*., 2014) it would be valuable to determine if MITF is important for survival in these recurrent melanomas. One approach would be to test identified targets of MITF in *BRAF*^{V600E}*mitfa*^{vc7} melanomas that recurred after MITF activity was restored. Identifying differences in the degree of tumour recurrence in these zebrafish after MITF inhibition could help to establish whether MITF is a good target in recurrent melanomas.

BRAF and MEK inhibitors could also be used to treat *BRAF*^{V600E}*mitfa*^{vc7} zebrafish mutants to model resistance mechanisms and in combination with MITF inhibitors assess the potential for targeting MITF in resistant melanomas. Again, these experiments could be carried out using the *mitfa-GFP* fluorescent reporter line

crossed to *BRAF^{V600E}mitfa^{vc7}* mutants to visualise the effect of BRAF, MEK, MITF and combination inhibitor treatments in melanoma resistance.

6.2.2 A BRAF^{V600E}-independent, mitfa^{vc7}p53^{M214K} melanoma model

In addition to the BRAF^{V600E} melanoma models shown here, the *mitfa^{vc7}p53^{M214K}* zebrafish melanomas present a new model for BRAF^{V600E}-independent melanomas. These are important models for the development of therapeutic strategies to treat patients that do not harbour the *BRAF^{V600E}* mutation. Similar to the *BRAF^{V600E}mitfa^{vc7}* model, these melanomas depend on MITF activity for survival and therefore they could also be used to test modulators of MITF as potential new therapeutics.

Preliminary research showed that the *mitfa^{vc7}p53^{M214K}* melanomas were highly invasive, comparable to the *BRAF^{V600E}p53^{M214K}* tumour growth pattern. Similar experiments carried out to those used to compare *BRAF^{V600E}mitfa^{vc7}* and *BRAF^{V600E}p53^{M214K}* melanomas would allow further characterisation of the BRAF^{V600E}-independent phenotype. It would be interesting for example to assess the mitotic activity of these tumours in light of their invasive behaviour and the expression of MITF target genes compared to the BRAF^{V600E} melanomas. As described in section 3.2.4, the mitotic activity of *mitfa^{vc7}p53^{M214K}* melanomas could be determined using the phospho-Histone H3 antibody. If high numbers of phospho-Histone H3 stained cells, similar to those found in *BRAF^{V600E}p53^{M214K}* tumours, were found in *mitfa^{vc7}p53^{M214K}* melanomas this would indicate a high mitotic rate. As described by Thompson and colleagues (2011), the presence of mitotic figures within a tumour tissue implies that cells are actively dividing and usually that tumours will grow rapidly with an increased potential to metastasise. This study also confirmed that 'a high tumour mitotic rate reflects a more aggressive tumour that is associated with a worse survival outcome' (Thompson *et al*., 2011). A high mitotic rate in *mitfa^{vc7}p53^{M214K}* melanomas could help to explain their aggressive, invasive growth.

The relative expression of *C-MET* in *mitfa*^{vc7}*p53*^{M214K} melanoma would be also interesting to confirm. MET is frequently found overexpressed in human cancers and in particular contributes to the invasive capacity of tumour cells (Stella *et al*., 2010). In this study, I found that *BRAF*^{V600E}*mitfa*^{vc7} melanomas expressed higher levels of *C-MET* compared to *BRAF*^{V600E}*p53*^{M214K}, despite the latter genotype showing a more invasive behaviour. If *C-MET* was found highly expressed in *mitfa*^{vc7}*p53*^{M214K} melanomas, this could in part explain its striking invasive behaviour. Inhibitors of MET are currently in pre-clinical development (Flaherty, 2006) and if *mitfa*^{vc7}*p53*^{M214K} melanomas have high *C-MET* expression levels it could act as an in *vivo* model in which to test these drugs.

6.2.3 Identification of genes that distinguish between melanoma subtypes

The RNA-seq analysis of *BRAF*^{V600E}*mitfa*^{vc7} and *BRAF*^{V600E}*p53*^{M214K} zebrafish melanomas identified several interesting and biologically relevant groups of genes that were differentially expressed and that may help to understand the observed histopathological distinctions between these two subtypes. The phosphodiesterases were a promising example and although there was no significant difference in cAMP levels between the two subtypes, this may mean that the PDEs play an additional role to assisting degradation of cAMP in a tumour environment, or that the specific *PDE* genes identified to be differentially expressed do not assist with this role. Directly inhibiting the specific *PDEs* found to be differentially expressed in the tumours would allow us to identify how these genes contribute to the pathology of BRAF^{V600E} melanomas. As described in Chapter 5, a link between phosphodiesterases and melanoma has already been established in two separate studies. Arozarena and colleagues (2005) showed that expression of PDE5 suppresses the invasive capacity of BRAF^{V600E} mutant melanoma cells and that PDE5A is downregulated in a number of BRAF mutant melanoma cell lines. Hiramoto and colleagues (2014) showed that inhibiting PDE2 reduces the growth and invasion capacity of a human malignant

melanoma PMP cell line. Together these studies suggest an important role for PDEs in the invasive nature of melanoma cells and the potential to target these enzymes to reduce invasiveness of melanomas. As the *BRAF*^{V600E}*p53*^{M214K} melanoma subtype was characteristically invasive compared to its *BRAF*^{V600E}*mitfa*^{vc7} counterpart it would be extremely valuable to test whether inhibitors of those PDEs found differentially expressed would be able to reverse this aggressive behaviour and if so, whether these could become novel therapeutic targets for the disease.

The other interesting group of genes identified to be differentially expressed were the *GRINs* and as there is supporting data showing that other members of this gene family are involved in melanomagenesis, together the data highlights the significance of these genes as potential druggable targets in melanoma. Wei and colleagues (2011) found *GRIN2A* to be the highest mutated gene in a screen of metastatic melanomas, while Valsesia and colleagues (2011) identified gene amplifications in both *GRIN2B* and *GRIN2C* in melanoma cell lines. Prickett and colleagues (2011) found *GRM3*, a group 2 glutamate receptor, frequently mutated in metastatic melanomas. Together, these three studies highlight the significance of glutamate receptor signalling pathway in melanoma and suggest a potential novel therapeutic strategy. A link between glutamate receptors and cancer has previously been established in neuronal tumours (Takano *et al*., 2001). Malignant gliomas with high levels of glutamate release have a distinct growth advantage and grow more aggressively than parental glial cells (Takano *et al*., 2001). In a separate study, Shin and colleagues (2008) show that expression of GRM1 in melanocytes is sufficient to induce melanoma *in vivo* through activation of ERK. The natural ligand of GRM1 is glutamate and excess glutamate is released from GRM1 expressing melanocytic cells to promote melanomagenesis (Shin *et al*., 2008). Together, results from Takano and Shin imply a correlation between glutamate release and human cancers.

Suppression of glutamate signalling using glutamate antagonists has been shown to inhibit the proliferation of human tumour cells of colon adenocarcinoma, breast and lung cancer cell lines (Rzeski *et al*., 2001). The anti-proliferative effect of these

antagonists reduces cell division and motility and increases cell death and invasive growth of tumour (Rzeski *et al*., 2001), further emphasizing the potential to target glutamate receptors in anticancer therapies. In a recent review by Stepulak and colleagues (2014) the clinical relevance of glutamate receptors in cancer was described as well as the attempts to inhibit glutamate receptors using agonists. There has been very little success in effective targets of glutamate receptors despite the depth of research implicating these molecules in several cancer types including bone, breast and prostate (Ren *et al*., 2012; Speyer *et al*., 2014; Koochekpour *et al*., 2012; Stepulak *et al*., 2014). The authors encouraged additional research to define the clinical significance of glutamate receptor expression and signaling in cancer, which they hope would lead to improved targeting of this pathway in the future.

In a similar manner to the PDE inhibitors, it would be particularly interesting to test the effect of glutamate receptor inhibition on the $BRAF^{V600E}p53^{M214K}$ melanoma invasive subtype and identify whether inhibitors would alter the characteristic invasive nature. Glutamate antagonists used in previous studies (Rzeski *et al*., 2001) could be used to treat $BRAF^{V600E}$ melanomas *in vivo*, determine the role of GRINs in melanoma biology and validate if members of the glutamate signaling pathway are potential novel drug targets.

Chapter 7 – Materials and Methods

7.1 Solutions

E3 media

To prepare 60X stock solution:

34.8g NaCl

1.6g KCl

5.8g $CaCl_2.2H_2O$

9.78g $MgCl_2.6H_2O$

Dissolve above in H_2O to a final volume of 2L. Adjust to pH7.2 using NaOH. To prepare 1L of 1X E3 media use 16.5ml 60X stock, make up to 1L with H_2O, and add 100µl 1% methylene blue (Sigma Aldrich).

Tricaine

Also known as 3-amino benzoic acid ethyl ester or 3-amino benzoate:

400mg tricaine (Sigma Aldrich)

2.1ml Tris (pH9)

97.9ml distilled H_2O

Prepare the above, dissolve using hot plate and stirrer and adjust to pH7. To use as an anaesthetic, place 4.2ml tricaine solution in 100ml clean system water.

Paraformaldehyde

Commercial 16% paraformaldehyde is diluted to a 4% working concentration with PBS before use in fixation.

EDTA

0.5M Ethylenediaminetetraacetic acid (pH7.8) prepared for calcification steps during histology.

Ethanol

A range of ethanol percentages (30-100) were used in various protocols.

Bleach

A bleaching solution of 10-13% sodium hypochlorite (Sigma Aldrich) is used to bleach zebrafish embryos at 24hpf, prior to transfer to the aquarium system. 180µl of bleach is mixed with 100ml system water in the bleaching process.

TBS

A 10X stock of Tris buffered saline (TBS) is made using:

61g Trizma base (Sigma Aldrich)

90g NaCl

Prepare solution by dissolving reagents in 800ml of distilled H_2O. Adjust to pH8.4 using concentrated HCl and make up to final 1L volume using distilled H_2O. Dilute 1:10 with H_2O to make a 1X working solution.

TBST

TBS-Tween is prepared using 1L of 1XTBS and adding 500µl Tween-20.

PBS

A 10X stock of phosphate buffered saline (PBS) is made using:

80g NaCl

2g KCl

14.4g Na_2HPO_4

2.4g KH_2PO_4

Prepare solution by dissolving reagents in 800ml of distilled H_2O. Adjust to pH7.4 using concentrated HCl and make up to final 1L volume using distilled H_2O. Dilute 1:10 with H_2O to make a 1X working solution.

PBST

PBS-Tween is prepared using 1L of 1XPBS and adding 500µl Tween-20.

Citrate buffer

To prepare 1L 0.01M citrate buffer (pH6) for antigen retrieval:

18ml 0.1M citric acid

82ml sodium citrate

900ml distilled H_2O

Dissolve reagents in water using hot plate and stirrer and then adjust to pH6.

EDTA buffer

To prepare 1L EDTA buffer (pH8) for antigen retrieval:

3.72g EDTA

1L distilled H_2O

Dissolve EDTA in water using hot plate and stirrer and then adjust to pH8.

DPX

Commercial DPX (a mixture of distyrene, a plasticizer and xylene) is used as a mounting media for histological protocols.

Xylene

A solvent used to remove paraffin from microscope slides prior to staining in histology.

Hematoxylin

A basic dye used for staining in histology.

Eosin

An acidic dye used for staining in histology.

Lithium carbonate

A 1% lithium carbonate solution is used to blue-up fixed sections after H&E staining in histology.

Acid-alcohol solution

1% HCl in 70% alcohol is used to remove excess stain and define nuclei after H&E staining in histology.

PTU

1-phenyl 2-thiourea (PTU) is used to treat embryos and inhibit melanogenesis, therefore improving signal detection in whole mount in situ hybridisation experiments.

7.2 Zebrafish husbandry

Zebrafish were reared and raised according to the United Kingdom Home Office Animals (Scientific Procedures) Act (1986) and approved by the University of Edinburgh Ethical Review Committee.

7.2.1 Breeding

Wild type and transgenic adult zebrafish can be paired (male and one/two females in breeding tank with barrier) or marbled (plastic chamber with marbles and mesh layer) to collect embryos laid externally by females and fertilised by males. After collection, embryos are placed in a petri dish and incubated in E3 medium at 28°C until required for experiments or until 5 days post fertilization (dpf) when they can be transferred to the system.

7.2.2 Raising embryos

After 5dpf, embryos are large enough to be transferred to either static tanks or into the nursery contained within the zebrafish aquarium system. At this age they are fed twice daily with paramecium and ZM1000 powder. After 4-6 weeks, they are then moved to larger 30 litre tanks within the system and are fed twice daily with brine shrimp and dry food. At 3 months they are old enough to be paired for breeding.

7.2.3 Strain origins

BRAF^{V600E}

Gateway™ technology was employed to clone *BRAF^{V600E}* under the control of the *mitfa* promoter to generate mosaic *BRAF^{V600E}* zebrafish. Single site cloning was carried out between a pENT 3C entry clone, containing human BRAF^{V600E} and a

destination vector pT2Kmin-NP Dest RfA, carrying the *mitfa* promoter, flanked by Tol2 transposon sequences (provided by Dr. James Lister, USA). A single LR recombination reaction was carried out between these two vectors using an LR Clonase™ Mix (Invitrogen), according to the manufacturer's protocol. Co-injection of this plasmid with transposase RNA (both at a 25ng/µl concentration) was carried out directly into the single-celled embryo. Embryos were transferred to the nursery after 5 dpf and raised to adulthood.

mitfa^{vc7}

The *mitfa*^{vc7} transgenic line was identified from an ENU-mutagenesis screen and provided to us by Dr. James Lister, USA. Unlike previous *mitfa* mutants, in which melanocytes are completely absent, zebrafish homozygous for the *mitfa*^{vc7} allele have variable numbers of developing melanocytes when grown at standard temperatures and conditions (Johnson *et al*., 2011). The advantage of this mutant was its temperature-sensitivity – the ability to regulate the levels of MITF and therefore the number of melanocytes that are able to develop by simply changing the temperature of the water in which the mutant was reared. To generate *BRAF*^{V600E}*mitfa*^{vc7} double homozygotes, genetic crosses were made and all generations of offspring were genotyped by PCR/sequencing to confirm BRAF and mitfa allele status.

p53^{M214K}

Zebrafish with a missense mutation in the *tp53* DNA-binding domain were first identified using a target-selected mutagenesis study (Berghmans *et al*., 2005). The *p53*^{M214K} mutation, used in cooperation with *BRAF*^{V600E} in this study, causes malignant peripheral nerve sheath tumours (MPNST) in 28% of fish at 8.5 months of age (Berghmans *et al*., 2005). Patton *et al*. (2005) first showed that *BRAF*^{V600E}*p53*^{M214K} mutants develop melanoma.

7.3 Zebrafish procedures

7.3.1 Anaesthesia

To tail clip or image an adult zebrafish it must first be anaesthetised. To do this, 4.5ml tricaine is mixed with 100ml water in a small tank. The zebrafish is then caught with a net and placed into the tank containing the anaesthetic until this has taken effect (2-3 minutes). After the tail clip or other procedure has been carried out during anaesthesia, the zebrafish is placed into a tank of distilled water for recovery and then back into its original tank.

7.3.2 Tail clip

Once under anaesthesia, the zebrafish can be placed onto a petri dish lid and a small piece of tail fin cut with a scalpel. The tissue is placed into a tube and kept at -20°C until required. The zebrafish are usually isolated after the tail clipping procedure until genotyping results are confirmed.

7.3.3 Imaging

Imaging of adult zebrafish whilst under anaesthesia or after sacrificing was carried out using Nikon light microscope to which a standard digital camera is attached. Zebrafish are placed onto a clean petri dish in a pool of distilled water, distributed using a plastic pipette. The petri dish is placed onto a white disc under the light microscope and brought into focus on the digital display of the camera. Sections of the zebrafish are photographed individually and saved. After photography is complete, images are downloaded from the camera and edited using Adobe Photoshop CS5. Separate images of an individual fish can be merged using the 'Photomerge' tool.

7.4 Pathology

7.4.1 Fixation

After sacrificing the zebrafish by immersion in tricaine solution, according to Home Office Schedule 1 methods, the fish is dissected in half transversely to increase penetration of the fixative. Tissues are then incubated in 4% paraformaldehyde (16% paraformaldehyde diluted in PBS) at 3 days at 4°C with agitation. Samples are washed with PBS and decalcified in 0.5M EDTA (pH8) for 5 days at 4°C with agitation. Tissue is washed again in PBS and then stored in 70% ethanol at 4°C until required.

7.4.2 Embedding and sectioning

Fixed tissues, of embryos, adult, or tumour, are embedded in wax to be serially sectioned. Sections are cut transversely at 5μm thickness using a macroscope. Cut wax sections are floated onto water within a water bath at 55°C, placed onto a slide and left to dry on a hot plate.

7.4.3 Haematoxylin and eosin (H&E) staining

H&E staining was carried out on cut, prepared sections on slides. The slides were deparaffinised in xylene, 2 x 5 minutes, and then rehydrated through graded alcohol solutions (100%, 90%, 70%, 50%, 30%, 5 minutes each) before washing thoroughly in running water. Slides were stained for 4 minutes in Mayer's haematoxylin, washed with water, rinsed with 95% acid-alcohol solution for a few seconds, washed with water, then counterstained in eosin for 1-2 minutes. Slides were dehydrated with 95% alcohol (5 minutes) and absolute alcohol (2 x 5 minutes), and cleared with 2 x 5 min xylene. DPX was used to mount the slides with coverslips and left to dry in the air.

7.5 Immunohistochemistry and immunofluorescence

7.5.1 Immunohistochemistry

For immunohistological staining, slides are treated as prior to H&E staining to deparaffinise and rehydrate the sections. Slides are then washed in water for 2 x 5 minutes, bleached in 1% potassium hydroxide/3% hydrogen peroxidase for 15-30 minutes and washed again in water for 3 x 5 minutes. Antigen retrieval is carried out with either citric acid or EDTA buffer: the desired buffer is brought to boiling point in a pressure cooker (lid off) in a microwave for 12 minutes; slides are placed into the buffer immediately, lid closed, and heated for 2 minutes, then 5 minutes, before removing from the buffer and leaving to cool. The slides are then washed with water for 3 x 5 minutes, before ensuring all endogenous peroxidase activity is removed by incubating in 3% hydrogen peroxidase for 10 minutes. Slides are washed again for 2 x 5 minutes with water, then for 5 minutes with 1 x TBS and blocked with serum-free blocking solution (DAKO) for 30 minutes at room temperature. The blocking solution is then removed from the slides and the sections are incubated with the desired primary antibody (diluted in antibody diluent (DAKO)) overnight at 4°C. The primary antibody is removed and the slides are washed in PBS for 3 x 5 minutes, before incubation with HRP Rabbit/Mouse secondary antibody (DAKO EnVision detection kit) for 30 minutes at room temperature. The secondary antibody is removed, washed in PBS for 2 x 5 minutes and the slides are incubated in DAB chromagen (DAKO) for 10 minutes to visualise the stain. The chromagen is washed off with water for 2 x 5 minutes, and the slides are counterstained: Mayer's haematoxylin for 4 minutes; wash with water; blue-up with lithium chloride (few seconds) and wash thoroughly with running water. The samples are then dehydrated with one minute incubations in increasing ethanol concentrations (70%, 90%, 2 x 100%), followed by 2 x 2 minute xylene washes and finally mounting with DPX mounting media and coverslips.

7.5.2 Immunofluorescence

For immunofluorescent staining, slides are treated as prior to H&E staining to deparaffinise and rehydrate the sections. Slides are then washed in water for 2 x 5 minutes and 1 x TBS for 3 x 5 minutes. Antigen retrieval is carried out with citric acid buffer, as in the protocol detailed in 7.5.1 and then the slides are washed in 1 x TBST for 3 x 5 minutes. Samples are blocked using 10% heat inactivated donkey serum (diluted in 1 x TBST) in a humidifying chamber for 90 minutes at room temperature. The serum is removed and the primary antibody, diluted in 1% donkey serum, is added to the slides, incubating overnight at 4°C. The slides are washed with 1 x TBST for 4 x 5 minutes, and the secondary antibody is added, incubating for 1 hour at room temperature in a humidifying chamber away from the light. Slides are washed again in 1 x TBST for 4 x 5 minutes, before coverslips are mounted using 1-2 drops of Prolong Gold (Molecular Probes) mounting media, covered and left to dry overnight, away from light, at 4°C. Coverslips are then sealed to the slides using a few drops of nail polish, left to dry and stored away from light at 4°C.

7.6 Molecular biology techniques

7.6.1 DNA extraction from tail clip

Prepare 100µl of DNA extraction buffer/tail clip and add to tube containing tail clip. Mix by flicking tube and then incubate at 56°C for ≥ 3 hours, flicking the tube every ½ -1 hour. Add 200µl ethanol/Na-acetate solution to each tube and mix by pipetting. Incubate at room temperature for 15 minutes. Centrifuge for 10-30 minutes at max speed (or until visible pellet forms). Remove supernatant and wash pellet by adding 500µl 70% ethanol to each tube, centrifuge for 10 minutes, remove supernatant and allow pellet to dry in air for ~2 minutes. Re-suspend DNA in 20-50µl TE buffer and store at -20°C.

7.6.2 RNA extraction from tail clip or tumour tissue

Homogenize sample by adding 500µl Trizol to the tube and using a powered tip/crushing with mortar and pestle. Transfer the homogenized sample into tube and add additional Trizol (1ml/50-100mg tissue). Incubate for 5 minutes at room temperature to permit the complete dissociation of nucleoprotein complexes. Add 200µl of chloroform per ml of Trizol, shake with hand for 15 seconds and incubate at room temperature for 2-3 minutes. Centrifuge at 12,000G for 15 minutes at 4°C. Transfer the upper aqueous phase to fresh tube using cut-off tip and mix with isopropanol (250µl isopropanol/500µl Trizol). Incubate the samples at room temperature for 10 minutes, then centrifuge at 12,000G for 10 minutes at 4°C. Make sure there is a visible pellet, then remove the supernatant and discard. Wash the RNA pellet once by adding 750µl 75% ethanol to the tube and pour off to leave pellet. Spin briefly and remove excess ethanol with tissue. Briefly dry the RNA pellet in the air, then re-suspend in RNase-free water (20-50µl) and incubate at 60°C for 10 minutes before storing at -80°C.

7.6.3 cDNA preparation from RNA

For RT-PCR/qRT-PCRs, use the Superscript II/III RT kit, using 1µg total RNA in a 10µl total reaction volume. Prepare a master mix of oligo $(dT)_{12-18}$ (500µg/ml) and dNTPs (5mM). For each reaction, a total of 3µl, use 2.25µl RNA (or RNA with RNase-free water) and 0.75µl master mix. Incubate at 65°C for 5 minutes, then quickly chill on ice. Prepare a master mix of 5 x First Strand buffer, DTT (0.1M), RNase OUT (40 units/µl) and Superscript II/III RT. To each 3µl reaction, add 2µl master mix, mix and place in PCR machine set with the following programme: Heated lid 110°C, 42°C for 5 minutes, 50°C for 1 hour, 70°C for 10 minutes, 4°C holding. The cDNA can then be stored at -20°C.

7.6.4 Genotyping

To genotype an adult zebrafish, a tail clip must be taken followed by extraction of the tail clip DNA and, using the DNA prepared, a PCR using the appropriate primer set can be carried out.

7.6.5 qRT-PCR

cDNA is prepared as described and relevant primers are diluted to 10µM concentration. The SYBR Green JumpStart Taq ReadyMix (Sigma) is used and contains a mixture of SYBR Green I (a commonly-used fluorescent DNA binding dye), JumpStart Taq DNA polymerase, deoxynucleotides and a reaction buffer. For gene of interest to be quantified by this method, a mastermix of SYBR Green JumpStart Taq ReadyMix, distilled water and primers are used. 4µl of cDNA is placed in wells of a 384-well plate to which the primer mastermix is added. β-actin primers are used to normalise the data and distilled water is added to wells instead of cDNA to act as a negative control. cDNA and primer mix are added to wells in triplicate as a technical replicate. Once cDNA and the primer/JumpStart Taq

mastermix has been added to the plate, it is covered and placed in a centrifuge where it is spun down (1000rpm for 1 minute) to mix and draw the contents of the wells to the bottom of the plate. The plate is then transferred to a Fast Real-Time PCR system (HT7900, Applied Biosystems).

7.6.6 Western Blotting

Preparation of the gels

8% Resolving gel. Makes 10ml for 2 gels

dH_2O	3.47ml
Tris (pH 8.8)	3.73ml
Acrylamide	2.7ml
TEMED	10µl
10% SDS	100µl
25% APS	40µl

Stacking gel. Makes 4ml for 2 gels

dH_2O	2.8ml
Tris (pH 6.8)	0.5ml
Acrylamide	0.67ml
TEMED	10µl
10% SDS	40µl
25% APS	20µl

Using the above recipes, 0.75 or 1.5mm SDS polyacrylamide gels were prepared. Approximately 4ml of resolving gel mixture was placed between glass plates (BioRad). To speed up polymerisation and ensure no bubbles formed on top of the gel layer, 1ml of isopropanol was pipetted onto the layer of resolving gel. When the gel polymerised, the isopropanol was poured off and 1.5ml stacking gel mixture was poured on top, before adding a 12 or 15-well comb between the plates.

Preparation of the lysates

To prepare lysates from embryos, these must first be collected, placed in skirted tubes with all media removed and snap-frozen for storage at -80°C. Embryos are usually aliquoted in 10s to allow ease of lysis and equal protein concentration preparation. The lysis buffer is prepared and can be stored at -20°C for subsequent use.

Lysis (RIPA) buffer. Makes 10ml

2M Tris HCl (pH 7.5)	250µl
5M NaCl	300µl
1% NPO_4	100µl
Na deoxycholate	0.5g
10% SDS	100µl
dH_20	to make up to 10ml

To lyse embryos, add 40µl prepared lysis buffer to each tube containing 10 embryos, as well as about 50 acid-washed glass beads. Ribolyse the samples using a ribolyser for 6 seconds at 6.5 speed. Incubate the samples on ice for 15 minutes and centrifuge using a table-top centrifuge at maximum speed for 15 minutes. Transfer the supernatant to a clean 1.7ml eppendorf tube. Measure the protein content of the

lysate by calculating the A_{380} absorbance using a NanoDrop 2000 Spectrophotometer.

Samples must be denatured prior to gel loading by adding respective volumes of Sample Buffer according to each lysate's protein content to make a final volume of 50µl. Lysate and Sample Buffer mixture is denatured at 95°C for 5 minutes, before loading into wells while still warm.

Performing Western Blots

Running the gel

After samples were loaded, the gel was run in a 1xSDS running buffer at 80V. Once the samples had reached the level at the bottom of the stacking gel, the voltage was increased to 120V until the samples had run out of the gel.

Semi-dry protein transfer

To transfer the proteins to synthetic membrane, semi-dry blotting equipment and protocol were used (BioRad). First, the gel and membrane were equilibrated in 1xTransfer Buffer for 15 minutes at room temperature. Filter paper was also soaked in 1xTransfer Buffer prior to protein transfer. Using the BioRad apparatus, the pre-soaked filter paper was placed onto the platinum anode, before placing the equilibrated membrane and subsequently the membrane, on top. Another layer of pre-soaked filter paper was placed on top of the membrane and air bubbles removed using a roller. Lastly, the cathode was placed onto the transfer stack and safely sealed. The assembly was connect to a power supply and run at 10V for 30 minutes. After successful transfer, the membrane can be removed and incubated with Ponceau S stain for 1-2 minutes to detect protein. Prior to blocking, the stain can be removed by washing with distilled water and one 5 minute rinse with 1xTBS.

Blocking

Subsequent to successful protein transfer, the membranes were incubated in a 1% milk/TBST solution for 30 minutes at room temperature with agitation.

Primary antibody incubation

The desired primary antibody concentration was prepared in 5ml 1% blocking solution. The membrane was placed in a sealed plastic sleeve and incubated with the primary antibody overnight at 4°C, with agitation. After overnight incubation, the primary antibody was poured off and the membrane washed with 0.1% blocking solution for 2 minutes at room temperature, with agitation. After the initial wash, the membrane was washed three times with 1xTBST for 5 minutes each at room temperature, with agitation.

Secondary antibody incubation

The desired secondary antibody concentration was prepared (usually between 1:1000-1:2000) in 5ml 1% blocking solution and the membrane incubated in the solution for 1 hour at room temperature, with agitation. After secondary antibody incubation, the membrane was washed four times with 1xTBST for 5 minutes each, at room temperature, with agitation.

Exposure and developing membranes

After the secondary antibody was washed off, the membrane was left briefly to air-dry. With the protein-side up, the membrane was incubated with 1ml of ECL Plus (GE Healthcare) for 5 minutes at room temperature. The membranes were then placed onto a glass plate within a developing cassette and sealed with cling film and directly exposed on x-ray film for varying lengths of time. The x-ray films were developed and scanned using an HP ScanJet 4300C scanner.

7.6.7 cAMP ELISA assay

Preparation of tissue samples

The cAMP assay was carried out using a cAMP ELISA kit (Enzo Life Sciences). To prepare samples from tumours, frozen tissue is ground to a fine powder under liquid nitrogen using a mortar and pestle. After the liquid nitrogen has evaporated, the tissue is weighed and homogenised in 10 volumes of 0.1M HCl. The sample is centrifuged for 10 minutes at max speed to pellet the debris. The supernatant is then used directly in the assay or frozen for a later analysis.

Preparation of cAMP standards

cAMP standards are prepared for the standard curve during analysis. As tissue samples were prepared using 0.1M HCl, this is also used as the standard diluent. To prepare the standards, a 2000pmol/ml cAMP stock (Enzo Life Sciences) is used and warmed to room temperature. 900µl of 0.1HCl is placed into five eppendorf tubes labelled numbers 1-5. 100µl of 2000pmol/ml standard stock is placed into tube 1 and vortexed thoroughly. 250µl of tube 1 is then transferred to tube 2 and vortexed thoroughly. 250µl of tube 2 is then transferred to tube 3 and vortexed thoroughly. This process is repeated for tubes 4 and 5 to prepare cAMP standards of 0.78, 3.13, 12.5, 50 and 200pmol/ml concentrations. The diluted standards must then be used for the assay within 1 hour of preparation.

Set-up and running of the cAMP assay

To prepare the assay, a Goat anti-Rabbit IgG 96-well microtitre plate (Enzo Life Sciences) is used. As well as standards and samples, two blanks (B), two total activity (TA), two non-specific binding (NSB) and two zero standard (Bo) wells are prepared. Into each well except the blank and TA wells, 50µl of Neutralizing

Reagent (Enzo Life Sciences) is added. 100µl of 0.1M HCl is then added to the NSB and Bo wells. 50µl of 0.1M HCl is added to the NSB wells. 100µl of each standard (1-5) is pipetted into duplicate standard wells and 100µl of each sample is then added to each sample well, also in duplicate. 50µl of blue conjugate (Enzo Life Sciences) then placed into each well except the blank and TA wells. 50µl of the yellow antibody (Enzo Life Sciences) is then placed into each well except the blank, TA and NSB wells. The plate is then sealed and incubated for 2 hours on a plate shaker at room temperature. After incubation, the contents of the wells are emptied and washed three times by adding 400µl of wash buffer (Enzo Life Sciences) to each well. After the final wash, the plate is firmly tapped onto a clean, lint-free paper towel to remove any remaining wash buffer. 5µl of blue conjugate is then placed into the TA wells and 200µl of the substrate solution is pipetted into each well. The plate is incubated for a second time for 1 hour at room temperature without shaking. After incubation 50µl of stop solution (Enzo Life Sciences) is added to each well to stop the reaction. To analyse the reactions, a microplate reader (1420 Multilabel Counter, PerkinElmer) is used. The plate reader is blanked using the substrate blank and then the optical density (OD) of each well is read at 405nm. To calculate cAMP concentration (pmol/ml) a standard curve is drawn using the OD values of the standard cAMP concentrations used. From the regression line equation of this curve, the cAMP concentration of each unknown sample can be calculated.

References

Acharya UH, Jeter JM. (2013) Use of ipilimumab in the treatment of melanoma. *Clin Pharmacol.* 5(Suppl 1): 21-27.

Adams DS, Masi A, Levin M. (2007) H+ pump-dependent changes in membrane voltage are an early mechanism necessary and sufficient to induce Xenopus tail regeneration. *Development*. 134(7): 1323-35.

Amae S, Fuse N, Yasumoto K, Sato S, Yajima I, Yamamoto H, Udono T, Durlu YK, Tamai M, Takahashi K, Shibahara S. (1998) Identification of a novel isoform of microphthalmia-associated transcription factor that is enriched in retinal pigment epithelium. *Biochem Biophys Res Commun*. 247(3): 710-5.

Amatruda JF, Shepard JL, Stern HM, Zon LI. (2002) Zebrafish as a cancer model system. *Cancer Cell*. 1(3): 229-31.

Amiel J, Watkin PM, Tassabehji M, Read AP, Winter RM. (1998) Mutation of the MITF gene in albinism-deafness syndrome (Tietz syndrome). *Clin Dysmorphol*. 7(1): 17-20.

Amsterdam A, Sadler KC, Lai K, Farrington S, Bronson RT, Lees JA, Hopkins N. (2004) Many ribosomal protein genes are cancer genes in zebrafish. *PLoS Biol.* 2(5): E139.

Anders F, Schartl M, Barnekow A. (1984) Xiphophorus as an in vivo model for studies on oncogenes. *Natl Cancer Inst Monogr*. 65: 97-109.

Anders S, Huber W. (2010) Differential expression analysis for sequence count data. *Genome Biol*. 11(10): R106.

Aparicio S, Chapman J, Stupka E, Putnam N, Chia JM, Dehal P, Christoffels A, Rash S, Hoon S, Smit A et al. (2002) Whole-genome shotgun assembly and analysis of the genome of Fugu rubripes. *Science*. 297(5585): 1301-10.

Arnheiter H. (2010) The discovery of the microphthalmia locus and its gene, Mitf. *Pigment Cell Melanoma Res*. 23(6): 729-35.

Arozarena I, Sanchez-Laorden B, Packer L, Hidalgo-Carcedo C, Hayward R, Viros A, Sahai E, Marais R. (2011) Oncogenic BRAF induces melanoma cell invasion by downregulating the cGMP-specific phosphodiesterase PDE5A. *Cancer Cell*. 19(1): 45-57.

Asher JH Jr, Friedman TB. (1990) Mouse and hamster mutants as models for Waardenburg syndromes in humans. *J Med Genet.* 27(10): 618-26.

Attia P, Phan GQ, Maker AV, Robinson MR, Quezado MM, Yang JC, Sherry RM, Topalian SL, Kammula US, Royal RE et al. (2005) Autoimmunity correlates with tumor regression in patients with metastatic melanoma treated with anti-cytotoxic T-lymphocyte antigen-4. *J Clin Oncol*. 23(25): 6043-53.

Azzola MF, Shaw HM, Thompson JF, Soong SJ, Scolyer RA, Watson GF, Colman MH, Zhang Y. (2003) Tumor mitotic rate is a more powerful prognostic indicator than ulceration in patients with primary cutaneous melanoma: an analysis of 3661 patients from a single center. *Cancer*. 97(6): 1488-98.

Balch CM, Buzaid AC, Soong SJ, Atkins MB, Cascinelli N, Coit DG, Fleming ID, Gershenwald JE, Houghton A Jr, Kirkwood JM et al. (2001) Final version of the American Joint Committee on Cancer staging system for cutaneous melanoma. *J Clin Oncol.* 19(16): 3635-48.

Bamford S, Dawson E, Forbes S, Clements J, Pettett R, Dogan A, Flanagan A, Teague J, Futreal PA, Stratton MR, Wooster R. (2004) The COSMIC (Catalogue of Somatic Mutations in Cancer) database and website. *Br J Cancer*. 91(2): 355-8.

Bardeesy N, Bastian BC, Hezel A, Pinkel D, DePinho RA, Chin L. (2001) Dual inactivation of RB and p53 pathways in RAS-induced melanomas. *Mol Cell Biol*. 21(6): 2144-53.

Beckwith LG, Moore JL, Tsao-Wu GS, Harshbarger JC, Cheng KC. (2000) Ethylnitrosourea induces neoplasia in zebrafish (Danio rerio). *Lab Invest*. 80(3): 379-85.

Béjar J, Hong Y, Schartl M. (2003) Mitf expression is sufficient to direct differentiation of medaka blastula derived stem cells to melanocytes. *Development*. 130(26): 6545-53.

Berger MF, Hodis E, Heffernan TP, Deribe YL, Lawrence MS, Protopopov A, Ivanova E, Watson IR, Nickerson E, Ghosh P et al. (2012) Melanoma genome sequencing reveals frequent PREX2 mutations. *Nature*. 485(7399): 502-6.

Berger MF, Levin JZ, Vijayendran K, Sivachenko A, Adiconis X, Maguire J, Johnson LA, Robinson J, Verhaak RG, Sougnez C et al. (2010) Integrative analysis of the melanoma transcriptome. *Genome Res*. 20(4): 413-27.

Berghmans S, Murphey RD, Wienholds E, Neuberg D, Kutok JL, Fletcher CD, Morris JP, Liu TX, Schulte-Merker S, Kanki JP et al. (2005) tp53 mutant zebrafish develop malignant peripheral nerve sheath tumors. *Proc Natl Acad Sci U S A*. 102(2): 407-12.

Bertolotto C, Lesueur F, Giuliano S, Strub T, de Lichy M, Bille K, Dessen P, d'Hayer B, Mohamdi H, Remenieras A et al. (2011) A SUMOylation-defective MITF germline mutation predisposes to melanoma and renal carcinoma. *Nature*. 480(7375): 94-8.

Bollag G, Hirth P, Tsai J, Zhang J, Ibrahim PN, Cho H, Spevak W, Zhang C, Zhang Y, Habets G et al. (2010) Clinical efficacy of a RAF inhibitor needs broad target blockade in BRAF-mutant melanoma. *Nature*. 467(7315): 596-9.

Boni A, Cogdill AP, Dang P, Udayakumar D, Njauw CN, Sloss CM, Ferrone CR, Flaherty KT, Lawrence DP, Fisher DE, Tsao H, Wargo JA. (2010) Selective BRAFV600E inhibition enhances T-cell recognition of melanoma without affecting lymphocyte function. *Cancer Res.* 70(13): 5213-9.

Box NF, Terzian T. (2008) The role of p53 in pigmentation, tanning and melanoma. *Pigment Cell Melanoma Res*. 21(5): 525-33.

Breslow A. (1970) Thickness, cross-sectional areas and depth of invasion in the prognosis of cutaneous melanoma. *Ann Surg*. 172(5): 902-8.

Broekaert SM, Roy R, Okamoto I, van den Oord J, Bauer J, Garbe C, Barnhill RL, Busam KJ, Cochran AJ, Cook MG et al. (2010) Genetic and morphologic features for melanoma classification. *Pigment Cell Melanoma Res*. 23(6): 763-70.

Bucheit AD and Davies MA. (2014) Emerging insights into resistance to BRAF inhibitors in melanoma. *Biochem Pharmacol.* 87(3): 381-9.

Busam KJ, Charles C, Lee G, Halpern AC. (2001) Morphologic features of

melanocytes, pigmented keratinocytes, and melanophages by in vivo confocal scanning laser microscopy. *Mod Pathol*. 14(9): 862-8.

Busam KJ, Jungbluth AA. (1999) Melan-A, a new melanocytic differentiation marker. *Adv Anat Pathol*. 6(1): 12-8.

Buscà R, Berra E, Gaggioli C, Khaled M, Bille K, Marchetti B, Thyss R, Fitsialos G, Larribère L, Bertolotto C, Virolle T, Barbry P, Pouysségur J, Ponzio G, Ballotti R. (2005) Hypoxia-inducible factor 1{alpha} is a new target of microphthalmia-associated transcription factor (MITF) in melanoma cells. *J Cell Biol*. 170(1): 49-59.

Cancer Research UK, 2011. *Skin cancer statistics* [online] Available at: http://www.cancerresearchuk.org/cancer-info/cancerstats/types/skin/ [Accessed 15th May 2014]

Cancer Research UK, 2013. *Treating melanoma* [online] Available at: http://www.cancerresearchuk.org/cancer-help/type/melanoma/treatment/ [Accessed 24th March 2014]

Carreira S, Goodall J, Aksan I, La Rocca SA, Galibert MD, Denat L, Larue L, Goding CR. (2005) Mitf cooperates with Rb1 and activates p21Cip1 expression to regulate cell cycle progression. *Nature*. 433(7027): 764-9.

Carreira S, Goodall J, Denat L, Rodriguez M, Nuciforo P, Hoek KS, Testori A, Larue L, Goding CR. (2006) Mitf regulation of Dia1 controls melanoma proliferation and invasiveness. *Genes Dev.* 20(24): 3426-39.

Carreira S, Liu B, Goding CR. (2000) The gene encoding the T-box factor Tbx2 is a

target for the microphthalmia-associated transcription factor in melanocytes. *J Biol Chem*. 275(29): 21920-7.

Carvajal RD, Antonescu CR, Wolchok JD, Chapman PB, Roman RA, Teitcher J, Panageas KS, Busam KJ, Chmielowski B, Lutzky J et al. (2011) KIT as a therapeutic target in metastatic melanoma. *JAMA*. 305(22): 2327-34.

Ceol CJ, Houvras Y, Jane-Valbuena J, Bilodeau S, Orlando DA, Battisti V, Fritsch L, Lin WM, Hollmann TJ, Ferré F et al. (2011) The histone methyltransferase SETDB1 is recurrently amplified in melanoma and accelerates its onset. *Nature*. 471(7339): 513-7.

Cerroni L, Soyer HP, Kerl H. (1995) bcl-2 protein expression in cutaneous malignant melanoma and benign melanocytic nevi. *Am J Dermatopathol*. 17(1): 7-11.

Chabner BA. (2011) Early accelerated approval for highly targeted cancer drugs. *N Engl J Med*. 364(12): 1087-9.

Chapman PB, Hauschild A, Robert C, Haanen JB, Ascierto P, Larkin J, Dummer R, Garbe C, Testori A, Maio M et al. (2011) Improved survival with vemurafenib in melanoma with BRAF V600E mutation. *N Engl J Med*. 364(26): 2507-16.

Cheli Y, Ohanna M, Ballotti R, Bertolotto C. (2010) Fifteen-year quest for microphthalmia-associated transcription factor target genes. *Pigment Cell Melanoma Res*. 23(1): 27-40.

Chin L. (2003) The genetics of malignant melanoma: lessons from mouse and man. *Nat Rev Cancer*. 3(8): 559-70.

Clark WH Jr, Elder DE, Guerry D 4th, Braitman LE, Trock BJ, Schultz D, Synnestvedt M, Halpern AC. (1989) Model predicting survival in stage I melanoma based on tumor progression. *J Natl Cancer Inst*. 81(24): 1893-904.

Clark WH Jr, From L, Bernardino EA, Mihm MC. (1969) The histogenesis and biologic behavior of primary human malignant melanomas of the skin. *Cancer Res.* 29(3): 705-27.

Corona G, Mondaini N, Ungar A, Razzoli E, Rossi A, Fusco F. (2011) Phosphodiesterase type 5 (PDE5) inhibitors in erectile dysfunction: the proper drug for the proper patient. *J Sex Med*. 8(12): 3418-32.

Cronin JC, Wunderlich J, Loftus SK, Prickett TD, Wei X, Ridd K, Vemula S, Burrell AS, Agrawal NS, Lin JC, Banister CE, Buckhaults P, Rosenberg SA, Bastian BC, Pavan WJ, Samuels Y. (2009) Frequent mutations in the MITF pathway in melanoma. *Pigment Cell Melanoma Res.* 22(4): 435-44.

Crotty KA, Menzies SW. (2004) Dermoscopy and its role in diagnosing melanocytic lesions: a guide for pathologists. *Pathology*. 36(5): 470-7.

Curtin JA, Fridlyand J, Kageshita T, Patel HN, Busam KJ, Kutzner H, Cho KH, Aiba S, Bröcker EB, LeBoit PE et al. (2005) Distinct sets of genetic alterations in melanoma. *N Engl J Med*. 353(20): 2135-47.

Daniotti M, Oggionni M, Ranzani T, Vallacchi V, Campi V, Di Stasi D, Torre GD, Perrone F, Luoni C, Suardi S et al. (2004) BRAF alterations are associated with complex mutational profiles in malignant melanoma. *Oncogene*. 23(35): 5968-77.

Das Thakur M, Salangsang F, Landman AS, Sellers WR, Pryer NK, Levesque MP, Dummer R, McMahon M, Stuart DD. (2013) Modelling vemurafenib resistance in melanoma reveals a strategy to forestall drug resistance. *Nature*. 494(7436): 251-5.

Davies H, Bignell GR, Cox C, Stephens P, Edkins S, Clegg S, Teague J, Woffendin H, Garnett MJ, Bottomley W et al. (2002) Mutations of the BRAF gene in human cancer. *Nature*. 417(6892): 949-54.

Davies MA. (2012) The role of the PI3K-AKT pathway in melanoma. *Cancer J*. 18(2): 142-7.

Davies MA, Kopetz S. (2013) Overcoming resistance to MAPK pathway inhibitors. *J Natl Cancer Inst.* 105(1): 9-10.

Dhomen N, Reis-Filho JS, da Rocha Dias S, Hayward R, Savage K, Delmas V, Larue L, Pritchard C, Marais R. (2009) Oncogenic Braf induces melanocyte senescence and melanoma in mice. *Cancer Cell*. 15(4): 294-303.

Dooley CM, Mongera A, Walderich B, Nüsslein-Volhard C. (2013) On the embryonic origin of adult melanophores: the role of ErbB and Kit signalling in establishing melanophore stem cells in zebrafish. *Development*. 140(5): 1003-13.

Dorvault CC, Weilbaecher KN, Yee H, Fisher DE, Chiriboga LA, Xu Y, Chhieng DC. (2001) Microphthalmia transcription factor: a sensitive and specific marker for malignant melanoma in cytologic specimens. *Cancer*. 93(5): 337-43.

Du J, Widlund HR, Horstmann MA, Ramaswamy S, Ross K, Huber WE, Nishimura EK, Golub TR, Fisher DE. (2004) Critical role of CDK2 for melanoma growth

linked to its melanocyte-specific transcriptional regulation by MITF. *Cancer Cell*. 6(6): 565-76.

Emery CM, Vijayendran KG, Zipser MC, Sawyer AM, Niu L, Kim JJ, Hatton C, Chopra R, Oberholzer PA, Karpova MB et al. (2009) MEK1 mutations confer resistance to MEK and B-RAF inhibition. Proc Natl Acad Sci USA. 106(48): 20411-6.

Fang D, Tsuji Y, Setaluri V. (2002) Selective down-regulation of tyrosinase family gene TYRP1 by inhibition of the activity of melanocyte transcription factor, MITF. *Nucleic Acids Res.* 30(14): 3096-106.

Fidler IJ. (1978) Tumor heterogeneity and the biology of cancer invasion and metastasis. *Cancer Res*. 38(9): 2651-60.

Flaherty KT. (2006) Chemotherapy and targeted therapy combinations in advanced melanoma. Clin Cancer Res. 12(7 Pt 2): 2366s-2370s.

Flaherty KT, Infante JR, Daud A, Gonzalez R, Kefford RF, Sosman J, Hamid O, Schuchter L, Cebon J, Ibrahim N et al. (2012) Combined BRAF and MEK inhibition in melanoma with BRAF V600 mutations. *N Engl J Med*. 367(18): 1694-703.

Flaherty KT, Puzanov I, Kim KB, Ribas A, McArthur GA, Sosman JA, O'Dwyer PJ, Lee RJ, Grippo JF, Nolop K, Chapman PB. (2010) Inhibition of mutated, activated BRAF in metastatic melanoma. *N Engl J Med.* 363(9): 809-19.

Franceschini A, Szklarczyk D, Frankild S, Kuhn M, Simonovic M, Roth A, Lin J, Minguez P, Bork P, von Mering C, Jensen LJ. (2013) STRING v9.1: protein-protein

interaction networks, with increased coverage and integration. *Nucleic Acids Res*. 41(Database issue): D808-15.

Furge KA, Kiewlich D, Le P, Vo MN, Faure M, Howlett AR, Lipson KE, Vande Woude GF, Webb CP. (2001) Suppression of Ras-mediated tumorigenicity and metastasis through inhibition of the Met receptor tyrosine kinase. *Proc Natl Acad Sci U S A*. 98(19): 10722-7.

Garraway LA, Widlund HR, Rubin MA, Getz G, Berger AJ, Ramaswamy S, Beroukhim R, Milner DA, Granter SR, Du J et al. (2005) Integrative genomic analyses identify MITF as a lineage survival oncogene amplified in malignant melanoma. *Nature*. 436(7047): 117-22.

Ghiorzo P, Pastorino L, Queirolo P, Bruno W, Tibiletti MG, Nasti S, Andreotti V; Genoa Pancreatic Cancer Study Group, Paillerets BB, Bianchi Scarrà G. (2013) Prevalence of the E318K MITF germline mutation in Italian melanoma patients: associations with histological subtypes and family cancer history. *Pigment Cell Melanoma Res*. 26(2): 259-62.

Goding C, Meyskens FL Jr. (2006) Microphthalmic-associated transcription factor integrates melanocyte biology and melanoma progression. *Clin Cancer Res*. 12(4): 1069-73.

Goodall J, Wellbrock C, Dexter TJ, Roberts K, Marais R, Goding CR. (2004) The Brn-2 transcription factor links activated BRAF to melanoma proliferation. *Mol Cell Biol*. 24(7): 2923-31.

Gown AM, Vogel AM, Hoak D, Gough F, McNutt MA. (1986) Monoclonal antibodies specific for melanocytic tumors distinguish subpopulations of

melanocytes. *Am J Pathol*. 123(2): 195-203.

Gray-Schopfer V, Wellbrock C, Marais R. (2007) Melanoma biology and new targeted therapy. *Nature.* 445(7130): 851-7.

Greenman C, Stephens P, Smith R, Dalgliesh GL, Hunter C, Bignell G, Davies H, Teague J, Butler A, Stevens C et al. (2007) Patterns of somatic mutation in human cancer genomes. *Nature*. 446(7132): 153-8.

Grill C, Bergsteinsdóttir K, Ogmundsdóttir MH, Pogenberg V, Schepsky A, Wilmanns M, Pingault V, Steingrímsson E. (2013) MITF mutations associated with pigment deficiency syndromes and melanoma have different effects on protein function. *Hum Mol Genet*. 22(21): 4357-67.

Guo J, Si L, Kong Y, Flaherty KT, Xu X, Zhu Y, Corless CL, Li L, Li H, Sheng X et al. (2011) Phase II, open-label, single-arm trial of imatinib mesylate in patients with metastatic melanoma harboring c-Kit mutation or amplification. *J Clin Oncol*. 29(21): 2904-9.

Halaban R, Rubin JS, Funasaka Y, Cobb M, Boulton T, Faletto D, Rosen E, Chan A, Yoko K, White W, et al. (1992) Met and hepatocyte growth factor/scatter factor signal transduction in normal melanocytes and melanoma cells. *Oncogene*. 7(11): 2195-206.

Hauschild A. (2009) Adjuvant interferon alfa for melanoma: new evidence-based treatment recommendations? *Curr Oncol.* 16(3): 3-6.

Hauschild A, Grob JJ, Demidov LV, Jouary T, Gutzmer R, Millward M, Rutkowski

P, Blank CU, Miller WH Jr, Kaempgen E. (2012) Dabrafenib in BRAF-mutated metastatic melanoma: a multicentre, open-label, phase 3 randomised controlled trial. *Lancet*. 380(9839): 358-65.

Hawkins WE, Overstreet RM, Fournie JW, Walker WW. (1985) Development of aquarium fish models for environmental carcinogenesis: tumor induction in seven species. *J Appl Toxicol*. 5(4): 261-4.

He X, Zhu Z, Johnson C, Stoops J, Eaker AE, Bowen W, DeFrances MC. (2008) PIK3IP1, a negative regulator of PI3K, suppresses the development of hepatocellular carcinoma. *Cancer Res*. 68(14): 5591-8.

Hemminki K, Lönnstedt I, Vaittinen P. (2001) A population-based study of familial cutaneous melanoma. *Melanoma Res.* 11(2): 133-40.

Hendrix MJ, Seftor EA, Seftor RE, Kirschmann DA, Gardner LM, Boldt HC, Meyer M, Pe'er J, Folberg R. (1998) Regulation of uveal melanoma interconverted phenotype by hepatocyte growth factor/scatter factor (HGF/SF). *Am J Pathol*. 152(4): 855-63.

Hiramoto K, Murata T, Shimizu K, Morita H, Inui M, Manganiello VC, Tagawa T, Arai N. (2014) Role of Phosphodiesterase 2 in Growth and Invasion of Human Malignant Melanoma Cells. *Cell Signal*. pii: S0898-6568(14)00133-8.

Hodgkinson CA, Moore KJ, Nakayama A, Steingrímsson E, Copeland NG, Jenkins NA, Arnheiter H. (1993) Mutations at the mouse microphthalmia locus are associated with defects in a gene encoding a novel basic-helix-loop-helix-zipper protein. *Cell*. 74(2): 395-404.

Hodi FS, O'Day SJ, McDermott DF, Weber RW, Sosman JA, Haanen JB, Gonzalez R, Robert C, Schadendorf D, Hassel JC et al. (2010) Improved survival with ipilimumab in patients with metastatic melanoma. *N Engl J Med*. 363(8): 711-23.

Hodis E, Watson IR, Kryukov GV, Arold ST, Imielinski M, Theurillat JP, Nickerson E, Auclair D, Li L, Place C et al. (2012) A landscape of driver mutations in melanoma. *Cell*. 150(2): 251-63.

Hoeflich KP, Gray DC, Eby MT, Tien JY, Wong L, Bower J, Gogineni A, Zha J, Cole MJ, Stern HM et al. (2006) Oncogenic BRAF is required for tumor growth and maintenance in melanoma models. *Cancer Res*. 66(2): 999-1006.

Hoek KS, Goding CR. (2010) Cancer stem cells versus phenotype-switching in melanoma. *Pigment Cell Melanoma Res.* 23(6): 746-59.

Hoek KS, Schlegel NC, Brafford P, Sucker A, Ugurel S, Kumar R, Weber BL, Nathanson KL, Phillips DJ, Herlyn M, Schadendorf D, Dummer R. (2006) Metastatic potential of melanomas defined by specific gene expression profiles with no BRAF signature. *Pigment Cell Res*. 19(4): 290-302.

Hoek KS, Schlegel NC, Eichhoff OM, Widmer DS, Praetorius C, Einarsson SO, Valgeirsdottir S, Bergsteinsdottir K, Schepsky A, Dummer R, Steingrimsson E. (2008) Novel MITF targets identified using a two-step DNA microarray strategy. *Pigment Cell Melanoma Res.* 21(6): 665-76.

Horn S, Figl A, Rachakonda PS, Fischer C, Sucker A, Gast A, Kadel S, Moll I, Nagore E, Hemminki K et al. (2013) TERT promoter mutations in familial and sporadic melanoma. *Science*. 339(6122): 959-61.

Hornyak TJ, Hayes DJ, Chiu LY, Ziff EB. (2001) Transcription factors in melanocyte development: distinct roles for Pax-3 and Mitf. *Mech Dev*. 101(1-2): 47-59.

Hou L, Panthier JJ, Arnheiter H. (2000) Signaling and transcriptional regulation in the neural crest-derived melanocyte lineage: interactions between KIT and MITF. *Development.* 127(24): 5379-89.

Howe K, Clark MD, Torroja CF, Torrance J, Berthelot C, Muffato M, Collins JE, Humphray S, McLaren K, Matthews L et al. (2013) The zebrafish reference genome sequence and its relationship to the human genome. *Nature*. 496(7446): 498-503.

Huang FW, Hodis E, Xu MJ, Kryukov GV, Chin L, Garraway LA. (2013) Highly recurrent TERT promoter mutations in human melanoma. *Science*. 339(6122): 957-9.

Hussussian CJ, Struewing JP, Goldstein AM, Higgins PA, Ally DS, Sheahan MD, Clark WH Jr, Tucker MA, Dracopoli NC. (1994) Germline p16 mutations in familial melanoma. *Nat Genet*. 8(1): 15-21.

Hwang WY, Fu Y, Reyon D, Maeder ML, Tsai SQ, Sander JD, Peterson RT, Yeh JR, Joung JK. (2013) Efficient genome editing in zebrafish using a CRISPR-Cas system. *Nat Biotechnol.* 31(3): 227-9.

Johannessen CM, Boehm JS, Kim SY, Thomas SR, Wardwell L, Johnson LA, Emery CM, Stransky N, Cogdill AP, Barretina J et al. (2010) COT drives resistance to RAF inhibition through MAP kinase pathway reactivation. Nature. 468(7326): 968-72.

Johannessen CM, Johnson LA, Piccioni F, Townes A, Frederick DT, Donahue MK,

Narayan R, Flaherty KT, Wargo JA, Root DE, Garraway LA. (2013) A melanocyte lineage program confers resistance to MAP kinase pathway inhibition. *Nature*. 504(7478): 138-42.

Johnson SL, Nguyen AN, Lister JA. (2011) mitfa is required at multiple stages of melanocyte differentiation but not to establish the melanocyte stem cell. *Dev Biol.* 350(2): 405-13.

King R, Peterson AC, Peterson KC, Mihm MC Jr, Fisher DE, Googe PB. (2002) Microphthalmia transcription factor expression in cutaneous mast cell disease. *Am J Dermatopathol.* 24(3): 282-4.

King R, Weilbaecher KN, McGill G, Cooley E, Mihm M, Fisher DE. (1999) Microphthalmia transcription factor. A sensitive and specific melanocyte marker for Melanoma Diagnosis.*Am J Pathol*. 155(3): 731-8.

Koochekpour S, Majumdar S, Azabdaftari G, Attwood K, Scioneaux R, Subramani D, Manhardt C, Lorusso GD, Willard SS, Thompson H et al. (2012) Serum glutamate levels correlate with Gleason score and glutamate blockade decreases proliferation, migration, and invasion and induces apoptosis in prostate cancer cells. *Clin Cancer Res*. 18(21): 5888-901.

Krauthammer M, Kong Y, Ha BH, Evans P, Bacchiocchi A, McCusker JP, Cheng E, Davis MJ, Goh G, Choi M et al. (2012) Exome sequencing identifies recurrent somatic RAC1 mutations in melanoma. *Nat Genet*. 44(9): 1006-14.

Kumar N, Goldminz AM, Kim N, Gottlieb AB. (2013) Phosphodiesterase 4-targeted treatments for autoimmune diseases. *BMC Med*. 11: 96.

Kumar R, Angelini S, Snellman E, Hemminki K. (2004) BRAF mutations are common somatic events in melanocytic nevi. *J Invest Dermatol.* 122(2): 342-8.

Kumar SM, Dai J, Li S, Yang R, Yu H, Nathanson KL, Liu S, Zhou H, Guo J, Xu X. (2013) Human skin neural crest progenitor cells are susceptible to BRAF(V600E)-induced transformation. *Oncogene*. doi: 10.1038/onc.2012.642

Langmead B, Trapnell C, Pop M, Salzberg SL. (2009) Ultrafast and memory-efficient alignment of short DNA sequences to the human genome. *Genome Biol*. 10(3): R25.

Lassen A, Atefi M, Robert L, Wong DJ, Cerniglia M, Comin-Anduix B, Ribas A. (2014) Effects of AKT inhibitor therapy in response and resistance to BRAF inhibition in melanoma. *Mol Cancer*. 13(1): 83.

Lee KC, Goh WL, Xu M, Kua N, Lunny D, Wong JS, Coomber D, Vojtesek B, Lane EB, Lane DP. (2008) Detection of the p53 response in zebrafish embryos using new monoclonal antibodies. *Oncogene*. 27(5): 629-40.

Levy C, Lee YN, Nechushtan H, Schueler-Furman O, Sonnenblick A, Hacohen S, Razin E. (2006) Identifying a common molecular mechanism for inhibition of MITF and STAT3 by PIAS3. *Blood*. 107(7): 2839-45.

Levy C, Khaled M, Fisher DE. (2006) MITF: master regulator of melanocyte development and melanoma oncogene. *Trends Mol Med.* 12(9): 406-14.

Li A, Ma Y, Yu X, Mort RL, Lindsay CR, Stevenson D, Strathdee D, Insall RH, Chernoff J, Snapper SB et al. (2011) Rac1 drives melanoblast organization during

mouse development by orchestrating pseudopod- driven motility and cell-cycle progression. *Dev Cell*. 21(4): 722-34.

Lister JA, Capper A, Zeng Z, Mathers ME, Richardson J, Paranthaman K, Jackson IJ, Patton EE. (2014) A conditional zebrafish MITF mutation reveals MITF levels are critical for melanoma promotion vs. regression in vivo. *J Invest Dermatol.* 134(1): 133-40.

Lister JA, Close J, Raible DW. (2001) Duplicate mitf Genes in Zebrafish: Complementary Expression and Conservation of Melanogenic Potential. *Dev Biol*. 237(2): 333-44.

Lister JA, Robertson CP, Lepage T, Johnson SL, Raible DW. (1999) nacre encodes a zebrafish microphthalmia-related protein that regulates neural-crest-derived pigment cell fate. *Development*. 126(17): 3757-67.

Liu LS, Colegio OR. (2013) Molecularly targeted therapies for melanoma. *Int J Dermatol*. 52(5): 523-30.

Liu S, Leach SD. (2011) Zebrafish models for cancer. *Annu Rev Pathol*. 6: 71-93.

Liu L, Lassam NJ, Slingerland JM, Bailey D, Cole D, Jenkins R, Hogg D. (1995) Germline p16INK4A mutation and protein dysfunction in a family with inherited melanoma. *Oncogene*. 11(2): 405-12.

Loercher AE, Tank EM, Delston RB, Harbour JW. (2005) MITF links differentiation with cell cycle arrest in melanocytes by transcriptional activation of INK4A. *J Cell Biol*. 168(1): 35-40.

McCallum CM, Comai L, Greene EA, Henikoff S. (2000) Targeted screening for induced mutations. *Nat Biotechnol*. 18(4): 455-7.

McGill GG, Haq R, Nishimura EK, Fisher DE. (2006) c-Met expression is regulated by Mitf in the melanocyte lineage. *J Biol Chem*. 281(15): 10365-73.

McGill GG, Horstmann M, Widlund HR, Du J, Motyckova G, Nishimura EK, Lin YL, Ramaswamy S, Avery W, Ding HF et al. (2002) Bcl2 regulation by the melanocyte master regulator Mitf modulates lineage survival and melanoma cell viability. *Cell*. 109(6): 707-18.

McGovern VJ, Mihm MC Jr, Bailly C, Booth JC, Clark WH Jr, Cochran AJ, Hardy EG, Hicks JD, Levene A, Lewis MG et al. (1973) The classification of malignant melanoma and its histologic reporting. *Cancer*. 32(6): 1446-57.

Meierjohann S, Schartl M, Volff JN. (2004) Genetic, biochemical and evolutionary facets of Xmrk-induced melanoma formation in the fish Xiphophorus. *Comp Biochem Physiol C Toxicol Pharmacol.* 138(3): 281-9.

Michaloglou C, Vredeveld LC, Soengas MS, Denoyelle C, Kuilman T, van der Horst CM, Majoor DM, Shay JW, Mooi WJ, Peeper DS. (2005) BRAFE600-associated senescence-like cell cycle arrest of human naevi. *Nature*. 436(7051): 720-4.

Miller AJ, Mihm MC Jr. (2006) Melanoma. *N Engl J Med*. 355(1): 51-65.

Mitchell MS, Abrams J, Thompson JA, Kashani-Sabet M, DeConti RC, Hwu WJ, Atkins MB, Whitman E, Ernstoff MS, Haluska FG et al. (2007) Randomized trial of an allogeneic melanoma lysate vaccine with low-dose interferon Alfa-2b compared

with high-dose interferon Alfa-2b for Resected stage III cutaneous melanoma. *J Clin Oncol*. 25(15): 2078-85.

Mullins MC, Hammerschmidt M, Haffter P, Nüsslein-Volhard C. (1994) Large-scale mutagenesis in the zebrafish: in search of genes controlling development in a vertebrate. *Curr Biol*. 4(3): 189-202.

Nakayama A, Nguyen MT, Chen CC, Opdecamp K, Hodgkinson CA, Arnheiter H. (1998) Mutations in microphthalmia, the mouse homolog of the human deafness gene MITF, affect neuroepithelial and neural crest-derived melanocytes differently. *Mech Dev*. 70(1-2): 155-66.

Natali PG, Nicotra MR, Di Renzo MF, Prat M, Bigotti A, Cavaliere R, Comoglio PM. (1993) Expression of the c-Met/HGF receptor in human melanocytic neoplasms: demonstration of the relationship to malignant melanoma tumour progression. *Br J Cancer*. 68(4): 746-50.

Nazarian R, Shi H, Wang Q, Kong X, Koya RC, Lee H, Chen Z, Lee MK, Attar N, Sazegar H et al. (2010) Melanomas acquire resistance to B-RAF(V600E) inhibition by RTK or N-RAS upregulation. *Nature*. 468(7326): 973-7.

Nguyen M, Arnheiter H. (2000) Signaling and transcriptional regulation in early mammalian eye development: a link between FGF and MITF. *Development*. 127(16): 3581-91.

Nikolaev SI, Rimoldi D, Iseli C, Valsesia A, Robyr D, Gehrig C, Harshman K, Guipponi M, Bukach O, Zoete V et al. (2011) Exome sequencing identifies recurrent somatic MAP2K1 and MAP2K2 mutations in melanoma. *Nat Genet.* 44(2): 133-9.

Nishimura EK, Granter SR, Fisher DE. (2005) Mechanisms of hair graying: incomplete melanocyte stem cell maintenance in the niche. *Science*. 307(5710): 720-4.

Nishimura EK, Jordan SA, Oshima H, Yoshida H, Osawa M, Moriyama M, Jackson IJ, Barrandon Y, Miyachi Y, Nishikawa S. (2002) Dominant role of the niche in melanocyte stem-cell fate determination. *Nature*. 416(6883): 854-60.

Nobukuni Y, Watanabe A, Takeda K, Skarka H, Tachibana M. (1996) Analyses of loss-of-function mutations of the MITF gene suggest that haploinsufficiency is a cause of Waardenburg syndrome type 2A. *Am J Hum Genet*. 59(1): 76-83.

Oberholzer PA, Kee D, Dziunycz P, Sucker A, Kamsukom N, Jones R, Roden C, Chalk CJ, Ardlie K, Palescandolo E et al. (2012) RAS mutations are associated with the development of cutaneous squamous cell tumors in patients treated with RAF inhibitors. *J Clin Oncol*. 30(3): 316-21.

Oxford English Dictionary Online. (2014) "melanoma, n.". *Oxford University Press*. http://www.oed.com/view/Entry/116044?redirectedFrom=melanoma (accessed April 29, 2014).

Paraiso KH, Xiang Y, Rebecca VW, Abel EV, Chen YA, Munko AC, Wood E, Fedorenko IV, Sondak VK, Anderson AR et al. (2011) PTEN loss confers BRAF inhibitor resistance to melanoma cells through the suppression of BIM expression. *Cancer Res*. 71(7): 2750-60.

Parkin DM, Mesher D, Sasieni P. (2011) 13. Cancers attributable to solar (ultraviolet) radiation exposure in the UK in 2010. *Br J Cancer*. 105 Suppl 2: S66-9.

Patton EE, Mathers ME, Schartl M. (2011) Generating and analyzing fish models of melanoma. *Methods Cell Biol*. 105: 339-66.

Patton EE, Nairn RS. (2010) Xmrk in medaka: a new genetic melanoma model. *J Invest Dermatol*. 130(1): 14-7.

Patton EE, Widlund HR, Kutok JL, Kopani KR, Amatruda JF, Murphey RD, Berghmans S, Mayhall EA, Traver D, Fletcher CD, Aster JC, Granter SR, Look AT, Lee C, Fisher DE, Zon LI. (2005) BRAF mutations are sufficient to promote nevi formation and cooperate with p53 in the genesis of melanoma. *Curr Biol.* 15(3): 249-54.

Planque N, Raposo G, Leconte L, Anezo O, Martin P, Saule S. (2004) Microphthalmia transcription factor induces both retinal pigmented epithelium and neural crest melanocytes from neuroretina cells. *J Biol Chem*. 279(40): 41911-7.

Planque N, Turque N, Opdecamp K, Bailly M, Martin P, Saule S. (1999) Expression of the microphthalmia-associated basic helix-loop-helix leucine zipper transcription factor Mi in avian neuroretina cells induces a pigmented phenotype. *Cell Growth Differ*. 10(7): 525-36.

Pleasance ED, Cheetham RK, Stephens PJ, McBride DJ, Humphray SJ, Greenman CD, Varela I, Lin ML, Ordóñez GR, Bignell GR et al. (2010) A comprehensive catalogue of somatic mutations from a human cancer genome. *Nature*. 463(7278): 191-6.

Pogenberg V, Ogmundsdóttir MH, Bergsteinsdóttir K, Schepsky A, Phung B, Deineko V, Milewski M, Steingrímsson E, Wilmanns M. (2012) Restricted leucine zipper dimerization and specificity of DNA recognition of the melanocyte master

regulator MITF. *Genes Dev*. 26(23): 2647-58.

Pollock PM, Harper UL, Hansen KS, Yudt LM, Stark M, Robbins CM, Moses TY, Hostetter G, Wagner U, Kakareka J et al. (2003) High frequency of BRAF mutations in nevi. *Nat Genet*. 33(1): 19-20.

Postovit LM, Seftor EA, Seftor RE, Hendrix MJ. (2006) Influence of the microenvironment on melanoma cell fate determination and phenotype. *Cancer Res.* 66(16): 7833-6.

Poulikakos PI, Persaud Y, Janakiraman M, Kong X, Ng C, Moriceau G, Shi H, Atefi M, Titz B, Gabay MT et al. (2011) RAF inhibitor resistance is mediated by dimerization of aberrantly spliced BRAF(V600E). *Nature*. 480(7377): 387-90.

Prickett TD, Agrawal NS, Wei X, Yates KE, Lin JC, Wunderlich JR, Cronin JC, Cruz P, Rosenberg SA, Samuels Y. (2009) Analysis of the tyrosine kinome in melanoma reveals recurrent mutations in ERBB4. *Nat Genet*. 41(10): 1127-32.

Prickett TD, Wei X, Cardenas-Navia I, Teer JK, Lin JC, Walia V, Gartner J, Jiang J, Cherukuri PF, Molinolo A et al. (2011) Exon capture analysis of G protein-coupled receptors identifies activating mutations in GRM3 in melanoma. *Nat Genet*. 43(11): 1119-26.

Ramsay JA, From L, Kahn HJ. (1995) bcl-2 protein expression in melanocytic neoplasms of the skin. *Mod Pathol*. 8(2): 150-4.

Ren BX, Gu XP, Zheng YG, Liu CL, Wang D, Sun YE, Ma ZL. (2012) Intrathecal injection of metabotropic glutamate receptor subtype 3 and 5 agonist/antagonist

attenuates bone cancer pain by inhibition of spinal astrocyte activation in a mouse model. *Anesthesiology*. 116(1): 122-32.

Richardson J, Lundegaard PR, Reynolds NL, Dorin JR, Porteous DJ, Jackson IJ, Patton EE. (2008) mc1r Pathway regulation of zebrafish melanosome dispersion. *Zebrafish*. 5(4): 289-95.

Robert C, Thomas L, Bondarenko I, O'Day S, M D JW, Garbe C, Lebbe C, Baurain JF, Testori A, Grob JJ et al. (2011) Ipilimumab plus dacarbazine for previously untreated metastatic melanoma. *N Engl J Med*. 364(26): 2517-26.

Rzeski W, Turski L, Ikonomidou C. (2001) Glutamate antagonists limit tumor growth. *Proc Natl Acad Sci U S A*. 98(11): 6372-7.

Salti GI, Manougian T, Farolan M, Shilkaitis A, Majumdar D, Das Gupta TK. (2000) Microphthalmia transcription factor: a new prognostic marker in intermediate-thickness cutaneous malignant melanoma. *Cancer Res*. 60(18): 5012-6.

Schartl M, Hornung U, Gutbrod H, Volff JN, Wittbrodt J. (1999) Melanoma loss-of-function mutants in Xiphophorus caused by Xmrk-oncogene deletion and gene disruption by a transposable element. *Genetics*. 153(3): 1385-94.

Schartl M, Schmidt CR, Anders A, Barnekow A. (1985) Elevated expression of the cellular src gene in tumors of differing etiologies in Xiphophorus. *Int J Cancer*. 36(2): 199-207.

Selzer E, Wacheck V, Lucas T, Heere-Ress E, Wu M, Weilbaecher KN, Schlegel W, Valent P, Wrba F, Pehamberger H, et al. (2002) The melanocyte-specific isoform of

the microphthalmia transcription factor affects the phenotype of human melanoma. *Cancer Res*. 62(7): 2098-103.

Sharma A, Singh K, Almasan A. (2012) Histone H2AX phosphorylation: a marker for DNA damage. *Methods Mol Biol*. 920: 613-26.

Sheffield MV, Yee H, Dorvault CC, Weilbaecher KN, Eltoum IA, Siegal GP, Fisher DE, Chhieng DC. (2002) Comparison of five antibodies as markers in the diagnosis of melanoma in cytologic preparations. *Am J Clin Pathol*. 118(6): 930-6.

Shekar SN, Duffy DL, Youl P, Baxter AJ, Kvaskoff M, Whiteman DC, Green AC, Hughes MC, Hayward NK, Coates M, Martin NG. (2009) A population-based study of Australian twins with melanoma suggests a strong genetic contribution to liability. *J Invest Dermatol.* 129(9): 2211-9.

Shepard JL, Amatruda JF, Stern HM, Subramanian A, Finkelstein D, Ziai J, Finley KR, Pfaff KL, Hersey C, Zhou Y et al. (2005) A zebrafish bmyb mutation causes genome instability and increased cancer susceptibility. *Proc Natl Acad Sci U S A.* 102(37): 13194-9.

Shi H, Moriceau G, Kong X, Lee MK, Lee H, Koya RC, Ng C, Chodon T, Scolyer RA, Dahlman KB et al. (2012) Melanoma whole-exome sequencing identifies (V600E)B-RAF amplification-mediated acquired B-RAF inhibitor resistance. *Nat Commun*. 3: 724.

Shibahara S, Takeda K, Yasumoto K, Udono T, Watanabe K, Saito H, Takahashi K. (2001) Microphthalmia-associated transcription factor (MITF): multiplicity in structure, function, and regulation. *J Investig Dermatol Symp Proc*. 6(1): 99-104.

Shidham VB, Qi DY, Acker S, Kampalath B, Chang CC, George V, Komorowski R. (2001) Evaluation of micrometastases in sentinel lymph nodes of cutaneous melanoma: higher diagnostic accuracy with Melan-A and MART-1 compared with S-100 protein and HMB-45. *Am J Surg Pathol*. 25(8): 1039-46.

Shields JM, Thomas NE, Cregger M, Berger AJ, Leslie M, Torrice C, Hao H, Penland S, Arbiser J, Scott G et al. (2007) Lack of extracellular signal-regulated kinase mitogen-activated protein kinase signaling shows a new type of melanoma. *Cancer Res*. 67(4): 1502-12.

Shin SS, Namkoong J, Wall BA, Gleason R, Lee HJ, Chen S. (2008) Oncogenic activities of metabotropic glutamate receptor 1 (Grm1) in melanocyte transformation. *Pigment Cell Melanoma Res.* 21(3): 368-78.

Siegel R, DeSantis C, Virgo K, Stein K, Mariotto A, Smith T, Cooper D, Gansler T, Lerro C, Fedewa S et al. (2012) Cancer treatment and survivorship statistics, 2012. *CA Cancer J Clin*. 62(4): 220-41.

Smith MP, Ferguson J, Arozarena I, Hayward R, Marais R, Chapman A, Hurlstone A, Wellbrock C. (2013) Effect of SMURF2 targeting on susceptibility to MEK inhibitors in melanoma. *J Natl Cancer Inst.* 105(1): 33-46.

Smith SD, Kelley PM, Kenyon JB, Hoover D. (2000) Tietz syndrome (hypopigmentation/deafness) caused by mutation of MITF. *J Med Genet*. 37(6): 446-8.

Spatz A, Shaw HM, Crotty KA, Thompson JF, McCarthy SW. (1998) Analysis of histopathological factors associated with prolonged survival of 10 years or more for patients with thick melanomas (> 5 mm). *Histopathology*. 33(5): 406-13.

Speyer CL, Hachem AH, Assi AA, Johnson JS, DeVries JA, Gorski DH. (2014) Metabotropic glutamate receptor-1 as a novel target for the antiangiogenic treatment of breast cancer. *PLoS One.* 9(3): e88830.

Spitsbergen JM, Tsai HW, Reddy A, Miller T, Arbogast D, Hendricks JD, Bailey GS. (2000) Neoplasia in zebrafish (Danio rerio) treated with 7,12-dimethylbenz[a]anthracene by two exposure routes at different developmental stages. *Toxicol Pathol*. 28(5): 705-15.

Stark MS, Woods SL, Gartside MG, Bonazzi VF, Dutton-Regester K, Aoude LG, Chow D, Sereduk C, Niemi NM, Tang N et al. (2011) Frequent somatic mutations in MAP3K5 and MAP3K9 in metastatic melanoma identified by exome sequencing. *Nat Genet. 44*(2): 165-9.

Steingrímsson E, Copeland NG, Jenkins NA. (2004) Melanocytes and the microphthalmia transcription factor network. *Annu Rev Genet*. 38: 365-411.

Stella GM, Benvenuti S, Comoglio PM. (2010) Targeting the MET oncogene in cancer and metastases. *Expert Opin Investig Drugs*. 19(11): 1381-94.

Stepulak A, Rola R, Polberg K, Ikonomidou C (2014) Glutamate and its receptors in cancer. *J Neural Transm*. [Epub ahead of print]

Stern HM, Zon LI. (2003) Cancer genetics and drug discovery in the zebrafish. *Nat Rev Cancer*. 3(7): 533-9.

Straussman R, Morikawa T, Shee K, Barzily-Rokni M, Qian ZR, Du J, Davis A, Mongare MM, Gould J, Frederick DT et al. (2012) Tumour micro-environment

elicits innate resistance to RAF inhibitors through HGF secretion. *Nature*. 487(7408): 500-4.

Sturm RA, Fox C, McClenahan P, Jagirdar K, Ibarrola-Villava M, Banan P, Abbott NC, Ribas G, Gabrielli B, Duffy DL, Soyer HP. (2014) Phenotypic characterization of nevus and tumor patterns in MITF E318K mutation carrier melanoma patients. *J Invest Dermatol.* 134(1): 141-9.

Su F, Viros A, Milagre C, Trunzer K, Bollag G, Spleiss O, Reis-Filho JS, Kong X, Koya RC, Flaherty KT et al. (2012) RAS mutations in cutaneous squamous-cell carcinomas in patients treated with BRAF inhibitors. *N Engl J Med*. 366(3): 207-15.

Tachibana M. (1997) Evidence to suggest that expression of MITF induces melanocyte differentiation and haploinsufficiency of MITF causes Waardenburg syndrome type 2A. Pigment Cell Res. 10(1-2): 25-33.

Tachibana M. (2000) MITF: a stream flowing for pigment cells. *Pigment Cell Res*. 13(4): 230-40.

Tachibana M, Perez-Jurado LA, Nakayama A, Hodgkinson CA, Li X, Schneider M, Miki T, Fex J, Francke U, Arnheiter H. (1994) Cloning of MITF, the human homolog of the mouse microphthalmia gene and assignment to chromosome 3p14.1-p12.3. *Hum Mol Genet*. 3(4): 553-7.

Tachibana M, Takeda K, Nobukuni Y, Urabe K, Long JE, Meyers KA, Aaronson SA, Miki T. (1996) Ectopic expression of MITF, a gene for Waardenburg syndrome type 2, converts fibroblasts to cells with melanocyte characteristics. *Nat Genet.* 14(1): 50-4.

Takano T, Lin JH, Arcuino G, Gao Q, Yang J, Nedergaard M. (2001) Glutamate release promotes growth of malignant gliomas. *Nat Med*. 7(9): 1010-5.

Tassabehji M, Newton VE, Read AP. (1994) Waardenburg syndrome type 2 caused by mutations in the human microphthalmia (MITF) gene. *Nat Genet.* 8(3): 251-5.

Taylor KL, Lister JA, Zeng Z, Ishizaki H, Anderson C, Kelsh RN, Jackson IJ, Patton EE. (2011) Differentiated melanocyte cell division occurs in vivo and is promoted by mutations in Mitf. *Development*. 138(16): 3579-89.

The Skin Cancer Foundation, 2014. *Melanoma* [online] Available at: http://www.skincancer.org/skin-cancer-information/melanoma [Accessed 28th March 2014]

Thompson JF, Soong SJ, Balch CM, Gershenwald JE, Ding S, Coit DG, Flaherty KT, Gimotty PA, Johnson T, Johnson MM et al. (2011) Prognostic significance of mitotic rate in localized primary cutaneous melanoma: an analysis of patients in the multi-institutional American Joint Committee on Cancer melanoma staging database. *J Clin Oncol*. 29(16): 2199-205.

Tietz W. (1963) A syndrome of deaf-mutism associated with albinism showing dominant autosomal inheritance. *Am J Hum Genet.* 15: 259-64.

To CT1, Tsao MS. (1998) The roles of hepatocyte growth factor/scatter factor and met receptor in human cancers. *Oncol Rep*. 5(5): 1013-24.

Trapnell C, Pachter L, Salzberg SL. (2009) TopHat: discovering splice junctions with RNA-Seq. *Bioinformatics*. 25(9): 1105-11.

Trapnell C, Williams BA, Pertea G, Mortazavi A, Kwan G, van Baren MJ, Salzberg SL, Wold BJ, Pachter L. (2010) Transcript assembly and quantification by RNA-Seq reveals unannotated transcripts and isoform switching during cell differentiation. *Nat Biotechnol*. 28(5): 511-5.

Tsai J, Lee JT, Wang W, Zhang J, Cho H, Mamo S, Bremer R, Gillette S, Kong J, Haass NK et al. (2008) Discovery of a selective inhibitor of oncogenic B-Raf kinase with potent antimelanoma activity. *Proc Natl Acad Sci U S A*. 105(8): 3041-6.

Tsao H, Chin L, Garraway LA, Fisher DE. (2012) Melanoma: from mutations to medicine. *Genes Dev*. 26(11): 1131-55.

Udono T, Yasumoto K, Takeda K, Amae S, Watanabe K, Saito H, Fuse N, Tachibana M, Takahashi K, Tamai M, Shibahara S. (2000) Structural organization of the human microphthalmia-associated transcription factor gene containing four alternative promoters. *Biochim Biophys Acta*. 1491(1-3): 205-19.

Valsesia A, Rimoldi D, Martinet D, Ibberson M, Benaglio P, Quadroni M, Waridel P, Gaillard M, Pidoux M, Rapin B et al. (2011) Network-guided analysis of genes with altered somatic copy number and gene expression reveals pathways commonly perturbed in metastatic melanoma. *PLoS One*. 6(4): e18369.

Van Allen EM, Wagle N, Sucker A, Treacy DJ, Johannessen CM, Goetz EM, Place CS, Taylor-Weiner A, Whittaker S, Kryukov GV et al. (2014) The genetic landscape of clinical resistance to RAF inhibition in metastatic melanoma. *Cancer Discov*. 4(1): 94-109.

Vance KW, Carreira S, Brosch G, Goding CR. (2005) Tbx2 is overexpressed and plays an important role in maintaining proliferation and suppression of senescence in

melanomas. *Cancer Res*. 65(6): 2260-8.

van 't Veer LJ, Burgering BM, Versteeg R, Boot AJ, Ruiter DJ, Osanto S, Schrier PI, Bos JL. (1989) N-ras mutations in human cutaneous melanoma from sun-exposed body sites. *Mol Cell Biol*. 9(7): 3114-6.

Villanueva J, Vultur A, Lee JT, Somasundaram R, Fukunaga-Kalabis M, Cipolla AK, Wubbenhorst B, Xu X, Gimotty PA, Kee D et al. (2010). Acquired resistance to BRAF inhibitors mediated by a RAF kinase switch in melanoma can be overcome by cotargeting MEK and IGF-1R/PI3K. *Cancer Cell.* 18(6): 683-95.

Viros A, Fridlyand J, Bauer J, Lasithiotakis K, Garbe C, Pinkel D, Bastian BC. (2008) Improving melanoma classification by integrating genetic and morphologic features. *PLoS Med.* 5(6): e120.

von Mering C, Huynen M, Jaeggi D, Schmidt S, Bork P, Snel B. (2003) STRING: a database of predicted functional associations between proteins. *Nucleic Acids Res*. 31(1): 258-61.

Wagle N, Emery C, Berger MF, Davis MJ, Sawyer A, Pochanard P, Kehoe SM, Johannessen CM, Macconaill LE, Hahn WC et al. (2011) Dissecting therapeutic resistance to RAF inhibition in melanoma by tumor genomic profiling. *J Clin Oncol.* 29(22): 3085-96.

Walia V, Mu EW, Lin JC, Samuels Y. (2012) Delving into somatic variation in sporadic melanoma. *Pigment Cell Melanoma Res*. 25(2): 155-70.

Wang Z, Gerstein M, Snyder M. (2009) RNA-Seq: a revolutionary tool for transcriptomics. *Nat Rev Genet*. 10(1): 57-63.

Webb CP, Taylor GA, Jeffers M, Fiscella M, Oskarsson M, Resau JH, Vande Woude GF. (1998) Evidence for a role of Met-HGF/SF during Ras-mediated tumorigenesis/metastasis. *Oncogene*. 17(16): 2019-25.

Weber J. (2007) Review: anti-CTLA-4 antibody ipilimumab: case studies of clinical response and immune-related adverse events. *Oncologist*. 12(7): 864-72.

Webster DE, Barajas B, Bussat RT, Yan KJ, Neela PH, Flockhart RJ, Kovalski J, Zehnder A, Khavari PA. (2014) Enhancer-targeted genome editing selectively blocks innate resistance to oncokinase inhibition. *Genome Res*. 24(5): 751-760.

Wei X, Walia V, Lin JC, Teer JK, Prickett TD, Gartner J, Davis S; NISC Comparative Sequencing Program, Stemke-Hale K, Davies MA et al. (2011) Exome sequencing identifies GRIN2A as frequently mutated in melanoma. *Nat Genet*. 43(5): 442-6.

Weilbaecher KN, Hershey CL, Takemoto CM, Horstmann MA, Hemesath TJ, Tashjian AH, Fisher DE. (1998) Age-resolving osteopetrosis: a rat model implicating microphthalmia and the related transcription factor TFE3. *J Exp Med*. 187(5): 775-85.

Wellbrock C, Marais R. (2005) Elevated expression of MITF counteracts B-RAF-stimulated melanocyte and melanoma cell proliferation. *J Cell Biol*. 170(5): 703-8.

Wellbrock C, Ogilvie L, Hedley D, Karasarides M, Martin J, Niculescu-Duvaz D, Springer CJ, Marais R. (2004) V599EB-RAF is an oncogene in melanocytes. *Cancer Res*. 64(7): 2338-42.

Wellbrock C, Rana S, Paterson H, Pickersgill H, Brummelkamp T, Marais R. (2008) Oncogenic BRAF regulates melanoma proliferation through the lineage specific factor MITF. *PLoS One.* 3(7): e2734.

White RM and Zon LI. (2008) Melanocytes in development, regeneration and cancer. *Cell Stem Cell.* 3(3): 242-52.

Whiteman DC, Pavan WJ, Bastian BC. (2011) The melanomas: a synthesis of epidemiological, clinical, histopathological, genetic, and biological aspects, supporting distinct subtypes, causal pathways, and cells of origin. *Pigment Cell Melanoma Res*. 24(5): 879-97.

Wienholds E, Plasterk RH. (2004) Target-selected gene inactivation in zebrafish. *Methods Cell Biol*. 77: 69-90.

Wilhelm S, Carter C, Lynch M, Lowinger T, Dumas J, Smith RA, Schwartz B, Simantov R, Kelley S. (2006) Discovery and development of sorafenib: a multikinase inhibitor for treating cancer. *Nat Rev Drug Discov*. 5(10): 835-44.

Wong AK, Park CY, Greene CS, Bongo LA, Guan Y, Troyanskaya OG. (2012) IMP: a multi-species functional genomics portal for integration, visualization and prediction of protein functions and networks. *Nucleic Acids Res*. 40(Web Server issue): W484-90.

Wu H, Goel V, Haluska FG. (2003) PTEN signaling pathways in melanoma. *Oncogene.* 22(20): 3113-22.

Yasumoto K, Takeda K, Saito H, Watanabe K, Takahashi K, Shibahara S. (2002)

Microphthalmia-associated transcription factor interacts with LEF-1, a mediator of Wnt signaling. *EMBO J.* 21(11): 2703-14.

Yeh JE, Toniolo PA, Frank DA. (2013) Targeting transcription factors: promising new strategies for cancer therapy. *Curr Opin Oncol*. 25(6): 652-8.

Yen J, White RM, Wedge DC, Van Loo P, de Ridder J, Capper A, Richardson J, Jones D, Raine K, Watson IR et al. (2013) The genetic heterogeneity and mutational burden of engineered melanomas in zebrafish models. *Genome Biol*. 14(10): R113.

Yokoyama S, Feige E, Poling LL, Levy C, Widlund HR, Khaled M, Kung AL, Fisher DE. (2008) Pharmacologic suppression of MITF expression via HDAC inhibitors in the melanocyte lineage. *Pigment Cell Melanoma Res*. 21(4): 457-63.

Yokoyama S, Woods SL, Boyle GM, Aoude LG, MacGregor S, Zismann V, Gartside M, Cust AE, Haq R, Harland M et al. (2011) A novel recurrent mutation in MITF predisposes to familial and sporadic melanoma. *Nature*. 480(7375): 99-103.

Yu H, McDaid R, Lee J, Possik P, Li L, Kumar SM, Elder DE, Van Belle P, Gimotty P, Guerra M et al. (2009) The role of BRAF mutation and p53 inactivation during transformation of a subpopulation of primary human melanocytes. *Am J Pathol.* 174(6): 2367-77.

Zheng W, Li Z, Nguyen AT, Li C, Emelyanov A, Gong Z. (2014) Xmrk, kras and myc transgenic zebrafish liver cancer models share molecular signatures with subsets of human hepatocellular carcinoma. *PLoS One*. 9(3): e91179.

Zon LI. (1999) Zebrafish: a new model for human disease. *Genome Res*. 9(2): 99-

100.

Zuo L, Weger J, Yang Q, Goldstein AM, Tucker MA, Walker GJ, Hayward N, Dracopoli NC. (1996) Germline mutations in the p16INK4a binding domain of CDK4 in familial melanoma. *Nat Genet.* 12(1): 97-9.

Appendix I – Supplementary Data

Table A-1 Genes derived from STRING network analysis

Each cluster is shown and referred to by row and number, as shown by Cytoscape (Figure 5.3). Both Ensembl gene ID and name are given, as well as the results of functional analysis using DAVID.

Cluster	Ensemble gene ID	Ensembl gene name	DAVID functional anaylsis
Row 1 (1)	ENSDARG00000027169	kpna7	Transmembrane transport, ion binding, membrane
	ENSDARG00000069401	si:dkeyp-114g9.1	
	ENSDARG00000045601	cax1	
	ENSDARG00000069428	zgc:158856	
	ENSDARG00000052375	zgc:66455	
	ENSDARG00000042215	pias4b	
	ENSDARG00000054786	faah2b	
	ENSDARG00000020289	pif1	
	ENSDARG00000086340	qdprb2	
	ENSDARG00000034989	retsatl	
	ENSDARG00000014565	eif4e1b	
	ENSDARG00000060346	zgc:162592	
	ENSDARG00000036247	tmem144b	
	ENSDARG00000016908	zgc:171779	
	ENSDARG00000039828	zp3b	
	ENSDARG00000014208	zgc:55413	
	ENSDARG00000054374	alg13	
	ENSDARG00000055655	birc5b	

	ENSDARG00000075113	nanog	
	ENSDARG00000070618	tatdn2	
	ENSDARG00000054211	st8sia7.1	
	ENSDARG00000040161	zgc:92287	
	ENSDARG00000004823	asz1	
	ENSDARG00000010437	fam46c	
	ENSDARG00000073787	CU075911.1	
	ENSDARG00000055934	si:ch1073-416j23.1	
	ENSDARG00000044638	map1lc3c	
	ENSDARG00000068593	CU326366.3	
	ENSDARG00000022813	dnd	
	ENSDARG00000040344	h1m	
	ENSDARG00000037002	zgc:152968	
	ENSDARG00000059252	zpcx	
	ENSDARG00000038271	zgc:113293	
	ENSDARG00000040022	si:dkey-208k4.2	
	ENSDARG00000071083	si:dkeyp-34c12.1	
	ENSDARG00000004529	zgc:173742	
	ENSDARG00000037532	mcm3l	
	ENSDARG00000070611	zgc:152986	
	ENSDARG00000079452	rbm46	
	ENSDARG00000035171	btg4	
	ENSDARG00000070166	EVA1B (2 of 5)	
	ENSDARG00000055973	zar1l	

	ENSDARG00000008807	bokb	
	ENSDARG00000070178	si:ch211-225p5.3	
	ENSDARG00000044844	zgc:66483	
	ENSDARG00000071541	si:dkey-42i9.8	
	ENSDARG00000032156	zgc:171776	
	ENSDARG00000052717	fbxo43	
	ENSDARG00000008541	chia.4	
	ENSDARG00000040510	ca15b	
	ENSDARG00000077077	CU695216.1	
	ENSDARG00000040081	zgc:66432	
	ENSDARG00000015543	s100a1	
Row 1 (2)	ENSDARG00000036159	trhrb	ATP binding, ion binding
	ENSDARG00000004026	chrm5a	
	ENSDARG00000043341	npy4r	
	ENSDARG00000002773	htr1fa	
	ENSDARG00000057029	htr2a	
	ENSDARG00000011091	drd2b	
	ENSDARG00000077167	nmbb	
	ENSDARG00000068557	htr5al	
	ENSDARG00000079395	pdyn	
	ENSDARG00000023722	hcrtr2	
	ENSDARG00000020744	bdkrb1	
	ENSDARG00000060702	npffr2.2	
	ENSDARG00000056230	ghsra	

	ENSDARG00000074851	s1pr4	
	ENSDARG00000039434	oprm1	
	ENSDARG00000035632	zgc:194112	
	ENSDARG00000071209	oprl1	
	ENSDARG00000014477	sstr3	
	ENSDARG00000053580	htf1fb	
	ENSDARG00000018616	agtr1a	
	ENSDARG00000078828	npb	
	ENSDARG00000038363	drd4a	
	ENSDARG00000042081	SSTR5	
	ENSDARG00000004869	penka	
	ENSDARG00000077638	F2R (5 of 7)	
	ENSDARG00000074661	gper	
	ENSDARG00000075112	tacr3a	
Row 1 (3)	ENSDARG00000051852	kcnc1a	Voltage-gated potassium channel
	ENSDARG00000069117	kcnh5b	
	ENSDARG00000002241	KCNA2	
	ENSDARG00000029511	KCNS3 (2 of 2)	
	ENSDARG00000062906	kcnv2b	
	ENSDARG00000059935	KCNA10 (2 of 2)	
	ENSDARG00000060085	kcnq3	
	ENSDARG00000046014	kcna6	
	ENSDARG00000070092	KCNV1	
	ENSDARG00000079491	KCNA3	

	ENSDARG00000040741	KCNAB1 (3 of 3)	
	ENSDARG00000061288	kcnc4	
	ENSDARG00000076854	KCNA10 (1 of 2)	
Row 1 (4)	ENSDARG00000037874	si:dkey-21n8.3	Cytochrome p450
	ENSDARG00000053966	cyp17a2	
	ENSDARG00000070021	cyp3c4	
	ENSDARG00000092091	CT737190.1	
	ENSDARG00000038369	cyp2k17	
	ENSDARG00000068493	CU928854.1	
	ENSDARG00000034070	cyp2aa3	
	ENSDARG00000037873	cyp3c1l2	
	ENSDARG00000009874	CYP2W1 (9 of 10)	
	ENSDARG00000070020	cyp2aa9	
	ENSDARG00000058458	cyp2k16	
Row 1 (5)	ENSDARG00000013014	or101-1	Odorant receptor
	ENSDARG00000094080	or103-1	
	ENSDARG00000041019	or111-11	
	ENSDARG00000043142	or108-3	
	ENSDARG00000041030	or111-1	
	ENSDARG00000025658	or111-2	
	ENSDARG00000004598	or102-2	
	ENSDARG00000041024	or111-6	
	ENSDARG00000068659	or104-2	
	ENSDARG00000003090	or103-4	

	ENSDARG00000074966	or102-3	
Row 2 (1)	ENSDARG00000089869	EVA1B (5 of 5)	Coiled-coil domain containing
	ENSDARG00000090768	zgc:173556	
	ENSDARG00000042130	zp3a.2	
	ENSDARG00000027639	zgc:165539	
	ENSDARG00000008835	si:dkey-46g23.5	
	ENSDARG00000078917	zgc:195245	
	ENSDARG00000079034	wu:fi38e01	
	ENSDARG00000094370	si:ch211-125e6.13	
	ENSDARG00000076949	zgc:173837	
	ENSDARG00000070709	wu:fi42e03	
Row 2 (2)	ENSDARG00000024047	tmem38a	Ion binding
	ENSDARG00000019202	ldb3b	
	ENSDARG00000036371	acta1a	
	ENSDARG00000003081	mybphb	
	ENSDARG00000058158	trim55b	
	ENSDARG00000021265	mybpc2b	
	ENSDARG00000013752	tnni2a.3	
	ENSDARG00000029995	tnni2b.2	
	ENSDARG00000029321	MYL3 (2 of 2)	
	ENSDARG00000045592	tnni2a.1	
Row 2 (3)	ENSDARG00000071070	PTHRP2	Cell membrane, G protein-coupled receptor
	ENSDARG00000078247	vip	
	ENSDARG00000020957	pth1ra	

	ENSDARG00000017437	adcy3b	
	ENSDARG00000019660	rxfp2a	
	ENSDARG00000028845	calcr	
	ENSDARG00000079443	VIP2	
	ENSDARG00000054946	mc5rb	
	ENSDARG00000021186	PTH2R (2 of 2)	
Row 2 (4)	ENSDARG00000045835	si:dkey-14d8.6	Proteolysis
	ENSDARG00000043722	cpa4	
	ENSDARG00000043173	CELA1 (2 of 8)	
	ENSDARG00000012539	dnase1	
	ENSDARG00000061858	zgc:153968	
	ENSDARG00000053853	slc13a2	
	ENSDARG00000018361	sult1st3	
	ENSDARG00000041848	rh50	
Row 2 (5)	ENSDARG00000070892	si:ch211-262h13.5	Membrane
	ENSDARG00000075614	zgc:193682	
	ENSDARG00000041034	zgc:152857	
	ENSDARG00000074547	si:ch211-240l19.8	
	ENSDARG00000019492	shbg	
	ENSDARG00000042613	crp3	
	ENSDARG00000091136	zgc:174259	
	ENSDARG00000056498	si:ch211-234p6.10	
Row 2 (6)	ENSDARG00000033542	nitr12	Novel immune-type receptors
	ENSDARG00000069925	nitr7a	

	ENSDARG00000074330	CU179759.1	
	ENSDARG00000068018	CU672228.1	
	ENSDARG00000068001	nitr1c	
	ENSDARG00000057956	nitr6a	
	ENSDARG00000068014	nitr1k	
	ENSDARG00000076114	CR847950.2	
Row 3 (1)	ENSDARG00000070597	prelp	Leucine-rich repeat containing
	ENSDARG00000062303	GP5	
	ENSDARG00000078790	lrrc18a	
	ENSDARG00000045811	BX897714.3	
	ENSDARG00000079654	st3gal1	
	ENSDARG00000076236	lrrc18b	
	ENSDARG00000040037	st3gal1l3	
	ENSDARG00000044895	fmoda	
Row 3 (2)	ENSDARG00000037840	actc1b	Ion binding, ATP-related
	ENSDARG00000028625	jph2	
	ENSDARG00000040565	ckmb	
	ENSDARG00000070835	tnnc2	
	ENSDARG00000035327	ckma	
	ENSDARG00000001993	myhb	
	ENSDARG00000018321	lbx1a	
Row 3 (3)	ENSDARG00000069293	AHSG	Aminotransferases
	ENSDARG00000042953	cyp2n13	
	ENSDARG00000017882	rdh1	

	ENSDARG00000052099	agxta	
	ENSDARG00000035602	dao.1	
	ENSDARG00000018478	agxtb	
	ENSDARG00000041787	cx32.3	
Row 3 (4)	ENSDARG00000056652	SLC22A7 (2 of 5)	Transmembrane, synaptic vesicle related
	ENSDARG00000060711	SV2B (1 of 3)	
	ENSDARG00000053961	SLC2A11	
	ENSDARG00000056643	slc22a7b	
	ENSDARG00000056833	svopa	
	ENSDARG00000059945	SV2A	
	ENSDARG00000014951	svopb	
Row 3 (5)	ENSDARG00000093844	zgc:136461	Proteolysis
	ENSDARG00000060350	APOD (2 of 3)	
	ENSDARG00000043168	CELA1 (7 of 8)	
	ENSDARG00000079274	zgc:66382	
	ENSDARG00000055539	epdl2	
	ENSDARG00000038296	tmem86b	
Row 3 (6)	ENSDARG00000022503	pkd2l1	Taste receptor
	ENSDARG00000059397	tas1r2.2	
	ENSDARG00000053135	tas1r2.1	
	ENSDARG00000006341	tas1r3	
	ENSDARG00000079880	tas2r200.1	
	ENSDARG00000074066	tas2r200.2	
Row 4	ENSDARG00000001915	phc2b	DNA binding

(1)	ENSDARG00000077741	ZGC:165551	
	ENSDARG00000070714	zgc:173544	
	ENSDARG00000073811	wu:fi34b01	
	ENSDARG00000078457	si:ch211-250e5.16	
Row 4 (2)	ENSDARG00000044278	synpr	N/A
	ENSDARG00000028846	arl3l1	
	ENSDARG00000020814	faimb	

Table A-2 Genes derived from IMP network analysis

Each cluster is shown and referred to by row and number, as shown by Cytoscape (Figure 5.4). Both Ensembl gene ID and gene symbol are given, as well as the results of functional analysis using DAVID.

Cluster	Ensemble gene ID	Gene symbol	DAVID functional analysis
Row 1 (1)	ENSDARG00000018259	ATP1A3A	Ion binding, cytoskeleton, membrane
	ENSDARG00000052765	GRIA2B	
	ENSDARG00000032565	CACNG2A	
	ENSDARG00000063018	FP102157.1	
	ENSDARG00000012772	ZGC:153845	
	ENSDARG00000024299	C1QTNF4	
	ENSDARG00000024299	C1QTNF4	
	ENSDARG00000062323	ADAM23A	
	ENSDARG00000008407	TSPAN7B	
	ENSDARG00000007654	NSFA	
	ENSDARG00000000503	STX1B	
	ENSDARG00000055455	GPM6AA	
	ENSDARG00000026247	C18H15ORF59	
	ENSDARG00000021595	LHFPL3	
	ENSDARG00000023228	VSNL1A	
	ENSDARG00000041062	CALB2A	

	ENSDARG00000055874	CPE	
	ENSDARG00000043448	ITM2CA	
	ENSDARG00000036344	CALB2B	
	ENSDARG00000004386	SI:DKEY-153K10.9	
	ENSDARG00000009621	CACNG2B	
	ENSDARG00000039256	SPEG	
	ENSDARG00000045945	SYN2A	
	ENSDARG00000078671	CDK5R2B	
	ENSDARG00000073755	PCDH1G22	
	ENSDARG00000059601	MAP1AA	
	ENSDARG00000054794	PLCXD3	
	ENSDARG00000020758	TMEM178	
	ENSDARG00000041627	SNCB	
	ENSDARG00000053130	PCP4A	
	ENSDARG00000004148	APLP1	
	ENSDARG00000077940	VSTM2B	
	ENSDARG00000045639	ELAVL4	
	ENSDARG00000015775	GAP43	
	ENSDARG00000053248	INAB	
	ENSDARG00000010029	SPON1A	
	ENSDARG00000071493	OLFM3A	
	ENSDARG00000009563	SLC1A2B	
	ENSDARG00000039647	SLC6A1B	
	ENSDARG00000005470	KIF5AA	

	ENSDARG00000016301	ZGC:65894	
	ENSDARG00000039123	TRIM9	
	ENSDARG00000012281	ZGC:65851	
	ENSDARG00000037921	GNG13B	
	ENSDARG00000071011	CDK5R2A	
	ENSDARG00000076987	SLITRK5	
	ENSDARG00000055740	MARCH	
	ENSDARG00000018997	CPLX2L	
	ENSDARG00000012482	PCLOB	
	ENSDARG00000060656	SI:CH211-10A23.2	
Row 1 (2)	ENSDARG00000006894	OPRK1	G protein-coupled receptor
	ENSDARG00000025024	PNOCA	
	ENSDARG00000077167	NMBB	
	ENSDARG00000044561	CCR7	
	ENSDARG00000007553	OPN4.1	
	ENSDARG00000063088	SI:DKEY-211G8.6	
	ENSDARG00000053833	MTNR1BA	
	ENSDARG00000079423	NPBWR2A	
	ENSDARG00000056230	GHSRA	
	ENSDARG00000054124	HTR1BD	
	ENSDARG00000068557	HTR5AL	
	ENSDARG00000074509	TACR2	
	ENSDARG00000039970	CNR2	
	ENSDARG00000014490	TAC1	

	ENSDARG00000053987	HTR1B	
	ENSDARG00000023722	HCRTR2	
	ENSDARG00000079395	PDYN	
	ENSDARG00000004026	CHRM5A	
	ENSDARG00000009020	CNR1	
	ENSDARG00000069669	ADRA2C	
	ENSDARG00000045788	AVPR1B	
	ENSDARG00000005522	GALR1	
	ENSDARG00000053580	HTF1FB	
	ENSDARG00000042081	SSTR5	
	ENSDARG00000014477	SSTR3	
	ENSDARG00000043341	NPY4R	
	ENSDARG00000054152	NMBR	
	ENSDARG00000020744	BDKRB1	
	ENSDARG00000036159	TRHRB	
	ENSDARG00000060702	NPFFR2.2	
	ENSDARG00000074851	S1PR4	
	ENSDARG00000002773	HTR1FA	
Row 1 (3)	ENSDARG00000027285	KCNF1B	Voltage-gated potassium channel
	ENSDARG00000060085	KCNQ3	
	ENSDARG00000035861	SI:RP71-39B20.4	
	ENSDARG00000051852	KCNC1A	
	ENSDARG00000070092	KCNV1	
	ENSDARG00000027940	KCNF1A	

	ENSDARG00000032799	KCND2	
	ENSDARG00000062906	KCNV2B	
	ENSDARG00000062640	KCNH8	
	ENSDARG00000074746	KCND1	
	ENSDARG00000008140	KCNAB1	
	ENSDARG00000055855	KCNC3A	
	ENSDARG00000079491	KCNA3	
	ENSDARG00000069560	KCNH3	
	ENSDARG00000069117	KCNH5B	
	ENSDARG00000002241	KCNA2	
	ENSDARG00000062942	KCNA1	
Row 1 (4)	ENSDARG00000004598	OR102-2	Odorant receptor
	ENSDARG00000068659	OR104-2	
	ENSDARG00000003090	OR103-4	
	ENSDARG00000041024	OR111-6	
	ENSDARG00000041030	OR111-1	
	ENSDARG00000013014	OR101-1	
	ENSDARG00000043142	OR108-3	
	ENSDARG00000094080	OR103-1	
	ENSDARG00000074966	OR102-3	
	ENSDARG00000041019	OR111-11	
	ENSDARG00000025658	OR111-2	
Row 2 (1)	ENSDARG00000054211	ST8SIA7.1	N/A
	ENSDARG00000055655	BIRC5B	

Row 2 (2)	ENSDARG00000012718	WEE2	N/A
	ENSDARG00000060346	ZGC:162592	
Row 2 (3)	ENSDARG00000045856	FGF6B	Fibroblast growth factors
	ENSDARG00000056074	FGF22	
	ENSDARG00000076510	FGF22	
	ENSDARG00000009351	FGF6A	
Row 2 (4)	ENSDARG00000059397	TAS1R2.2	Taste receptors
	ENSDARG00000053135	TAS1R2.1	
	ENSDARG00000006341	TAS1R3	
	ENSDARG00000079880	TAS2R200.1	
Row 2 (5)	ENSDARG00000070492	FGF21	Fibroblast growth factors, interleukin
	ENSDARG00000045854	FGF23	
	ENSDARG00000040982	FGF14	
	ENSDARG00000035377	FGF5	
Row 2 (6)	ENSDARG00000056643	SLC22A7B	Transmembrane transport
	ENSDARG00000059945	SV2A	
	ENSDARG00000015869	SLC22A16	
	ENSDARG00000053961	SLC2A11	
Row 3 (1)	ENSDARG00000030961	AK8	Phospho-diesterases
	ENSDARG00000012555	AK5	
	ENSDARG00000032344	PDE4A	
	ENSDARG00000076650	CR848033.1	
	ENSDARG00000017023	AK7B	
	ENSDARG00000063732	PDE11A	

	ENSDARG00000060875	PDE1A	
	ENSDARG00000068130	C5H9ORF9	
	ENSDARG00000075714	C5H11ORF88	
	ENSDARG00000061899	IQUB	
	ENSDARG00000040254	HORMAD1	
Row 3 (2)	ENSDARG00000017274	OPN1SW2	Visual perception, membrane
	ENSDARG00000014840	PRPH2B	
	ENSDARG00000027424	SLC25A3A	
	ENSDARG00000017634	PDCB	
	ENSDARG00000056915	SI:CH211-237L4.6	
Row 3 (3)	ENSDARG00000058053	SERPING1	Immunoglobulin subtype, receptor
	ENSDARG00000053973	FETUB	
	ENSDARG00000031046	NR1H5	
	ENSDARG00000045516	ITIH2	
	ENSDARG00000087359	C3B	
Row 3 (4)	ENSDARG00000070543	GRIN2AB	G protein-coupled receptor, transmembrane
	ENSDARG00000034493	GRIN2AA	
	ENSDARG00000030376	GRIN2BB	
	ENSDARG00000052765	GRIA2B	
	ENSDARG00000009563	SLC1A2B	
Row 3 (5)	ENSDARG00000058158	TRIM55B	Ion binding
	ENSDARG00000075433	CR847973.1	
	ENSDARG00000035958	TNNI2B.1	
	ENSDARG00000045592	TNNI2A.1	

	ENSDARG00000024047	TMEM38A	
Row 3 (6)	ENSDARG00000086340	QDPRB2	Ion binding, nucleus
	ENSDARG00000069401	SI:DKEYP-114G9.1	
	ENSDARG00000069129	ZGC:153126	
	ENSDARG00000037532	MCM3L	
	ENSDARG00000079452	RBM46	
	ENSDARG00000055934	SI:CH1073-416J23.1	
	ENSDARG00000037002	ZGC:152968	
	ENSDARG00000040022	SI:DKEY-208K4.2	
	ENSDARG00000034989	RETSATL	
	ENSDARG00000016538	ZGC:55888	
Row 3 (7)	ENSDARG00000070835	TNNC2	Microtubule
	ENSDARG00000018321	LBX1A	
	ENSDARG00000059259	PABPC4	
	ENSDARG00000053254	MYLPFA	
	ENSDARG00000035327	CKMA	
	ENSDARG00000037840	ACTC1B	
	ENSDARG00000001993	MYHB	
	ENSDARG00000040565	CKMB	
Row 3 (8)	ENSDARG00000007971	CKS1B	Mitosis, cell cycle
	ENSDARG00000069917	SKA3	
	ENSDARG00000002403	NUSAP1	
	ENSDARG00000044437	CDCA5	
	ENSDARG00000070656	SI:CH211-69G19.2	

	ENSDARG00000075621	BIRC5A	
Row 4 (1)	ENSDARG00000044261	SI:CH211-243G18.2	Ion binding, nucleus
	ENSDARG00000021265	MYBPC2B	
	ENSDARG00000014196	MYL1	
	ENSDARG00000029995	TNNI2B.2	
	ENSDARG00000003081	MYBPHB	
Row 4 (2)	ENSDARG00000056643	SLC22A7B	Transmembrane transport
	ENSDARG00000054690	SI:DKEY-166K12.1	
	ENSDARG00000015869	SLC22A16	
	ENSDARG00000053961	SLC2A11	
	ENSDARG00000056028	SLC22A7A	

Appendix II – Relevant Publications

JID Open

A Conditional Zebrafish MITF Mutation Reveals MITF Levels Are Critical for Melanoma Promotion vs. Regression *In Vivo*

James A. Lister[1,5,6], Amy Capper[2,3,5], Zhiqiang Zeng[2,3], Marie E. Mathers[4], Jennifer Richardson[2,3], Karthika Paranthaman[2,3], Ian J. Jackson[2] and E. Elizabeth Patton[2,3,6]

The microphthalmia-associated transcription factor (MITF) is the "master melanocyte transcription factor" with a complex role in melanoma. MITF protein levels vary between and within clinical specimens, and amplifications and gain- and loss-of-function mutations have been identified in melanoma. How MITF functions in melanoma development and the effects of targeting MITF *in vivo* are unknown because MITF levels have not been directly tested in a genetic animal model. Here, we use a temperature-sensitive *mitf* zebrafish mutant to conditionally control endogenous MITF activity. We show that low levels of endogenous MITF activity are oncogenic with $BRAF^{V600E}$ to promote melanoma that reflects the pathology of the human disease. Remarkably, abrogating MITF activity in $BRAF^{V600E}$*mitf* melanoma leads to dramatic tumor regression marked by melanophage infiltration and increased apoptosis. These studies are significant because they show that targeting MITF activity is a potent antitumor mechanism, but also show that caution is required because low levels of wild-type MITF activity are oncogenic.

Journal of Investigative Dermatology (2014) **134,** 133–140; doi:10.1038/jid.2013.293; published online 15 August 2013

INTRODUCTION

Driver genes that stimulate proliferation and survival are important drug targets in cancer. The discovery of $BRAF^{V600E}$ mutations in nevi and melanoma has directly led to the development of small-molecule inhibitors with clear clinical benefit (Flaherty *et al.*, 2012). Despite these dramatic improvements, drug resistance remains a critical problem, and most patients with metastatic melanoma eventually succumb to the disease within a year. It is therefore necessary to identify additional therapeutic targets in melanoma that can be used in combination with available treatments (Tsao *et al.*, 2012).

One of the important genes in melanocyte development and melanoma is the highly conserved ''master melanocyte transcription factor'' microphthalmia-associated transcription factor (MITF) (Levy *et al.*, 2006). MITF responds to multiple signaling cascades to orchestrate genes involved in melanocyte growth, differentiation, and survival (Cheli *et al.*, 2010). Although MITF mutations in development lead to similar phenotypes across species, the function of MITF in melanoma is complex and not fully understood. MITF is expressed in most melanomas, although MITF protein levels vary between melanoma specimens, with some subsets of melanoma showing high levels and others showing low levels of MITF (Flaherty *et al.*, 2012). MITF activity can also vary within an individual melanoma, such that low levels of MITF promote invasion and stem-cell like phenotypes and moderate levels of MITF activity promote cell cycle progression (Goodall *et al.*, 2008; Hoek and Goding, 2010; Cheli *et al.*, 2011; Strub *et al.*, 2011; Cheli *et al.*, 2012). The ability of MITF to activate cancer hallmark genes makes it an important mediator of oncogenic signaling in cancer. This is underscored by evidence that MITF is at least partially responsible for the oncogenic potential of BRAF in cells (Wellbrock and Marais, 2005; Wellbrock *et al.*, 2008). Studies from melanoma cells indicate that a key function of $BRAF^{V600E}$ seems to be to maintain MITF activity at a critical threshold where it promotes proliferation, invasion, and survival, without promoting differentiation (at higher levels) or apoptosis or senescence (at lower levels) (Giuliano *et al.*, 2010; Hoek and Goding, 2010; Cheli *et al.*, 2011; Strub *et al.*, 2011; Cheli *et al.*, 2012)

However, MITF may have additional cooperating functions in melanoma. MITF is amplified in some melanomas, and expression of ectopic MITF can cooperate with $BRAF^{V600E}$ to transform primary human melanocytes and neural crest cells (Garraway *et al.*, 2005; Kumar *et al.*, 2013). In addition, MITF

[1]*Department of Human and Molecular Genetics and Massey Cancer Center, Virginia Commonwealth University, Richmond, Virginia, USA;* [2]*MRC Human Genetics Unit, Western General Hospital, Edinburgh, UK;* [3]*University of Edinburgh Cancer Research UK Centre, Institute of Genetics and Molecular Medicine, University of Edinburgh, Edinburgh, UK and* [4]*Department of Pathology, Western General Hospital, Edinburgh, UK*

[5]*These authors contributed equally to this work.*

[6]*These authors are co-submitting authors.*

Correspondence: James A. Lister or E. Elizabeth Patton, Department of Human and Molecular Genetics and Massey Cancer Center, Virginia Commonwealth University, P.O. Box 980033, 1101 E. Marshall Street, Richmond, Virginia 23298-0033, USA. E-mail: jalister@vcu.edu or e.patton@igmm.ed.ac.uk

Abbreviation: MITF, microphthalmia-associated transcription factor

Received 13 March 2013; revised 10 May 2013; accepted 26 May 2013; accepted article preview online 5 July 2013; published online 15 August 2013

mutations have been identified in $BRAF^{V600E}$ melanomas including somatic mutations with either hypomorphic or increased activity (Cronin *et al.*, 2009), and a germline SUMOylation E318K mutation that is a melanoma risk factor and confers differential gene expression of MITF target genes (Bertolotto *et al.*, 2011; Yokoyama *et al.*, 2011). Thus, MITF is important in melanoma because it is an effector of oncogenic signaling, and also because it may have additional activity that contributes to melanomagenesis.

How MITF activity contributes to melanoma development and survival in an animal is unknown. Animal models are fundamental in establishing how genetic mutations contribute to cancer *in vivo*. Although many *Mitf* mutant mouse lines exist (Hou and Pavan, 2008), they do not permit conditional control of MITF activity in melanoma development or survival. Here, we address the importance of MITF activity in melanoma *in vivo* using a conditional *mitfa* temperature-sensitive zebrafish mutant ($mitfa^{vc7}$) in which endogenous MITF activity can be altered by changing the temperature of the water (Johnson *et al.*, 2011; Taylor *et al.*, 2011). In zebrafish, there are two *mitf* genes (*mitfa* and *mitfb*), and *mitfa* is essential for the development of neural crest–derived melanocytes (Lister *et al.*, 1999). Thus, by using a *mitfa* mutant we specifically control endogenous MITF activity in skin melanocytes, and avoid the potential complication of MITF activity in other tissues, such as those described in mouse mutants (Hou and Pavan, 2008). We show that low levels of wild-type MITF activity are oncogenic with $BRAF^{V600E}$ to promote melanoma *in vivo*, and that abrogating MITF activity in melanoma leads to rapid tumor regression. These results reveal that critical thresholds of MITF lead to dramatically different melanoma outcomes, and indicate that although targeting MITF activity is a potent antitumor approach, simply reducing MITF activity is sufficient to drive melanoma in $BRAF^{V600E}$ melanocytes.

RESULTS

Hypomorphic MITF is oncogenic with $BRAF^{V600E}$ in melanomagenesis

We sought to test whether hypomorphic levels of MITF activity could contribute to melanoma development *in vivo* using a zebrafish *mitf* temperature-sensitive mutant, $mitfa^{vc7}$ (Figure 1a–d; Johnson *et al.*, 2011; originally characterized as *fh53*) and a transgenic line expressing $BRAF^{V600E}$ in melanocytes that we have previously developed and has been effective in the identification of cooperating driver genes (Figure 1e) (Patton *et al.*, 2005; Ceol *et al.*, 2011). The $mitfa^{vc7}$allele is a splice site mutation at the intron 6 splice donor site that leads to a reduction in melanocytes when zebrafish are reared at $<26\,^{\circ}C$, and an almost complete loss of melanocytes at $>28\,^{\circ}C$ (Figure 1b–d) (Johnson *et al.*, 2011). We performed two generations of genetic crosses with the $BRAF^{V600E}$ transgenic fish to the $mitfa^{vc7}$ mutant zebrafish to generate $BRAF^{V600E/V600E}mitfa^{vc7/vc7}$ ($BRAF^{V600E}mitf$) zebrafish. As expected, $BRAF^{V600E}mitf$ zebrafish did not develop melanocytes at the restrictive temperature ($28.5\,^{\circ}C$) because there is not sufficient MITF activity to generate melanocytes (Figure 1f). Importantly, at $<26\,^{\circ}C$, $BRAF^{V600E}mitf$ zebrafish developed nevi (Figure 1g), some of which progressed to melanoma ($n=18/67$; Figure 1h–j). The $mitfa^{vc7}$ allele is a splice site mutation, and we confirmed that the $BRAF^{V600E}mitf$ melanomas expressed the mis-spliced + *intron6* variant with hypomorphic levels of correctly spliced *mitfa* (Figure 1k). As controls, neither $BRAF^{V600E}$ transgenic fish carrying wild-type *mitfa* alleles nor *mitfa* mutants lacking the $BRAF^{V600E}$ transgene developed melanoma at any temperature (Patton *et al.*, 2005; Johnson *et al.*, 2011; data not shown). We compared the incidence of melanoma in $BRAF^{V600E}mitf$ compared with $BRAF^{V600E/V600E}p53^{M214K/M214K}$ ($BRAF^{V600E}p53$) zebrafish, and found that the incidence was similar between the two genotypes ($n=48/177$; Figure 1j). These results show that hypomorphic levels of MITF activity interact genetically with $BRAF^{V600E}$ to promote melanoma *in vivo*.

$BRAF^{V600E}mitf$ melanomas display characteristic histopathological features

We wanted to know whether the *mitf* and *p53* cooperating mutations contributed to melanoma pathology. We found that most $BRAF^{V600E}mitf$ melanomas displayed a superficial spreading growth pattern with some invasion into the underlying muscle (Figure 2a; $n=22/26$). This pattern was reminiscent of superficial spreading melanoma, the most common subtype of human melanoma. A striking characteristic feature of $BRAF^{V600E}mitf$ melanomas was the presence of large, heavily pigmented cells throughout the tumor ($n=26/26$), and often found in the kidney (the site of the hematopoietic compartment in zebrafish). Macrophages laden with melanin (melanophages) are often a feature of human malignant melanoma, and express CD68. We found these large cells to correspond to CD68-positive cells in the $BRAF^{V600E}mitf$ melanomas and characterized them as melanophages (Supplementary Figure S1 online). $BRAF^{V600E}mitf$ melanomas were composed of spindle- and epithelioid-shaped tumor cells, marked by few mitoses and showing only mild nuclear pleomorphism. These histological features were characteristic of $BRAF^{V600E}mitf$ melanomas, and allowed reliable identification of these tumors on blind assessment by a clinical skin pathologist (MEM; $n=26/26$; Figure 2a). By comparison, most $BRAF^{V600E}p53$ melanomas progressed rapidly, displaying a nodular and a highly invasive growth pattern into multiple organs ($n=19/21$; Figure 2b). No melanophages were observed in $BRAF^{V600E}p53$ melanomas, and the tumors were composed primarily of epithelioid cells, with features indicative of aggressive cancers including numerous mitoses and moderate-to-severe nuclear pleomorphism.

We analyzed the activation state of the MAPK cascade in the $BRAF^{V600E}mitf$ and $BRAF^{V600E}p53$ mutant melanoma by performing immunohistochemical analysis with anti-phospho-extracellular signal–regulated kinase (ERK; Figure 2c). As expected, phospho-ERK signal was detected in the majority of melanoma cells in both $BRAF^{V600E}mitf$ and $BRAF^{V600E}p53$ melanoma, and $BRAF^{V600E}p53$ had increased levels of p53 mutant protein (Figure 2d). Both melanomas stained positively for Melan-A, a MITF target gene and marker for melanoma and melanocytes in human specimens (Du *et al.*, 2003) (Figure 2e). Increased mitotic activity in $BRAF^{V600E}p53$

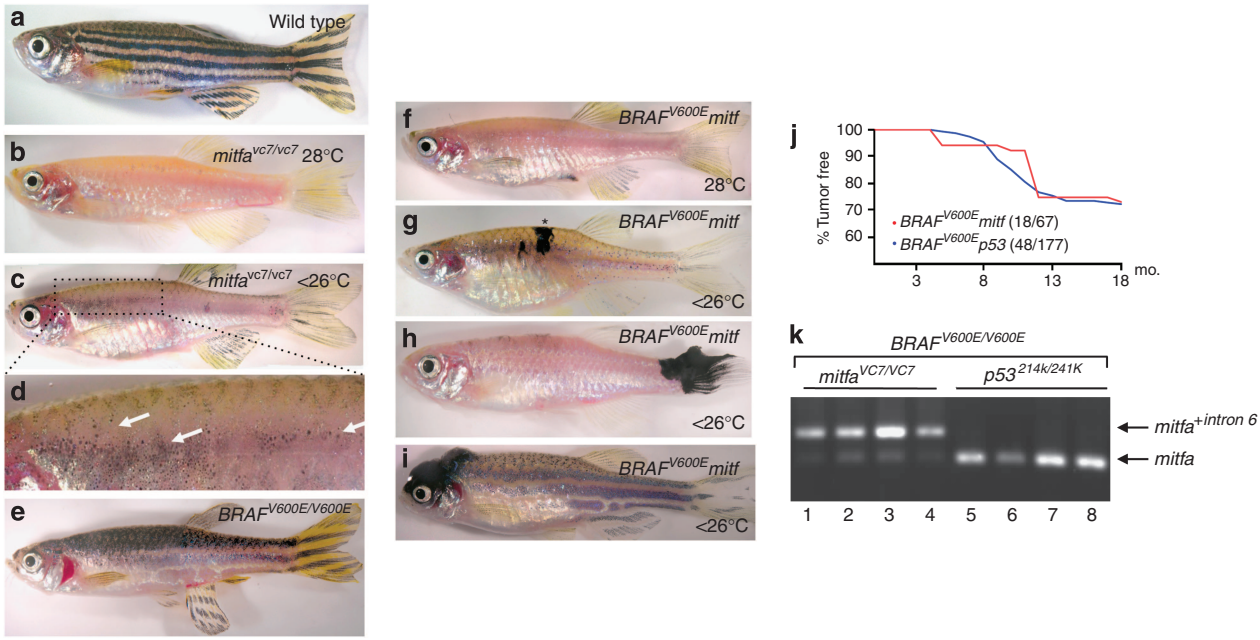

Figure 1. The microphthalmia-associated transcription factor (MITF) is oncogenic with BRAF^{V600E} in melanomagenesis. (**a**) Adult wild-type zebrafish or (**b**) adult *mitfa*^{vc7} mutant zebrafish living in water at 28 °C or (**c**, **d**) <26 °C. At <26 °C some melanocytes are visible in the body (**d**: enlarged region, white arrows). (**e**) Adult transgenic line expressing human *BRAF*^{V600E} in the melanocytes. (**f–i**) Genetic crosses of *BRAF*^{V600E}*mitf* at the semirestrictive temperatures develop nevi (*) and melanoma (on the tail of the middle fish, and on the head of the bottom fish). (**j**) Melanoma incidence curves of *BRAF*^{V600E}*p53* and *BRAF*^{V600E}*mitf* (<26 °C) genetic crosses. (**k**) Real-time PCR (RT-PCR) analysis of the *mitfa* transcript in *BRAF*^{V600E}*p53* and *BRAF*^{V600E}*mitf* melanomas.

melanomas compared with *BRAF*^{V600E}*mitf* melanoma cells was confirmed by immunostaining for phospho-histone H3, a marker of late-G2/M phase (Figure 2f and g). These results show that there is a strong genotype–phenotype correlation for cooperating mutations that can directly affect growth features and cellular histology.

Differential MITF target gene expression between melanoma genotypes

We wanted to understand how hypomorphic MITF activity contributed to melanoma, and hypothesized that MITF target genes may be differentially expressed between the melanoma genotypes. We performed quantitative real-time PCR on MITF target genes involved in proliferation (*cdk2*), cell cycle arrest (*p16*, *p21*), differentiation (*tyr*, *dct*), and survival (*bcl-2*, *hif1α*, *c-met*) (Figure 3). Despite the differences in phospho-histone H3 staining between the genotypes, the differences in *cdk2*, *p16*, and *p21* cycle threshold (Ct) values between melanoma genotypes were not statistically significant (Figure 3a–c). Neither was there a significant difference in the cycle threshold values for expression of *p53*, *bcl-2*, or *hif1α* between melanoma genotypes (Figure 3f–h). These results indicate that despite the reduced levels of MITF activity in *BRAF*^{V600E}*mitf* melanomas, there is sufficient MITF activity to control MITF target genes involved in cell proliferation and survival. Strikingly, *BRAF*^{V600E}*mitf* melanomas expressed lower levels of differentiation genes (*tyr* and *dct*), as indicated by higher cycle threshold values (Figure 3d and e). Unexpectedly, we found that *BRAF*^{V600E}*mitf* melanomas expressed significantly higher levels of *c-met* compared with *BRAF*^{V600E}*p53* melanoma (Figure 3i). *c-met* is a MITF target gene, but is also transcriptionally regulated by Pax3 in melanoblasts and melanomas (McGill *et al.*, 2006; Beuret *et al.*, 2007; Mascarenhas *et al.*, 2010). The tumor-initiating potential of cell types can vary within a lineage and differing tumor potentials may exist within the melanocyte lineage (Kumar *et al.*, 2013). Although the tumors are heterogeneous, the low expression of differentiation genes (*tyr* and *dct*) coupled with high *c-met* gene expression pattern suggests that hypomorphic MITF activity may maintain melanocytes in a less differentiated state that is more susceptible to BRAF^{V600E} transformation.

Loss of MITF causes melanoma regression

MITF is a lineage survival oncogene in cells, but the effect of abrogating MITF activity in an animal model of melanoma *in vivo* is unknown. To develop an animal system that could directly validate MITF as a drug target, we tested the effects of dramatically reducing MITF activity on melanoma survival by increasing the water temperature to the restrictive conditions (32 °C); none of the aberrant *mitfa*^{vc7} splice products are sufficient for melanocyte development at these restrictive temperatures (Johnson *et al.*, 2011), and MITF activity is not required to maintain the activity of the *mitfa* promoter fragment driving the BRAF^{V600E} transgene (Supplementary Figure S2 online; Dooley *et al.*, 2013). *BRAF*^{V600E}*mitf*^{vc7} zebrafish were reared at <26 °C to promote melanoma development, and then the temperature of the water was raised to 32 °C to turn off MITF activity. Within 2 weeks, 8/12 melanomas had dramatically regressed (Figure 4a; fish 1 and 2). Melanoma regression was the result of the *mitfa*^{vc7}

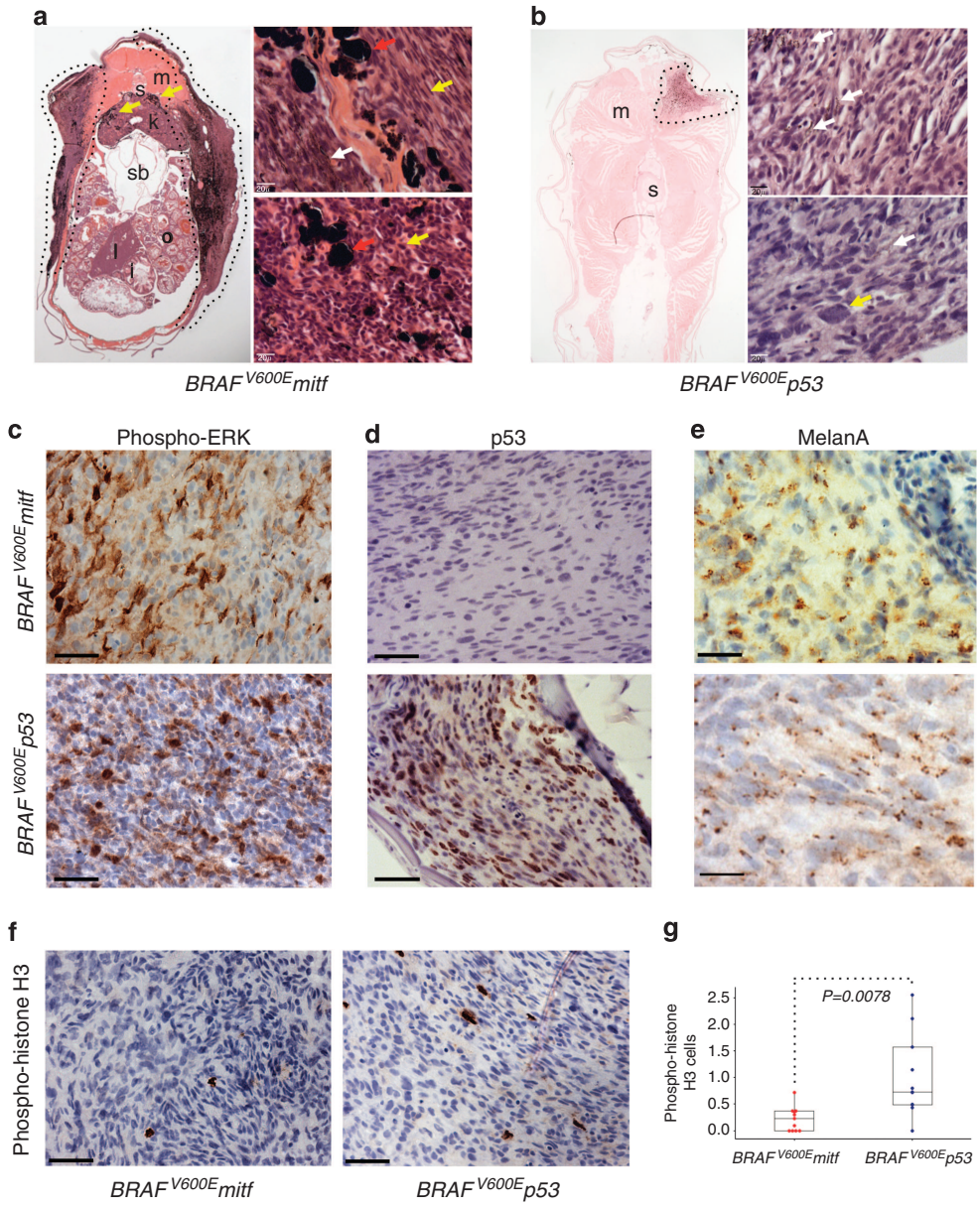

Figure 2. Comparative histopathology of BRAF^{V600E} melanomas. (**a**) Cross-section of adult *BRAF^{V600E}mitf* zebrafish with superficial spreading melanoma (dotted line). Infiltrating melanophages in the kidney are indicated (yellow arrows). i, intestine; k, kidney; l, liver; m, muscle; o, ovary; s, spinal column; sb, swimbladder. (Top and bottom panels) Hematoxylin and eosin (H&E) stain of *BRAF^{V600E}mitf* melanoma, indicating large melanophages (red arrows), spindle or epithelioid cell shapes (yellow arrows), and pigmented melanoma cells (white arrow). Scale bars = 20 μm. (**b**) Cross-section of adult *BRAF^{V600E}p53* zebrafish with invasive melanoma (dotted line). (Top and bottom panels) H&E stain of *BRAF^{V600E}p53* melanoma, indicating pigmented melanoma cells (white arrows) and nuclear pleomorphisms (yellow arrow). Scale bars = 20 μm. (**c–f**) Immunohistochemistry staining for (**c**) phospho-extracellular signal–regulated kinase (ERK), (**d**) p53, (**e**) Melan-A, and (**f**) phospho-histone H3. Scale bars = 50 μm. (**g**). Box plot of mean percentage phospho-histone H3–stained cells in *BRAF^{V600E}mitf* and *BRAF^{V600E}p53* tumors (n = 11 melanomas of each genotype). Bars represent interquartile range; Student's t-test P = 0.0078.

mutation and not just the water temperature because *BRAF^{V600E}p53* zebrafish upshifted to 32 °C for 2 weeks showed no tumor regression and even continued growth (n = 6/6; Figure 4b). By 2 months, 12/15 very large tumors showed regression, and 6 of these fish showed complete regression and even healing at the tumor site (Figure 4c; fish 3 and 4). Interestingly, despite the striking levels of melanoma regression, melanomas recurred following a temperature shift to <26 °C, indicating that a subpopulation of melanoma cells with very low MITF activity survive and are capable of repopulating the tumor site (Supplementary Figure S3 online).

To understand the process of melanoma regression, we shifted *BRAF^{V600E}mitf* zebrafish to the restrictive temperature (32 °C) for 7 days to analyze melanoma regression in progress. Histological analysis of the regressing melanomas showed evidence of tumor regression, characterized by marked loss of tumor cell density and accumulation of heavily pigmented melanophages (n = 7/7; Figure 5a and b). To address whether

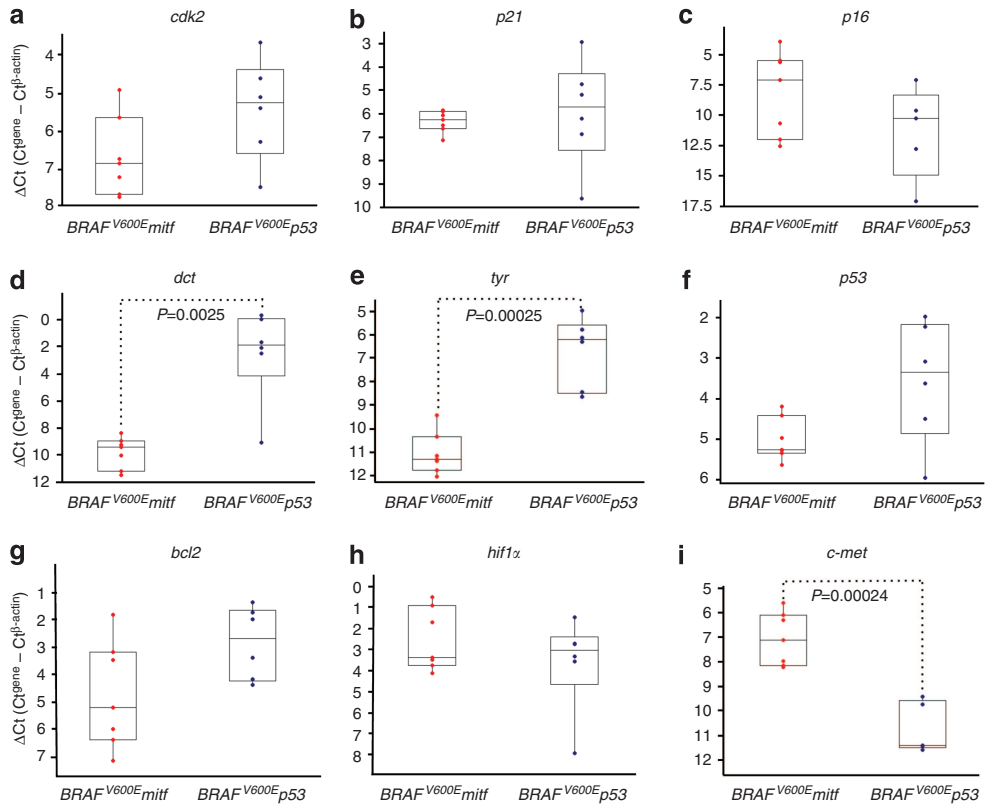

Figure 3. MITF target gene expression. (**a–i**) Box plots of quantitative real-time PCR (qRT-PCR) of MITF target genes and *p53*. The *y*-axis indicates the difference between the cycle threshold (Ct) value of the gene of interest and the Ct value of β-actin in each sample. Note that the *y*-axis is inverted for ease of interpretation. Bars represent interquartile range; *P*-values determined by Student's *t*-test. Also see Supplementary Table S1 online. MITF, microphtholmia associated transcription factor.

apoptosis contributed to regression, we stained sections of the regressing *BRAF*^{V600E}*mitf* melanomas with antibodies to detect active (cleaved) Caspase-3. We found high levels of active Caspase-3 in the regressing tumors compared with *BRAF*^{V600E}*mitf* melanomas at $<26\,^{\circ}C$ ($n=5$ in each group; Figure 5c). We conclude that there is a genetic dependency on MITF activity in *BRAF*^{V600E}*mitf* melanoma.

DISCUSSION

Identifying BRAF^{V600E} cooperating mutations that drive melanoma progression is critical for developing new therapeutic approaches and tackling drug resistance. Accumulating evidence indicates that MITF activity is a key contributing factor in melanoma (Tsao *et al.*, 2012). We now show in an animal that a low level of wild-type MITF activity is oncogenic with BRAF^{V600E} and that abrogating MITF activity in melanoma leads to tumor regression.

The BRAF^{V600E}*mitf* model is relevant to human melanoma, because for some patients, low expression of MITF is associated with disease progression and poor prognosis (Salti *et al.*, 2000; Levy *et al.*, 2006). In these contexts, exogenous expression of MITF leads to inhibition of proliferation (Selzer *et al.*, 2002; Wellbrock and Marais, 2005). This is in apparent contrast to evidence that MITF amplification is also an indicator of poor prognosis, and that MITF cooperates with BRAF^{V600E} to transform melanocytes (Garraway *et al.*, 2005). These differences in MITF activity may reflect distinct subtypes of melanoma; however, another possibility is that MITF amplification indicates the need for melanoma cells to maintain sufficient MITF activity for survival in the context of high BRAF^{V600E} signaling (Garraway *et al.*, 2005; Wellbrock *et al.*, 2008). Thus, a common feature of melanoma may involve maintaining sufficient MITF activity for survival and proliferation while at the same time restricting higher levels of MITF activity that promote cell cycle arrest and differentiation or lower levels that lead to cell cycle arrest and apoptosis (Gray-Schopfer *et al.*, 2007; Hoek and Goding, 2010). Here, the temperature-sensitive nature of the zebrafish *mitfa*^{vc7} mutant allele enables MITF activity to be varied within an individual animal by altering the water temperature, thereby revealing the role of MITF activity levels in melanomagenesis and survival *in vivo*, although we cannot exclude the possibility that the *mitfa*^{vc7} mutant has additional functions that contribute to melanoma.

Histopathological characteristics of melanoma are determined by a number of factors, and at least some are genetically determined (Whiteman *et al.*, 2011). This is illustrated by the clinical classification of BRAF^{V600E} melanomas as a subgroup based on histomorphological features (Viros *et al.*, 2008). We show here that cooperating mutations also have an important role in determining the pathological features

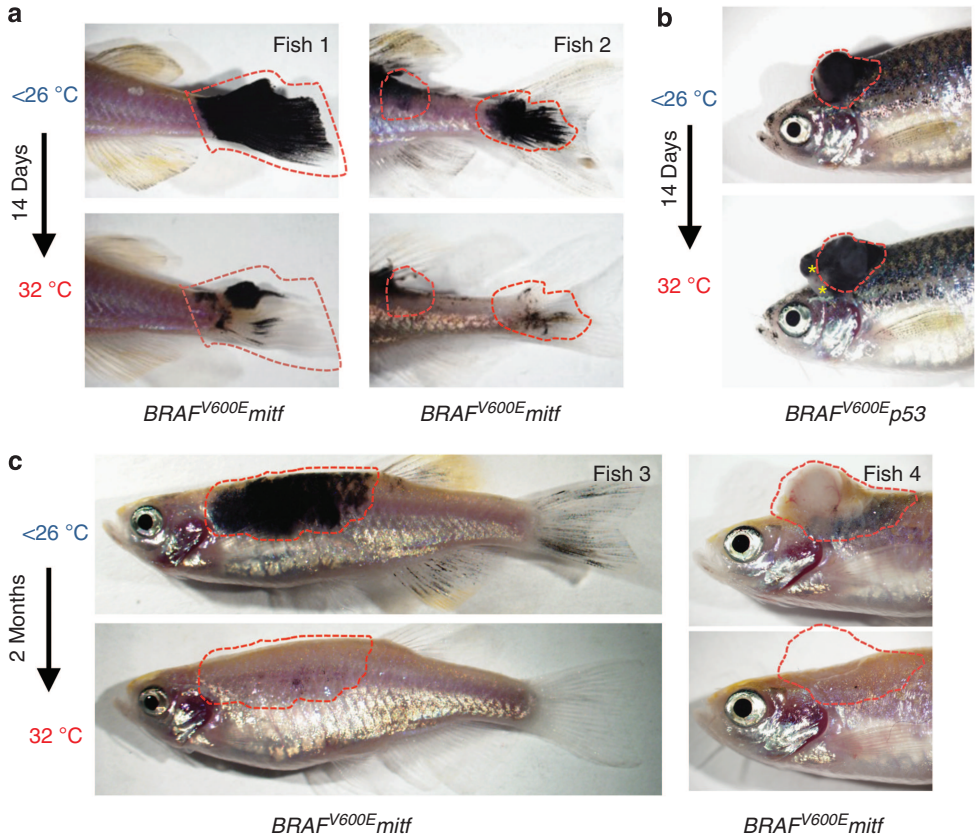

Figure 4. Abrogation of MITF activity causes melanoma regression. (**a**) Images of adult *BRAF*^{V600E}*mitf* zebrafish at <26 °C, and transferred to water at 32 °C for 14 days (bottom images). Red dotted lines outline the tumors before and after the temperature shift. (**b**) Control *BRAF*^{V600E}*p53* melanoma fish at <26 °C and at 32 °C. Areas of increased tumor growth are indicated with yellow asterisks. (**c**) Adult *BRAF*^{V600E}*mitf* zebrafish at <26 °C and after 2 months at 32 °C. MITF, microphtholmia associated transcription factor.

of melanoma. We find that low, oncogenic levels of MITF activity contribute to melanoma pathology, possibly by maintaining melanoma cells in a progenitor-like state. Notably, macrophages laden with melanin (melanophages) were a diagnostic feature of the *BRAF*^{V600E}*mitf* melanomas. Melanophages are found in human melanomas, are indicative of an immune response, and predict an improved prognosis for patients, possibly because of tumor regression through macrophage engulfment of melanoma cells (Handerson *et al.*, 2007). Thus, BRAF^{V600E} cooperating mutations can directly influence tumor morphology, as well as tumor–immune cell interactions.

The dramatic recurrence of melanomas in patients following treatment with the BRAF^{V600E} inhibitor, vemurafenib, indicates that combination therapies that target multiple pathways in melanoma may be necessary to improve patient outcome. MITF activity has been implicated as an important drug target (Flaherty *et al.*, 2012; Tsao *et al.*, 2012), and we now show that shutting off endogenous MITF activity *in vivo* leads to dramatic and rapid melanoma regression, characterized by melanophage infiltration and apoptosis. The melanomas recur at the same location following reactivation of MITF activity (Supplementary Figure S3 online), although at this stage we cannot distinguish whether this reflects incomplete tumor regression or a cancer-initiating population that can survive with low-to-no MITF activity. Notably, although melanophages are presumably participating in melanoma regression and/or clearance (Figure 5), we do not know their function in melanoma growth (Figure 2a): macrophages can lead to both melanoma regression (Nakashima *et al.*, 2012) and promotion (Zaidi *et al.*, 2011), or form melanoma–macrophage hybrids (Pawelek, 2007).

In conclusion, our zebrafish model provides *in vivo* genetic evidence that targeting MITF activity—either directly or through regulators of MITF—may be an effective approach to melanoma therapy. Critically, our studies show that although targeting MITF activity is a potent antitumor mechanism, it must be done with caution because partial or ineffective targeting of MITF is oncogenic.

MATERIALS AND METHODS

All zebrafish work was done in accordance with the United Kingdom Home Office Animals (Scientific Procedures) Act (1986) and approved by the University of Edinburgh Ethical Review Committee, and in the United States in compliance with protocol AM10415, approved by the Institutional Animal Care and Use Committee of Virginia Commonwealth University. The temperature-sensitive *mitfa*^{vc7} mutant is described in Johnson *et al.* (2011), and the *mitfa*^{vc7} phenotypes were first inadvertantly ascribed to the *mitfa*^{fh53}mutant.

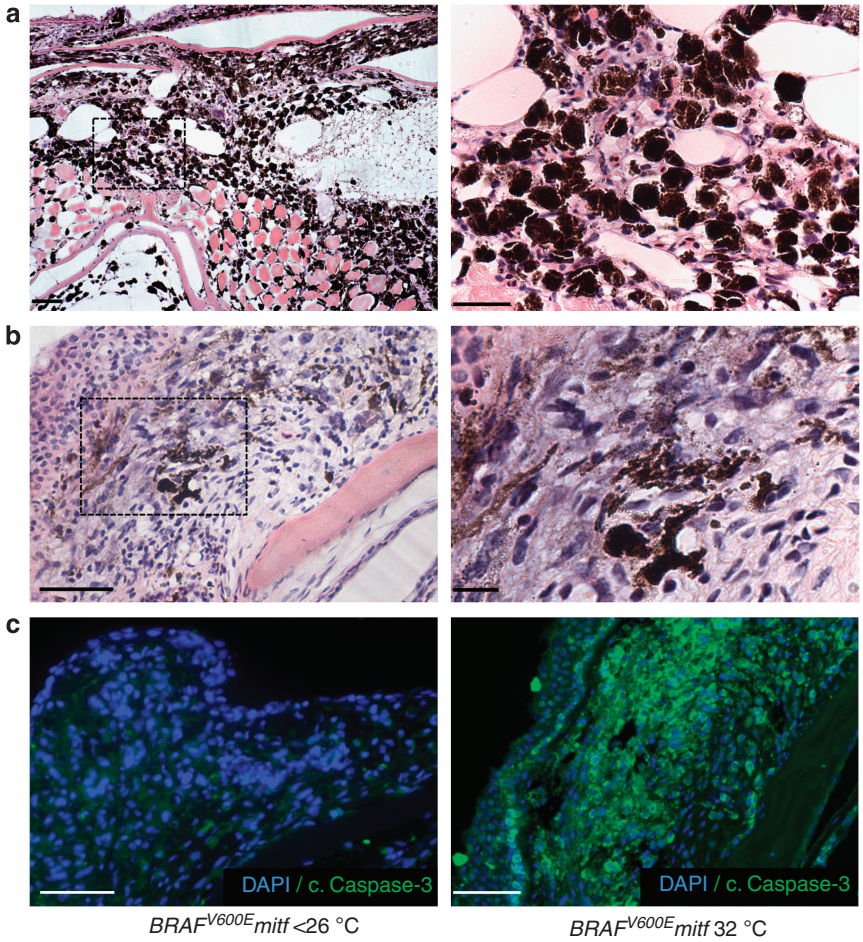

Figure 5. Melanoma regression is associated with melanophage and apoptotic activity. (**a**) Hematoxylin and eosin (H&E) staining of a regressing *BRAF*^{V600E}*mitf* melanoma showing almost total regression with prominent melanophages (scale bar = 200 μm). Boxed region is enlarged in right panel (scale bar = 100 μm). (**b**) A regressing tumor, showing subtotal regression with melanoma cells present (scale bar = 100 μm). Boxed region is enlarged in right panel (scale bar = 50 μm). (**c**) Images of nonregressing (<26 °C) and regressing (32 °C) *BRAF*^{V600E}*mitf* melanomas (as shown in **b**), stained with an antibody to detect cleaved-Caspase-3 (scale bar = 50 μm).

Histopathology

Adult zebrafish were prepared for histopathology as described previously (Patton *et al.*, 2011). Antibodies and antigen retrieval methods were as follows: anti-phospho-extracellular signal–regulated kinase 1/2, 1:1,000, EDTA buffer (Cell Signaling Technology, Danvers, MA); p53 5.1, 1:500, citrate buffer; phospho-histone H3, 1:1,000, citrate buffer (Cell Signaling Technology); Melan-A, 1:75, citrate buffer (DAKO, Cambridge, UK). For the proliferation analysis, the total melanoma cell population in each of the six images was counted (between 1,000 and 3,000 cells) and the percentage of phospho-histone H3–stained cells calculated.

PCR analysis

Total RNA was isolated using TRIzol reagent (Invitrogen, Paisley, UK). First-strand complementary DNA was synthesized from 1 μg of total RNA in a 10 μl reaction using SuperScript III Reverse Transcriptase (Invitrogen). Complementary DNA was then amplified by PCR using primers covering the alternative splicing region in the *mitfa*^{vc7} gene. Quantitative real-time PCR was performed using SYBR Green Jumpstart Taq Readymix for high-throughput real-time PCR (Sigma, St Louis, MO). Reactions were run in an ABI PRISM 7900 HT Sequence Detection System (Applied Biosystems, Paisley, UK) using the SYBR Green protocol. The zebrafish *β-actin* gene was used as reference. Primers sequences are presented in Supplementary Table S1 online.

CONFLICT OF INTEREST

The authors state no conflict of interest.

ACKNOWLEDGMENTS

We are grateful to Nick Hastie, Margaret Frame, James Amatruda, and Kerrie Marie for the critical reading of the manuscript; Katie Lunney and Leyla Peachy for zebrafish husbandry; and David Lane for the zebrafish p53 antibody. This work was funded by a Concern Foundation for Cancer Research CONCERN (CONquer canCER Now) Award (to JAL), a FP7-Framework ZF-Cancer grant (to EEP), the Wellcome Trust (to EEP), Medical Research Scotland (to JR and EEP), and the Medical Research Council (to AC, JR, ZZ, KP, IJJ, and EEP).

SUPPLEMENTARY MATERIAL

Supplementary material is linked to the online version of the paper at http://www.nature.com/jid

REFERENCES

Bertolotto C, Lesueur F, Giuliano S *et al.* (2011) A SUMOylation-defective MITF germline mutation predisposes to melanoma and renal carcinoma. *Nature* 480:94–8

Beuret L, Flori E, Denoyelle C *et al.* (2007) Up-regulation of MET expression by alpha-melanocyte-stimulating hormone and MITF allows hepatocyte growth factor to protect melanocytes and melanoma cells from apoptosis. *J Biol Chem* 282:14140–7

Ceol CJ, Houvras Y, Jane-Valbuena J *et al.* (2011) The histone methyltransferase SETDB1 is recurrently amplified in melanoma and accelerates its onset. *Nature* 471:513–7

Cheli Y, Giuliano S, Fenouille N *et al.* (2012) Hypoxia and MITF control metastatic behaviour in mouse and human melanoma cells. *Oncogene* 10:2461–70

Cheli Y, Giuliano S, Botton T *et al.* (2011) Mitf is the key molecular switch between mouse or human melanoma initiating cells and their differentiated progeny. *Oncogene* 30:2307–18

Cheli Y, Ohanna M, Ballotti R *et al.* (2010) Fifteen-year quest for microphthalmia-associated transcription factor target genes. *Pigment Cell Melanoma Res* 23:27–40

Cronin JC, Wunderlich J, Loftus SK *et al.* (2009) Frequent mutations in the MITF pathway in melanoma. *Pigment Cell Melanoma Res* 22:435–44

Dooley CM, Mongera A, Walderich B *et al.* (2013) On the embryonic origin of adult melanophores: the role of ErbB and Kit signalling in establishing melanophore stem cells in zebrafish. *Development* 140:1003–13

Du J, Miller AJ, Widlund HR *et al.* (2003) MLANA/MART1 and SILV/PMEL17/GP100 are transcriptionally regulated by MITF in melanocytes and melanoma. *Am J Pathol* 163:333–43

Flaherty KT, Hodi FS, Fisher DE (2012) From genes to drugs: targeted strategies for melanoma. *Nat Rev Cancer* 12:349–61

Garraway LA, Widlund HR, Rubin MA *et al.* (2005) Integrative genomic analyses identify MITF as a lineage survival oncogene amplified in malignant melanoma. *Nature* 436:117–22

Giuliano S, Cheli Y, Ohanna M *et al.* (2010) Microphthalmia-associated transcription factor controls the DNA damage response and a lineage-specific senescence program in melanomas. *Cancer Res* 70:3813–22

Goodall J, Carreira S, Denat L *et al.* (2008) Brn-2 represses microphthalmia-associated transcription factor expression and marks a distinct subpopulation of microphthalmia-associated transcription factor-negative melanoma cells. *Cancer Res* 68:7788–94

Gray-Schopfer V, Wellbrock C, Marais R (2007) Melanoma biology and new targeted therapy. *Nature* 445:851–7

Handerson T, Berger A, Harigopol M *et al.* (2007) Melanophages reside in hypermelanotic, aberrantly glycosylated tumor areas and predict improved outcome in primary cutaneous malignant melanoma. *J Cutan Pathol* 34:679–86

Hoek KS, Goding CR (2010) Cancer stem cells versus phenotype-switching in melanoma. *Pigment Cell Melanoma Res* 23:746–59

Hou L, Pavan WJ (2008) Transcriptional and signaling regulation in neural crest stem cell-derived melanocyte development: do all roads lead to Mitf? *Cell Res* 18:1163–76

Johnson SL, Nguyen AN, Lister JA (2011) mitfa is required at multiple stages of melanocyte differentiation but not to establish the melanocyte stem cell. *Dev Biol* 350:405–13

Kumar SM, Dai J, Li S *et al.* (2013) Human skin neural crest progenitor cells are susceptible to BRAF(V600E)-induced transformation. *Oncogene* 1–10

Levy C, Khaled M, Fisher DE (2006) MITF: master regulator of melanocyte development and melanoma oncogene. *Trends Mol Med* 12:406–14

Lister JA, Robertson CP, Lepage T *et al.* (1999) nacre encodes a zebrafish microphthalmia-related protein that regulates neural-crest-derived pigment cell fate. *Development* 126:3757–67

Mascarenhas JB, Littlejohn EL, Wolsky RJ *et al.* (2010) PAX3 and SOX10 activate MET receptor expression in melanoma. *Pigment Cell Melanoma Res* 23:225–37

McGill GG, Haq R, Nishimura EK *et al.* (2006) c-Met expression is regulated by Mitf in the melanocyte lineage. *J Biol Chem* 281:10365–73

Nakashima H, Miyake K, Clark CR *et al.* (2012) Potent antitumor effects of combination therapy with IFNs and monocytes in mouse models of established human ovarian and melanoma tumors. *Cancer Immunol Immunother* 61:1081–92

Patton EE, Mathers ME, Schartl M (2011) Generating and analyzing fish models of melanoma. *Methods Cell Biol* 105:339–66

Patton EE, Widlund HR, Kutok JL *et al.* (2005) BRAF mutations are sufficient to promote nevi formation and cooperate with p53 in the genesis of melanoma. *Curr Biol* 15:249–54

Pawelek JM (2007) Viewing malignant melanoma cells as macrophage-tumor hybrids. *Cell Adh Migr* 1:2–6

Salti GI, Manougian T, Farolan M *et al.* (2000) Micropthalmia transcription factor: a new prognostic marker in intermediate-thickness cutaneous malignant melanoma. *Cancer Res* 60:5012–6

Selzer E, Wacheck V, Lucas T *et al.* (2002) The melanocyte-specific isoform of the microphthalmia transcription factor affects the phenotype of human melanoma. *Cancer Res* 62:2098–103

Strub T, Giuliano S, Ye T *et al.* (2011) Essential role of microphthalmia transcription factor for DNA replication, mitosis and genomic stability in melanoma. *Oncogene* 30:2319–32

Taylor KL, Lister JA, Zeng Z *et al.* (2011) Differentiated melanocyte cell division occurs in vivo and is promoted by mutations in Mitf. *Development* 138:3579–89

Tsao H, Chin L, Garraway LA *et al.* (2012) Melanoma: from mutations to medicine. *Genes Dev* 26:1131–55

Viros A, Fridlyand J, Bauer J *et al.* (2008) Improving melanoma classification by integrating genetic and morphologic features. *PLoS Med* 5:e120

Wellbrock C, Marais R (2005) Elevated expression of MITF counteracts B-RAF-stimulated melanocyte and melanoma cell proliferation. *J Cell Biol* 170:703–8

Wellbrock C, Rana S, Paterson H *et al.* (2008) Oncogenic BRAF regulates melanoma proliferation through the lineage specific factor MITF. *PLoS One* 3:e2734

Whiteman DC, Pavan WJ, Bastian BC (2011) The melanomas: a synthesis of epidemiological, clinical, histopathological, genetic, and biological aspects, supporting distinct subtypes, causal pathways, and cells of origin. *Pigment Cell Melanoma Res* 24:879–97

Yokoyama S, Woods SL, Boyle GM *et al.* (2011) A novel recurrent mutation in MITF predisposes to familial and sporadic melanoma. *Nature* 480: 99–103

Zaidi MR, Davis S, Noonan FP *et al.* (2011) Interferon-gamma links ultraviolet radiation to melanomagenesis in mice. *Nature* 469:548–53

Zebrafish as a model system to investigate the function of MITF in melanoma

Amy Capper and E. Elizabeth Patton*

Background

Melanoma is the most lethal form of skin cancer, and incidence continues to rise rapidly in Western populations. The American Cancer Society currently estimates that there are 120,000 new cases of melanoma diagnosed in the U.S. each year with UV exposure playing a major role in susceptibility. $BRAF^{V600E}$ is one of the most common somatic mutations associated with melanoma and the recent development of drugs that target $BRAF^{V600E}$ has led to clinically significant improvements in outcomes for melanoma patients. Despite these improvements, many patients with metastatic melanoma eventually succumb to the disease, making it imperative that new therapeutic strategies are developed to identify additional melanoma target pathways (1).

One such important and emerging melanoma target is microphthalmia-associated transcription factor (MITF; Fig. 1). MITF is the "master" transcription factor in melanocyte development, and it plays a complex role in melanoma. Germline MITF mutations have been identified as risk factors for melanoma, and amplifications of the MITF gene, as well as somatic MITF mutations have been identified in melanoma (2). In human cancers and zebrafish melanoma models, MITF activity is finely balanced to provide sufficient activity for melanoma survival and proliferation, but not differentiation (higher activity levels) or senescence/apoptosis (low to no activity levels). In this educational session, we discuss how the zebrafish has been developed as a preclinical model for testing the function of MITF mutations in melanoma.

Discussion

MITF is a highly conserved transcription factor required for melanocyte development

Melanocytes are the pigment producing cells that color our hair, skin and eyes, and function as an important barrier against the harmful effects of UV-irradiation. Melanocytes are found in all vertebrate species, including the zebrafish, where these cells help to form the stripes for which the fish is named. As small, aquarium fish, zebrafish are now widely used as a vertebrate model system because they share many genomic, developmental, anatomical and clinical features with humans (3).

Authors' Affiliations: MRC Institute of Genetics and Molecular Medicine, MRC Human Genetics Unit and University of Edinburgh Cancer Research UK Center, University of Edinburgh, Western General Hospital, Edinburgh EH4 2XR UK

***Corresponding Author:** E-mail: e.patton@igmm.ed.ac.uk

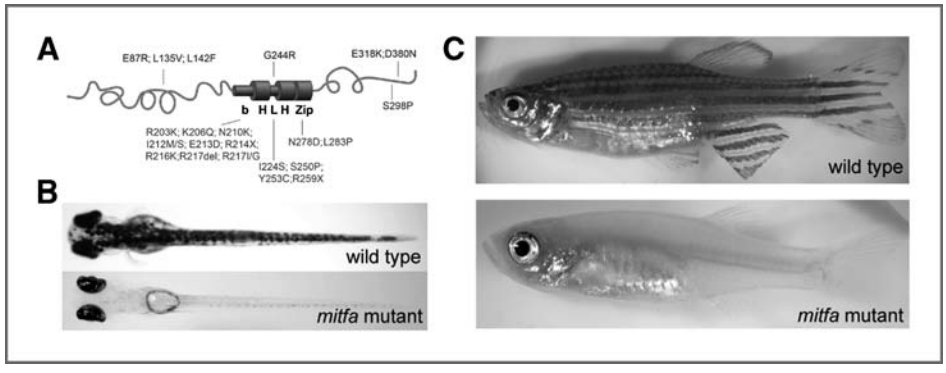

Fig. 1. Human cancer and developmental mutations in MITF, and a loss of function mutation in zebrafish *mitfa*. A. MITF is a basic helix-loop-helix leucine zipper transcription factor, and mutations have been identified that lead to Waardenburg Type IIA and Tietz syndrome (bottom) and melanoma (top). B. A loss of function mutation in *mitfa* leads to a complete loss of all neural crest melanocytes in the zebrafish embryo, and C. in adult zebrafish. The eyes remain pigmented due to expression of a *mitfb*, a paralog of mitfa that arose through an ancient genome duplication event. Fig. 1A kindly provided by Eirikur Steingrimsson (25).

One of the critical melanocyte genetic factors in both fish and humans is MITF. MITF is a transcription factor that regulates a suite of target genes involved in melanocyte specification, proliferation, and differentiation (4). MITF is required for melanocyte development during embryogenesis in fish and mammals, and human germline mutations in MITF lead to Waardenburg Type IIa and Teitz syndromes, characterized by hypopigmentation, deafness, and facial features (Fig. 1A). In zebrafish, an ancestral genome duplication event gave rise to two mitf genes, *mitfa* and *mitfb*, and loss of function mutations in *mitfa* lead to a complete loss of all neural crest derived melanocytes that pigment the skin of the fish (Fig. 1B and C) (5).

MITF is mutated and amplified in melanoma, and is a melanoma-predisposition gene

While it is well established that MITF is essential for melanocyte development, its function in melanoma is less well understood. Germline MITF mutations have been identified as risk factors for melanoma, and MITF amplifications as well as somatic MITF mutations have been identified in melanoma (6–10). An important issue in the field is to understand and reconcile how differing MITF mutations contribute to melanoma. For example, some somatic MITF mutations have reduced activity (6), while the germline $MITF^{E318K}$ mutation has a dominant function by altering MITF target gene expression and conferring increased nevi numbers and non-blue eye color (9, 10). One explanation for the varied MITF activity observed between melanoma samples is that MITF is a lineage survival oncogene: Sufficient MITF activity is required to maintain melanoma survival, but higher MITF activity leads to differentiation and cell cycle arrest, while loss of MITF leads to senescence and/or apoptosis (11–16). Thus, the levels of MITF activity in every melanoma is finely tuned to be "just right" to promote melanoma without leading to differentiation or cell cycle arrest/apoptosis (11, 12).

Zebrafish as a model system for MITF activity in melanoma

An essential part of the challenge to identify melanoma target pathways is the development of animal disease models that reproduce the aetiology and progression of the disease within the context of a whole animal. Zebrafish cancers, including melanomas, are histopathologically similar to the human disease, and parallel molecular mechanisms underlie melanoma in both species (17). We have previously demonstrated that expression of $BRAF^{V600E}$ in zebrafish melanocytes leads to the development of nevi, and when combined with a mutation in *p53*, many nevi progress to melanoma (Fig. 2A) (18). The $BRAF^{V600E}$*p53* mutant melanomas are highly aggressive and invasive, have a high mitotic index, are genetically unstable, and can be transplanted into wild type zebrafish.

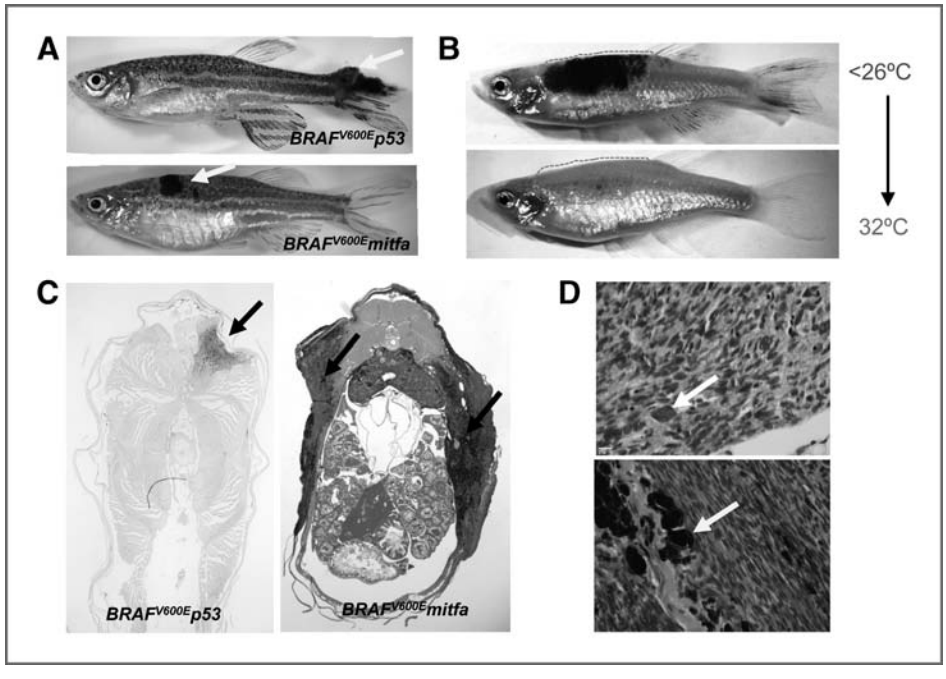

Fig. 2. MITF mutations with lowered activity cooperate with $BRAF^{V600E}$ in melanoma. A. Adult zebrafish with melanoma (arrows). Top fish: $BRAF^{V600E}$ *p53* mutant zebrafish. Bottom fish: $BRAF^{V600E}$ co-operates with low levels of MITF activity to promote melanoma. B. Complete loss of MITF activity in $BRAF^{V600E}$*mitfa* melanomas causes melanoma regression. Here, the *mitfa* genetic mutation is temperature sensitive, and shifting the fish to 32C leads to complete loss of MITF activity in body melanocytes and melanoma regression (outlined area). C. $BRAF^{V600E}$*p53* (left panel) and $BRAF^{V600E}$*mitfa* (right panel) melanomas have characteristically distinct growth patterns. Cross section of adult zebrafish with melanomas indicated (arrows). $BRAF^{V600E}$*p53* melanomas are highly invasive into the underlying musculature, while $BRAF^{V600E}$*mitfa* melanomas display superficial spreading along the skin, with very little invasion and have an abundance of infiltrating melanophages that darkly pigment the tumor. D. $BRAF^{V600E}$*p53* (top panel) and $BRAF^{V600E}$*mitfa* (bottom panel) melanomas are histopathologically distinct and represent different melanoma subtypes. Arrows indicate nuclear pleomorphisms (top panel) and infiltrating macromelanophages (bottom panel). Note differences in melanoma cell shape and organization between subtypes.

While evidence from human melanoma suggested that MITF activity could be oncogenic, there was no genetic animal model to address MITF activity in melanoma promotion and survival. Recently, Lister and colleagues have identified a temperature-sensitive mutant allele of *mitfa*, such that when the fish are grown in water at 24C, MITF is active and the animals develop pigmented melanocytes (19). However, when the temperature of the water is raised to above 28C, MITF is inactive and the fish are white. This enables control of MITF activity by simply altering the temperature of the water. Utilizing this *mitfa* temperature sensitive allele, we found that lowered levels of MITF activity cooperated with $BRAF^{V600E}$ mutations to promote nevi and melanoma *in vivo*, and that loss of MITF in established melanomas led to rapid melanoma regression (Fig. 2A and B) (20). Furthermore, while melanoma incidence was similar in $BRAF^{V600E}$*p53* and $BRAF^{V600E}$*mitf* fish, the histopathology of the melanomas were strikingly different. $BRAF^{V600E}$*mitf* melanomas were characterized by a high degree of pigmentation, low mitotic index and superficial spreading through the skin, in contrast to the aggressive and invasive nature of $BRAF^{V600E}$*p53* melanoma (Fig. 2C and D). An important implication from this animal model is the validation of MITF as a drug target in melanoma, but also that caution would be needed in this approach, because insufficient targeting of MITF activity (leading to simply a reduction in MITF activity) could be oncogenic (20).

Future Directions

With an animal model of MITF activity in melanoma in hand, the next series of challenges can begin to be addressed:

Develop conditional genetic models of melanoma that recapitulate MITF mutations found in humans

New technological advances in genome editing in zebrafish using the CRISPR/Cas9 system now make this possible (21). This is important to directly test the function of MITF cancer genes *in vivo*, and would enable direct validation of MITF as a target in otherwise MITF wild type cancers. Additional zebrafish MITF models could also illuminate the mechanisms underlying MITF oncogenic activity, and enable the identification of MITF cooperating pathways (such as by exome sequencing of zebrafish melanomas, as recently described (22)).

Understand MITF activity in melanocyte and melanoma stem cells

In zebrafish, low expressing *mitf+* cells associated with the dorsal root ganglia may mark melanocyte stem cells (23), and low *MITF* expression is associated with a tumor-promoting population in human melanoma (24). It will be of great interest to establish the impact of MITF cancer mutations on the melanocyte stem cell in development, in melanoma initiation and progression, and response to therapy.

Develop zebrafish as a pre-clinical system to test and validate drug-leads and drug-targets

A unique feature of the zebrafish vertebrate system is the ability to perform whole animal small molecule screens for drug-leads that target melanocyte and MITF pathways *in vivo*. Zebrafish

embryos are fertilized outside the mother and are transparent, enabling visualization and manipulation of development from a single cell embryo through organogenesis and disease. This system provides the potential to identify target pathways in development that can then be applied in the adult zebrafish melanoma and mammalian systems (3).

References

1. Flaherty KT, Hodi FS, Fisher DE. From genes to drugs: Targeted strategies for melanoma. Nat Rev Cancer 2012;12:349–61.

2. Tsao H, Chin L, Garraway LA, Fisher DE. Melanoma: from mutations to medicine. Genes Dev 2012;26:1131–55.

3. White R, Rose K, Zon L. Zebrafish cancer: The state of the art and the path forward. Nat Rev Cancer 2013;13:624–36.

4. Cheli Y, Ohanna M, Ballotti R, Bertolotto C. Fifteen-year quest for microphthalmia-associated transcription factor target genes. Pigment Cell Melanoma Res 2010;23:27–40.

5. Lister JA, Close J, Raible DW. Duplicate mitf genes in zebrafish: complementary expression and conservation of melanogenic potential. Dev Biol 2001;237:333–44.

6. Cronin JC, Wunderlich J, Loftus SK, Prickett TD, Wei X, Ridd K, et al. Frequent mutations in the MITF pathway in melanoma. Pigment Cell Melanoma Res 2009;22:435–44.

7. Garraway LA, Widlund HR, Rubin MA, Getz G, Berger AJ, Ramaswamy S, et al. Integrative genomic analyses identify MITF as a lineage survival oncogene amplified in malignant melanoma. Nature 2005;436:117–22.

8. Hodis E, Watson IR, Kryukov GV, Arold ST, Imielinski M, Theurillat JP, et al. A landscape of driver mutations in melanoma. Cell 2012;150:251–63.

9. Bertolotto C, Lesueur F, Giuliano S, Strub T, de Lichy M, Bille K, et al. A SUMOylation-defective MITF germline mutation predisposes to melanoma and renal carcinoma. Nature 2011;480:94–8.

10. Yokoyama S, Woods SL, Boyle GM, Aoude LG, MacGregor S, Zismann V, et al. A novel recurrent mutation in MITF predisposes to familial and sporadic melanoma. Nature 2011;480:99–103.

11. Gray-Schopfer V, Wellbrock C, Marais R. Melanoma biology and new targeted therapy. Nature 2007;445:851–7.

12. Hoek KS, Goding CR. Cancer stem cells versus phenotype-switching in melanoma. Pigment Cell Melanoma Res 2010;23:746–59.

13. Carreira S, Goodall J, Aksan I, La Rocca SA, Galibert MD, Denat L, et al. Mitf cooperates with Rb1 and activates p21Cip1 expression to regulate cell cycle progression. Nature 2005;433:764–9.

14. Carreira S, Goodall J, Denat L, Rodriguez M, Nuciforo P, Hoek KS, et al. Mitf regulation of Dia1 controls melanoma proliferation and invasiveness. Genes Dev 2006;20:3426–39.

15. Strub T, Giuliano S, Ye T, Bonet C, Keime C, Kobi D, et al. Essential role of microphthalmia transcription factor for DNA replication, mitosis and genomic stability in melanoma. Oncogene 2011;30:2319–32.

16. Giuliano S, Cheli Y, Ohanna M, Bonet C, Beuret L, Bille K, et al. Microphthalmia-associated transcription factor controls the DNA damage response and a lineage-specific senescence program in melanomas. Cancer Res 2010;70:3813–22.

17. Amatruda JF, Patton EE. Genetic models of cancer in zebrafish. Int Rev Cell Mol Biol 2008;271:1–34.

18. Patton EE, Widlund HR, Kutok JL, Kopani KR, Amatruda JF, Murphey RD, et al. BRAF mutations are sufficient to promote nevi formation and cooperate with p53 in the genesis of melanoma. Curr Biol 2005;15:249–54.

19. Johnson SL, Nguyen AN, Lister JA. mitfa is required at multiple stages of melanocyte differentiation but not to establish the melanocyte stem cell. Dev Biol 2011;350:405–13.

20. Lister JA, Capper A, Zeng Z, Mathers ME, Richardson J, Paranthaman K, et al. A conditional zebrafish MITF mutation reveals MITF levels are critical for melanoma promotion vs. regression *in vivo*. J Invest Dermatol 2014;134:133–40.

21. Hwang WY, Fu Y, Reyon D, Maeder ML, Tsai SQ, Sander JD, et al. Efficient genome editing in zebrafish using a CRISPR-Cas system. Nat Biotechnol 2013;31:227–9.

22. Yen J, White RM, Wedge DC, Van Loo P, de Ridder J, Capper A, et al. The genetic heterogeneity and mutational burden of engineered melanomas in zebrafish models. Genome Biol 2013;14:R113.

23. Dooley CM, Mongera A, Walderich B, Nusslein-Volhard C. On the embryonic origin of adult melanophores: The role of ErbB and Kit signalling in establishing melanophore stem cells in zebrafish. Development 2013;140:1003–13.

24. Cheli Y, Giuliano S, Botton T, Rocchi S, Hofman V, Hofman P, et al. Mitf is the key molecular switch between mouse or human melanoma initiating cells and their differentiated progeny. Oncogene 2011;30:2307–18.

25. Grill C, Bergsteinsdottir K, Ogmundsdottir MH, Pogenberg V, Schepsky A, Wilmanns M, et al. MITF mutations associated with pigment deficiency syndromes and melanoma have different effects on protein function. Hum Mol Genet 2013;22: 4357–67.